Regulation of Rps6 phosphorylation by TOR complexes in Saccharomyces cerevisiae

Yerlikaya, Seda

UNIVERSITE DE GENEVE
Section de Biologie
Département de Biologie Moléculaire

FACULTE DES SCIENCES
Professeur Robbie Loewith

Regulation of Rps6 Phosphorylation by TOR Complexes in *Saccharomyces cerevisiae*

THÈSE

Présentée à la faculté des sciences de l'Université de Genève pour obtenir le grade de Docteur ès Sciences, mention Biologie

par

Seda YERLIKAYA
de
Ankara (TURQUIE)

Thèse n° 4613

GENÈVE
Atelier d'impression Repromail
2013

UNIVERSITÉ
DE GENÈVE

FACULTÉ DES SCIENCES

Doctorat ès sciences
Mention biologie

Thèse de *Madame Seda YERLIKAYA*

intitulée :

" Regulation of Rps6 Phosphorylation by TOR Complexes in *Saccharomyces cerevisiae* "

La Faculté des sciences, sur le préavis de Messieurs R. LOEWITH, professeur associé et directeur de thèse (Département de biologie moléculaire), D. SHORE, professeur ordinaire (Département de biologie moléculaire) et M. PENDE, docteur (Centre de recherche Croissance et Signalisation, Université Paris Descartes, Site Necker, Paris, France), autorise l'impression de la présente thèse, sans exprimer d'opinion sur les propositions qui y sont énoncées.

Genève, le 18 novembre 2013

Thèse - 4613 -

Le Doyen, Jean-Marc TRISCONE

N.B.- La thèse doit porter la déclaration précédente et remplir les conditions énumérées dans les "Informations relatives aux thèses de doctorat à l'Université de Genève".

Table of Contents

ACKNOWLEDGEMENTS

Five years.. Five years of PhD which let me learn, enjoy and change with great contributions from many people. Many thanks..

To Robbie for being a great support from the first moment we met, for creating an atmosphere which does not let us know what an “I hate Mondays” syndrome is, for giving all the freedom to enjoy science and most importantly for being open to any discussion any time. I do hope that you never change the way you are.

To the lab people for all the great moments, friendship, support and discussion. I am well aware of the fact that having not only colleagues but also great friends in a work environment is precious. Special thanks to Michael, Manuele, Marie, Alex, Karo and Christl for this.

To Madeleine for making this thesis possible by handing down a very-well established project and also to Sedef and Margot for their contributions to this work.

To all our collaborators for the help we received during this journey.

To all the great people I met in Geneva for making me love even Geneva. Special thanks to Cansel, Remzi, Fabi and Eve for being there for me and for filling these last five years with great friendship, joy, fun and lots of good memories.

To my amazing friends İrem, Gülin, Pınar, Özgün, Kemal for their long-distance support.

To Nilhan. It is useless to try to express how much having you there by my side means to me.

To my family /aileme, her biriniz cansınız. Olduğum insan olma sebebimsiniz. Sağolasınız.

To all the #occupygezi supporters for refreshing my belief in resistance, solidarity and a better world.

To Modern Sabahlar for making me laugh all the time in the lab even on a bad day and for keeping me motivated at work.

To all the beautiful books to be read under sun.

To all the good music, especially to Gevende, which let me appreciate every single moment of life.

Hepinize yürekten bir “eyvallah”. Bu tezde, her birinizin emeği çok.

Finally, this work is dedicated..

..to Ali İsmail, Ethem, Mehmet, Abdullah, Medeni, Ahmet, the ones we lost in Roboski, and to Ceylan (Önkol) and to Uğur (Kaymaz).

..also to “zuzu”.

ABSTRACT

English

The central dogma of molecular biology as first proposed by Francis Crick in 1958 states the route of genetic information in a cell as the “transfer of sequential information” from DNA to RNA and then to protein (Crick, 1958). Accordingly, messenger RNAs (mRNAs) carry out a major role in transferring the information from DNA to protein. Thus, regulation of the fate of an mRNA once transcribed from DNA is crucial for the steady-state gene expression levels in the cell. Following its transport from nucleus into cytoplasm, there are various paths waiting for an mRNA; translation, degradation, and storage.

The *T*arget *O*f *R*apamycin (TOR) pathway is a central regulator of cell growth in response to various environmental and cell intrinsic cues. TOR signaling has already been implicated in the regulation of translation. With the aim of addressing the role of TOR in mRNA degradation, we focused on how Ccr4, the major deadenylase in budding yeast, is regulated by TOR complex 1 (TORC1). We showed that Ccr4 was a phosphoprotein whose phosphorylation levels were highly responsive to nutrient depletion and TORC1 activity. We hypothesized that phosphorylation of Ccr4 might influence global mRNA turnover but we obtained no evidence to support this idea. We pinpointed a number of kinases which mediated the phosphorylation of Ccr4, giving us future directions on which specific processes might be affected by this phosphorylation event.

Ribosomal protein S6 (Rps6) was shown to be a phosphoprotein more than three decades ago. Yet, one fundamental question still remains to be elucidated: What is the physiological role of this phosphorylation? To address this question, we characterized the major players of the pathway signaling to Rps6 in *Saccharomyces cerevisiae*. We showed that phosphorylation of two highly conserved sites on Rps6 were differentially regulated downstream of TOR complexes 1 and 2. We characterized the novel TORC1 effector Ypk3 and *bona fide* TORC2 effectors Ypk1 and Ypk2 as S6 kinases in budding yeast. Moreover, Glc7/Shp1 emerged as the phosphatase branch which

antagonized the Rps6 phosphorylation. We explored a role for Rps6 phosphorylation in global translation and translation decoding but such functions were not apparent. Currently, we are working to unveil the mystery of physiological function of Rps6 phosphorylation in the cell taking advantage of the novel players of this pathway which we have identified.

Altogether, our study provides further insights into the mechanisms by which both TORC1 and TORC2 contribute to posttranscriptional regulation of gene expression in *Saccharomyces cerevisiae*.

Français

En 1958, Francis Crick instaura pour la première fois le dogme central de la biologie moléculaire, qui établit le cheminement de l'information génétique dans une cellule comme un "transfert d'informations séquentielles" de l'ADN à l'ARN, puis aux protéines (Crick, 1958). En conséquence, les ARN messagers (ARNm) ont un rôle majeur dans le transfert de l'information de l'ADN aux protéines. Ainsi, la régulation du devenir d'un ARNm issu de la transcription de l'ADN est cruciale pour le niveau basal d'expression des gènes dans une cellule. Après son transport du noyau au cytoplasme, plusieurs voies possibles existent pour un ARNm : traduction, dégradation et stockage.

La voie de signalisation *T*arget *O*f *R*apamycin (TOR) est un régulateur central de la croissance cellulaire répondant à divers signaux environnementaux et intracellulaires. TOR est aussi impliquée dans la régulation de la traduction d'ARNm en protéines. Dans le but d'établir le rôle de TOR dans la dégradation des ARNm, nous nous sommes concentrés sur Ccr4, la déadénylase majeure de la levure *S*. *cerevisiae*, et sa régulation par le complexe TOR 1 (TORC1). Nous avons montré que Ccr4 était une phosphoprotéine dont les niveaux de phosphorylation répondaient fortement aux niveaux de nutriments disponibles ainsi qu'à TORC1. Nous avons alors proposé que la phosphorylation de Ccr4 pourrait influencer le recyclage des ARNm, mais nous n'avons obtenu aucune preuve confirmant cette idée. Nous avons identifié un certain nombre de kinases qui jouent un rôle dans la phosphorylation de Ccr4, nous permettant d'envisager plusieurs directions dans lesquelles poursuivre nos recherches concernant les processus spécifiques engendrés par cette phosphorylation.

La protéine ribosomale S6 (Rps6) a été identifiée comme étant une phosphoprotéine il y a plus de trente ans. Néanmoins, une question fondamentale reste à élucider : quel est le rôle physiologique de cette phosphorylation? Afin de répondre à cette question, nous avons caractérisé les principaux acteurs de la voie de signalisation régulant Rps6 chez *S. cerevisiae*. Nous avons démontré que la phosphorylation de deux résidus très conservés dans Rps6 était régulée différemment, en aval des

complexes TORC1 et TORC2. Nous avons caractérisé Ypk3, un nouvel effecteur de TORC1, ainsi que Ypk1 et Ypk2, deux effecteurs *bona fide* de TORC2, en tant que S6 kinases dans la levure. De plus, les protéines Glc7/Shp1 sont apparues comme le complexe de phosphatases antagonisant la phosphorylation de Rps6. Nous avons également exploré le rôle de la phosphorylation de Rps6 dans la traduction en général, ainsi que dans l'étape de décodage, mais aucun rôle n'a pu être mis en évidence. Actuellement, nous continuons à travailler sur le rôle physiologique de la phosphorylation de Rps6 dans la cellule, ceci grâce aux nouveaux acteurs que nous venons d'identifier.

Dans l'ensemble, notre étude nous fournit des connaissances plus précises des mécanismes par lesquels TORC1 et TORC2 contribuent à la régulation post-transcriptionnelle de l'expression des gènes chez la levure *S. cerevisiae*.

Introduction

The *T*arget *O*f *R*apamycin Signaling Pathway in *Saccharomyces cerevisiae*

Cells sense changes in their environment and adapt to these changes. This adaptation is crucial for their survival. The *T*arget *O*f *R*apamycin (TOR) signaling pathway plays an important role in this process by linking environmental cues as well as cell-intrinsic cues to the major cellular processes which regulate growth. Specifically, Tor controls cell growth by regulating gene transcription, translation, ribosome biogenesis, lipid synthesis and actin polarization. In yeast, there are two *TOR* genes, *TOR1* and *TOR2*, while there is only one in higher eukaryotes. Tor kinases are found in two functionally and structurally distinct multiprotein complexes, Tor Complex 1 (TORC1) and Tor Complex 2 (TORC2) (Figure 1). In *Saccharomyces cerevisiae*, TORC1 contains either Tor1 or Tor2 in addition to Kog1, Tco89 and Lst8. Only Tor2 is found in TORC2 together with Avo1, Avo2, Avo3, Lst8, Bit2 and Bit61. Both TORCs perform essential functions. Rapamycin, an anti-fungal and immunosuppressant drug, inhibits TORC1, but not TORC2. On the other hand, a newly characterized drug, BHS345 (BHS) inhibits both of the complexes in *Saccharomyces cerevisiae* (Shimada et al, 2013). TORC1 is localized at the vacuolar membrane, whereas TORC2 is mainly associated with the plasma membrane through its Avo1 component (Berchtold & Walther, 2009).

Tor kinases belong to the family of phosphatidylinositol 3-kinase-related kinases (PIKK) (Rubenstein & Schmidt, 2007). They share common domains with the other members of the family: FAT (FRAP-ATM-TRRAP), PRD (PIKK regulatory domain) and FATC domains. The FAT domain follows HEAT repeats found at the N-terminal part of the Tor kinases. The tandem HEAT (Huntington, Elongation factor 3, PR65/A, TOR) repeats mediate protein-protein interactions. Between the FAT domain and the central kinase domain, there is the FRB domain (FKBP12-rapamycin binding domain). FKBP12, a proline isomerase, is also the “receptor” of rapamycin and binding of the FKBP12-rapamycin heterocomplex to the FRB domain inhibits the enzymatic activity of Tor in the context of TORC1 (Heitman et al, 1991; Koltin et al, 1991).

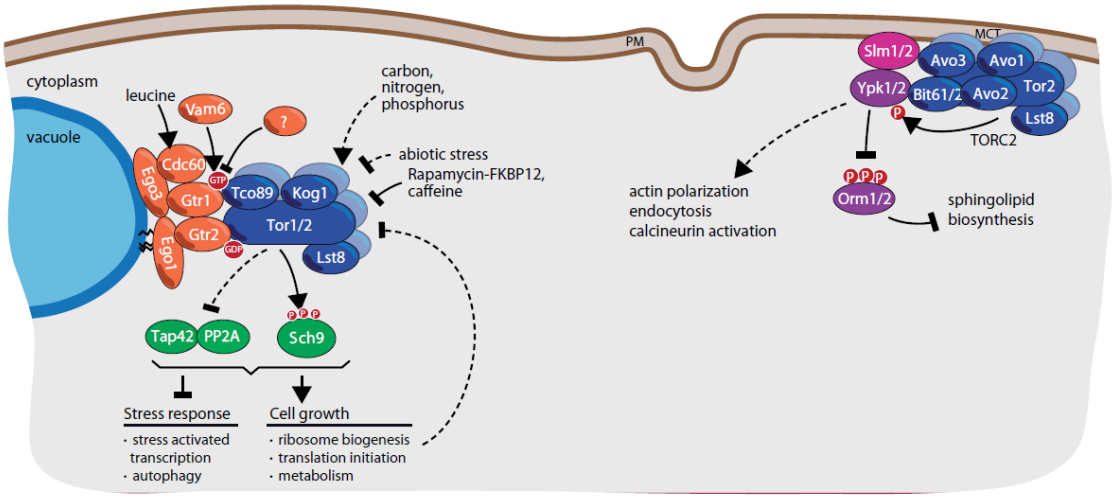

Figure 1. TORC1 and TORC2 signaling pathways in *Saccharomyces* cerevisiae

Although rapamycin still remains as the only specific inhibitor of TORC1 in budding yeast, many other compounds are known to strongly affect the activity of Tor kinases. Caffeine emerged as another TORC1 inhibitor although its specificity remains rather questionable as it also inhibits other PIKK family members in mammalian cells (Reinke et al, 2006; Sarkaria et al, 1999; Wanke et al, 2008). Wortmannin, a phosphatidylinositol kinase inhibitor, inhibits both TORC1 and TORC2 activities *in vitro* and *in vivo* in budding yeast (Chen et al, 2012; Liu et al, 2012). On the other hand, the translation elongation inhibitor cycloheximide hyperactivates both of the TOR complexes; presumably by elevating the intracellular amino acid concentration (Beugnet et al, 2003; Urban et al, 2007), (Loewith Lab, unpublished data). In mammalian cells, there are many commonly used Tor inhibitors including pp242 and Torin1 (Feldman et al, 2009; Thoreen et al, 2009). Characterization of these two inhibitors paved the way to the elucidation of rapamycin-resistant functions of TORC1 in mammalian cells. Inhibition of mTORC1 with either pp242 or Torin1 has a more profound effect on cap-dependent translation and autophagy compared to rapamycin. So far, evidence for rapamycin-resistant TORC1 activity is still lacking in yeast.

AGC Kinases as Effectors of TOR

In yeast as well as in higher eukaryotes, the best characterized substrates of Tor are members of the AGC family of kinases. The AGC kinases propagate the signal from Tor and regulate a wide range of targets in the cell. In human, there are 63 members of this family, whereas in budding yeast there are only 20 (Jacinto & Lorberg, 2008).The mammalian TORC1 (mTORC1) substrate, S6 kinase and the mammalian TORC2 (mTORC2) substrates Akt and Sgk1 are among the members of the AGC kinase family. Similarly, in yeast, the *bona fide* effectors of TOR complexes (Sch9, Ypk1 and Ypk2) belong to the same family. AGC kinases share common motifs which are important for their activity and regulation. One of these motifs is the highly conserved hydrophobic motif (HM) at the carboxyl-terminus. The HM motif is critical for the AGC kinase activity (Jacinto & Lorberg, 2008). The motif often bears a phosphorylatable Ser/Thr residue. In many cases, phosphorylation of the HM triggers the phosphorylation of another common motif, the turn motif (TM) prompting the full activation of the kinase (Jacinto & Lorberg, 2008). Tor targets the HM of its targets as well as the TM (Oh et al, 2010). Beside these motifs, Tor also phosphorylates Ser/Thr residues followed by proline at the C-terminal domain of its substrates (Brunn et al, 1997; Urban et al, 2007). Another important phosphorylation site on AGC kinases is located in the activation loop (T-loop) of the kinase domain. PDK1 in higher eukaryotes and Pkh1/2/3 kinases in yeast are responsible for the phosphorylation of this site. Mutations of the T-loop completely impair the enzymatic activity of the kinases, emphasizing the significant role of this site in the activity of the AGC kinases (Roelants et al, 2004). In turn, the AGC kinases recognize their substrates through a consensus recognition motif (RxRxxS/T or RxxS/T) (Pearce et al, 2010).

The TORC1 Signaling Pathway

TORC1 in *Saccharomyces cerevisiae* propagates its signal through two major effectors; Tap42 and Sch9. Tap42 is a regulator of Type 2A phosphatase (PP2A) and PP2A-related phosphatases such as Sit4. Association of Tap42 with these phosphatases is regulated by nutrients via TORC1 (Di Como &

Arndt, 1996; Jiang & Broach, 1999). Another component of this branch is the Tap42-interacting protein, Tip41. Tip41 is thought to interact with Tap42 leading to inhibition of the association between Tap42 and the phosphatases in a TORC1-dependent manner (Jacinto et al, 2001). Although major players of this branch are conserved in higher eukaryotes, the mode of regulation of the pathway seems to differ from that in yeast (Nakashima et al, 2013). TORC1 coordinates translation initiation, activity of nutrient permeases and stress-activated transcription via the Tap42-branch (Loewith, 2010).

Another major effector of TORC1 is Sch9, which is an AGC kinase family member (Urban et al, 2007). Via Sch9, TORC1 regulates translation initiation and transcription (Huber et al, 2009; Huber et al, 2011; Urban et al, 2007). TORC1-dependent inhibitory phosphorylation of Gcn2, a Ser-Thr kinase, leads to accumulation of the non-phosphorylated form of the alpha subunit of the translation initiation factor eIF2, subsequently promoting global translation initiation (Cherkasova & Hinnebusch, 2003; Urban et al, 2007). Both the Tap42 and Sch9 branches are involved in the regulation of translation initiation via Gcn2. However, the details of this regulation remain to be elucidated.

Considering its role in translation and its ability to phosphorylate ribosomal protein S6 *in vitro*, Sch9 was proposed to be the functional ortholog of S6 kinase in higher eukaryotes (Urban et al, 2007). Sch9 activity also has global effects not only on translation, but also on transcription through the regulation of all three RNA polymerases (Figure 2). Maf1 transmits the signal from Sch9 to RNA polymerase III, while Stb3, Dot6 and Tod6 in collaboration with the histone deacetylase complex RPD3L regulate ribosomal protein (RP) and ribosome biogenesis (Ribi) gene expression in response to TORC1-dependent Sch9 activity (Huber et al, 2009; Huber et al, 2011). In parallel to Sch9, a transcription factor, Sfp1, contributes to the regulation of RP and Ribi gene expression downstream of TORC1 (Lempiainen et al, 2009; Marion et al, 2004). Direct phosphorylation of Sfp1 by TORC1 prompts its nuclear translocation, where it enhances gene expression (Lempiainen et al, 2009). Moreover, Sch9 modulates entry into G1 arrest via phosphorylation of a PAS kinase Rim15 (Pedruzzi

et al, 2003). Following inactivation of TORC1, Rim15 becomes hypophosphorylated and accumulates in the nucleus where it phosphorylates targets required for proper entry into stationary phase.

Expression of a phosphomimetic allele of *SCH9* and the temperature-sensitive allele of *TAP42* (*tap42-11*) is sufficient to restore growth of cells lacking TORC1 function. This ability to bypass TORC1 supports the idea that these are the two major branches downstream of TORC1 (Huber et al, 2009). Yet, there are other elements engaged in TORC1-dependent regulation of cell growth. For instance, Kns1 and Mck1, highly conserved kinases from the LAMMER/Cdc-like and GSK3 families respectively, function downstream of TORC1 to regulate ribosome and transfer RNA (tRNA) synthesis under a variety of stress conditions (Lee et al, 2012; Roelants et al, 2004). Atg13 is another known substrate of TORC1. Direct phosphorylation of Atg13 by TORC1 hinders its association with the Atg1 kinase complex, thereby inhibiting the autophagy under normal conditions (Kamada et al, 2010).

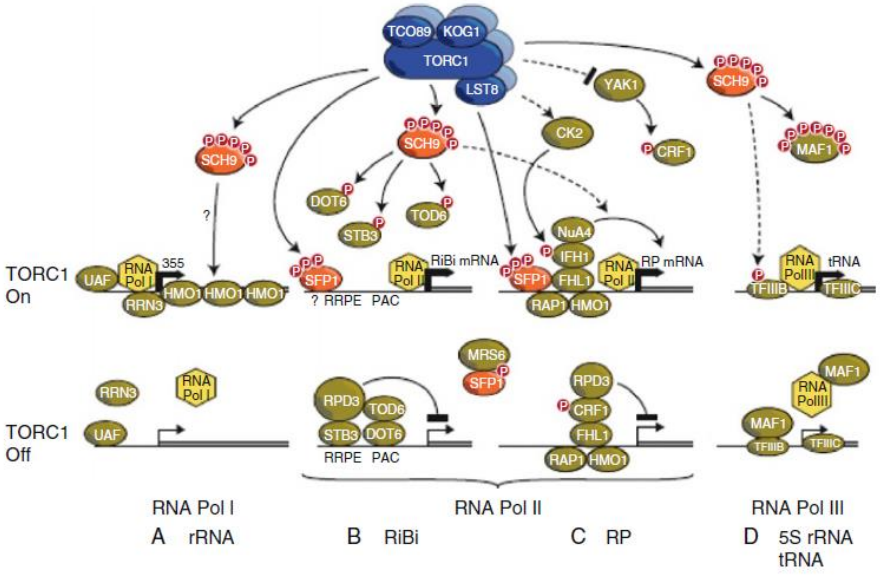

Figure 2. Regulation of transcription by TORC1 (Loewith, 2010)

The TORC2 Signaling Pathway

TORC2 is in charge of polarized cell growth, actin cytoskeleton organization, and ceramide and sphingolipid synthesis, mainly via the redundant AGC kinases, Ypk1 and Ypk2 (Aronova et al, 2008; Berchtold et al, 2012; Kamada et al, 2005; Niles et al, 2012). Expression of a hyperactive allele of

YPK2 (*YPK2*^{D239A}) rescues the lethality of inhibition of TORC2, suggesting that Ypk1/2 kinases are the major downstream elements of this pathway. Individual deletion of *YPK1* and *YPK2* is not lethal whereas the combinatorial deletion of these genes is inviable. Given that Ypk1 is more abundant than Ypk2, and ypk1 cells are much sicker than ypk2 cells, Ypk1 is thought to be the predominant kinase among these two.

Redundant proteins Slm1 and Slm2 were also shown to be phosphorylated in a TORC2-dependent manner, suggesting that Slm proteins function downstream of TORC2 (Audhya et al, 2004). Slm1 and Slm2 are phosphoinositide PI(4,5)P_2-binding proteins. Recently, Slm proteins were found to contribute to the regulation of TORC2 activity towards Ypk1/2 kinases in response to plasma membrane stress, eventually modulating the sphingolipid synthesis pathway (Berchtold et al, 2012).

Ypk1/2 is not only phosphorylated by TORC2, but also by Fpk1 and Fpk2 on its N-terminus (Roelants et al, 2010). Phospholipid flippase kinases Fpk1/2 are redundant kinases which phosphorylate phospholipid translocases called flippases (Nakano et al, 2008). Phosphorylation of Ypk1/2 by Fpk1/2 has an inhibitory effect on its enzymatic activity (Roelants et al, 2010). On the other hand, Fpk1/2 proteins are also phosphorylated and inhibited by Ypk1/2, indicating a negative feedback loop which regulates the activity of both sets of kinases.

Ypk1 was shown to interfere with eIF4G protein levels in yeast and thereby to inhibit translation initiation (Gelperin et al, 2002). The synthesis of sphingoid base was implicated in the regulation of translation initiation under heat stress conditions affecting the stability of eIF4G in a similar way to inactivation of Ypk1 (Meier et al, 2006). Considering the role of Ypks in sphingolipid synthesis, these findings point at a role for Ypk kinases, and possibly TORC2, in translation regulation. However, the mechanism so far remains obscure.

Phosphoproteomic Analysis of TOR Signaling Pathways

Analysis of rapamycin- and BHS-sensitive phosphoproteomes in combination with large-scale studies investigating the localization changes of GFP-tagged proteins in response to rapamycin treatment has extended our understanding of cellular processes regulated by TOR signaling pathway (Table 1) (Huber et al, 2009; Shin et al, 2009), (Loewith Lab, unpublished data).

Intriguingly, multiple factors which are involved in the main mRNA degradation pathway in yeast were found to be rapamycin-sensitive phosphoproteins such as Ccr4, Not3 and Pat1, thereby suggesting that TORC1 regulates mRNA degradation (Table 1). Moreover, many ribosomal proteins and translation initiation factors, including Rps6 which is a well-established target of mammalian TORC1 (Meyuhas, 2008), came out as TORC1- and TORC2-dependent phosphoproteins. Another interesting candidate identified is Shp1, which is a positive regulator of the catalytic subunit of Type 1 protein phosphatase Glc7 and an interacting partner of the AAA ATPase Cdc48.

Table 1. Factors whose phosphorylation/localization is affected by the inhibition of TOR complexes (Adapted from (Loewith, 2010))

Gene Name	Function of encoded protein	Localization (L) altered by Rapamycin Phosphorylation altered by rapamycin (R) / BHS (B) / Ypk1 inhibition (Y)
	Ribosome biogenesis factors, ribosomal proteins and translation factors	
FAP7	Small subunit synthesis	R
SRP40	Preribosome assmebly/transport	R
LHP1	Maturation of tRNA and U6 snRNA precursors	R
RRP14	Constituent of 66S preribosomal particles	R
RRN3	RNA Pol I initiation factor	R, L
NOP9	90S preribosome/ SSU processome	L
NHP2	rRNA processing	L
NSR1	rRNA processing	L
CBF5	90S preribosome/ SSU processome	L
UTP4	90S preribosome/ SSU processome	L
UTP5	90S preribosome/ SSU processome	L
UTP18	90S preribosome/ SSU processome	L
UTP22	90S preribosome/ SSU processome	L
UTP25	90S preribosome/ SSU processome	L
PWP2	90S preribosome/ SSU processome	L
BFR2	90S preribosome/ SSU processome	L
NOP58	90S preribosome/ SSU processome	L
NOP56	90S preribosome/ SSU processome	L
RRP5	90S preribosome/ SSU processome	L
RPC10	Subunit of RNA Pol I, II, III	L
RPA12	Subunit of RNA Pol I	L
RPA135	Subunit of RNA Pol I	L
RPA34	Subunit of RNA Pol I	L
RPA43	Subunit of RNA Pol I	L
RPA49	Subunit of RNA Pol I	L
RPA190	Subunit of RNA Pol I	L
MRT4	Large subunit synthesis	L
NOG1	Small subunit synthesis	L
NAF1	rRNA processing	L
SHQ1	rRNA processing	L
DED1	ATP-dependent DEAD-box RNA helicase	R, B, Y
RPL12B	Ribosomal 60S subunit protein	Y
RPL13A/B	Ribosomal 60S subunit protein	B
RPL24	Ribosomal 60S subunit protein	B
RPL26B	Ribosomal 60S subunit protein	B
RPL4A	Ribosomal 60S subunit protein	Y
RPS10A/B	Ribosomal 40S subunit protein	B
RPS12	Ribosomal 40S subunit protein	Y
RPS19A/B	Ribosomal 40S subunit protein	B, Y
RPS21A/B	Ribosomal 40S subunit protein	R, B
RPS21B	Ribosomal 40S subunit protein	Y
RPS28B	Ribosomal 40S subunit protein	Y
RPS6A/B	Ribosomal 40S subunit protein	R, B
SUI3	Beta subunit of the translation initiation factor eIF2	Y
TIF3	Translation initiation factor eIF4B	B
TIF4631	Translation initiation factor eIF4G	R, B
TIF4632	Translation initiation factor eIF4G	R, B, Y
FUN12	Translation initiation factor eIF5B	Y
TIF5	Translation initiation factor eIF5	R, B, Y
TEF2	Translational elongation factor EF-1 alpha	Y
	mRNA processing factors	
CWC2	Pre-mRNA splicing	L
PRP9	Pre-mRNA splicing	L
SNU66	SR protein kinase	R
SKY1	SR protein involved in mRNA transport	R
GBP2	SR protein involved in mRNA transport	R
HRB1	Deadenylation-dependent mRNA decay	R
PAT1	Deadenylation-dependent mRNA decay	R, B
CCR4	Deadenylation-dependent mRNA decay	R
NOT3	Deadenylation-dependent mRNA decay	R
MPP6	Degradation of cryptic noncoding mRNAs	R

Glc7 and Shp1

Glc7 is the essential catalytic subunit of the highly conserved Type 1 protein phosphatase (PP1) which regulates a wide range of processes in the cell including ion homeostasis, glycogen metabolism, septin organization and chromosome segregation (Bharucha et al, 2008; Francisco et al, 1994; Tan et al, 2003; Williams-Hart et al, 2002). Its function and substrate specificity are strictly regulated by various regulatory proteins. To date, 17 regulatory subunits of Glc7 have been characterized in budding yeast with Shp1 being one of these accessory proteins (Table 2).

Table 2. Regulatory subunits of protein phosphatase type-1 in *Saccharomyces cerevisiae* (Adapted from *Saccharomyces* Genome Database)

Gene Name	Function of encoded protein
REG1	Regulatory subunit of Glc7, involved in negative regulation of glucose-repressible genes
REG2	Regulatory subunit of the Glc7 ; involved with Reg1, Glc7, and Snf1 in regulation of glucose-repressible genes, also involved in glucose-induced proteolysis of maltose permease
PIG1	Putative targeting subunit for Glc7 that tethers it to the Gsy2 glycogen synthase
PIG2	Putative targeting subunit for Glc7 that tethers it to the Gsy2 glycogen synthase
GLC8	Regulatory subunit of Glc7, involved in glycogen metabolism and chromosome segregation
RED1	Protein component of the synaptonemal complex axial elements, involved in chromosome segregation during the first meiotic division
GAC1	Putative targeting subunit for Glc7 that tethers it to the Gsy2 glycogen synthase
GIP1	Meiosis-specific regulatory subunit of the Glc7 , regulates spore wall formation and septin organization, required for expression of some late meiotic genes and for normal localization of Glc7
GIP2	Putative regulatory subunit of Glc7, involved in glycogen metabolism
GIP3	Glc7-interacting protein whose overexpression relocalizes Glc7 from the nucleus and prevents chromosome segregation
SHP1	UBX (ubiquitin regulatory X) domain-containing protein that regulates Glc7 phosphatase activity and interacts with Cdc48; interacts with ubiquitylated proteins in vivo and is required for degradation of a ubiquitylated model substrate
BNI4	Targeting subunit for Glc7, localized to the bud neck, required for localization of chitin synthase III to the bud neck via interaction with the chitin synthase III regulatory subunit Skt5
SCD5	Protein required for normal actin organization and endocytosis; targeting subunit for Glc7; undergoes Crm1-dependent nuclear-cytoplasmic shuttling; multicopy suppressor of clathrin deficiency
SIP5	Protein of unknown function; interacts with both the Reg1/Glc7 phosphatase and the Snf1p kinase
BUD14	Protein involved in bud-site selection, Bud14-Glc7 complex is a cortical regulator of dynein; inhibitor of the actin assembly factor Bnr1 (formin)
SDS22	Conserved and essential nuclear regulatory subunit of Glc7, functions positively with Glc7 to promote dephosphorylation of nuclear substrates required for chromosome transmission during mitosis
YPI1	Essential inhibitor of Glc7; overproduction causes decreased cellular content of glycogen

Attempts to identify suppressors of the lethality due to *GLC7* overexpression paved the way to the characterization of Shp1 as a regulatory subunit of Glc7 (Zhang et al, 1995). Deletion of the *SHP1* gene resulted in lower activity of Glc7 *in vitro* suggesting that Shp1 is a positive regulator of Glc7. Shp1 contains three characteristic domains; the C-terminal ubiquitin regulatory X (UBX), a central SEP domain and the N-terminal ubiquitin-binding UBA domain (Schuberth & Buchberger, 2008). The UBX

domain mediates the interaction between Shp1 and Cdc48 ATPase, whereas the UBA domain is the ubiquitin-associated domain. Cdc48 is a member of the AAA (*A*TPases *A*ssociated with diverse cellular *A*ctivities) ATPase family (Lupas & Martin, 2002). Cdc48 functions by binding to its cofactors Ufd1-Npl4 and Shp1 in a mutually exclusive manner (Schuberth & Buchberger, 2008). Cdc48-Shp1 complex has so far been implicated in chromosome positioning, autophagosome biogenesis, protein degradation by the 26S proteasome and cell cycle progression (Bohm & Buchberger, 2013; Cheng & Chen, 2010; Krick et al; Schuberth et al, 2004). The role of Shp1 in these processes is mostly linked to its ability to regulate Glc7 (Bohm & Buchberger, 2013; Cheng & Chen, 2010). For instance, in the case of regulation of the spindle assembly checkpoint, the Shp1/Cdc48 complex is required for accumulation of Glc7 in nucleus (Cheng & Chen). Proper assembly of kinetochores during mitosis is assured by the activity of the Ipl1 kinase (the yeast homolog of Aurora B). The role of Glc7 in this process is to balance Ipl1 activity and to promote the bipolar attachment of chromosomes. Furthermore, mutations in *GLC7*, *SHP1* and the TORC1 component *TCO89* suppress the growth defect of a temperature sensitive allele of *IPL1*, thereby attributing a role to all these components in chromosome segregation and mitosis (Robinson et al, 2012). A recent study shows that the toxicity of *GLC7* overexpression can be partially rescued by several mutants of *SHP1* as well as its deletion (Bohm & Buchberger, 2013). More interestingly, the ability of Shp1 mutants to rescue the lethality due to *GLC7* overexpression correlates with its ability to interact with Cdc48, linking the Glc7- and Cdc48-dependent functions of Shp1. Yet, the details of the crosstalk between Cdc48/Shp1 and Glc7/Shp1 complexes still remain to be elucidated.

Strains deleted for *SHP1* share phenotypes with strains carrying a loss-of-function allele of *GLC7*. Both strains are deficient in glycogen accumulation and cell cycle progression (Zhang et al, 1995). Moreover, Glc7 and three of its regulatory subunits Reg1, Shp1 and Glc8 were shown to function in fructose-1,6-bisphosphatase (an enzyme involved in gluconeogenesis) trafficking and degradation in the vacuole upon glucose stimulation (Cui et al, 2004). Glc7 is highly responsive to glucose levels in a Shp1- and Reg1-dependent manner (Castermans et al, 2012). Accordingly, absence of Shp1 activity

abolished the glucose-induced activity of Glc7. In addition, deletion of the *SHP1* gene resulted in high levels of *SUC2* expression compared to wild type cells. Suc2 is an invertase enzyme which is responsible for the catalysis of di-/tri-saccharides. Several attempts to elucidate how Shp1 regulates Glc7 activity suggested that Shp1 promotes nuclear accumulation of Glc7 (Cheng & Chen, 2010; Hu et al, 2012). However, the effect of Shp1 activity on Glc7 localization is blurred by conflicting results (Bohm & Buchberger, 2013; Zhang et al, 1995). As an alternative model, Shp1 was recently shown to inhibit the interaction between Glc7 and Glc8, another regulatory subunit of Glc7 (Bohm & Buchberger, 2013).

Shp1, itself, and its function as an accessory protein of Cdc48 is conserved in higher eukaryotes. In fact, p47, the mammalian homolog of Shp1 is one of the first characterized binding partners of p97/VCP, the mammalian Cdc48 homolog (Kondo et al, 1997). One of the first cellular roles attributed to p97 was the regulation of disassembly and reassembly of Golgi stacks during mitosis, and later p47 was found to regulate the ATPase activity of p97/VCP during this process (Meyer et al, 1998; Rabouille et al, 1995). Later on, the role of p47/p97 in the regulation of membrane fusion was extended to other organelles like the endoplasmic reticulum (ER) (Uchiyama et al, 2002). Similarly, Cdc48 is involved in the self-fusion of ER membranes in budding yeast (Latterich et al, 1995). In addition, phosphorylation of p47 by Cdc2 kinase on Ser140 in a cell cycle-dependent manner is crucial for its role in Golgi membrane fusion (Uchiyama et al, 2003). During interphase, p47 has a nuclear localization but retains a small cytoplasmic population (Uchiyama et al, 2003). The role of Shp1 in the proteasomal degradation pathway is also conserved in mammalian cells. Recently, p47 was shown to inhibit the IκB kinase complex by binding to a polyubiquitinated subunit of the complex and targeting the subunit for lysosomal degradation (Shibata et al, 2012).

Regulation of mRNA Fate by TOR Signaling

Gene expression levels are determined by the balance between transcription, translation, mRNA and protein decay rates. Messenger RNAs (mRNAs) are the critical players of this multi-step process

which carry the genetic information from DNA to protein. Once transcribed, an mRNA can be translated, stored in processing bodies (P-bodies) and stress granules, or degraded (Figure 3). Extrinsic elements, such as mRNP complexes, as well as intrinsic elements, such as the 5'-N7-methyl guanosine cap and the 3'-poly(A) tail, are the major determinants of which path an mRNA will follow. The 5'-cap promotes translation of the mRNA while protecting the mRNA from 5'-to-3' degradation, whereas shortening of the poly(A) tail marks the mRNA for degradation.

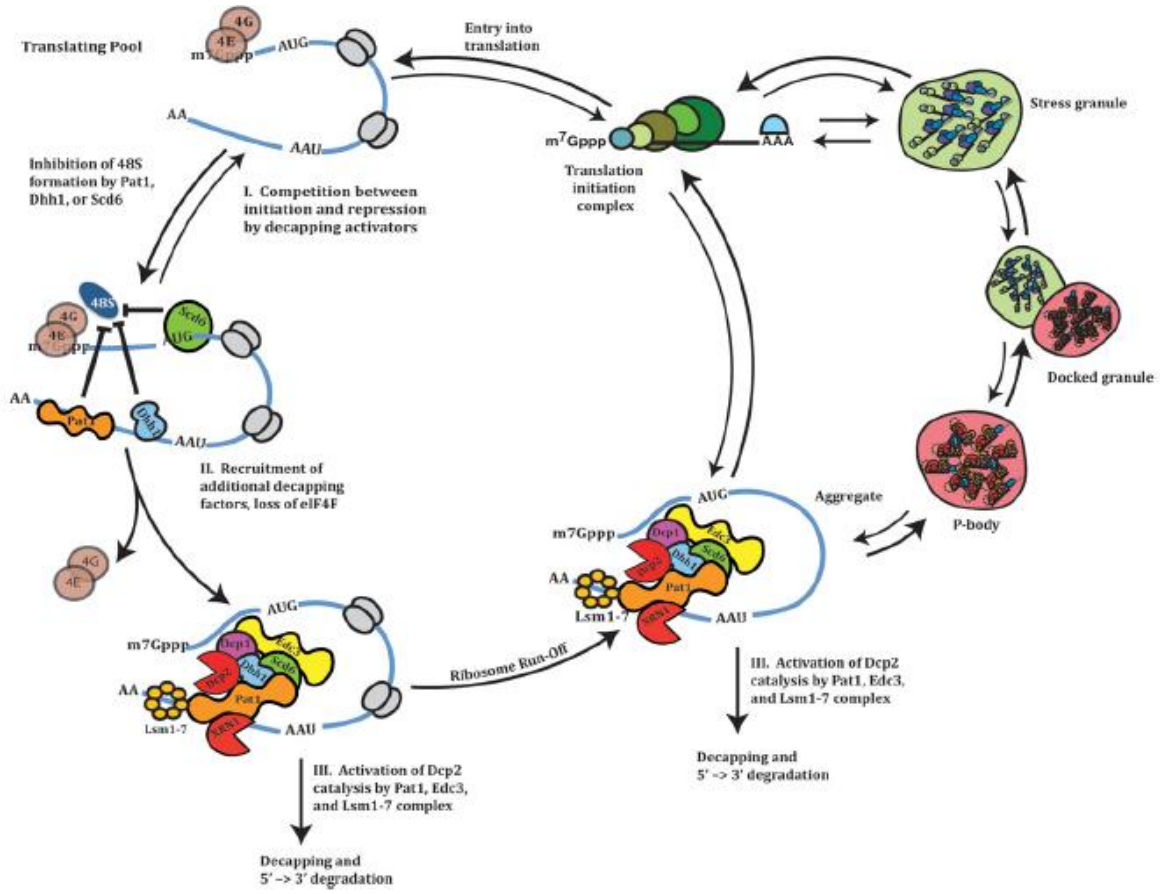

Figure 3. mRNA cycle in budding yeast (Parker, 2012)

Translation

Ribosomes are large ribonucleoprotein (RNP) complexes composed of two main subunits: 40s and 60S in eukaryotes. The large subunit (60S) of a yeast ribosome is composed of 25S, 5.8S and 5S ribosomal RNAs (rRNA) and 46 ribosomal proteins, whereas the small subunit is composed of 18S rRNA in complex with 33 ribosomal proteins. Ribosome biogenesis begins in the nucleolus and

continues in the cytoplasm. Each subunit is synthesized and transported into the cytoplasm separately. Every single step of ribosome maturation is under tight control of numerous trans-acting factors. Once maturation of the ribosome is completed in the cytoplasm, the ribosomes are ready to be employed for translation.

Translation is a complex process that requires the concerted activity of numerous factors. Formation of a ternary complex composed of eIF2, GTP and the initiator methionyl-tRNA (Met-tRNA$_i$) is the initial step of translation initiation. Next, the ternary complex associates with eIF1, eIF1A, eIF3, eIF5 and a 40S ribosomal subunit to form a pre-initiation complex (PIC). Target mRNA marked by binding of the eIF4F complex (composed of the RNA helicase eIF4A, the cap-binding protein eIF4E and eIF4G), eIF4B, eIF3 and the poly(A)-binding protein (PABP) is recruited to the PIC. The PIC scans the 5' untranslated region of the mRNA until recognition of a start codon. Start codon recognition leads to dissociation of eIF1 and conversion of eIF2·GTP to eIF2·GDP by eIF5 activity and the scanning stops. Dissociation of eIF2·GDP and eIF5 is followed by recruitment of the 60S large ribosomal subunit to the mRNA by eIF5B GTPase resulting in formation of the 80S initiation complex. GTP hydrolysis by eIF5B occurs, eIF1A and eIF5B dissociate from the complex and translation elongation starts. Translation elongation requires three factors: eEF1A, eEF2, and eIF5A. Binding of aminoacyl-tRNA to the A-site of the ribosome and translocation of the peptidyl-tRNA from the A-site to the P-site are mediated by eEF1A and eEF2, respectively. eIF5A has a rather specific role in translation elongation: it promotes the translation of proline repeats (Doerfel et al, 2013; Gutierrez et al, 2013; Ude et al, 2013). eRF1 and eRF3 are factors required for the termination step of translation.

As mentioned before, TORC1 regulates translation initiation mainly via the control of Gcn2 activity. Accordingly, rapamycin treatment results in a rapid inhibition of translation initiation as reflected by an increase in the 80S monosome-to-polysomes ratio (Urban et al, 2007). In mammalian cells, TORC1 directly phosphorylates two translational components: S6 kinases (S6K1 and S6K2) and 4E-BP1 (Ma & Blenis, 2009). S6 kinases were identified as kinases responsible for the phosphorylation of ribosomal

protein S6 (Rps6), a small ribosomal subunit component (Erikson & Maller, 1985). 4E-BP1 is an inhibitor of eukaryotic initiation factor 4E. 4E-BP1 and eIF4G competitively bind eIF4E. Phosphorylation of 4E-BP1 by mTORC1 inhibits its association with eIF4E, promoting translation initiation. In the absence of mTORC1 activity, hypophosphorylated 4E-BP1 has higher affinity for eIF4E, leading to diminished interaction between eIF4E and eIF4G and thereby to decreased translation initiation.

Interestingly, recent studies showed that mTORC2 associates with ribosomes to cotranslationally phosphorylate some of its targets such as Akt and an RNA-binding protein IMP1 (Dai et al, 2013; Oh et al, 2010). In addition, association of mTORC2 with ribosomes was found to promote mTORC2 activity (Zinzalla et al, 2011).

Ribosomal Protein S6 Phosphorylation

Phosphorylation of Rps6 is a highly conserved event from yeast to mammalian cells. In higher eukaryotes, there are five phosphorylation sites on its C-terminal end, while only two of these sites (Ser232 and Ser233) corresponding to Ser235 and Ser236 in higher eukaryotes are conserved in yeast (Figure 4). Rps6 is one of the first ribosomal proteins to be found to undergo phosphorylation (Gressner & Wool, 1974; Kabat, 1970). Following its discovery, Rps6 phosphorylation was shown to be highly sensitive to nutrients, hormones, growth factors and a variety of stress conditions (Meyuhas, 2008). S6 kinases, S6K1 and S6K2 are the major kinases phosphorylating Rps6 in an mTORC1-dependent manner on several sites (S235/S236/S240/S244) (Pende et al, 2004). Yet, RSKs (90kDa ribosomal protein S6 kinases) also play a role in MAP kinase pathway-dependent phosphorylation of Rps6 specifically targeting the S235/S236 residues (Roux et al, 2007). Recently, members of casein kinase I kinase family were found to phosphorylate Rps6 on Ser247 in response to mitogenic stimuli (Hutchinson et al, 2011). Intriguingly, not only TORC1, but also TORC2 is involved in Rps6 phosphorylation in fission yeast (Du et al, 2012). Current data suggest that Rps6 phosphorylation in fission yeast is dependent on Psk1 (the ortholog of Ypk3 in budding yeast) and

Gad8 (the ortholog of Ypk1/2 in budding yeast) (Du et al, 2012; Nakashima et al, 2012). On the other hand, the type 1 protein phosphatase (PP1) appears to antagonize Rps6 phosphorylation in mammals (Belandia et al, 1994; Hutchinson et al, 2011).

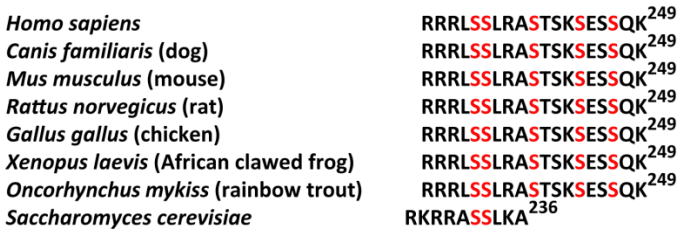

Figure 4. Rps6 phosphorylation from budding yeast to mammals (Meyuhas, 2008)

Multiple reports indicate that the phosphorylation of Rps6 on multiple sites in higher eukaryotes takes place in an ordered fashion (Flotow & Thomas, 1992; Martin-Perez & Thomas, 1983; Radimerski et al, 2000; Wettenhall et al, 1992). Ser236 is the first site to be phosphorylated and this phosphorylation event is followed by phosphorylation of Ser235, Ser240, Ser244 and Ser247 sequentially (Martin-Perez & Thomas, 1983; Wettenhall et al, 1992). Accordingly, phosphorylation of Ser247 requires residues Ser240/244 to be phosphorylated (Hutchinson et al, 2011). More interestingly, mutation of Ser247 partially abolishes the phosphorylation of Ser240/244, pointing at a crosstalk between these sites.

After years of research, the physiological role of Rps6 phosphorylation still remains mysterious. Rps6 knock-in mice carrying the alanine-substituted non-phosphorylatable version of Rps6 exhibited severe phenotypes like reduced size, glucose intolerance and muscle weakness (Ruvinsky et al, 2005). Conflicting results on the role of Rps6 phosphorylation in global protein synthesis prompted the idea that rather than being a general regulator of translation, Rps6 phosphorylation could be regulating the translation of a subset of mRNAs. Accordingly, Rps6 phosphorylation was proposed to promote the translation of mRNAs with 5'-terminal oligopyrimidine tracts, so called TOP mRNAs (Fumagalli, 2000). TOP mRNAs often encode ribosomal proteins and elongation factors (Iadevaia et al, 2008; Levy et al, 1991). However, following studies weakened the role of Rps6 phosphorylation in TOP

mRNA translation while further supporting the contribution of mTORC1 in this process: analyses of the mRNAs interacting with actively translating ribosomes following inhibition of mTORC1 revealed that TOP mRNAs are major targets of translation regulation by mTORC1 (Hsieh et al, 2012; Tang et al, 2001; Thoreen et al, 2012). On the other hand, cells isolated from knock-in mice expressing non-phosphorylatable Rps6 displayed no observable defect in TOP mRNA translation (Ruvinsky et al, 2005; Tang et al, 2001). Considering the lack of TOP mRNAs in yeast, it seems plausible to claim that phosphorylation of Rps6 has other functional roles in the cell.

Earlier studies in yeast suggested that Rps6 phosphorylation had no observable effect on the growth of cells under different conditions (Johnson & Warner, 1987; Tang et al, 2001). However, mammalian studies showed that cells from S6K-double knockout mice and Rps6 knock-in mice had a significantly reduced size compared to wild type cells, suggesting a role for Rps6 phosphorylation in cell growth (Ohanna et al, 2005; Pende et al, 2004; Ruvinsky et al, 2005). Recently, S6 kinases and Rps6 phosphorylation were shown to regulate the synthesis of ribosome biogenesis factors during feeding following starvation (Chauvin et al, 2013).

Biochemical crosslinking assays proposed that Rps6 lies on the surface of the 40S subunit at the interface between the 40S and 60S subunits and in close proximity to the decoding center (Metspalu et al, 1978; Nygard & Nika, 1982; Takahashi & Ogata, 1981). However, recent structural studies confuted these ideas and showed that Rps6 is located far away from the decoding center. In fact, one of the most recently reported structures of eukaryotic ribosomes suggested that Rps6 is located in the close vicinity to the binding site for eIF4G (Ben-Shem et al, 2011). In addition, the C-terminal domain of Rpl24 and Rps6 strongly interact according to this structure. Translation of polycistronic mRNAs require efficient reinitiation, which depends upon the retention of eIF3 on actively scanning 40S, and the C-terminal domain of Rpl24 is crucial for the retention of eIF3 (Zhou et al, 2010). Taking all these findings together, it seems feasible to suggest that Rps6 phosphorylation may play a role in the recruitment of regulatory factors involved in initiation/re-initiation events as suggested in the

paper despite the fact that the last 10 amino acids of Rps6 where the phosphorylation sites are located in were missing in that structure (Ben-Shem et al, 2011).

S6 Kinases

In mammals, there are two S6K genes: *S6K1* and *S6K2*. Both S6K1 and S6K2 have multiple isoforms with kinase activities (p31/p70/p85 and p54/p56, respectively). Just like other AGC kinases, S6 kinases bear functionally important domains: an acidic N-terminal domain, the kinase domain, a linker domain and a basic C-terminal domain (Magnuson et al, 2012). The N-terminus of S6 kinases contains a TOR signaling motif, called a TOS motif, with the sequence of FDIDL. This TOS motif is also shared by another target of mTORC1, 4E-BP1 (Schalm & Blenis, 2002). The TOS motif is thought to be important for the interaction with Raptor, an mTORC1 component and Kog1 homolog. Mutation of this motif impairs S6K activity. Other critical motifs in relation to S6 kinase activity are the HM and the TM which lie in the linker region between the kinase domain and the C-terminal domain of the protein. Phosphorylation of the HM (Thr389 on S6K1 and Thr 388 on S6K2) by mTORC1 promotes kinase activity. A phosphorylatable TM (Ser371 on S6K1 and Ser370 on S6K2) is also crucial for S6 kinase activity. However, the role of mTORC1 in this phosphorylation event remains rather confusing. Although some reports showed that rapamycin affected the levels of phosphorylation of this site, the correlation between phosphorylation of the TM and mTORC1 activity remained rather weak compared to that of the HM and mTORC1 activity (Ferrari et al, 1993; Saitoh et al, 2002). S6 kinases are also phosphorylated on the T-loop as well as on multiple proline-directed sites on their C-terminal end. Ordered phosphorylation of all these sites contribute to the full activation of S6 kinases.

Subcellular localization of S6 kinases has so far remained controversial. Both S6 kinases are thought to contain a nuclear localization signal (NLS) suggesting that these proteins shuttle between the nucleus and the cytoplasm (Magnuson et al, 2012). In accordance with this idea, p70 isoform of S6K1 was recently shown to localize both to nucleus and to cytoplasm. More interestingly, inhibition of

mTORC1 activity triggered the cytoplasmic accumulation of p70 (Rosner & Hengstschlager, 2011; Rosner et al, 2012). On the other hand, the p85 isoform was found to be predominantly cytoplasmic, while p31 was nuclear without refuting the possibility that they also shuttle between the cellular compartments under different conditions (Rosner & Hengstschlager, 2011).

Beside its well-established target Rps6, S6 kinases have a wide range of translation-related substrates such as eIF4B and eEF2 kinase. Phosphorylation of eIF4B by S6K1 enhances its interaction with eIF4A and eIF3 (Raught et al, 2004). In addition, S6K1 triggers the degradation of an eIF4A inhibitor, PDCD4 through phosphorylation, thereby promoting translation initiation (Dorrello et al, 2006). S6 kinases are not only involved in the regulation of initiation but also in the elongation step. S6K1 fosters elongation via phosphorylating and inactivating eEF2 kinase, which inhibits eEF2 activity by phosphorylation (Wang et al, 2001).

S6 kinases contribute to translation regulation partly, via regulation of ribosome biogenesis. S6K1 stimulates the rRNA transcriptional program in response to growth factors via phosphorylation of the rDNA transcription factor UBF (Hannan et al, 2003). Moreover, S6K1 is able to promote RNA polymerase I-dependent transcription *in vitro* (Mayer et al, 2004). Lastly, in a recent study, S6Ks were clearly shown to be indispensable for the proper transcription of about 75% of genes encoding ribosome biogenesis factors after feeding (Chauvin et al, 2013).

Mammalian TORC1-regulated S6K activity has been linked to numerous cellular processes besides translation and ribosome biogenesis. For instance, they contribute to DNA damage response by modulating Mdm2 activity downstream of nutrient availability (Lai et al, 2010). Moreover, S6Ks promote cell survival via phosphorylation and inhibition of pro-apoptotic proteins (Harada et al, 2001).

The RSK (90 kDa ribosomal protein S6 kinase) Family of Protein Kinases

The kinases responsible for the RAS/MAPK-dependent phosphorylation of Rps6 are the RSKs. Mammalian cells carry four isoforms: RSK1-4. S6K-double knockout cells still display residual

phosphorylation on Ser235 and Ser236 (Pende et al, 2004). Later, RSKs were found to be the kinases which phosphorylate these sites *in vitro* and *in vivo* (Roux et al, 2007). Interestingly, RSKs contain two separate kinase domains, one at the C-terminus and the other at the N-terminus of the protein. The N-terminal kinase domain resembles the AGC kinase domain, whereas the C-terminal kinase domain is similar to the CAMK (Ca^{2+}/ calmodulin-dependent protein kinase) family kinase domain. The N-terminal kinase domain appears to be the major functional kinase domain as it is required for the phosphorylation of all known substrates of RSKs (Romeo et al, 2012). All four isoforms of RSKs are primarily cytoplasmic just like S6 kinases. However, RSK1-3 are able to shuttle between the cytoplasm and nucleus in a stimuli-dependent manner (Chen et al, 1992; Zhao et al, 1995). RSK4 is the only isoform which does not translocate into the nucleus but rather remains cytoplasmic even upon mitogenic stimulation (Dummler et al, 2005). RSKs regulate various cellular processes such as transcriptional regulation, cell cycle progression, cell growth and survival by targeting a wide range of substrates (Romeo et al, 2012). The role of RSKs in translational regulation is partly due to phosphorylation of Rps6. RSK-dependent phosphorylation of Rps6 was implicated in cap-dependent translation (Roux et al, 2007). Accordingly, the recruitment of ribosomes to the 5'-cap complex is boosted by the phosphorylation of Rps6 on Ser235/236 by RSKs.

Ypk3

In budding yeast, Rps6 phosphorylation is conserved. However, the pathways signaling to Rps6 are still not elucidated. As mentioned earlier, Sch9 was proposed to be the S6K in yeast based on its ability to phosphorylate Rps6 *in vitro* (Urban et al, 2007). Nonetheless, *in vivo* evidence is still missing. In the meantime, phylogenetic analyses of TOR signaling pathway recently suggested that Ypk3 is the S6 kinase ortholog in *Saccharomyces cerevisiae* (van Dam et al). Besides, Psk1, the Ypk3 ortholog in fission yeast, was recently shown to phosphorylate Rps6 in a rapamycin-sensitive manner (Nakashima et al, 2012). Ypk3 is a poorly characterized member of the AGC kinase family in budding yeast. The understanding of how Ypk3 is regulated remains limited. High-throughput studies supported by *in vitro* experiments revealed that Ypk3, itself, is a phosphoprotein which is targeted by

PKA (cAMP-dependent protein kinase A) (Budovskaya et al, 2005; Ptacek et al, 2005). Furthermore, it was shown that phosphorylation of Ypk3 by PKA was dependent on TORC1 *in vivo* (Soulard et al). The kinase domains and C-terminal domains of AGC kinases are highly conserved. Accordingly, there is 42% homology between the kinase domains of Ypk1/2 and Ypk3, and 20% homology between their C-terminal domains. On the other hand, the N-terminal domains of Ypk3 and Ypk1/2 are rather divergent. Similarly, the kinase domains of Ypk3 and Sch9 share a 37% homology, while their C-terminal domains have a 24% homology.

Regulation of Translation Efficiency

Wobble Decoding

The universal genetic code is composed of 61 codons encoding for 20 amino acids and 3 termination codons, suggesting that some of the tRNAs recognize more than one codon. This is achieved by a so-called wobble interaction of the first base of the anti-codon with multiple bases at the third position of the codon (Crick, 1966). tRNAs are post-transcriptionally modified at the wobble position by the Elongator complex to enable this interaction. In yeast, the Elongator complex consists of six major components, Elp1-6 in addition to other accessory components (Versees et al, 2010). Wobble decoding influences translation efficiency and fidelity as the repeats of the codons which require a wobble interaction on the third base can be “strongly inhibitory” to translation (Letzring et al, 2010). Moreover, it was recently shown that proper tRNA modifications and the wobble interactions at the codon-anticodon pairs were crucial for translational reprogramming and for survival under stress conditions (Fernandez-Vazquez et al, 2013).

Tandem Amino Acid Repeats

Another determinant of the translation efficiency is the amino acid repeats. Tandem amino acid repeats are common among eukaryotic proteins and enriched in transcription factors, DNA-binding proteins and signaling proteins (Alba & Guigo, 2004; Green & Wang, 1994; Mar Alba et al, 1999). The length of the repeats was proposed to affected translation efficiency (Feng et al, 1995; Usdin, 2008).

Moreover, in a recent study, Thomas Dever and his colleagues investigated how repeats of each amino acid affect the translation efficiency and showed that the repeats of arginine, cysteine and histidine impair translation, whereas glutamine and phenylalanine repeats enhances the translation rates (Gutierrez et al, 2013). The same study also revealed that the efficient translation of proline repeat motifs required a specific elongation factor, eIF5A. The role of eIF5a in translation elongation appeared to be conserved in prokaryotes (Doerfel et al, 2013; Ude et al, 2013). In accordance, a recent study which analyzed a previous ribosome profiling dataset to identify what stalls ribosomes during translation concluded that repeats of positively charged residues (Arg, His and Lys) are the major players influencing the rate of translation (Charneski & Hurst, 2013).

Reinitiation

About 50% of mammalian mRNAs, 30% of plant mRNAs and 13% of yeast mRNAs contain at least one short upstream open reading frame (uORF) on their N-terminal ends (Jackson et al, 2010; Zhou et al, 2010). Efficiency of translation of the downstream ORFs is very low in eukaryotes under normal conditions. However, the presence of short uORFs can be a means of regulation of translation of a downstream ORF under different conditions. To translate the downstream ORF, ribosomes initiate translation normally; however, the 40S subunit remains associated with the mRNA even after termination and continues scanning to resume translation on the following start codon. Availability of the ternary complex and the distance between the open reading frames are the main parameters affecting the efficiency of reinitiation. One well-studied example of reinitiation is the translation of *GCN4* mRNA in yeast. Gcn4 is a transcription factor which is required for the transcription of amino acid biosynthetic genes upon amino acid starvation. The *GCN4* mRNA contains four short upstream ORFs in its 5'-region. The first two uORFs are permissive for reinitiation, whereas the last two are inhibitory. Therefore, under normal conditions, the *GCN4* ORF is not translated. In response to amino acid starvation, the increase in eIF2α phosphorylation leads to lower ternary complex concentration. Thus, the 40S subunit scans through the inhibitory uORFs and initiates translation on *GCN4* ORF. Gcn2 is the primary regulator of eIF2α activity and thereby ternary complex availability in yeast. eIF3,

eIF4A and eIF4G have so far been characterized as the factors which permit efficient reinitiation (Poyry et al, 2004; Szamecz et al, 2008).

Ribosomal Frameshifting

Proper maintenance of the reading frame during protein synthesis is crucial for the fidelity of translation of genetic information into proteins. However, under special conditions, active ribosomes can be driven to shift by one base in 5' (+1) or 3' (-1) direction in response to specific cis-acting sequences on mRNA, a process called programmed ribosomal frameshifting (PRF) (Dinman, 2012). PRF is widely used by a variety of viruses as a mechanism to fine-tune the synthesis of multiple viral proteins. Recent studies suggest that PRF is also employed in regulation of gene expression in eukaryotes. Genome-wide analysis of putative PRF signals in yeast indicated that cellular PRF-inducing signals frequently direct the ribosomes to a premature termination codon targeting the mRNAs for degradation via non-sense mediated mRNA decay or no-go decay pathways (Belew et al, 2011; Jacobs et al, 2007). The translation elongation inhibitor anisomycin, which occupies the A-site, inhibits -1 PRF, whereas another inhibitor sparsomycin promotes it (Dinman et al, 1997).

mRNA Degradation

The major mRNA decay pathway in yeast begins with deadenylation of mRNAs, which is carried out by the Ccr4-Not complex. The Ccr4-Not complex is considered as the main deadenylase complex in yeast (Daugeron et al, 2001; Tucker et al, 2001). Ccr4 and Pop2 are the two nuclease components of the complex with Ccr4 being the predominant one (Chen et al, 2002; Tucker et al, 2002). The other deadenylase complex in yeast is the Pan2/Pan3 complex, which is mostly involved in the proper adjustment of the length of poly(A) tails of newly synthesized mRNAs (Brown & Sachs, 1998). Deadenylation was proposed to be the rate-limiting step of this pathway (He & Parker, 1999), thereby suggesting that regulation of mRNA deadenylation can be an important means of regulating mRNA degradation. The deadenylation step is followed either by 3'→5' decay by the exosome or by the decapping step. Decapping is mediated by the decapping enzymes Dcp1 and Dcp2 with the help

of several accessory proteins such as Sm-like (Lsm) proteins, Edc proteins, the DExD/H-box RNA helicase Dhh1 and Pat1 (Mrt1) (LaGrandeur & Parker, 1998; Parker & Song, 2004). Subsequently, deadenylated and decapped mRNAs are degraded by the 5'→3' exonuclease Xrn1 (Figure 5).

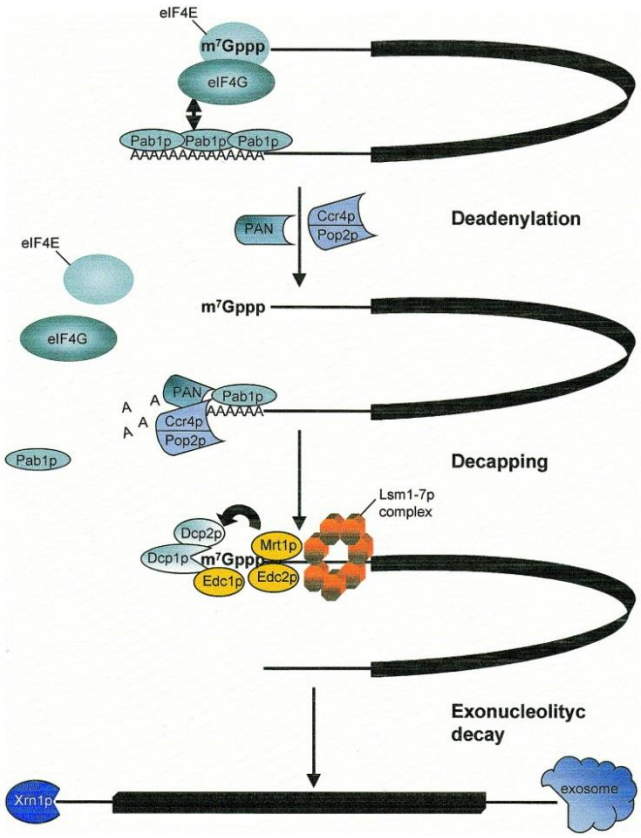

Figure 5. The major mRNA degradation pathway in budding yeast (Tourriere et al, 2002)

Like many other cellular processes, the mRNA decay pathway is also responsive to changes in the extracellular environment. As an example, mRNA decay rates change depending on the availability of glucose in yeast (Jona et al, 2000). More specifically, the stability of yeast ribosomal protein mRNAs is affected by both mild heat shock and glucose (Herruer et al, 1988; Yin et al, 2003). Exposure of the cells to stress conditions such as heat shock or hyperosmolarity inhibits mRNA degradation in mammalian cells as well (Gowrishankar et al, 2006).

The Ccr4-Not Complex

The Ccr4-Not complex is a conserved, essential, multi-functional complex, which is composed of nine core proteins (Not1, Not2, Not3, Not4, Not5, Ccr4, Pop2, Caf40 and Caf130) in yeast (Figure 6) (Chen

et al, 2001; Collart & Panasenko, 2012; Liu et al, 1998). Not1 is the scaffold protein of the complex (Maillet et al, 2000). Despite the fact that all these proteins are found in the same complex, different subunits play diverse roles in the regulation of gene expression. The first role attributed to the complex was in transcription. Whole genome microarray analysis indicated that deletion of *CCR4*, *POP2*, *NOT3*, *NOT4*, *NOT5*, *CAF40* or *CAF130* had a global effect on mRNA expression (Cui et al, 2008). In fact, Ccr4 was first identified as a transcription factor involved in the expression of the glucose-repressible alcohol dehydrogenase II (ADHII) (Denis, 1984). Similarly, Not proteins were initially defined as transcriptional repressors (Collart & Struhl, 1994; Oberholzer & Collart, 1998). More recently, the Ccr4-Not complex was linked to the promotion of transcription elongation (Kruk et al, 2011). However, although the first impression created by all these findings was that the complex was a global transcription regulator, versatile roles have been ascribed to the individual proteins found in the complex during the following years. For instance, Ccr4 and Pop2 were found to be "the major cytoplasmic mRNA deadenylases" in budding yeast (Tucker et al, 2001). The roles of Ccr4 and Pop2 are also conserved in higher eukaryotes (Bianchin et al, 2005; Yamashita et al, 2005). Ccr4 and Pop2 turned out to be members of the ExoIII family and the RNaseD family of nucleases, respectively (Daugeron et al, 2001; Dlakic, 2000). However, rather than being an active nuclease in the cell, Pop2 mostly functions as the link between Ccr4 and the rest of the complex (Tucker et al, 2002). Deletion of the *CCR4* gene produces a variety of phenotypes such as a strong defect in deadenylation, an increase in cell size, hypersensitivity to rapamycin, caffeine, SDS, and high/low temperatures (Coller et al, 2001; Huber et al, 2009; Manukyan et al, 2008). Deletion of *POP2* results in similar phenotypes such as temperature-sensitive growth, caffeine sensitivity and extended survival in stationary phase (Moriya et al, 2001). Beside its role in global deadenylation, Ccr4 plays various roles in specific processes in the cell by regulating deadenylation rates of specific mRNAs. For instance, a genome-wide analysis of mRNA decay rates revealed that although Ccr4 is a global regulator of mRNA stability, it shows some preference towards the mRNAs encoding ribosome biogenesis factors (Grigull et al, 2004). Moreover, Ccr4 was shown to contribute to septin

organization presumably via regulating the length of poly(A) tails of mRNAs encoding proteins involved in septin assembly (Traven et al, 2009). In accordance with this role, cells deleted for the *CCR4* gene exhibit defects in septin morphology in a Cdc28-inhibitory kinase Swe1-dependent manner. Ccr4 also modulates the half-life of *Whi5* mRNA, which encodes for a repressor of G1 transcription, thereby affecting cell size-dependent cell cycle progression (Manukyan et al, 2008).

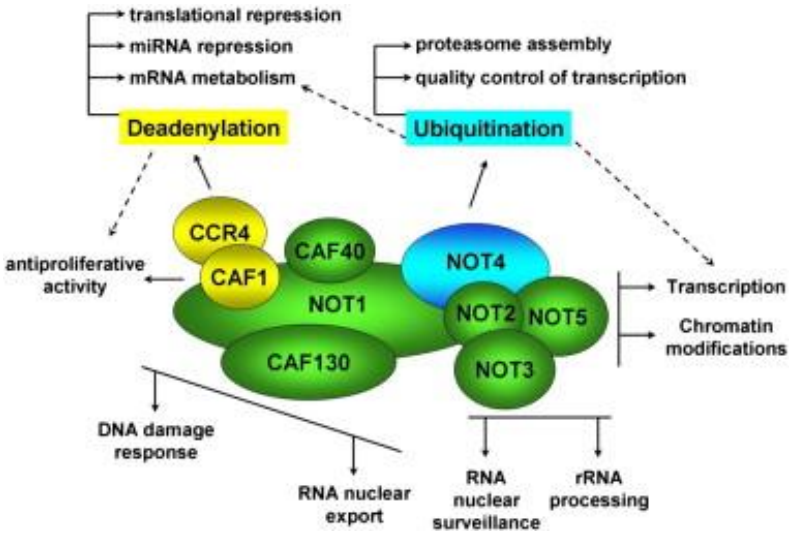

Figure 6. Composition of Ccr4-Not complex in *Saccharomyces cerevisiae* (Collart & Panasenko, 2012)

The question of how specific mRNAs are targeted by Ccr4 leads us to the RNA-binding proteins. One of the RNA-binding protein families whose members are known to recruit the Ccr4-Not complex to mRNAs is the evolutionary conserved Pumilio (PUF) family. In budding yeast, there are six members of this family. PUF proteins bind to the 3'-untranslated region of mRNAs so as to regulate their stability (Wickens et al, 2002). More specifically, Puf2, Puf4 and Puf5 recruit the Ccr4-Not complex through their direct interaction with Pop2 (Goldstrohm et al, 2006; Goldstrohm et al, 2007; Hook et al, 2007).

Pop2 was shown to be engaged in cell cycle progression. Under conditions where cells were starved for glucose, Pop2 was found to be phosphorylated on residue Thr 97 by Yak1 promoting G1 arrest (Manukyan et al, 2008). In the absence of glucose, Yak1 is localized in the nucleus suggesting that phosphorylation of Pop2 under this condition takes place in nucleus. In mammalian cells, the human

homolog of Pop2, hCAF1 was found to shuttle between the cytoplasm and the nucleus in a cell cycle-dependent manner (Morel et al, 2003). Altogether, these findings suggest that regulation of Pop2 localization might be a means of regulating its activity. There is no evidence to imply that Ccr4 also shuttles between the cytoplasm and the nucleus in a similar manner to Pop2. However, Ccr4 was also implicated in proper cell cycle progression in previous studies (Liu et al, 1997). Expression of *CCR4* and *POP2* seemed to be modulated through the cell cycle. Moreover, Ccr4 and Pop2 were found to interact with a cell cycle-regulated kinase Dbf2 *in vivo* (Liu et al, 1997).

Beyond deadenylation, the Ccr4-Not complex has also been found to possess ubiquitin ligase activity. The first clue for a role of the Ccr4-Not complex in protein ubiquitination came from mammalian studies where the human ortholog of Not4, CNOT4 was shown to function as an E3 ubiquitin ligase (Albert et al, 2002). Subsequently, E3 ligase activity of Not4 in budding yeast was also proven *in vitro* and *in vivo* (Mulder et al, 2007a; Mulder et al, 2007b; Panasenko et al, 2006). Lastly, functions of other Ccr4-Not components remain to be fully described. Not2, Not4 and Not5 seemed to be required for the efficient decapping of *EDC1* mRNA (Muhlrad & Parker, 2005). However, the mechanism of this regulation requires further investigation. Not2 has a conserved role in the maintenance of the structural integrity of the Ccr4-Not complex (Ito et al, 2011a; Russell et al, 2002). The specific roles of Caf40 and Caf130 in cell remain to be elucidated.

How the Ccr4-Not complex is regulated has so far remained nebulous. As mentioned before, Pop2 is phosphorylated by the Yak1 kinase upon glucose starvation (Moriya et al, 2001). In addition to Pop2, Not3 and Not5 are phosphoproteins which become hyper-phosphorylated in a Rim15/Yak1/PKA-dependent manner when cells are depleted for glucose (Lenssen et al, 2005). Mass spectrometry analysis of the Ccr4-Not complex revealed phosphorylation sites on Not1, Pop2 and Not4 (Lau et al, 2010). However, the functional significance of these phosphorylation events is still not understood.

Processing Bodies and Stress Granules

Attempts to characterize specific sites for mRNA degradation in the cell led to the characterization of processing bodies (P-bodies). Parker and his group defined P-bodies as "discrete cytoplasmic foci" where mRNA decapping and 5'-to-3' degradation take place (Sheth & Parker, 2003). The core of P-bodies consists of Ccr4, Pop2 and the decapping enzymes Dcp1/Dcp2 together with Edc3, Pat1, Dhh1, the Lsm1-7 complex, and Xrn1 (Balagopal & Parker, 2009). mRNAs and Nonsense Mediated Decay-related proteins are also found in P-bodies. In yeast, Edc3 is used as a marker of P-bodies given that a self-interaction domain of Edc3 is important for the assembly of P-bodies as well as an asparagine-glutamine rich domain of Lsm4 (Decker et al, 2007). P-bodies are not visible under the microscope under normal conditions. However, their assembly is strongly induced under a variety of stress conditions such as glucose deprivation, salt and heat stress (Balagopal & Parker, 2009; Shah et al, 2013). Although P-bodies were initially defined as the sites of mRNA degradation, mRNA degradation seemed to continue without any observable defect in the absence of P-bodies. These findings suggest that P-bodies are more likely to play specific roles under different stress conditions.

Stress granules are another well-studied cytoplasmic RNP complex. In addition to proteins which are shared with P-bodies, stress granules contain a number of translation initiation factors, the 40S ribosomal subunit and Pab1, the poly(A) binding protein (Anderson & Kedersha, 2008). Stress granules were proposed to be the sites for mRNA storage (Yamasaki & Anderson, 2008). Similarly to P-bodies, stress granules are induced in response to various stresses as well as to inhibition of translation initiation.

Recently, Protein Kinase A (PKA) was found to be the major regulator of P-body formation partly via its role in the phosphorylation of Pat1 (Ramachandran et al, 2011; Shah et al, 2013). TORC1 did not seem to be involved in this process as neither rapamycin nor nitrogen-source deprivation induced P-body formation (Ramachandran et al, 2011). Neither PKA nor TORC1 affect the assembly of stress granules (Shah et al, 2013). In accordance with the findings in yeast, rapamycin treatment does not

induce stress granule formation in mammalian cells (Brown et al, 2011). However, inhibition of mTORC1 with ATP-competitive inhibitors like Torin1 and pp242 as well as with siRNAs directed to mTOR or Raptor led to the formation of stress granules in an eIF4E pathway-dependent manner (Fournier et al, 2013). Furthermore, treatment of mammalian cells with wortmannin efficiently promoted stress granule formation through the inhibition of another PIKK family member SMG1 (Brown et al, 2011). In yeast, phosphorylation of the decapping enzyme Dcp2 by Ste20 was shown to be required for the recruitment of Dcp2 to P-bodies and efficient assembly of stress granules under stress conditions (Yoon et al, 2010). Even though evidence to support the role of TORC1 in stress granule formation in yeast is still missing, a recent study proposed that stress granules regulate TORC1 activity. Interestingly, TORC1 was found to be sequestered in stress granules induced by heat stress (Takahara & Maeda, 2012). Recruitment of TORC1 into stress granules appears to be a means of suppressing TORC1 activity and delaying its reactivation during recovery, eventually contributing to the protection of the cells from heat stress-dependent cellular damage. Intriguingly, this mechanism is conserved in higher eukaryotes. The dual specificity kinase DYRK3, putative homolog of Yak1 kinase, plays a crucial role in the sequestration of mTORC1 in stress granules in mammalian cells (Wippich et al, 2013). Another recently identified negative regulator of mTORC1 called Astrin was also shown to be involved in the recruitment of Raptor to the stress granules (Thedieck et al, 2013). Yet, the details of the mechanisms responsible for regulation of P-bodies and stress granules, and the functional importance of these mRNP complexes require further investigation.

Research Project

The major goal of this study is to reach a better understanding of the events downstream of TORC1/2. More specifically, we wanted to address how the fate of mRNA in the cell is regulated by the TOR complexes. To achieve this goal, we focused on the regulation of the major deadenylase Ccr4 and the small ribosomal subunit protein S6 through phosphorylation in a TORC1- and/or TORC2-dependent manner.

Article and Results

Section I. Regulation of Stb3, Dot6 and Tod6 by Sch9

Analysis of the rapamycin-responsive phosphoproteome had revealed Stb3, Dot6 and Tod6 as Sch9-dependent TORC1 effectors (Huber et al, 2009). In this follow-up story, we elucidated the mechanism by which Sch9 regulates ribosome biogenesis via these three transcriptional repressors.

Dot6 and Tod6 were previously characterized as Myb-like HTH transcription factors, which preferably bind to the PAC (Polymerase A and C) element commonly found in Ribi gene promoters (Lippman & Broach, 2009; Wade et al, 2006; Zhu et al, 2009). Stb3, on the other hand, binds to RRPE (rRNA processing elements) elements enriched again in Ribi gene promoters (Liko et al, 2007; Wade et al, 2006). Here, we demonstrated that Dot6/Tod6 abrogates the Ribi gene expression by recruiting the RPD3L histone deacetylase complex, whereas, Stb3 repressed not only the expression of Ribi genes but also the expression of RP genes, also by recruiting RPD3L. Moreover, Sch9 contributed to this process by inhibiting these three transcription factors via direct phosphorylation, and thereby promoting ribosome biogenesis.

Altogether, these data helped us to further understand the complex mechanisms by which TORC1 and Sch9 regulate ribosome biogenesis.

Personal contributions to the article:

Figure S5A: Protein extraction and analysis of protein levels of HA-tagged Stb3 by western blotting

Figure S6C: Protein extraction and analysis of protein levels of HA-tagged Dot6 and Tod6 proteins by western blotting

The EMBO Journal (2011) 30, 3052–3064 | © 2011 European Molecular Biology Organization | All Rights Reserved 0261-4189/11
www.embojournal.org

THE EMBO JOURNAL

Sch9 regulates ribosome biogenesis via Stb3, Dot6 and Tod6 and the histone deacetylase complex RPD3L

Alexandre Huber[1], Sarah L French[2], Hille Tekotte[3], Seda Yerlikaya[1], Michael Stahl[1], Mariya P Perepelkina[1], Mike Tyers[3], Jacques Rougemont[4], Ann L Beyer[2] and Robbie Loewith[1,*]

[1]Department of Molecular Biology and National Center for Competence in Research Program 'Frontiers in Genetics', University of Geneva, Geneva, Switzerland, [2]Department of Microbiology, University of Virginia Health System, Charlottesville, VA, USA, [3]Wellcome Trust Center for Cell Biology, University of Edinburgh, Edinburgh, Scotland and [4]Bioinformatics and Biostatistics Core Facility, Swiss Federal School of Engineering of Lausanne and Swiss Institute of Bioinformatics, Lausanne, Switzerland

TORC1 is a conserved multisubunit kinase complex that regulates many aspects of eukaryotic growth including the biosynthesis of ribosomes. The TOR protein kinase resident in TORC1 is responsive to environmental cues and is potently inhibited by the natural product rapamycin. Recent characterization of the rapamycin-sensitive phosphoproteome in yeast has yielded insights into how TORC1 regulates growth. Here, we show that Sch9, an AGC family kinase and direct substrate of TORC1, promotes *ribosome biogenesis* (*Ribi*) and *ribosomal protein* (*RP*) gene expression via direct inhibitory phosphorylation of the transcriptional repressors Stb3, Dot6 and Tod6. Deletion of *STB3*, *DOT6* and *TOD6* partially bypasses the growth and cell size defects of an *sch9* strain and reveals interdependent regulation of both *Ribi* and *RP* gene expression, and other aspects of Ribi. Dephosphorylation of Stb3, Dot6 and Tod6 enables recruitment of the RPD3L histone deacetylase complex to repress *Ribi/RP* gene promoters. Taken together with previous studies, these results suggest that Sch9 is a master regulator of ribosome biogenesis through the control of *Ribi*, *RP*, *ribosomal RNA* and *tRNA* gene transcription.

The EMBO Journal (2011) **30,** 3052–3064. doi:10.1038/emboj.2011.221; Published online 5 July 2011
Subject Categories: signal transduction; chromatin & transcription
Keywords: rapamycin; ribosome biogenesis; RPD3 histone deacetylase; Sch9; Stb3

*Corresponding author. Department of Molecular Biology, University of Geneva, 30, quai Ernest-Ansermet, Geneva 1211, Switzerland. Tel.: +41 22 379 6116; Fax: +41 22 379 6868; E-mail: robbie.loewith@unige.ch

Received: 3 January 2011; accepted: 8 June 2011; published online: 5 July 2011

Introduction

The budding yeast *Saccharomyces cerevisiae* synthesizes ~2000 ribosomes per minute per cell under optimal growth conditions. To ensure the proper transcription, processing and assembly of the 78 ribosomal proteins (RPs) and 4 ribosomal RNAs (rRNAs) that constitute a ribosome, hundreds of *trans*-acting assembly factors and other cofactors for translation regulation, tRNA biosynthesis or purine/pyrimidine synthesis must also be produced from a set of coregulated genes known as the *ribosome biogenesis* (*Ribi*) regulon (Jorgensen *et al*, 2004; Wade *et al*, 2006). Ribosome biogenesis thus requires the coordinated activities of all three RNA polymerases (RNAPI, II and III) and can commandeer up to 70–80% of total nuclear transcriptional capacity (Warner, 1999). To limit unnecessary energy expenditure under stress and/or starvation conditions, the synthesis of ribosomal components and their Ribi cofactors must be tightly controlled. This regulation is imposed in part by nutrient- and stress-sensitive signalling networks. Most notably, the TOR and PKA kinases regulate Ribi at the transcriptional level (De Virgilio and Loewith, 2006).

The TOR kinases in yeast (TOR1 and TOR2) are the catalytic subunits of two functionally distinct multiprotein complexes, TORC1 and TORC2 (De Virgilio and Loewith, 2006). In optimal growth conditions, TORC1 is active and promotes growth both by stimulating anabolic processes, such as protein synthesis, and by inhibiting catabolic processes, such as macroautophagy (De Virgilio and Loewith, 2006). Binding of the natural product macrolide rapamycin or exposure to cellular stress rapidly inactivates TORC1 (Heitman *et al*, 1991; Urban *et al*, 2007), inhibits anabolic processes and induces catabolic processes.

Ribosome biogenesis is the principal anabolic process that is stimulated by TORC1. The assembly of new ribosomes begins with the TORC1-dependent activation of RNAPI, II and III to promote the transcription of *rRNA*, *RP* and *Ribi*, and *tRNA* genes, respectively (Zaragoza *et al*, 1998; Jorgensen *et al*, 2004; Martin *et al*, 2004; Schawalder *et al*, 2004; Wade *et al*, 2004; Rudra *et al*, 2005). TORC1-dependent signals are mediated by a number of effectors kinases (Breitkreutz *et al*, 2010), the best characterized of which is Sch9, an AGC family Ser/Thr kinase and direct substrate of TORC1 (Urban *et al*, 2007). Sch9 regulates RNAPIII by phosphorylating and inactivating Maf1, a conserved repressor of RNAPIII activity (Upadhya *et al*, 2002; Oficjalska-Pham *et al*, 2006; Roberts *et al*, 2006; Huber *et al*, 2009; Lee *et al*, 2009; Wei and Zheng, 2009). TORC1 also stimulates RNAPI in both an Sch9-dependent and -independent manner, in part through regulation of the transcription initiation factor Rrn3 (Peyroche *et al*, 2000; Laferte *et al*, 2006; Huber *et al*, 2009). Finally, TORC1 regulates the activity of RNAPII at the large cohort of *Ribi* and *RP* genes, at least in part via Sch9 (Jorgensen *et al*, 2004; Urban *et al*, 2007).

Ribi and *RP* genes exhibit overlapping but non-identical kinetics of regulation due to their differing promoter structures, which bind both common and distinct transcription factors (Ju and Warner, 1994; Hughes *et al*, 2000; Jorgensen *et al*, 2004; Wade *et al*, 2006; Lempiainen and Shore, 2009). Among these factors, Fhl1/Ifh1/Crf1, Sfp1 and Hmo1 have all been shown to mediate TORC1 signals to *RP* and/or *Ribi* genes (Jorgensen *et al*, 2004; Martin *et al*, 2004; Schawalder *et al*, 2004; Wade *et al*, 2004; Rudra *et al*, 2005; Lempiainen *et al*, 2009; Singh and Tyers, 2009). However, genetic analysis suggests that Sch9 functions in parallel to Fhl1/Ifh1 and Sfp1 (Jorgensen *et al*, 2004; Lempiainen *et al*, 2009), by an as yet undeciphered mechanism.

Ribi gene promoters are enriched in two distinct motifs, the PAC element (Polymerase A and C) and the RRPE element (rRNA processing element) (Hughes *et al*, 2000; Jorgensen *et al*, 2004; Wade *et al*, 2006). Several independent studies recently identified two Myb-like HTH transcription factors, Dot6 and Tod6, as cognate factors for the PAC element (Badis *et al*, 2008; Freckleton *et al*, 2009; Zhu *et al*, 2009). Dot6 and Tod6 act as transcriptional repressors whose function is antagonized by signals from TORC1, Sch9 and PKA (Lippman and Broach, 2009). Despite its apparent lack of a DNA-binding domain, Stb3 recognizes the RRPE element, where it can apparently act as either a transcriptional activator (Liko *et al*, 2007) or a transcriptional repressor (Liko *et al*, 2010), depending on growth context. Like Dot6 and Tod6, Stb3 appears to lie downstream of the TORC1–Sch9 axis (Liko *et al*, 2010).

Histone acetylation within *Ribi* and *RP* gene promoters is also regulated by TORC1. Inhibition of TORC1 by rapamycin induces both the release of the Esa1 histone acetyltransferase and the recruitment of the Rpd3 histone deacetylase at *RP* gene promoters, and thereby represses transcription (Rohde and Cardenas, 2003; Humphrey *et al*, 2004). Rpd3 is also recruited to *Ribi* gene promoters upon TORC1 inhibition (Humphrey *et al*, 2004). Importantly, in the absence of Rpd3, but not other histone deacetylases, rapamycin effectively fails to repress both *RP* and *Ribi* regulons (Humphrey *et al*, 2004). Rpd3 resides in two functionally distinct complexes, RPD3L and RPD3S, which are characterized by specific essential subunits such as Sds3 and Sap30 (RPD3L) and Rco1 (RPD3S) (Carrozza *et al*, 2005b). RPD3S is thought to suppress spurious intragenic transcription by deacetylating histones in coding regions, while RPD3L functions to repress transcription initiation when recruited to promoter regions by various DNA-binding factors (Carrozza *et al*, 2005a, b).

The mechanism whereby TORC1 controls the *Ribi* and *RP* regulons remains only poorly characterized. Our recent analysis of the rapamycin-sensitive phosphoproteome revealed that Stb3, Dot6 and Tod6 become hypophosphorylated upon TORC1 inhibition in an Sch9-dependent manner, suggesting that these factors may be the missing effectors of TORC1 in the control of RNAPII-mediated transcription of *Ribi* and *RP* genes (Huber *et al*, 2009). Consistently, rapamycin treatment elicited dephosphorylation of Stb3 and Dot6 in a similar survey for novel TORC1 effectors (Soulard *et al*, 2010). Here, we demonstrate that Sch9 directly phosphorylates the Stb3, Dot6 and Tod6 transcription factors to abrogate the repression of *Ribi* and *RP* genes. Upon Sch9 inhibition, Stb3 and Dot6/Tod6 cooperate to recruit the RPD3L histone deacetylase complex to *Ribi* gene promoters, whereas Stb3 is responsible for recruitment of RPD3L to *RP* gene promoters. These observations consolidate the TORC1- and Sch9-dependent mechanisms of transcriptional regulation of the major promoter classes during ribosome biogenesis.

Results

Sch9 directly phosphorylates Stb3, Dot6 and Tod6 in vivo and in vitro

We first sought to determine whether the TORC1-dependent phosphorylation of Stb3, Dot6 and Tod6 is specifically mediated by Sch9. We also included PKA in these analyses as PKA has been shown previously to phosphorylate Stb3 and Dot6 *in vitro* (Budovskaya *et al*, 2005; Deminoff *et al*, 2006) and this kinase often has overlapping functions with Sch9 (De Virgilio and Loewith, 2006; Zaman *et al*, 2008; Ramachandran and Herman, 2011). We used analogue-sensitive alleles of *SCH9* (*sch9*^{as}) and *PKA* (*pka*^{as}*: tpk1*^{as}*tpk2*^{as} *tpk3*^{as} as PKA activity is encoded by three partially redundant *TPK* genes in yeast) (Jorgensen *et al*, 2004; Yorimitsu *et al*, 2007), which encode a point mutation in the kinase domain that specifically renders the enzyme sensitive to inhibition by the bulky ATP analogue 1NM-PP1 (Shokat and Velleca, 2002). We observed that HA-tagged Stb3 analysed from untreated cells migrated as a smear in SDS–PAGE, suggesting phosphorylation on multiple sites (Supplementary Figure S1). This migration pattern was not dramatically altered by rapamycin treatment or by inhibition of Sch9^{as} and/or PKA^{as} with 1NM-PP1 (Figure 1A; Supplementary Figure S1). We and others have previously observed that Sch9 and PKA share preferences for Ser/Thr residues preceded by an Arg at the −3 position and Arg/Lys at −2, that is, a consensus motif of R[R/K]x[S/T]* (Huber *et al*, 2009; Lee *et al*, 2009). We probed for potential changes in Stb3 phosphorylation using an antibody against this phosphorylated consensus motif (see Supplementary Figure S1A for antibody specificity controls). We observed rapid dephosphorylation of Stb3 after Sch9 inhibition but not after PKA inhibition, suggesting that Stb3 phosphorylation at the consensus R[R/K]x[S/T] sites is specifically regulated by Sch9 *in vivo* (Figure 1A). Inhibition of either Sch9 or PKA also resulted in an apparent rapid dephosphorylation of both Dot6 (Figure 1B) and Tod6 (Figure 1C). Combined inhibition of the two kinases caused a more pronounced dephosphorylation of both substrates, suggesting that Sch9 and PKA act in parallel on Dot6 and Tod6.

To determine if the three transcription factors might be direct substrates of Sch9, recombinant Stb3, Dot6 and Tod6 were tested for their ability to be phosphorylated by Sch9 in an *in vitro* kinase assay. A constitutively active form, Sch9^{3E} (Urban *et al*, 2007), but not catalytically impaired Sch9, could directly phosphorylate all three proteins *in vitro* (Figure 1D–G). Together, these *in vivo* and *in vitro* results suggest that Sch9 directly phosphorylates Stb3, Dot6 and Tod6.

Sch9 regulates Ribi and RP genes via Stb3, Dot6, Tod6 and the histone deacetylase RPD3L

Next, we wished to examine the biological function for Stb3, Dot6 and Tod6 phosphorylation downstream of TORC1/Sch9. Dot6 and Tod6 function as repressors of *Ribi/RP* transcription (Lippman and Broach, 2009) presumably via their intrinsic affinity for PAC promoter elements, which are enriched upstream of *Ribi* genes (Freckleton *et al*, 2009; Zhu *et al*, 2009).

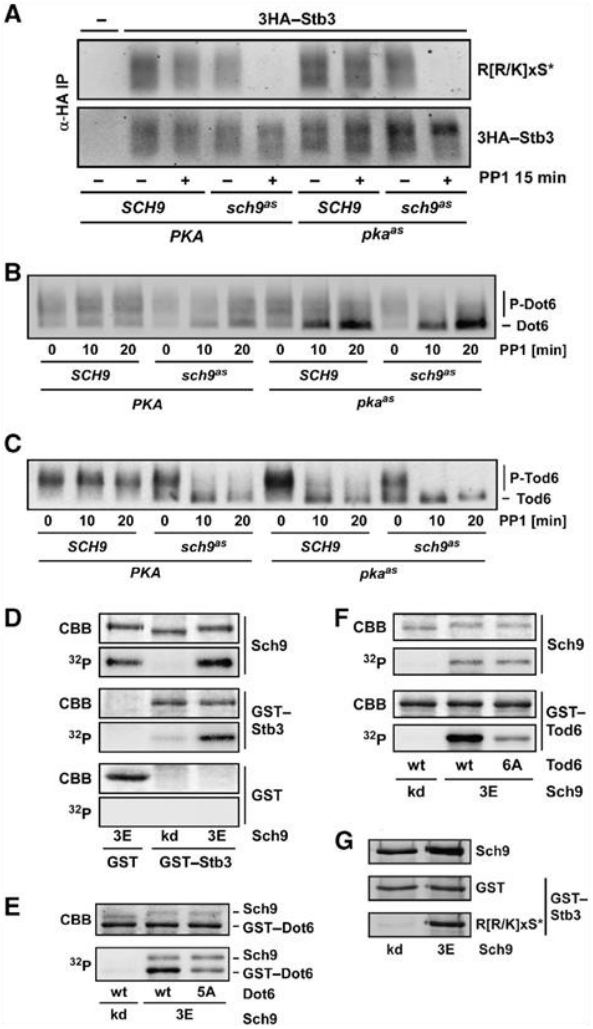

Figure 1 Stb3, Dot6 and Tod6 are directly phosphorylated by Sch9 *in vivo* and *in vitro*. (**A**–**C**) Strains of indicated genotype and expressing 3HA–Stb3 (**A**), Dot6–5HA (**B**) or Tod6–5HA (**C**) were grown exponentially in YPD at 30°C and subjected to the indicated treatments. (**A**) 3HA–Stb3 was immunoprecipitated after denaturing protein extraction and phosphorylation status (anti-R[R/K]xS*) and abundance (anti-HA) determined by western blot. A strain transformed with empty vector was used as a mock IP control (left lane) (**B**, **C**) Dot6–5HA and Tod6–5HA phosphorylation status was determined by migration in SDS–PAGE and anti-HA western blot. (**D**–**G**) *In vitro* kinase assays. GST–Stb3 (**D**, **G**), GST–Dot6^{wt} and GST–Dot6^{5A} (**E**) and GST–Tod6^{wt} and GST–Tod6^{6A} (**F**) were tested as substrates for Sch9^{3E} (Urban *et al*, 2007) in presence of γ-^{32}P-ATP (**D**–**F**) or unlabelled ATP only (**G**). Reactions with GST as the substrate (**D**) or Sch9^{kd}, a point mutant lacking catalytic activity, as the kinase (**D**–**G**) were performed to control for specificity. Reactions were resolved by SDS–PAGE, stained with coomassie (CBB) and ^{32}P incorporation detected by autoradiography (**D**–**F**). Alternatively, reactions were analysed by western blot against the Protein A and GST tags and the phosphorylated R[R/K]x[S/T]* motif (**G**).

Stb3 also appears to function as a downstream transcriptional effector of Sch9, but curiously seems to act as both a transcriptional activator and repressor (Liko *et al*, 2007, 2010). To clarify the role of Stb3 and to comprehensively characterize the functional relationships of Stb3, Dot6 and Tod6 as downstream effectors of Sch9, we used mRNA-Seq transcriptome profiles to delineate the sets of genes that respond to each factor. As expected (Jorgensen *et al*, 2004), inhibition of Sch9 resulted in downregulation of many genes (12% of 5025 genes detected were downregulated >1.5-fold), among which *Ribi* (79% of 457 genes; $P<10^{-31}$) and *RP* (99% of 137 genes; $P<10^{-37}$) genes were highly enriched (Figure 2A). As observed in the mRNA-Seq data and confirmed by RT–qPCR (Supplementary Figure S2A and B), this repression was partially alleviated when *STB3* or *DOT6* and *TOD6* were deleted. This effect was not due to a prior lack of induction of the *Ribi/RP* genes in these deletion strains (Supplementary File F1 and data not shown). Strikingly, disruption of *STB3* abrogated the repression of *RP* genes following Sch9 inhibition ($P<10^{-37}$; Figure 2A; Supplementary Figure S2A–C; Supplementary Table S1); conversely Sch9 appeared to regulate *Ribi* genes preferentially via Dot6 and Tod6 ($P<10^{-31}$). The combined deletion of all three factors had an additive effect, as observed by the near total failure of Sch9 inhibition to repress *Ribi/RP* gene expression in the *stb3*Δ *dot6*Δ *tod6*Δ background. In agreement with the known DNA motif preferences, *Ribi* genes that harboured only RRPE elements in their promoters were preferentially regulated via Stb3 ($P<10^{-4}$; Figure 2A; Supplementary Figure S2C; Supplementary Table S1), whereas genes bearing only PAC elements were preferentially regulated by Dot6/Tod6 ($P<0.001$).

In addition to these effects, we observed hyper-induction of Gcn4 target genes upon Sch9 inhibition in a *dot6*Δ *tod6*Δ strain and to an even greater extent in a *stb3*Δ strain (Supplementary Figure S2B). Although we have not pursued this effect further, we suspect that imbalanced repression of *Ribi* genes under these conditions may result in increased *GCN4* mRNA translation, and consequently in the observed increase in expression of Gcn4 targets.

Stb3 was originally identified as a binding partner of Sin3 (Kasten and Stillman, 1997), a component of the RPD3L and RPD3S histone deacetylase complexes. Dot6 and Tod6 also bind to the RPD3L complex (Shevchenko *et al*, 2008). In addition, Rpd3, which is the shared catalytic subunit of these deacetylase complexes, is implicated in *Ribi* and *RP* gene regulation downstream of TORC1 (Rohde and Cardenas, 2003; Humphrey *et al*, 2004). The interaction of Stb3, Dot6 and Tod6 with RPD3 could thus explain their reported activities as transcriptional repressors. We, therefore, determined whether either of the RPD3 complexes function downstream of Sch9 in the regulation of *Ribi/RP* genes. We examined the transcriptional profile caused by Sch9 inhibition in strains that lacked Rpd3, Rco1 (a specific and essential component of RPD3S) or Sds3 (a specific and essential component of RPD3L) (Carrozza *et al*, 2005b). While the absence of Rco1 had virtually no effect, deletion of the RPD3L components dramatically alleviated the repression of *Ribi/RP* genes that would otherwise be observed upon Sch9 inhibition (Figure 2A; Supplementary Figure S2A and B). These observations strongly suggest that Stb3, Dot6 and Tod6 repress transcription of the *Ribi* and *RP* regulons via RPD3L.

Effects of Stb3, Dot6 and Tod6 on cell growth and cell size

Cells in which *Ribi* gene expression is compromised exhibit a reduced growth rate and a small cell size (Jorgensen *et al*, 2004). The absence of Sch9 activity in particular causes

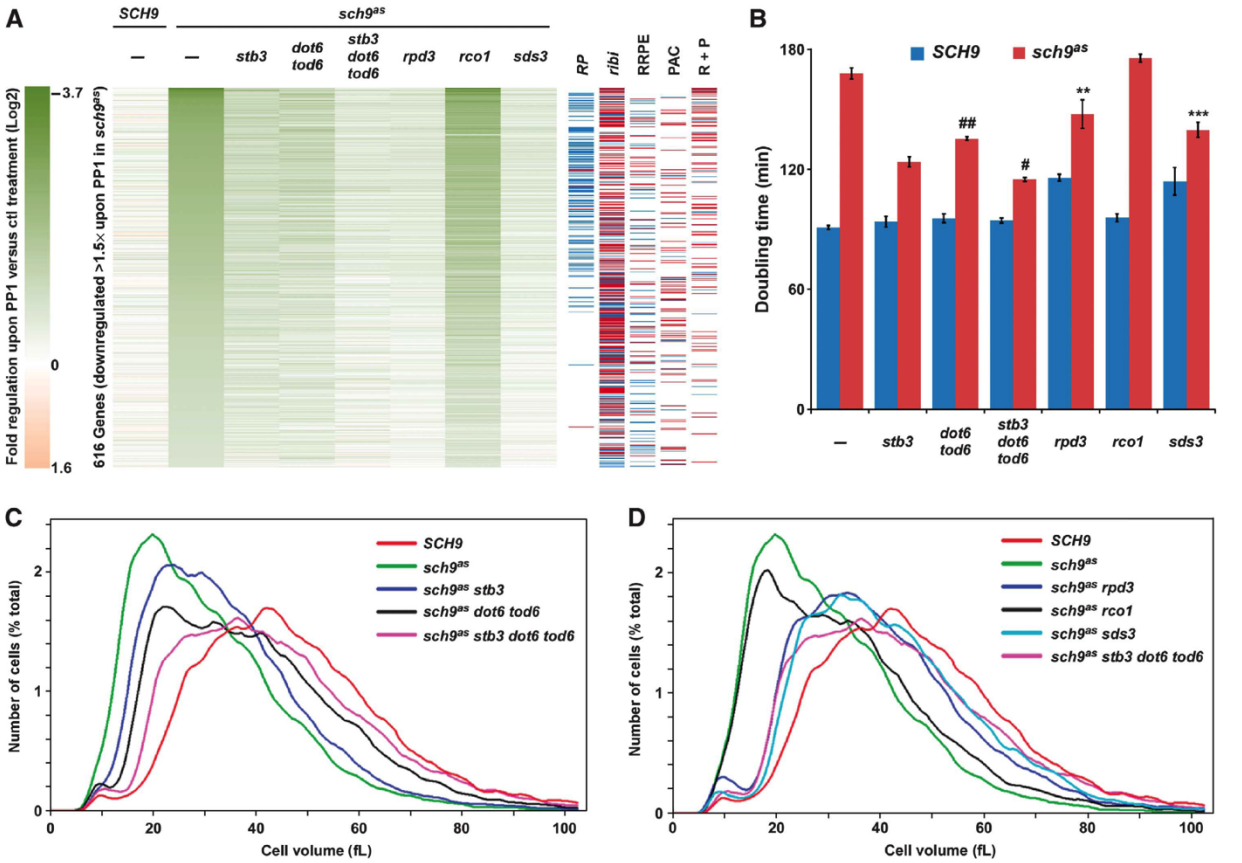

Figure 2 Sch9 regulates cell growth via Stb3, Dot6, Tod6 and RPD3L. (**A**) Regulation of *Ribi* and *RP* transcription. Strains of the indicated genotype were grown to exponential phase in YPD at 30°C, treated for 30 min with 1NM-PP1 (PP1) or drug vehicle, followed by determination of mRNA-Seq transcriptome profiles. All genes downregulated >1.5-fold by 1NM-PP1 versus drug vehicle in the *sch9*^{as} strain are shown, as sorted by magnitude of change. In the right panels, genes belonging to the *Ribi* or *RP* regulons or whose promoters contain RRPE or PAC promoter elements or both (R + P) (Jorgensen and Tyers, 2004) are indicated with blue dashes if derepressed preferentially by *STB3* deletion or red dashes if derepressed preferentially by *DOT6/TOD6* deletion. (**B**) Regulation of growth rate. *SCH9* and *sch9*^{as} strains harbouring the indicated gene deletions were grown to exponential phase at 30°C in YPD in the presence of 1NM-PP1 and doubling times calculated from quantitative growth curves. Growth rate effects were recapitulated in spot assays; the phenotypes of the *stb3*Δ and *dot6*Δ *tod6*Δ strains were confirmed by complementation with plasmid-encoded wild-type alleles (Supplementary Figure S3A and B). Data are means of three independent experiments ± s.d. $^{**}P<0.01$; $^{***}P<0.001$ versus *sch9*^{as}. $^{\#}P<0.05$; $^{\#\#}P<0.01$ versus *sch9*^{as}*stb3*Δ. (**C**, **D**) Regulation of cell size. Strains of the indicated genotypes were grown as in (**B**) and cell size distributions determined on a Z2 Coulter counter. Size profiles are shown in two separate panels with the same scales for clarity. Corresponding *SCH9*^{wt} control distributions were also determined (Supplementary Figure S3B and C; see Supplementary Table S2 for all quantitative size parameters).

a severe small size (Whi) phenotype and a marked growth defect (Jorgensen *et al*, 2002). We determined if these phenotypes are mediated via Stb3, Dot6, Tod6 and the RPD3L complex. Our wild-type strain had a doubling time (t_d) of ~90 min and a mode cell volume of 41 fL (Figure 2B–D; Supplementary Figure S3C and D; Supplementary Table S2); inhibition of an *sch9*^{as} strain with 1NM-PP1 increased the doubling time to about 170 min and decreased mode cell volume to about 20 fL. This decreased cell size is attributable to a reduced critical size threshold at the point of commitment to division (Start), as estimated by the half height value of the daughter cell (left hand) side of the size distribution (half height daughter size for wild type = 24 fL and for *sch9*^{as} with 1NM-PP1 = 12 fL). Deletion of *STB3* in the *sch9*^{as} strain strongly suppressed the slow growth phenotype (t_d = 125 min) and partially suppressed the cell size defect (daughter size = 14 fL). Importantly, the *stb3*Δ strain itself was wild type in size (Supplementary Figure S3C), thereby demonstrating that the size rescue effect was epistatic rather than additive. Deletion of *DOT6* and *TOD6* more potently rescued the size defect (daughter size = 17 fL) but suppressed the slow growth phenotype to a lesser extent (t_d = 135 min). As the *dot6*Δ *tod6*Δ strain had a somewhat larger size than wild type (Supplementary Figure S3C), the increase in size was more pronounced in the *sch9*^{as} background (42% increase in *sch9*^{as} versus 23% increase in wild type), again consistent with an epistatic interaction. Combined deletion of the three genes further suppressed both phenotypes (t_d = 115 min; daughter size = 20 fL), consistent with the observed synthetic transcriptional effects. As predicted, deletion of either *RPD3* or *SDS3* fully recapitulated the size suppression by the deletion of *STB3*, *DOT6* and *TOD6* (daughter sizes = 20 and 22 fL, respectively). However, the *rpd3*Δ and *sds3*Δ mutations only slightly rescued the growth rate phenotype of *sch9*^{as} cells (t_d = 145 and 140 min, respectively), in part due to an Sch9-independent slow growth phenotype (t_d = 115 min

in both strains). Deletion of the RPD3S subunit, *RCO1*, did not suppress either *sch9* phenotype ($t_d = 175$ min doubling time; daughter size = 12 fL). Independent flow cytometric determination of total cell protein content confirmed that the suppression of cell size defects was due to differences in biomass and not due to increased vacuolarization (Supplementary Figure S3E). We note that even the strongest size suppression effects did not fully restore size to wild type, suggesting that additional Sch9 effectors likely influence the size threshold. Collectively, these results indicate that Stb3 and Dot6/Tod6 function in concert with the RPD3L complex to regulate growth rate and cell size.

Sch9 regulates RNA polymerase I and III via Stb3, Dot6 and Tod6

TORC1/Sch9 regulates rRNA transcription by RNAPI through an Rrn3-independent pathway (Huber *et al*, 2009; Wei and Zheng, 2009; Philippi *et al*, 2010); in addition, Sch9 regulates rRNA processing (Huber *et al*, 2009). Since the *Ribi* regulon contains many genes involved in rRNA transcription and processing, and since RPs appear to have indirect roles in these processes (Reiter *et al*, 2011), we wondered if Sch9 indirectly promotes rRNA transcription and/or processing via the *Ribi* and *RP* regulons. We assayed RNAPI transcription by Miller chromatin spreads (Figure 3A and B) and found that Sch9 inhibition reduced the number of polymerases per 35S rRNA gene by >60%. This defect was partially suppressed by the disruption of *STB3*, *DOT6/TOD6* or *RPD3*. We then performed metabolic pulse-labelling experiments with ^{3}H-uracil to examine effects on rRNA synthesis and processing (Huber *et al*, 2009). Sch9 inhibition reduced the incorporation of radioactivity into rRNA and caused a defect in 27S–25S and 20S–18S rRNA maturation (Figure 3C). Disruption of *STB3* partially rescued both effects, while disruption of *DOT6* and *TOD6* resulted in a relative accumulation of 27S and 20S species, suggesting that rRNA transcription was partially restored but that the processing phenotype was not. Again, deletion of all three transcription factors, or deletion of *RPD3* alone, further rescued the rRNA transcription and processing defects. Interestingly, the downregulation of

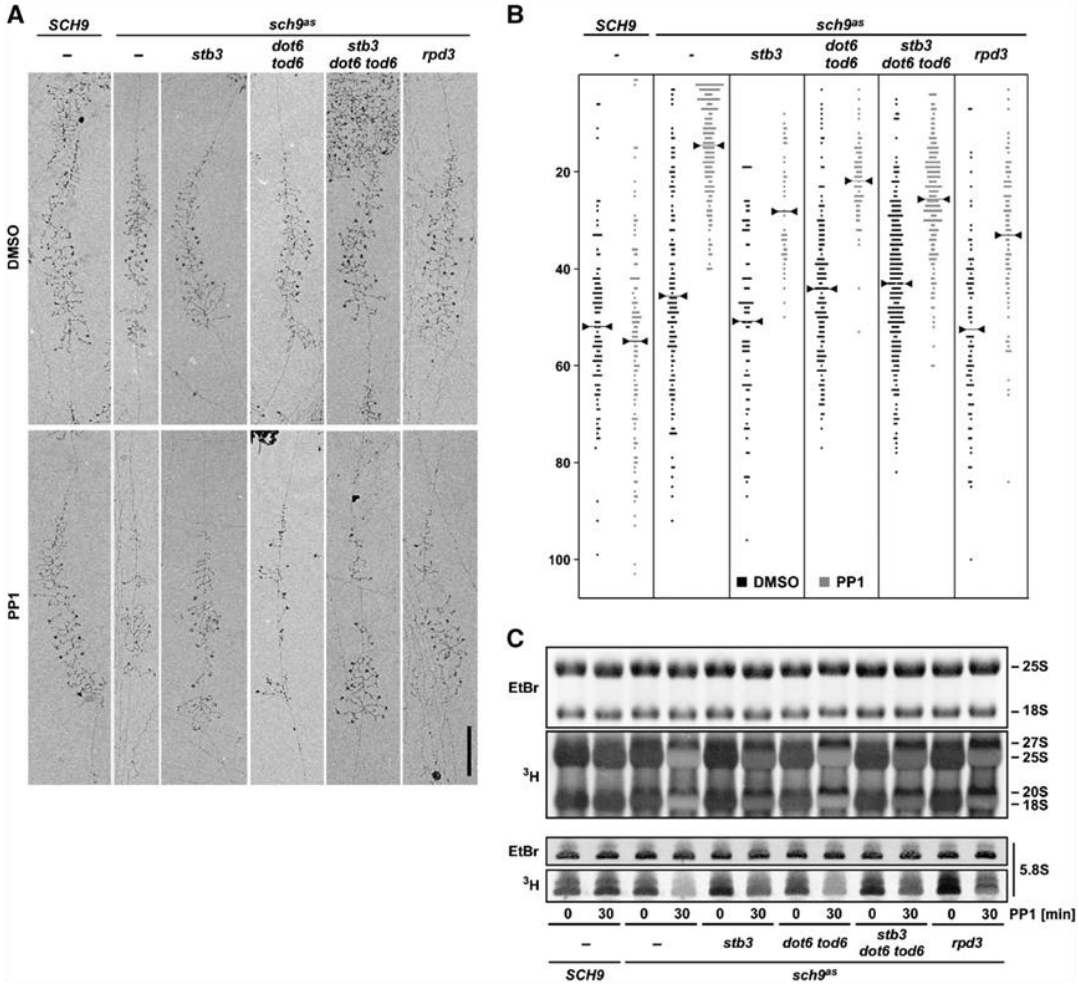

Figure 3 Stb3, Dot6 and Tod6 regulate RNA Pol I transcription initiation and rRNA processing. (**A**, **B**) Miller chromatin spreads were prepared from the indicated strains treated for 30 min with 1NM-PP1 or DMSO. (**A**) Representative electron micrographs of transcribed rDNA genes in Miller spreads. (**B**) The number of polymerases of each active *rDNA* repeat was determined and plotted. Averages are marked for each group with a line bounded by triangles. (**C**) RNA synthesis in the indicated strains following DMSO or 1NM-PP1 treatment was determined by metabolic pulse labelling with ^{3}H-uracil. Total RNA loaded was visualized by staining with ethidium bromide (EtBr). Mature rRNA (25S and 18S) and pre-rRNA (27S and 20S) species are indicated.

5S rRNA and tRNA production upon Sch9 inhibition was also partially ameliorated by elimination of *STB3*, *DOT6/TOD6* or RPD3L function (Supplementary Figure S4). These findings reveal that Sch9 regulates both rRNA transcription/processing and tRNA synthesis via the same cohort of Rpd3-associated effectors that govern *Ribi* and *RP* gene expression.

Phosphorylation of Stb3, Dot6 and Tod6 regulates their repressive activities

Given that Stb3, Dot6 and Tod6 phosphorylation negatively correlated with their repressive activity (Figures 1A–C and 2A), we mutated the known Sch9 sites in each protein and assessed the phenotypic consequences. Five sites in Stb3 match the R[R/K]x[S/T] Sch9/PKA consensus motif, three of which (S254, S285 and S286) have been reported in phosphoproteomic profiles (Chi *et al*, 2007; Bodenmiller *et al*, 2008; Huber *et al*, 2009; Soulard *et al*, 2010; Stark *et al*, 2010). Replacing all three sites with non-phosphorylatable Ala residues yielded a variant ($Stb3^{3A}$) that was not recognized by a phosphospecific antibody *in vivo* (Supplementary Figure S1A and B). Overexpression of $STB3^{3A}$ but not wild-type *STB3* impaired cell growth and decreased *RP* gene expression (Figure 4A; Supplementary Figure S5A). While this *RP* defect was partially suppressed in an *sds3*Δ strain (Supplementary Figure S5A and B), consistent with a previous report (Liko *et al*, 2010), the toxicity of $STB3^{3A}$ overexpression was not suppressed by disruption of RPD3L function (Figure 4A). Unlike previous studies (Liko *et al*, 2010), we detected only marginal suppression of $STB3^{3A}$ toxicity upon disruption of the *HOS2* histone deacetylase gene. Furthermore, deletion of *HOS2* suppressed neither the defects in growth rate nor *Ribi* or *RP* gene expression of an $sch9^{as}$ strain in our genetic background

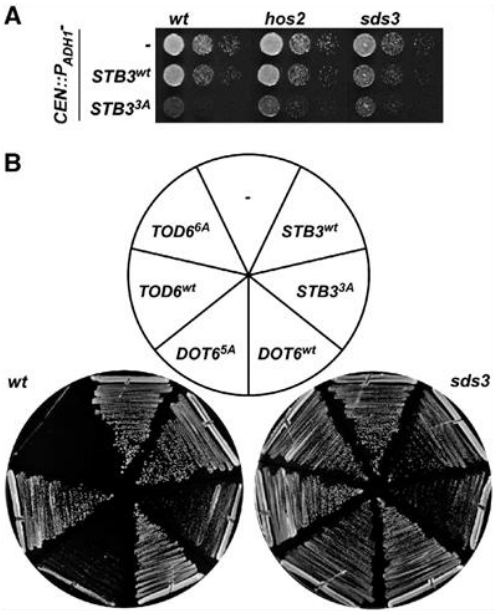

Figure 4 Stb3, Dot6 and Tod6 phosphorylation regulates their activity *in vivo*. (**A**, **B**) The indicated strains were transformed with *CEN*-based plasmids expressing the indicated alleles of *STB3*, *DOT6* or *TOD6* from the strong constitutive *ADH1* promoter. Cells were then plated in 10-fold dilution series (**A**) or restruck (**B**) onto selective synthetic medium and grown for 3 days at 30°C.

(Supplementary Figure S5C and D). These negative results are consistent with the previous reports that Hos2 has virtually no influence on the broad transcriptional profile elicited by rapamycin (Humphrey *et al*, 2004).

We had previously mapped five phosphorylation sites in Dot6 and six sites in Tod6, all of which corresponded to the R[R/K]x[S/T] consensus except for S247 in Dot6, which still fits a minimal RxxS consensus (Huber *et al*, 2009). Dot6 and Tod6 variants in which these sites were substituted with Ala residues ($Dot6^{5A}$ and $Tod6^{6A}$) were not as robustly phosphorylated by Sch9 in an *in vitro* kinase assay (Figure 1E and F). Overexpression of $DOT6^{5A}$ and $TOD6^{6A}$, but not wild-type alleles caused a severe slow growth phenotype that was largely suppressed by deletion of *SDS3* (Figure 4B). Because of the severity of the $DOT6^{5A}$- and $TOD6^{6A}$-associated growth phenotypes, we verified this result by conditional expression of each allele from the *GAL1* promoter (Supplementary Figure S6A). On galactose medium, overexpression of the non-phosphorylatable Dot6 and Tod6 variants again caused a strong growth phenotype, which was suppressed by deletion of *RPD3* or *SDS3* but not *RCO1*. Similar results were also obtained with a doxycycline-inducible system (Supplementary Figure S6B and C). In agreement with the growth defects, *Ribi* and *RP* gene transcription was strongly repressed upon overexpression of the non-phosphorylatable variants of Dot6 and Tod6 compared with their wild-type counterparts, and was restored upon disruption of RPD3L function (Supplementary Figure S6D). Collectively, these data demonstrate that Sch9-dependent phosphorylation antagonizes the repressive functions of Stb3, Dot6 and Tod6.

Negative feedback regulation of Tod6 and homeostatic control of Ribi/RP genes

In several assays for Tod6 phosphorylation, we noticed that Tod6 levels were decreased when the protein was hypophosphorylated (Figure 1C). Tod6–5HA levels were diminished in a $sch9^{as}$ strain (the $sch9^{as}$ allele is slightly hypomorphic; Jorgensen *et al*, 2004) and further decreased upon treatment with 1NM-PP1 (Figure 5A). Similarly, the $Tod6^{6A}$–5HA phosphosite mutant was less abundant as compared with the wild-type protein (Figure 5B and C). In part, this effect was due to diminished expression of $TOD6^{6A}$*–5HA* as compared with wild-type *TOD6–5HA* mRNA (Figure 5C). The reduced abundance of the $TOD6^{6A}$*–5HA* transcript levels was not due to *cis* destabilization effects because expression of this allele also decreased the endogenous *TOD6* transcript (Figure 5D). These observations are consistent with the fact that *TOD6* is part of the *Ribi* regulon (Wade *et al*, 2006), with the down-regulation of *TOD6* upon Sch9 inhibition (Supplementary File F1), with the regulated recruitment of RPD3L to the *TOD6* promoter (see below) and with the specific effects of *TOD6* on *Ribi* gene expression (Supplementary Figure S7). In addition, the $Tod6^{6A}$–5HA protein/mRNA ratio was significantly decreased compared with the wild-type ratio (Figure 5C), suggesting that Tod6 dephosphorylation may destabilize the protein. We were unable to directly test this hypothesis because the effects of both translational inhibitors and nutrient shifts on Sch9 activity (Urban *et al*, 2007) would confound interpretation of wild-type Tod6 half-life data. We conclude that Tod6 negatively represses its own transcription in a manner that is antagonized by Sch9-dependent phosphorylation, and that Tod6 phosphorylation may promote its

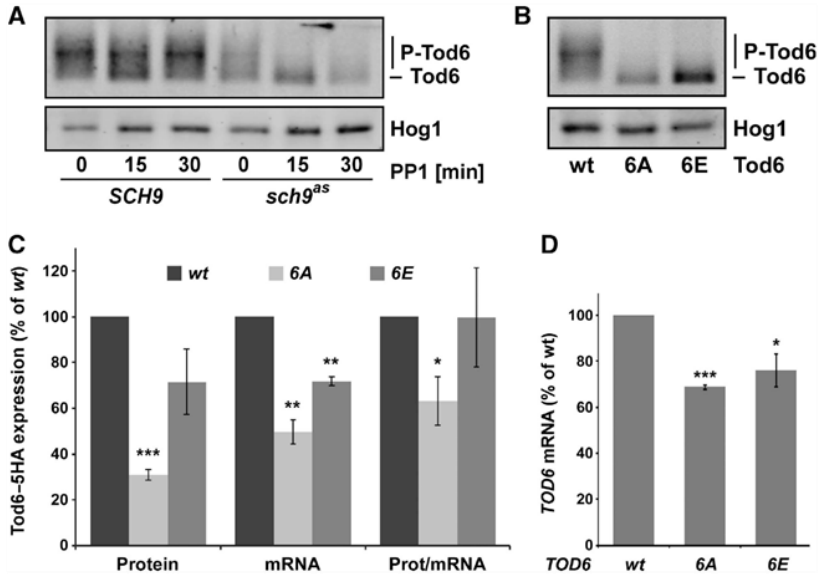

Figure 5 Regulation of Tod6 expression level and protein abundance. (**A**) *SCH9* and *sch9*^{as} cells expressing Tod6–5HA were grown in YPD at 30°C and subjected to 300 nM 1NM-PP1 treatment as indicated. Proteins were extracted under denaturing conditions and analysed by western blot against the HA epitope; an antibody specific to the Hog1 protein served as loading control. (**B**) Strains expressing the indicated TOD6–5HA alleles were grown to exponential phase in SC-URA at 30°C and proteins were extracted and analysed as in (**A**). (**C**) Quantification of Tod6–5HA versus Hog1 abundance shown in (**B**) and two other independent experiments. Quantification of TOD6–5HA versus ACT1 mRNA expression was determined from total RNA extracts from the same strains as in (**B**). The ratio of Tod6–5HA protein to TOD6–HA mRNA was calculated from these values and shown as mean ± s.d. of three independent experiments. (**D**) Endogenous TOD6 versus ACT1 expression levels for the same RNA extracts shown in (**C**). Values are mean ± s.d. of three independent experiments. $*P<0.05$; $**P>0.01$; $***P<0.001$ versus wild-type control.

stability. Altogether these data suggest that Tod6 is part of a homeostatic control mechanism of *Ribi* gene transcription involving negative feedback loops on its expression and possibly stability.

RPD3L is recruited to Ribi/RP gene promoters by Stb3, Dot6 and Tod6

As Stb3, Dot6 and Tod6 each interact with RPD3L subunits (Kasten and Stillman, 1997; Shevchenko *et al*, 2008), we hypothesized that these factors may recruit the RPD3L deacetylase complex to *RP* and *Ribi* promoter DNA. Coimmunoprecipitation experiments confirmed that each factor interacted with RPD3L and, somewhat surprisingly, revealed that the interactions were not sensitive to Sch9 activity (Supplementary Figure S8A and B). We next asked if RPD3L was recruited to the relevant promoter regions upon Sch9 inhibition and whether this recruitment was dependent on Stb3 and/or Dot6/Tod6. We used a TAP-tagged version of Sds3 for chromatin immunoprecipitation followed by high-throughput sequencing (ChIP-Seq). RPD3L-associated sequences were detected using the MACS algorithm and mapped to downstream ORFs on both DNA strands (Supplementary File F2). In comparison to a mock ChIP signal obtained with untagged Sds3, 875 peaks were mapped to the promoters of 943 genes in the Sds3–TAP immunoprecipitations. Of these, 223 peaks in 271 promoters were upregulated >1.5-fold in an *sch9*^{as} strain treated with 1NM-PP1 compared with the untagged control strain (Figure 6A; Supplementary Figure S9A and B; Supplementary Table S3). Analyses of these RPD3L ChIP-Seq profiles revealed that *RP* promoters were highly enriched ($P<10^{-9}$) and that *Ribi* promoters were enriched to a lesser extent ($P<0.01$). Assessment of the genetic dependencies of these profiles revealed that RPD3L peaks that depended on Stb3 were highly enriched in *RP* gene promoters ($P<10^{-12}$), whereas the majority of RPD3L peaks in *Ribi* gene promoters were preferentially but not exclusively dependent on Dot6 and Tod6 (20 *Ribi* genes; $P<0.05$). The Stb3- versus Dot6/Tod6-dependent RPD3L recruitment to *RP* and *Ribi* gene promoters was significantly correlated with the Stb3- versus Dot6/Tod6-dependent regulation of *RP* and *Ribi* genes by Sch9 (Supplementary Figure S10; $P<10^{-4}$). In the absence of all three repressive transcription factors, the RPD3L peaks at the promoters of both *RP* and *Ribi* promoters were equivalent to those in an *SCH9* control strain (Figure 6A; Supplementary Figure S9C). These ChIP-Seq data were confirmed by conventional ChIP–qPCR experiments for selected *Ribi* and *RP* genes (Supplementary Figure S11A). Overall, the influence of *STB3* and *DOT6/TOD6* deletions on RPD3L recruitment closely paralleled their effects on transcriptome profiles (Figure 2A; Supplementary Table S1). The combination of ChIP-Seq, transcriptome profiling and protein–protein interaction data strongly support a model whereby Stb3, Dot6 and Tod6 serve to physically recruit the RPD3L histone deacetylase complex upstream of *Ribi* and *RP* genes.

Our finding that RPD3L was recruited to *RP* gene promoters almost exclusively by Stb3 was somewhat puzzling given that Stb3 was identified as a sequence-specific partner for the RRPE element that is strongly enriched upstream of *Ribi* and not *RP* genes (Liko *et al*, 2007). We, therefore, located Stb3 interaction regions in the genome by repeating the ChIP-Seq analyses with an Stb3–TAP fusion protein. Compared with RPD3L, Stb3 showed strong occupancy at fewer loci, almost

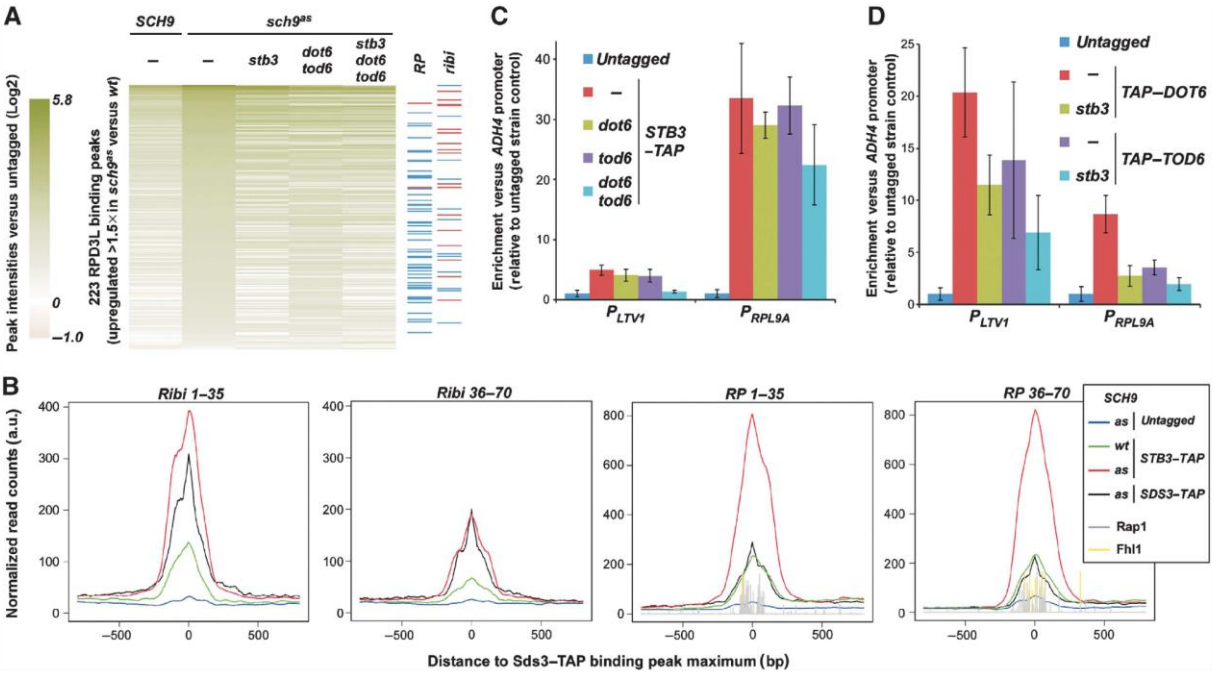

Figure 6 RPD3L recruitment to *Ribi* and *RP* promoters upon Sch9 inhibition in a Stb3- and Dot6/Tod6-dependent manner. (**A**) Strains of the indicated genotype expressing an Sds3–TAP fusion protein were grown exponentially in YPD at 30°C and treated with 300 nM 1NM-PP1 for 20 min followed by fixation, chromatin extraction and ChIP-Seq analysis. Sds3 (RPD3L)-associated sequences were detected by comparing read counts from the *sch9^{as}SDS3–TAP* strain to an *sch9^{as}* (untagged) mock control using the MACS algorithm. Peak intensities were calculated in all conditions at these loci (Supplementary File F2) and normalized to the untagged control counts. Peaks showing an upregulation >1.5-fold in the *sch9^{as}* strain compared with wild type are shown as sorted by magnitude of change. In the right panels, peaks mapping to *Ribi* or *RP* gene promoters are indicated with blue dashes if upregulation upon Sch9 inhibition was preferentially suppressed by *STB3* deletion, or with red dashes if upregulation upon Sch9 inhibition was preferentially suppressed by *DOT6/TOD6* deletion. (**B**) Strains of the indicated genotype expressing an Stb3–TAP fusion protein or untagged Stb3 (mock control) were grown, treated and processed for ChIP-Seq analysis as in (**A**). In all, 70 peaks of Sds3–TAP (RPD3L) binding mapping to *Ribi* gene promoters were sorted according to their score (Supplementary File F2) and divided into two sets (*Ribi* 1–35 and 36–70). Each set of peaks were aligned according to their maxima, summed and plotted for each condition (black line; left panels). Total read counts mapping to the aligned loci in the Stb3–TAP ChIP-Seq analyses (red and green) and their mock control (blue) were also plotted. A similar analysis for peaks mapping to *RP* gene promoters was performed (right panels). The relative position of Rap1 (grey) and Fhl1 (yellow) binding sites in these promoters was evaluated by scoring each loci using previously published position weight matrices of the corresponding motifs (Harbison *et al*, 2004). (**C**, **D**) Stb3 and Dot6/Tod6 cooperate to bind upstream of *Ribi* genes. *sch9^{as}* strains bearing the indicated gene deletions and expressing the indicated TAP-tagged proteins were grown exponentially in YPD at 30°C and treated with 300 nM 1NM-PP1 for 20 min. Cells were then fixed and processed for ChIP–qPCR analysis for the indicated loci. Data are shown as mean ± s.d. of four (**C**) and three (**D**) independent experiments.

all of which were upregulated upon Sch9 inhibition (635 out of 636 peaks) and coincident with the Sch9-sensitive RPD3L peaks in *Ribi* and *RP* promoters (Figure 6B; Supplementary Figure S9A and B). The Stb3 ChIP-Seq data were also confirmed by ChIP–qPCR for selected *Ribi* and *RP* genes (Supplementary Figure S11B). ChIP–qPCR also revealed that Dot6 interactions with the *LTV1* and *NOP14* promoters were strongly upregulated upon Sch9 inhibition (Supplementary Figure S11C). Tod6 also occupies these loci, but was not overtly responsive to Sch9 inhibition. This apparent lack of regulation should be interpreted with caution, however, as Tod6 levels are markedly lower in a *sch9^{as}* strain and decrease further upon 1NM-PP1 treatment (Figure 5A; Supplementary Figure S8B). In contrast to Stb3, we observed that both Dot6 and Tod6 preferentially occupied *Ribi* gene promoters as the ChIP–qPCR upstream of *RP* genes was only slightly above background (Supplementary Figure S11C).

As Stb3, Dot6 and Tod6 each showed detectable binding upstream of *Ribi* and *RP* genes, we asked whether their recruitment was interdependent. We thus examined the interactions of Stb3–TAP at the *LTV1* (*Ribi*) and *RPL9A* (*RP*) promoters in a 1NM-PP1-treated *sch9^{as}* strain upon *DOT6* and/or *TOD6* deletion. The single deletions had little or no impact on the Stb3 signal at either loci. In the *dot6*Δ *tod6*Δ background, however, Stb3 recruitment upstream of *LTV1* was reduced to background levels, whereas its interaction with the *RPL9A* promoter was only slightly affected (Figure 6C). We then asked whether Dot6/Tod6 recruitment to these loci was dependent upon *STB3*. The interaction of both Dot6 and Tod6 was partially impaired at the *LTV1* promoter and completely absent at the *RPL9A* promoter in the *stb3*Δ background (Figure 6D). These ChIP data suggest that upon Sch9 inhibition, Stb3 and Dot6/Tod6 bind upstream of *Ribi* genes in a cooperative manner to recruit the RPD3L histone deacetylase complex, while RPD3L tethering to *RP* gene promoters depends mainly on Stb3, with only a minor influence of Dot6/Tod6. These observations consistently correlate with the relative effects of Stb3, Dot6 and Tod6 on the transcriptional regulation of *Ribi* and *RP* genes.

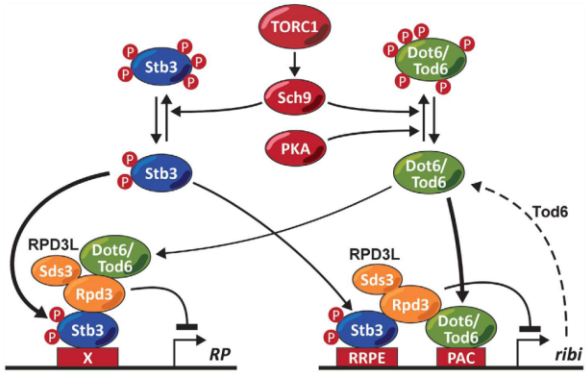

Figure 7 Sch9 regulates ribosome biogenesis via Stb3, Dot6 and Tod6 and the histone deacetylase complex RPD3L. Sch9 directly phosphorylates the transcription repressors Stb3, Dot6 and Tod6 to antagonize their ability to recruit the RPD3L histone deacetylase to *RP* and *ribi* promoters. The thicker arrows indicate that Stb3 primarily mediates suppression of *RP* genes while Dot6/Tod6 primarily mediate suppression of *ribi* genes. The dashed arrow labelled Tod6 is included to highlight the fact that *TOD6* belongs to the *ribi* regulon and thus participates in a feedback loop to maintain homeostasis of *ribi* gene expression. Please see text for further details.

Discussion

We show here that the three transcriptional repressors, Stb3, Dot6 and Tod6, are directly phosphorylated by the Sch9 kinase to allow physiological regulation of the *Ribi* and *RP* regulons in response to TORC1-mediated nutrient signals. These observations build on our previous analysis of the rapamycin-sensitive phosphoproteome (Huber *et al*, 2009), and on previous genetic data that implicate Stb3, Dot6 and Tod6 in the regulation of *Ribi* and *RP* genes downstream of TORC1/Sch9 and PKA (Lippman and Broach, 2009; Liko *et al*, 2010). Our analysis shows that Sch9-dependent regulation of *RP* gene transcription is mediated primarily by Stb3 whereas Sch9-dependent regulation of *Ribi* gene transcription is mediated by Dot6, Tod6 and, to a lesser extent, Stb3. We provide a mechanistic basis for the repressive activity of the three transcription factors, namely that the histone deacetylase complex RPD3L is recruited to *Ribi* and *RP* gene promoters upon Sch9 inhibition in an Stb3- and Dot6/Tod6-dependent manner. A model that encapsulates these results is presented in Figure 7.

Several observations suggest that RPD3L recruitment is the primary mechanism by which these three transcription factors repress *Ribi* and *RP* transcription: (i) Stb3, Dot6 and Tod6 interact physically with RPD3L (Supplementary Figure S8A and B) (Kasten and Stillman, 1997; Shevchenko *et al*, 2008); (ii) disruption of RPD3L phenocopies the derepression of *Ribi* and *RP* genes caused by deletion of *STB3*, *DOT6* and *TOD6* when Sch9 is inhibited (Figures 2A–C and 3A and B; Supplementary Figure S2A); (iii) the relative dependency on Stb3 versus Dot6/Tod6 for RPD3L recruitment to *Ribi* and *RP* gene promoters correlates with the transcriptional regulation of these regulons (Figures 2A and 6A; Supplementary Figure S10); and (iv) overexpression of non-phosphorylatable Dot6 and Tod6 variants impairs growth in an RPD3L-dependent manner (Figure 4B; Supplementary Figure S6A–D).

Recently, it has been suggested that Stb3 acts by recruiting the Hos2 histone deacetylase to repress transcription because deletion of *HOS2* but not *RPD3* suppressed the growth defect caused by Stb3 overexpression (Liko *et al*, 2010). However, in our strain background, deletion of *HOS2* does not suppress the severe growth phenotype observed upon $Stb3^{3A}$ overexpression (Figure 4A), nor does it alleviate the repression of Stb3-dependent *Ribi* and *RP* genes observed upon inhibition of Sch9 (Supplementary Figure S6B). In agreement with our data, two independent studies showed that Rpd3, but not Hos2, couples TORC1 signals to *Ribi* and *RP* genes (Rohde and Cardenas, 2003; Humphrey *et al*, 2004). Nevertheless, it is puzzling that RPD3L disruption did not suppress the $Stb3^{3A}$-induced slow growth phenotype in our strain background (Figure 4B). Although several explanations can be envisioned, at present we favour the hypothesis that $Stb3^{3A}$ represses *Ribi/RP* transcription not only via recruitment of RPD3L but also by displacing and/or otherwise interfering with Fhl1/Rap1 function. This hypothesis is based on our ChIP-Seq profiles, which indicate that RPD3L and Stb3 chromatin binding sites are very close to, if not coincident with, Fhl1 and Rap1 binding sites (Figure 6B). This observation suggests that $Stb3^{3A}$ could effectively interfere with Fhl1/Rap1 functions, for example by antagonizing recruitment of the critical transcriptional activator Ifh1. The predictions of this model remain to be tested.

How does Sch9 regulate Stb3, Dot6 and Tod6? Sch9 was previously shown to antagonize the nuclear accumulation of Stb3 (Liko *et al*, 2010). Notably, unlike many other regulated transcription factor complexes, we did not detect any change in Stb3 affinity for RPD3L upon Sch9 inhibition (Supplementary Figure S8A). Nucleocytoplasmic shuttling and/or the affinity of its association with chromatin are other potential points of Stb3 regulation. In contrast to Stb3, Dot6 and Tod6 localize to the nucleus in rapidly growing cells and this localization is not apparently regulated by Sch9 (data not shown). Similar to Stb3, the interactions between Dot6 or Tod6 and RPD3L also did not seem to be altered upon Sch9 inhibition (Supplementary Figure S9B). Thus, we hypothesize that Sch9-dependent phosphorylation regulates the ability of Dot6 and Tod6 to interact with chromatin. As the recruitment of Stb3 and Dot6/Tod6 appears to be interdependent (Figure 6C and D), these factors may physically interact at chromatin and/or alter the local chromatin environment to facilitate mutual interactions.

Delineating the precise roles of individual phosphorylation events in Stb3, Dot6 and Tod6 will be a challenge. Large-scale mass spectrometric studies (Chi *et al*, 2007; Bodenmiller *et al*, 2008; Huber *et al*, 2009; Soulard *et al*, 2010; Stark *et al*, 2010) suggest that these factors are phosphorylated on >50 sites in total. Furthermore, although we could not confirm previous reports that Stb3 phosphorylation is regulated by PKA (Budovskaya *et al*, 2005), we did confirm that Dot6 and Tod6 phosphorylation is regulated downstream of PKA (Figure 1B and C) (Deminoff *et al*, 2006). Thus, like Maf1 (Huber *et al*, 2009; Lee *et al*, 2009; Wei and Zheng, 2009; Ramachandran and Herman, 2011), Dot6 and Tod6 represent a convergence point for growth regulation mediated by TORC1 and PKA.

Previously, we showed that Sch9 regulates RNAPI and III transcription (Huber *et al*, 2009). Here, we demonstrate that at least part of this regulation is mediated on a relatively short timescale by Stb3 and Dot6/Tod6 (30 min Sch9 inhibition; Figure 3A–C). As we have been unable to detect binding

of any of these transcription factors to the rDNA locus (Supplementary Figure S11A–C), we speculate that this regulation occurs indirectly via the expression of *Ribi* genes, many of which encode factors involved in RNAPI/III transcription (Jorgensen *et al*, 2004; Wade *et al*, 2006). However, as deletion of *STB3*, *DOT6* and *TOD6* only partially blocks the reduction in rRNA transcription observed upon Sch9 inhibition, it is likely that another target of Sch9 involved in RNAPI regulation remains to be identified.

We also found that Stb3 influences rRNA processing. This observation was not in itself surprising as many *Ribi* gene products are implicated in this process (Jorgensen *et al*, 2004; Wade *et al*, 2006). However, the result that Stb3, which regulates primarily *RP* rather than *Ribi* transcription, seems to have an exclusive role in regulating 27S–25S and 20S–18S rRNA processing (Figure 3B) was unexpected. We note that RP synthesis and incorporation into the 40S and 60S ribosomal subunits is coupled with the maturation of the corresponding rRNAs (Ferreira-Cerca *et al*, 2005; Poll *et al*, 2009; Reiter *et al*, 2011).

We have shown previously that Ribi influences not only growth rate but also the critical cell size threshold (Jorgensen *et al*, 2002, 2004). This effect of Ribi on cell size is independent from effects on protein synthesis *per se* (Jorgensen *et al*, 2004). We found that Stb3 affects the rate of cell growth more potently than Dot6/Tod6 (Figure 2B), consistent with the predominant effects of Stb3 on *RP* gene expression. In contrast, Dot6/Tod6 have a greater influence on cell size than Stb3 (Figure 2C), also consistent with their primary effect on the *Ribi* regulon. As deletion of *STB3*, *DOT6* and *TOD6* did not completely alleviate the small size caused by Sch9 inhibition, we again infer the existence of other Sch9 effectors for cell size. These observations will serve as a starting point to further dissect how the Ribi machinery communicates growth potential to the cell division machinery at Start.

Finally, our studies have uncovered an additional feedback loop in ribosome biogenesis, namely the autoregulation of Tod6 activity in the control of *Ribi* gene expression (Figure 5C and D; Supplementary Figures S6 and S7). This negative transcriptional feedback mechanism in principle imposes homeostatic control on Ribi (Supplementary Figure S6), and may act in concert with previously reported signalling feedback loops on Sch9 and Sfp1 (Jorgensen *et al*, 2004; Mnaimneh *et al*, 2004; Lempiainen *et al*, 2009). Understanding the complex interactions of these feedback loops as the primary means of establishing homeostatic control of ribosome biogenesis will be an intriguing and challenging area of future research.

Materials and methods

Yeast strains and growth assays

S. cerevisiae strains and plasmids are described in Supplementary Tables S4 and S5, respectively. Strains were constructed according to the standard protocols. Unless specified otherwise, rapamycin was used at 200 nM (from a 1-mM stock solution in 90% ethanol, 10% Tween-20), and 1NM-PP1 at 300 nM (from 1 mM or 10 mM stocks in DMSO).

For growth rate assays, cells growing exponentially were diluted in the indicated media to an OD_{600} of $\leqslant 0.025$ and 200 μl aliquots were dispensed in transparent 96-well plates. Wells were loaded with medium without cells to serve as reference. The plates were incubated at 30°C and OD_{600} was measured every 15 min for each well in a Sunrise microplate reader (Tecan, Switzerland). Reference values measured from medium alone were subtracted from all measurements. Doubling times were calculated from the slopes of linear regressions on the OD_{600} after Log2 transformation as a function of time once the cultures reached an OD_{600} of 0.2.

Cell size assays were performed on exponential phase cultures using a Z2 Coulter counter, as described previously (Jorgensen *et al*, 2002).

Denaturing protein extraction and immunoprecipitation

Denaturing protein extracts were performed using the TCA-Urea method as described previously (Urban *et al*, 2007). For immunoprecipitation, denatured extracts were diluted 10-fold in native lysis buffer (PBS 10% glycerol 0.5% Tween-20) supplemented with 10 mM NaF, 10 mM *p*-nitrophenylphosphate, 10 mM $Na_2P_2O_4$, 10 mM β-glycerophosphate, 1 × Roche protease inhibitor cocktail and 1 mM PMSF and cleared by centrifugation at full speed in a microcentrifuge. A total of 10 μl anti-HA sepharose beads was added to the supernatants, incubated for 2 h at 4°C and washed 3 × with native lysis buffer. Immunoprecipitated proteins were analysed by western blotting with anti-HA and anti R[R/K]x[S/T]* (Cell Signaling) antibodies.

Sch9 kinase assays

TAP–Sch9 variants were expressed and purified as described previously (Huber *et al*, 2009) except that magnetic beads coated with rabbit IgG (Invitrogen) were used instead of glutathione-coated sepharose beads and the purified kinase was not eluted from the beads. Recombinant GST, GST–Stb3, GST–Dot6 and GST–Tod6 fusion protein variants were expressed using the pGEX6P1 system as described previously (Huber *et al*, 2009) except that the proteins were eluted using PBS 20% glycerol 0.5% Tween-20 supplemented with 20 mM reduced glutathione for 15 min at room temperature. Sch9 kinase assays were performed as described previously (Huber *et al*, 2009).

mRNA sequencing

RNA extracts were purified of genomic DNA contaminations using RNeasy kits (Qiagen). Libraries were prepared from pools of equivalent amounts of RNA from four independent experiments and sequenced using version 4 kits and single read flow cells on Genome Analyzer IIx machine according to the manufacturer's instructions (Illumina). Sequencing reads were mapped to the transcriptome of *S. cerevisiae* using the QSeq software with standard parameters (DNAStar). Minimal thresholds of 20 reads in each condition and 100 reads in at least one condition were applied to all transcripts. The relative expression of 5083 transcripts meeting these criteria was calculated by normalizing their reads counts to the total number of reads in each condition. A summary of the libraries' sequencing and reads mapping to yeast ORFs is shown in Supplementary Table S6. We defined as *Ribi* genes the first 500 non-*RP* genes in the ranking list of Wade *et al* (2006). Raw sequence files are available in the GEO database (http://www.ncbi.nlm.nih.gov/geo/; accession number: GSE29122).

Miller spreads

'Miller' chromatin spreads were prepared according to French *et al* (2003). All areas of the grids containing dispersed nucleoli were photographed. The number of RNA polymerase I molecules on each visible 35S rRNA gene was counted by hand on enlarged micrographs. To be included, the chromatin strand on which the gene occurred needed to be sufficiently long to encompass the entire length of the gene.

^{3}H-uracil pulse-labelling assays

^{3}H-uracil pulse-labelling assays were performed as described previously (Huber *et al*, 2009) with the following modifications. Briefly, cells were made prototroph and grown in SC-URA at 25°C. In all, 10 ml aliquots were removed and pulsed with 25 μCi ^{3}H-uracil for 20 min. Cold uracil was added at a 100-fold molar excess and cells were grown 20 more minutes before harvest and total RNA extraction. RNA was resolved by gel electrophoresis and transferred to membranes. Its loading was controlled by ethidium bromide staining and the incorporation of ^{3}H-uracil was determined by exposure to phosphorimager screens.

Quantitative western blotting

The Li-Cor infrared fluorescent system was used for quantitative western blotting. All antibodies were incubated in PBS 0.01%

Tween-20 (PBST) supplemented with 5% BSA. Washing steps were performed using PBST. After 1 h blocking in PBST 5% BSA, membranes were probed overnight with mouse anti-HA and rabbit anti-Hog1 antibodies. Membranes were washed three times with PBST and the primary antibodies were detected with anti-mouse and anti-rabbit secondary antibodies coupled to the infrared dyes IRDye800® (Rockland, PA, USA) and IRDye680® (Li-Cor, NE, USA), respectively. After three washes, fluorescence was detected using the Odyssey® IR imaging system (Li-Cor). The ImageJ software was used for quantification (Abramoff *et al*, 2004).

ChIP assays

ChIP assays were performed and quantified by qPCR using the SYBR Green system as described previously (Bianchi *et al*, 2004) with slight modifications. Briefly, cells were fixed with 1% formaldehyde for 10 min at room temperature. Fixation was stopped with 125 mM glycine and cells were harvested by centrifugation. The extracted chromatin was sheared in a bioruptor sonicator (Diagenode) for 20 min (30 s on; 30 s off) at full power. IPs were performed using pan-mouse IgG beads (Dynal, Invitrogen) and were quantified using primers (Supplementary Table S7) for the indicated loci and normalized by qPCR DNA purified from the IP input. IP efficiency was normalized with a similar quantification for the *ADH4* locus as a control.

For ChIP-Seq experiments, ChIPs were scaled up by a factor of six (240 ml of culture at an OD_{600} of 0.5) and chromatin was sheared in aliquots of 300 µl for 30 min instead of 20 with otherwise identical settings. ChIPs were repeated three times (untagged controls were repeated nine times). The immunopurified DNA was pooled, crosslinks were reversed overnight at 65°C and the DNA was purified using Qiagen PCR purification kits. The DNA was eluted with 40 µl of the supplied elution buffer and stored at −80°C until further analysis. Libraries were prepared using ChIP-Seq sample preparation kits (Illumina) according to the manufacturer's instructions. DNA fragments ends were repaired using a mix of Klenow DNA polymerase, T4 DNA polymerase and T4 polynucleotide kinase. DNA was then purified and 3′ A overhangs were added using a Klenow fragment (3′–5′ exo minus). DNA was purified again and ligated to adapters. In all, 190 ± 10 bp fragments were selected using the E-Gel SizeSelect system (Invitrogen) and purified. Fragments with adapters were finally enriched with 18 cycles of PCR and purified. High-throughput sequencing of libraries was performed on a Genome Analyzer IIx machine (Illumina) each in a separate channel. Sequencing reads were mapped on SGD1.01 genome assembly using Bowtie 0.12.1 (Langmead *et al*, 2009), with parameters *-n 3 –best –strata –solexa1.3-quals -a -m 20* and viewed with the USCS Genome Browser (Kent *et al*, 2002). Libraries sequencing and reads alignment to the yeast genome are summarized in Supplementary Table S8. The MACS algorithm v 1.7.3.1 (Zhang *et al*, 2008) was used to detect Sds3–TAP binding peaks by comparing the mapped read counts obtained from the *sch9^{as}SDS3–TAP* versus the untagged *sch9^{as}* strains with parameters *–mfold = 2 –P value = 1e−5*. Raw sequence files are available in the GEO database (GSE29124).

Supplementary data

Supplementary data are available at *The EMBO Journal* Online (http://www.embojournal.org).

Acknowledgements

We thank David Shore and RL laboratory members for comments on draft manuscripts. We are grateful for all the high-throughput sequencing performed at the Genomics platform of the National Center of Competence in Research 'Frontiers in Genetics' and their computational analysis performed at the Vital-IT Center for high-performance computing of the Swiss Institute of Bioinformatics (http://www.vital-it.ch). AH was recipient of a fellowship from the Novartis Foundation for Biology and Medicine. RL is the recipient of a professorship from the Swiss National Science Foundation (PP00P3-110770/3100A0-108114) and receives generous support from the canton of Genève, the National Centers of Competence in Research 'Frontiers in Genetics' and 'Chemical Biology', the Leenaards Foundation, and the European Research Council (ERC-2007-StG 206173-TOR signalling). ALB acknowledges funding by the NIH (GM63952). MT acknowledges support from the Wellcome Trust, a Royal Society Wolfson Research Merit Award and the Scottish Universities Life Sciences Alliance. JR is supported by the SystemsX.ch initiative and the EPFL.

Author contributions: Miller chromatin spreads were performed by SF. Cell sizes were measured by HT. SY performed western blot analyses (Supplementary Figures S5A and S6C). MS carried out western blot analysis (Figure 1B) and protein determinations by flow cytometry. MPP performed RT–qPCR measurements (Supplementary Figure S5B). High-throughput sequencing data mapping and analysis was carried out by JR. All other experiments and analyses were carried out by AH. MT, ALB and RL contributed to experimental design and supervision. AH wrote the manuscript with the help of HT, SF, MT, ALB and RL.

Conflict of interest

The authors declare that they have no conflict of interest.

References

Abramoff MD, Magalhaes PJ, Ram SJ (2004) Image processing with ImageJ. *Biophoton Int* **11:** 36–41

Badis G, Chan ET, van Bakel H, Pena-Castillo L, Tillo D, Tsui K, Carlson CD, Gossett AJ, Hasinoff MJ, Warren CL, Gebbia M, Talukder S, Yang A, Mnaimneh S, Terterov D, Coburn D, Li Yeo A, Yeo ZX, Clarke ND, Lieb JD *et al* (2008) A library of yeast transcription factor motifs reveals a widespread function for Rsc3 in targeting nucleosome exclusion at promoters. *Mol Cell* **32:** 878–887

Bianchi A, Negrini S, Shore D (2004) Delivery of yeast telomerase to a DNA break depends on the recruitment functions of Cdc13 and Est1. *Mol Cell* **16:** 139–146

Bodenmiller B, Campbell D, Gerrits B, Lam H, Jovanovic M, Picotti P, Schlapbach R, Aebersold R (2008) PhosphoPep—a database of protein phosphorylation sites in model organisms. *Nat Biotechnol* **26:** 1339–1340

Breitkreutz A, Choi H, Sharom JR, Boucher L, Neduva V, Larsen B, Lin ZY, Breitkreutz BJ, Stark C, Liu G, Ahn J, Dewar-Darch D, Reguly T, Tang X, Almeida R, Qin ZS, Pawson T, Gingras AC, Nesvizhskii AI, Tyers M (2010) A global protein kinase and phosphatase interaction network in yeast. *Science* **328:** 1043–1046

Budovskaya YV, Stephan JS, Deminoff SJ, Herman PK (2005) An evolutionary proteomics approach identifies substrates of the cAMP-dependent protein kinase. *Proc Natl Acad Sci USA* **102:** 13933–13938

Carrozza MJ, Florens L, Swanson SK, Shia W-J, Anderson S, Yates J, Washburn MP, Workman JL (2005a) Stable incorporation of sequence specific repressors Ash1 and Ume6 into the Rpd3L complex. *Biochim Biophys Acta* **1731:** 77–87

Carrozza MJ, Li B, Florens L, Suganuma T, Swanson SK, Lee KK, Shia WJ, Anderson S, Yates J, Washburn MP, Workman JL (2005b) Histone H3 methylation by Set2 directs deacetylation of coding regions by Rpd3S to suppress spurious intragenic transcription. *Cell* **123:** 581–592

Chi A, Huttenhower C, Geer LY, Coon JJ, Syka JE, Bai DL, Shabanowitz J, Burke DJ, Troyanskaya OG, Hunt DF (2007) Analysis of phosphorylation sites on proteins from Saccharomyces cerevisiae by electron transfer dissociation (ETD) mass spectrometry. *Proc Natl Acad Sci USA* **104:** 2193–2198

Deminoff SJ, Howard SC, Hester A, Warner S, Herman PK (2006) Using substrate-binding variants of the cAMP-dependent protein kinase to identify novel targets and a kinase domain important for substrate interactions in Saccharomyces cerevisiae. *Genetics* **173:** 1909–1917

De Virgilio C, Loewith R (2006) Cell growth control: little eukaryotes make big contributions. *Oncogene* **25:** 6392–6415

Ferreira-Cerca S, Poll G, Gleizes PE, Tschochner H, Milkereit P (2005) Roles of eukaryotic ribosomal proteins in maturation and transport of pre-18S rRNA and ribosome function. *Mol Cell* **20:** 263–275

Freckleton G, Lippman SI, Broach JR, Tavazoie S (2009) Microarray profiling of phage-display selections for rapid mapping of transcription factor-DNA interactions. *PLoS Genet* **5:** e1000449

French SL, Osheim YN, Cioci F, Nomura M, Beyer AL (2003) In exponentially growing Saccharomyces cerevisiae cells, rRNA synthesis is determined by the summed RNA polymerase I loading rate rather than by the number of active genes. *Mol Cell Biol* **23:** 1558–1568

Harbison CT, Gordon DB, Lee TI, Rinaldi NJ, Macisaac KD, Danford TW, Hannett NM, Tagne J-B, Reynolds DB, Yoo J, Jennings EG, Zeitlinger J, Pokholok DK, Kellis M, Rolfe PA, Takusagawa KT, Lander ES, Gifford DK, Fraenkel E, Young RA (2004) Transcriptional regulatory code of a eukaryotic genome. *Nature* **431:** 99–104

Heitman J, Movva NR, Hall MN (1991) Targets for cell cycle arrest by the immunosuppressant rapamycin in yeast. *Science* **253:** 905–909

Huber A, Bodenmiller B, Uotila A, Stahl M, Wanka S, Gerrits B, Aebersold R, Loewith R (2009) Characterization of the rapamycin-sensitive phosphoproteome reveals that Sch9 is a central coordinator of protein synthesis. *Genes Dev* **23:** 1929–1943

Hughes JD, Estep PW, Tavazoie S, Church GM (2000) Computational identification of cis-regulatory elements associated with groups of functionally related genes in Saccharomyces cerevisiae. *J Mol Biol* **296:** 1205–1214

Humphrey EL, Shamji AF, Bernstein BE, Schreiber SL (2004) Rpd3p relocation mediates a transcriptional response to rapamycin in yeast. *Chem Biol* **11:** 295–299

Jorgensen P, Nishikawa JL, Breitkreutz BJ, Tyers M (2002) Systematic identification of pathways that couple cell growth and division in yeast. *Science* **297:** 395–400

Jorgensen P, Rupes I, Sharom JR, Schneper L, Broach JR, Tyers M (2004) A dynamic transcriptional network communicates growth potential to ribosome synthesis and critical cell size. *Genes Dev* **18:** 2491–2505

Jorgensen P, Tyers M (2004) How cells coordinate growth and division. *Curr Biol* **14:** R1014–R1027

Ju Q, Warner JR (1994) Ribosome synthesis during the growth cycle of Saccharomyces cerevisiae. *Yeast* **10:** 151–157

Kasten MM, Stillman DJ (1997) Identification of the Saccharomyces cerevisiae genes STB1-STB5 encoding Sin3p binding proteins. *Mol Gen Genet* **256:** 376–386

Kent WJ, Sugnet CW, Furey TS, Roskin KM, Pringle TH, Zahler AM, Haussler D (2002) The human genome browser at UCSC. *Genome Res* **12:** 996–1006

Laferte A, Favry E, Sentenac A, Riva M, Carles C, Chedin S (2006) The transcriptional activity of RNA polymerase I is a key determinant for the level of all ribosome components. *Genes Dev* **20:** 2030–2040

Langmead B, Trapnell C, Pop M, Salzberg SL (2009) Ultrafast and memory-efficient alignment of short DNA sequences to the human genome. *Genome Biol* **10:** R25

Lee J, Moir RD, Willis IM (2009) Regulation of RNA polymerase III transcription involves SCH9-dependent and SCH9-independent branches of the target of rapamycin (TOR) pathway. *J Biol Chem* **284:** 12604–12608

Lempiainen H, Shore D (2009) Growth control and ribosome biogenesis. *Curr Opin Cell Biol* **21:** 855–863

Lempiainen H, Uotila A, Urban J, Dohnal I, Ammerer G, Loewith R, Shore D (2009) Sfp1 interaction with TORC1 and Mrs6 reveals feedback regulation on TOR signaling. *Mol Cell* **33:** 704–716

Liko D, Conway MK, Grunwald DS, Heideman W (2010) Stb3 plays a role in the glucose-induced transition from quiescence to growth in Saccharomyces cerevisiae. *Genetics* **185:** 797–810

Liko D, Slattery MG, Heideman W (2007) Stb3 binds to ribosomal RNA processing element motifs that control transcriptional responses to growth in Saccharomyces cerevisiae. *J Biol Chem* **282:** 26623–26628

Lippman SI, Broach JR (2009) Protein kinase A and TORC1 activate genes for ribosomal biogenesis by inactivating repressors encoded by Dot6 and its homolog Tod6. *Proc Natl Acad Sci USA* **106:** 19928–19933

Martin DE, Soulard A, Hall MN (2004) TOR regulates ribosomal protein gene expression via PKA and the Forkhead transcription factor FHL1. *Cell* **119:** 969–979

Mnaimneh S, Davierwala AP, Haynes J, Moffat J, Peng WT, Zhang W, Yang X, Pootoolal J, Chua G, Lopez A, Trochesset M, Morse D, Krogan NJ, Hiley SL, Li Z, Morris Q, Grigull J, Mitsakakis N, Roberts CJ, Greenblatt JF *et al* (2004) Exploration of essential gene functions via titratable promoter alleles. *Cell* **118:** 31–44

Oficjalska-Pham D, Harismendy O, Smagowicz WJ, Gonzalez de Peredo A, Boguta M, Sentenac A, Lefebvre O (2006) General repression of RNA polymerase III transcription is triggered by protein phosphatase type 2A-mediated dephosphorylation of Maf1. *Mol Cell* **22:** 623–632

Peyroche G, Milkereit P, Bischler N, Tschochner H, Schultz P, Sentenac A, Carles C, Riva M (2000) The recruitment of RNA polymerase I on rDNA is mediated by the interaction of the A43 subunit with Rrn3. *EMBO J* **19:** 5473–5482

Philippi A, Steinbauer R, Reiter A, Fath S, Leger-Silvestre I, Milkereit P, Griesenbeck J, Tschochner H (2010) TOR-dependent reduction in the expression level of Rrn3p lowers the activity of the yeast RNA Pol I machinery, but does not account for the strong inhibition of rRNA production. *Nucleic Acids Res* **38:** 5315–5326

Poll G, Braun T, Jakovljevic J, Neueder A, Jakob S, Woolford Jr JL, Tschochner H, Milkereit P (2009) rRNA maturation in yeast cells depleted of large ribosomal subunit proteins. *PLoS One* **4:** e8249

Ramachandran V, Herman PK (2011) Antagonistic interactions between the cAMP-dependent protein kinase and Tor signaling pathways modulate cell growth in Saccharomyces cerevisiae. *Genetics* **187:** 441–454

Reiter A, Steinbauer R, Philippi A, Gerber J, Tschochner H, Milkereit P, Griesenbeck J (2011) Reduction in ribosomal protein synthesis is sufficient to explain major effects on ribosome production after short-term TOR inactivation in Saccharomyces cerevisiae. *Mol Cell Biol* **31:** 803–817

Roberts DN, Wilson B, Huff JT, Stewart AJ, Cairns BR (2006) Dephosphorylation and genome-wide association of Maf1 with Pol III-transcribed genes during repression. *Mol Cell* **22:** 633–644

Rohde JR, Cardenas ME (2003) The tor pathway regulates gene expression by linking nutrient sensing to histone acetylation. *Mol Cell Biol* **23:** 629–635

Rudra D, Zhao Y, Warner JR (2005) Central role of Ifh1p-Fhl1p interaction in the synthesis of yeast ribosomal proteins. *EMBO J* **24:** 533–542

Schawalder SB, Kabani M, Howald I, Choudhury U, Werner M, Shore D (2004) Growth-regulated recruitment of the essential yeast ribosomal protein gene activator Ifh1. *Nature* **432:** 1058–1061

Shevchenko A, Roguev A, Schaft D, Buchanan L, Habermann B, Sakalar C, Thomas H, Krogan NJ, Stewart AF (2008) Chromatin central: towards the comparative proteome by accurate mapping of the yeast proteomic environment. *Genome Biol* **9:** R167

Shokat K, Velleca M (2002) Novel chemical genetic approaches to the discovery of signal transduction inhibitors. *Drug Discov Today* **7:** 872–879

Singh J, Tyers M (2009) A Rab escort protein integrates the secretion system with TOR signaling and ribosome biogenesis. *Genes Dev* **23:** 1944–1958

Soulard A, Cremonesi A, Moes S, Schutz F, Jeno P, Hall MN (2010) The rapamycin-sensitive phosphoproteome reveals that TOR controls protein kinase A toward some but not all substrates. *Mol Biol Cell* **21:** 3475–3486

Stark C, Su T-C, Breitkreutz A, Lourenco P, Dahabieh M, Breitkreutz B-J, Tyers M, Sadowski I (2010) PhosphoGRID: a database of experimentally verified *in vivo* protein phosphorylation sites from the budding yeast Saccharomyces cerevisiae. *Database* **2010:** bap026

Upadhya R, Lee J, Willis IM (2002) Maf1 is an essential mediator of diverse signals that repress RNA polymerase III transcription. *Mol Cell* **10:** 1489–1494

Urban J, Soulard A, Huber A, Lippman S, Mukhopadhyay D, Deloche O, Wanke V, Anrather D, Ammerer G, Riezman H, Broach JR, De Virgilio C, Hall MN, Loewith R (2007) Sch9 is a major target of TORC1 in Saccharomyces cerevisiae. *Mol Cell* **26:** 663–674

Wade CH, Umbarger MA, McAlear MA (2006) The budding yeast rRNA and ribosome biosynthesis (RRB) regulon contains over 200 genes. *Yeast* **23:** 293–306

Wade JT, Hall DB, Struhl K (2004) The transcription factor Ifh1 is a key regulator of yeast ribosomal protein genes. *Nature* **432:** 1054–1058

Warner JR (1999) The economics of ribosome biosynthesis in yeast. *Trends Biochem Sci* **24:** 437–440

Wei Y, Zheng XF (2009) Sch9 partially mediates TORC1 signaling to control ribosomal RNA synthesis. *Cell Cycle* **8:** 4085–4090

Yorimitsu T, Zaman S, Broach JR, Klionsky DJ (2007) Protein kinase A and Sch9 cooperatively regulate induction of autophagy in Saccharomyces cerevisiae. *Mol Biol Cell* **18:** 4180–4189

Zaman S, Lippman SI, Zhao X, Broach JR (2008) How Saccharomyces responds to nutrients. *Ann Rev Genet* **42:** 27–81

Zaragoza D, Ghavidel A, Heitman J, Schultz MC (1998) Rapamycin induces the G0 program of transcriptional repression in yeast by interfering with the TOR signaling pathway. *Mol Cell Biol* **18:** 4463–4470

Zhang Y, Liu T, Meyer C, Eeckhoute J, Johnson D, Bernstein B, Nusbaum C, Myers R, Brown M, Li W, Liu XS (2008) Model-based analysis of ChIP-Seq (MACS). *Genome Biol* **9:** R137

Zhu C, Byers K, McCord R, Shi Z, Berger M, Newburger D, Saulrieta K, Smith Z, Shah M, Radhakrishnan M, Philippakis A, Hu Y, De Masi F, Pacek M, Rolfs A, Murthy T, Labaer J, Bulyk ML (2009) High-resolution DNA binding specificity analysis of yeast transcription factors. *Genome Res* **19:** 556–566

Section II. Characterization of Ccr4 as a Downstream Effector of TORC1

TORC1-dependent Phosphorylation of Ccr4 and Pop2

In various large-scale studies, deletion strains of some components of the mRNA decay pathway such as *Ccr4, Pop2, Dhh1* or *Pat1* were found to be hypersensitive to rapamycin (Dudley et al, 2005; Huber et al, 2009; Xie et al, 2005). To probe this further, we compared the growth phenotypes of these strains in the presence of rapamycin or at different temperatures. The results showed that *ccr4, pop2* and *pat1* strains exhibit similar sensitivities to rapamycin and cold temperature, whereas the *dhh1* strain is relatively resistant, but still more sensitive to stress conditions than the wild type strain (Figure 7A). In contrast to the other strains, the *pop2* strain showed hypersensitivity to high temperature suggesting that different components of the mRNA degradation pathway have both related and distinct roles in the cell. Furthermore, we showed that overexpression of *Ccr4* and *Pop2* also render the cells hypersensitive to rapamycin (Figure 7B) implying that fine-tuned levels of these proteins are important for proper cellular functioning.

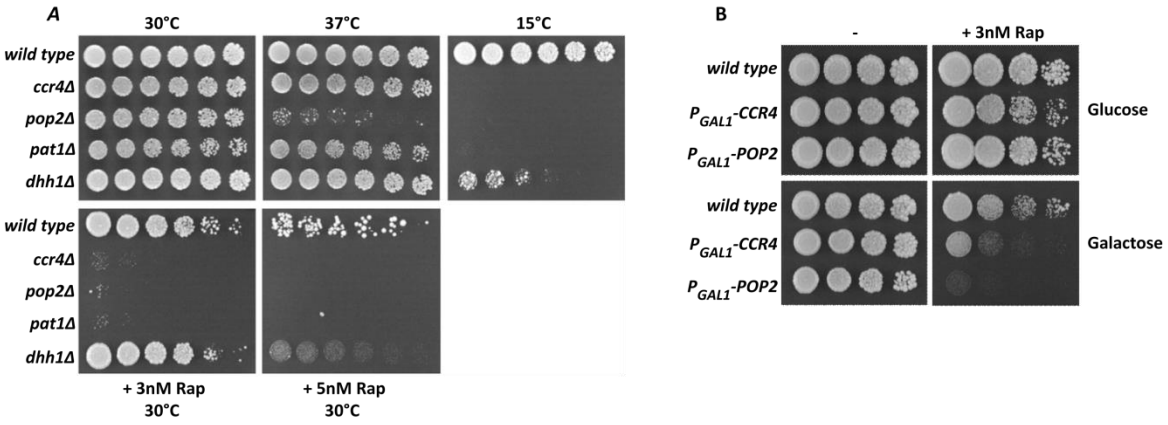

Figure 7. Phenotypes associated with deletion and overexpression of *CCR4* and *POP2*.

(A-B)Ten-fold dilutions of the indicated strains were spotted on YPD or YPGal with or without rapamycin and grown for 2-3 days.

In a recent study published by our laboratory, phosphoproteomes of rapamycin- and vehicle-treated cells were compared with the aim of finding novel downstream elements of TORC1-signaling

pathway (Huber et al, 2009). In this study, two rapamycin-responsive phosphopeptides were mapped to Ccr4 and Pat1. For further investigation of the rapamycin effect on these proteins, we analyzed their electrophoretic mobility in SDS-PAGE gel and showed that Ccr4 tagged with three HA-epitopes migrated as one slower band on the gel upon rapamycin and wortmannin treatments which inhibit TORC1. Cycloheximide treatment, which activates TORC1, resulted in a collapse into one faster migrating band (Figure 8A). However, we did not detect any change in the migration pattern of Pat1 (Yıldız Koca & Michael Stahl, unpublished data). That the changes in the electrophoretic mobility of Ccr4 were indeed due to the changes in its phosphorylation status was further confirmed by abolishment of the effect following phosphatase treatment (Figure 8B).

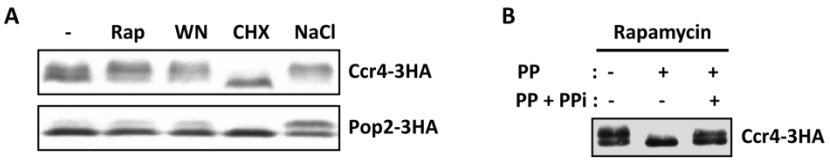

Figure 8. Rapamycin-sensitive phosphorylation of Ccr4 and Pop2

(A) Wild type cells expressing the indicated tagged proteins were grown in YPD to exponential phase and treated with either rapamycin (Rap), wortmannin (WN), cycloheximide (CHX) or sodium chloride (NaCl) for 20min. Anti-HA antibody was used for the detection of HA-tagged proteins. (B) Following the native preparation of the total extract, HA-tagged Ccr4 was immunoprecipitated using an anti-HA antibody. Three aliquots were prepared and were treated with either water, lambda phosphatase (PP) or lambda phosphatase with phosphatase inhibitor mix (PPi).

The deadenylation step was proposed to be the rate-limiting step of mRNA decay (He & Parker, 1999), suggesting that regulation of mRNA deadenylation can be an important means of regulation of gene expression. Taking all these into account, we decided to focus on the regulation of Ccr4 and Pop2 by TORC1. Pop2 displayed a very similar migration pattern to that of Ccr4 on the gel; hyperphosphorylation upon rapamycin and wortmannin, and dephosphorylation after cycloheximide treatment (Figure 8A). A time course of rapamycin treatment showed that hyperphosphorylation of Ccr4 was stable for up to two hours; however the protein, itself, was not (Figure 9A). Interestingly,

the phosphorylation status of Pop2 seemed to change throughout the time course (Figure 9A). Given that TORC1 is regulated by a variety of nutrient sources, we investigated whether Ccr4 and Pop2 phosphorylation levels were responsive to changes in nutrient levels. As expected, both proteins became hyperphosphorylated under carbon- and nitrogen-source starvation conditions (Figure 9B-C).

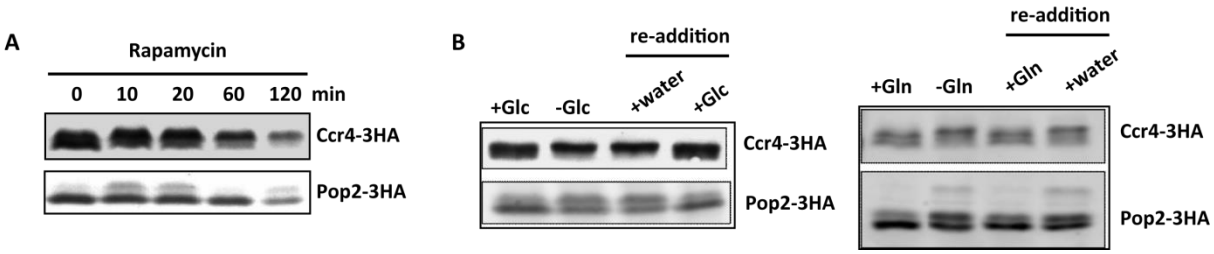

Figure 9. Phosphorylation of Ccr4 and Pop2 is regulated by rapamycin and nutrients.

(A) Exponentially growing cells were treated with 200nM rapamycin for the indicated time points. (B-C) Prototroph strains were grown in YNB(-N) with 2% glucose and 0.2% glutamine. First samples were collected as cells entered exponential growth phase. The rest of the cells were spun down, washed once and resuspended in YNB(-N) with either 0.2% glutamine or 2% glucose. Samples were collected following 20 minutes of incubation at 30°C. The rest of the cultures were split into two and treated with water or 2% glucose / 0.2% glutamine. After 20 minutes of incubation, all the samples were collected and treated with TCA to freeze metabolism prior to protein extraction.

Besides their well-defined roles in mRNA deadenylation, Ccr4 and Pop2 are known to be a part of a larger protein complex, the Ccr4-Not complex. Next, we wanted to see whether other proteins in the complex possessed rapamycin-dependent phosphorylation as well. Not4 and Not5 also displayed slower migration on the gel upon rapamycin treatment just like Ccr4 and Pop2 suggesting that the complex, itself, could be a target of TORC1 signaling pathway (Figure 10).

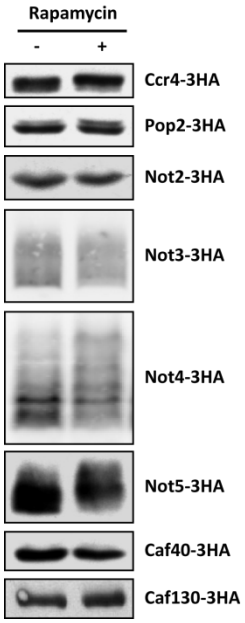

Figure 10. The Ccr4-Not complex as a target of TORC1

Exponentially growing cells with the indicated tagged-proteins were treated with 200nM rapamycin for 20 minutes.

Identification of the Components of TORC1 Pathway Involved in Ccr4/Pop2 Regulation

To further investigate the mechanism by which TORC1 controls Ccr4 and Pop2, we started to seek other components involved in this regulation. We first checked whether Ccr4 or Pop2 regulation was downstream of the known effectors of TORC1. Thus, we benefited from the *SCH9*^{DE} allele which renders the protein able to function independently from TORC1 (Urban et al, 2007), and the *tip41* strain which partially overcomes the rapamycin-dependency of Tap42-branch of TORC1 signaling pathway (Jacinto et al, 2001). We showed that rapamycin-dependent phosphorylation of Pop2 was mediated by Sch9 (Figure 11A). However, Sch9 dependency of Ccr4 phosphorylation upon rapamycin was only partial. Thereafter, we followed a biased approach to address the other kinases responsible for the phosphorylation of Ccr4 and Pop2. Thus, we focused on the kinases which were previously implicated in either TORC1 signaling or the Ccr4-Not complex function such as Yak1 (Moriya et al, 2001), Hsl1 (Traven et al, 2009), Dbf2 (Liu et al, 1997), Mck1, Kns1 (Lee et al, 2012) and Rim15 (Wei et al, 2008). We compared the electrophoretic mobility of Ccr4 and Pop2 in the deletion backgrounds

of the aforementioned kinases before and after rapamycin treatment. The absence of Rim15 resulted in the abolishment of rapamycin-dependent phosphorylation of Pop2 (Figure 11B) suggesting that Rim15 mediates the signal from TORC1 to Pop2. However, whether Rim15 is the kinase which directly phosphorylates Pop2 following the inhibition of TORC1 activity requires further investigation. No effect was detected in the deletion backgrounds for any other proteins tested (data not shown). We could confirm the role of Yak1 in phosphorylation of Pop2 upon glucose deprivation as published before but found no role for Yak1 upstream of Ccr4 (Figure 11C) (Moriya et al, 2001). Glucose-dependent phosphorylation of Ccr4 or Pop2 did not seem to be dependent on Sch9 suggesting that independent pathways regulating these phosphorylation events under different conditions (Figure 11D). Similarly, salt-dependent phosphorylation of Ccr4 was not mediated by Sch9 leaving open the question of which physiological condition regulates TORC1-dependent hyper-phosphorylation of Ccr4/Pop2 (Figure 11E).

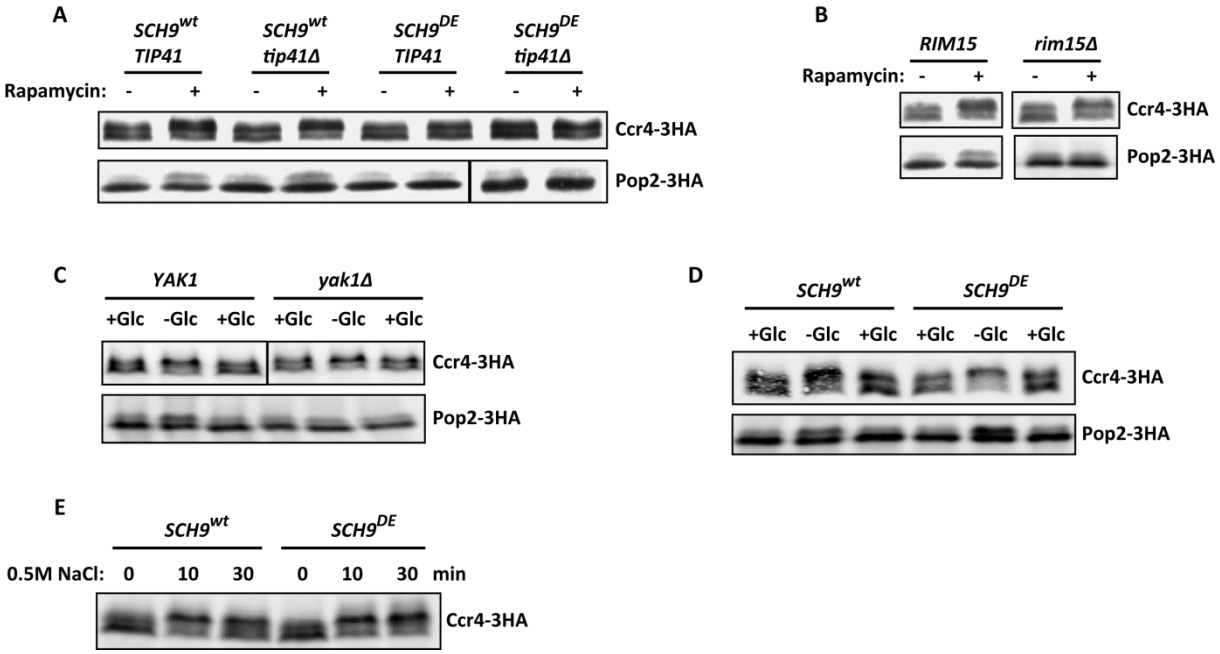

Figure 11. Sch9 contributes to rapamycin-dependent phosphorylation of both Ccr4 and Pop2.

(A-B) Indicated strains were treated with 200nM rapamycin or vehicle for 20 minutes. (C-D) When the cells reached exponential growth phase in YPD, the first set of samples were collected and treated with TCA. Following washing, cells were resuspended in YP and incubated for 20 minutes, and then cells were treated with 2% glucose and incubated for another 20 minutes. (E) Indicated strains were treated with 0.5M sodium chloride for 10 or 30 minutes.

Identification of the Rapamycin-sensitive Phosphorylation Sites on Ccr4 and Pop2

Next, we mapped the phosphorylation sites in TAP-tagged Ccr4 and Pop2 purified from rapamycin- or vehicle-treated samples by mass spectrometry. Three rapamycin-responsive phosphorylation sites were identified in Ccr4, whereas only one phosphorylation site was found in Pop2 (Figure 12A). The three sites in Ccr4 were found to be in close proximity to the central domain which includes several tandem copies of a leucine-rich-repeat domain (Malvar et al, 1992). This domain was proposed to be required for the interaction with Pop2, other components of the Ccr4-Not complex and also other potential binding partners (Draper et al, 1995; Liu et al, 2001) suggesting that TORC1-dependent phosphorylation of Ccr4 may be regulating its interaction with its binding partners. The single phosphorylation site in Pop2 was found to reside in the N-terminus of the protein.

Conversion of serine 278 to alanine abolished the phosphorylation of Ccr4, but we still observed a very slight response to rapamycin (Figure 12B). Therefore, we also mutated two more residues which came out in the mass spectrometry analysis, and are in close proximity to serine 278. In this case, Ccr4 appeared to lose all the phosphorylation under normal conditions, and also its hyperphosphorylation upon rapamycin (Figure 12B).

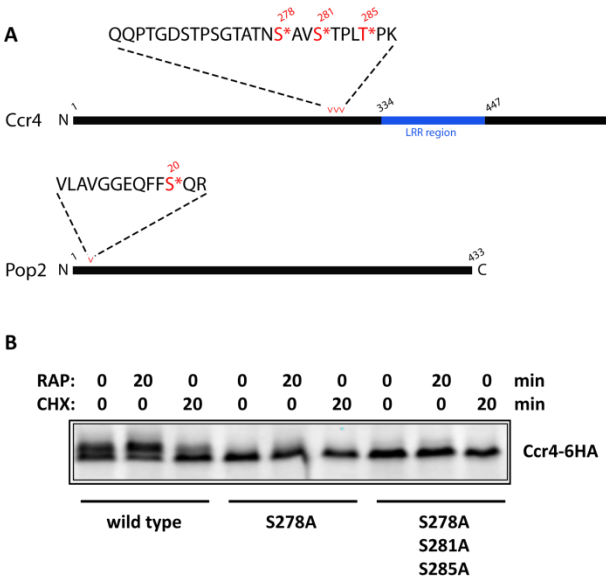

Figure 12. Rapamycin-sensitive phosphorylation sites on Ccr4 and Pop2

(A) TAP-tagged Ccr4 and Pop2 strains were treated with 200nM rapamycin for 20 minutes once they reached the exponential growth phase. Subsequently, proteins were extracted and tagged proteins were immunoprecipitated using IgG-coupled beads. Immunoprecipitated proteins were separated by SDS-PAGE gel and stained with coomassie. The bands corresponding to TAP-tagged Ccr4 and Pop2 were cut out and sent to Gustav Ammarer's laboratory in Vienna for mass spectrometric analysis of the phosphorylation sites. (B) The relevant phosphosites on Ccr4 were substituted with alanine using PCR-based techniques. The cells bearing the indicated plasmids were treated with 200nM rapamycin or 25µg/ml cycloheximide for 20 minutes.

However, this non-phosphorylatable version of Ccr4 ($Ccr4^{3A}$) seemed to function like the wild-type protein upon rapamycin since the expression of $Ccr4^{3A}$ was able to rescue the rapamycin-hypersensitive phenotype of *ccr4* strain (Figure 13). We also mutated these 3 phosphorylation sites into glutamate so as to obtain a phosphomimetic form of the protein and we sought out growth

phenotypes of these mutants under a variety of conditions. Deletion of *CCR4* rendered the cells hypersensitive to rapamycin, cycloheximide, low temperature and use of raffinose as a carbon source; however, all these sensitivities could be rescued by the expression of either of wild type, non-phosphorylatable or phosphomimetic alleles of *CCR4*, suggesting that phosphorylation of Ccr4 has no clear role in these conditions (Figure 13).

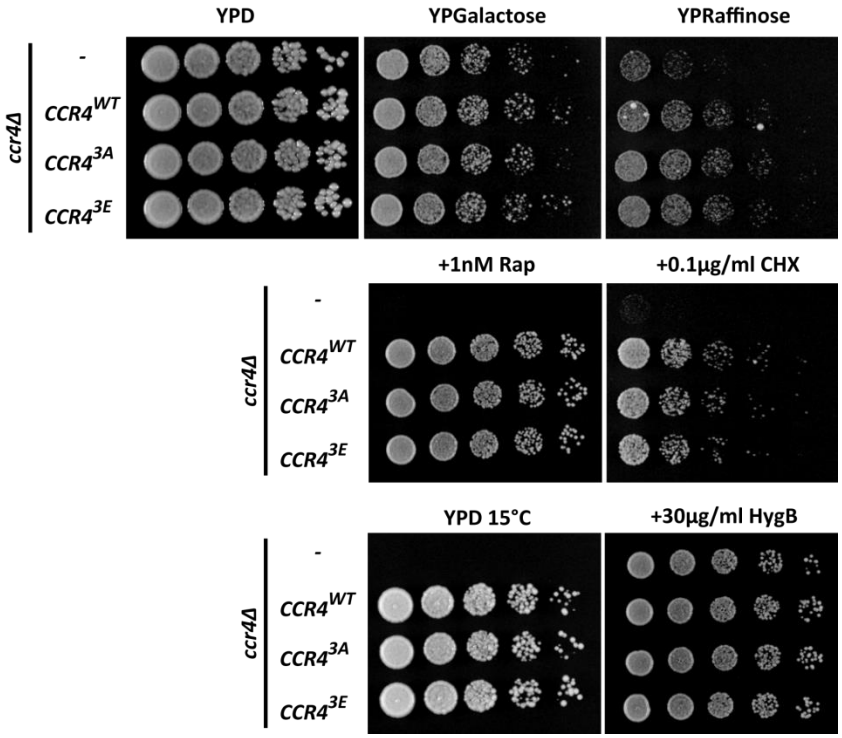

Figure 13. Ccr4 phosphomutants behave like the wild type under different stress conditions.

Growth abilities of the indicated strains under different conditions were analyzed with spot assay. The plates were kept for 2-3 days at 30°C (if not indicated otherwise).

Regulation of Ccr4 by the Casein Kinase I isoform, Yck1

The phosphorylation site Ser281 which we mapped on Ccr4 is found in a recognition motif for Casein Kinase I; S(P)XXS* (S(P) stands for a phosphoserine whereas S* is the residue targeted by the kinase.) (Kennelly & Krebs, 1991; Stark et al, 2010). Thus, we tested whether Casein Kinase I has a role in Ccr4 phosphorylation. In budding yeast, there are three isoforms of casein kinase I: Yck1, Yck2 and Yck3. Combinatorial deletion of *YCK1* and *YCK2* is lethal suggesting that Yck1 and Yck2 share redundant

functions (Wang et al, 1992). However, we observed that deletion of *YCK1* - but not that of *YCK2* or *YCK3* (data not shown) - led to a decrease at the phosphorylation level of Ccr4 (Figure 14A). Casein kinase I was previously shown to alter septin assembly (Robinson et al, 1999). Similarly, Ccr4 regulates the stability of a number of proteins involved in septin assembly, thereby contributing to proper septin organization (Traven et al, 2009). Thus, we asked the question whether kinases involved in septin organization such as Elm1 and Swe1 also affected the levels of Ccr4 phosphorylation. We found that deletion of *SWE1* gene abolished the rapamycin-dependent phosphorylation of Ccr4 (Figure 14A). In contrast, the deletion of *ELM1* resulted in constitutive hyperphosphorylation of Ccr4. Our observation was in accordance with the previous studies which had characterized Elm1 as a negative regulator of Swe1 (Ma et al, 1996; Sreenivasan & Kellogg, 1999). Accordingly, Elm1 is responsible for the hyper-phosphorylation of Swe1 in a mitosis-specific manner (Sreenivasan & Kellogg, 1999). Given the role of casein kinase 1, Swe1 and Elm1 in septin organization and cell cycle progression, we checked whether the phosphorylation of Ccr4 was regulated in a cell-cycle dependent manner. Preliminary experiments showed that levels of Ccr4 phosphorylation changed through one cycle of mitotic division (Figure 14B). Next, we investigated for any possible role for the phosphorylation of Ccr4 in cell cycle progression. However, the cells expressing wild type, non-phosphorylatable or phosphomimetic *CCR4* allele did not exhibit any difference in the cell cycle progression as assessed by the FACS analysis of the DNA content upon release from G1 arrest by alpha factor (data not shown).

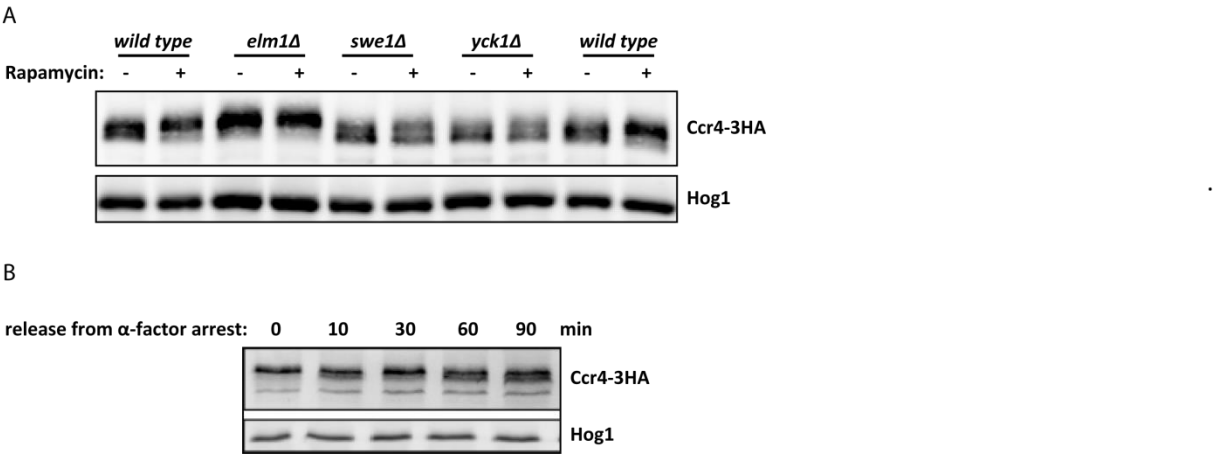

Figure 14. Rapamycin-dependent phosphorylation of Ccr4 is mediated by Swe1, Yck1 and Elm1.

(A) Indicated strains were treated with 200nM rapamycin or vehicle for 20 minutes prior to the TCA treatment and western analysis. (B) Exponentially growing cells were treated with mating factor alpha for 4hours to arrest the cell cycle in G1. Then, the cells were gently washed and resuspended in fresh medium to release the cells from the cell cycle arrest. Following release, samples were collected at the indicated time points. Samples were also collected for FACS analysis to follow the progression of the cell cycle.

Ccr4 Phosphorylation and Its Role in the Regulation of the Stability of Ribosomal Protein mRNAs

It is well documented that TORC1 regulates ribosome biogenesis through the control of transcription of ribosomal protein (*RP*) mRNAs (De Virgilio & Loewith, 2006). Considering that mRNA levels are controlled by both transcription and mRNA decay rates, we hypothesized that TORC1 may also regulate the stability of *RP mRNA*s. Based on the previous observations showing that under stress conditions Ccr4 has a preference for transcripts encoding ribosome biogenesis factors and ribosomal proteins (Grigull et al, 2004), we speculated that the regulation of *RP mRNA* stability by TORC1 may be mediated by Ccr4. To test this hypothesis, we focused on a number of *RP* mRNAs (*Rps4, Rpl3* and *Rpl21a*) which were shown to be stabilized by glucose (Yin et al, 2003). We also tested mating pheromone a-factor (*Mfa2*) and 3-phosphoglycerate kinase (*Pgk1*) mRNAs, whose stability are not affected by rapamycin treatment for short-time points that we used (Albig & Decker, 2001). To test the deadenylation levels of our candidate mRNAs, we decided to perform the ligation- mediated

poly(A)-test (LM-PAT), which is an RT-PCR-based method (Salles & Strickland, 1995). In this assay, the product size is a direct reflection of the length of poly(A) tail length of specific mRNAs. Our results showed that, as anticipated, poly(A) tail lengths of both *Mfa2* and *Pgk1* mRNAs were not responsive to rapamycin, but highly sensitive to deletion of *CCR4* or *POP2*. Strikingly, all three *RP* mRNAs that we tested were highly sensitive to rapamycin in view of the rapid deadenylation of these mRNAs upon rapamycin (Figure 15). However, this response did not seem to be dependent on Ccr4.

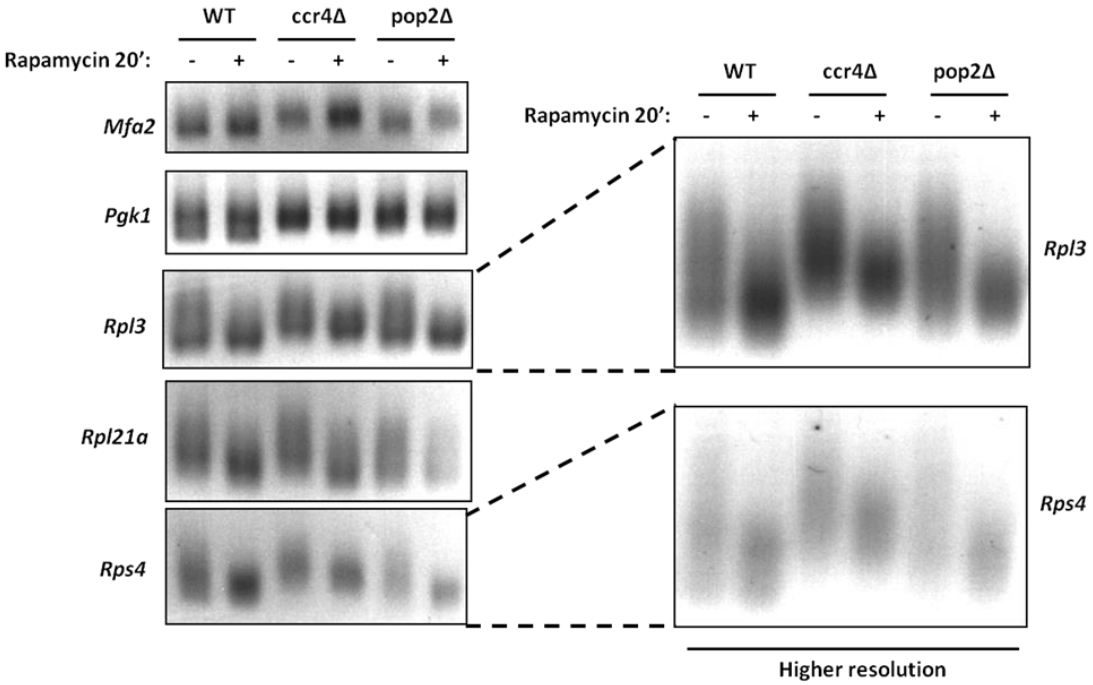

Figure 15. *RP* mRNAs become deadenylated upon rapamycin in a Ccr4-independent manner.

Poly(A) tail lengths of the indicated mRNAs were analyzed with LM-PAT technique using specific primers.

TORC1 was proposed to regulate transcription of ribosomal proteins via a corepressor Crf1 (Martin et al, 2004). We compared the deadenylation rates of *Rps4, Rpl3* and *Rpl21a* mRNAs following inhibition of TORC1 in wild type and crf1Δ strains in order to ensure that deadenylation of these mRNAs upon rapamycin is not an indirect effect due to inhibition of their transcription. None of the poly(A) tails which we tested showed any shortening difference between the wild type and the crf1Δ strains (Figure 16A). However, deletion of the *CRF1* gene did not block the repression of RP gene

transcription as assessed by quantitative real time-PCR in contrast to what was reported before (data not shown).

Rpd3 histone deacetylase was also shown to be required for TORC1-dependent repression of RP transcription (Huber et al, 2011; Humphrey et al, 2004). Thus, we compared the deadenylation of *Rpl3* upon rapamycin in wild type, rpd3Δ and sds3Δ strains. Sds3 is a component of the RPD3L deacetylase complex (Carrozza et al, 2005). In the deletion strains, rapamycin-dependent deadenylation of *Rpl3* mRNA was repressed in a manner correlating with the extent of loss of transcription (Figure 16B-C). With these results, we concluded that deadenylation of the *RP* mRNAs upon inhibition of TORC1 is an indirect consequence of repression of their transcription.

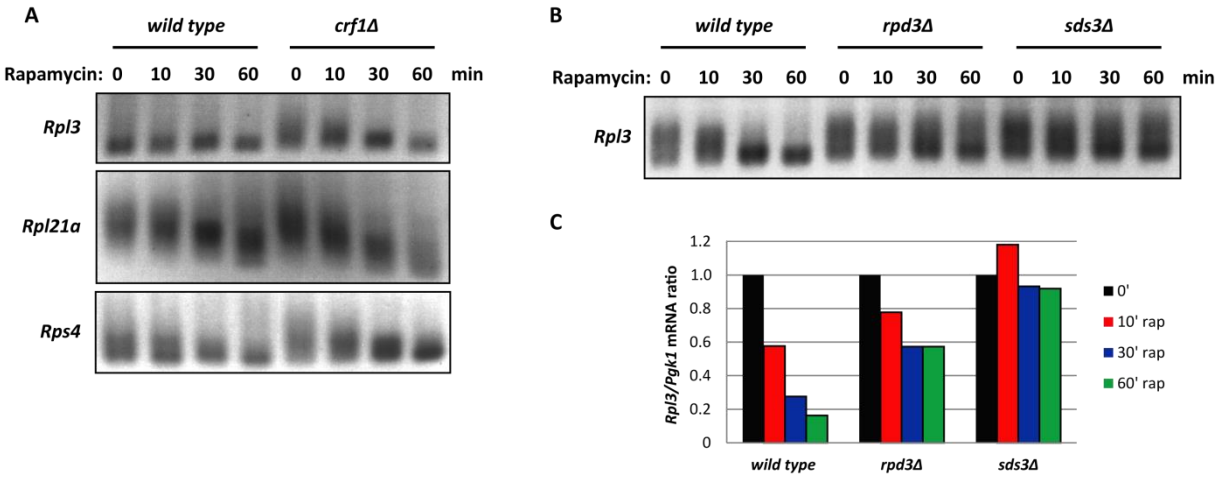

Figure 16. Shortening of poly(A) tails of *RP* mRNAs upon rapamycin is due to inhibition of transcription.

(A-B) Exponentially growing cells were treated with 200nM rapamycin and samples were collected at the indicated time-points. Following RNA extraction and cDNA synthesis, deadenylation of the indicated mRNAs were analyzed with LM-PAT. (C) Total mRNA levels were measured with quantitative Real Time-PCR using the same cDNA samples used for LM-PAT analysis.

Aro4 is an enzyme involved in the catalysis of the initial step of aromatic amino acid biosynthesis. *Aro4* mRNA is destabilized in a rapamycin-dependent manner due to the accelerated shortening of the poly(A) tail (Albig & Decker, 2001). We confirmed that *Aro4* mRNA was deadenylated upon rapamycin, however, in a Ccr4-independent manner (Figure 17A). Thereafter, we employed a

tetracycline-dependent activator/repressor dual system to inhibit expression of the *ARO4* gene and to measure the half-life of *Aro4* mRNA (Belli et al, 1998). In this system, addition of tetracycline promotes the binding of a repressor to the *ARO4* promoter and also suppresses the binding of an activator, thereby providing an acute and specific inhibition of transcription of the gene of interest (Figure 17B). Thus, we tested whether *Aro4* mRNA levels were sensitive to rapamycin as previously reported. In contrast to what was proposed, we found that treatment of the cells with rapamycin led to an extension of the *Aro4* mRNA half-life (Figure 17C). Similarly, deletion of the *CCR4* gene resulted in an increase of its half-life. Deletion of *CCR4* and rapamycin treatment had additive effect on stabilization of *Aro4* mRNA, suggesting that rapamycin-dependent increase is independent of Ccr4. This experiment led us to propose that TORC1 plays a role in the *Aro4* mRNA stability, but the mechanism of this regulation still remains to be elucidated.

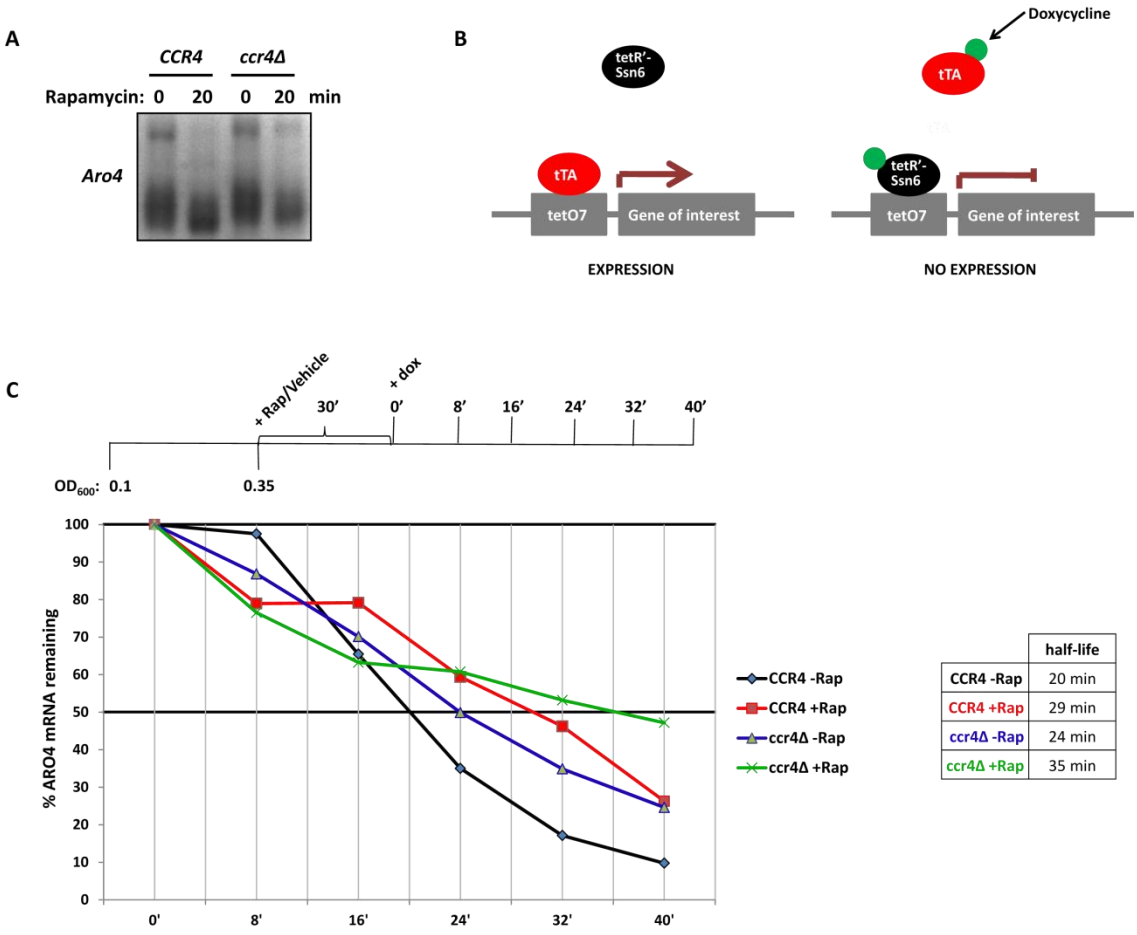

Figure 17. Half-life of *Aro4* mRNA is sensitive to rapamycin treatment.

(A) The indicated strains were treated with 200nM rapamycin or vehicle. LM-PAT was performed to analyze poly(A) tail lenghts of the mRNA with specific primers. (B) The cartoon depicts the dual-tet system which we employed to inhibit the transcription of the gene of interest so as to study the mRNA half-lives. tTA: the tetracycline transactivator; tetR'-Ssn6: the tetracycline repressor fused to the yeast repressor protein Ssn6; $tetO_7$: the tetracycline operator sequence. (C) Prior to inhibition of transcription with doxycycline (5µg/ml), the indicated strains were treated with 200nM rapamycin or the vehicle for 30 minutes. mRNA levels at specific time-points were determined with qRT-PCR using specific primers. *Aro4* mRNA levels were normalized to *Pgk1* mRNA levels.

We also measured the mRNA levels of a number of candidate genes during rapamycin treatment in cells expressing either wild type, phosphomutant or phosphomimetic alleles of *CCR4*. *Rps2*, *Rpl3* and *Aro4* mRNA levels decreased in response to rapamycin with the same kinetics in all three strains (Figure 18). On the contrary, *Hsp26* levels increased following inhibition of TORC1. However, again,

no significant difference was observed in the mutant cells compared to the wild type cells, suggesting that Ccr4 phosphorylation has no obvious role in the regulation of these specific mRNAs.

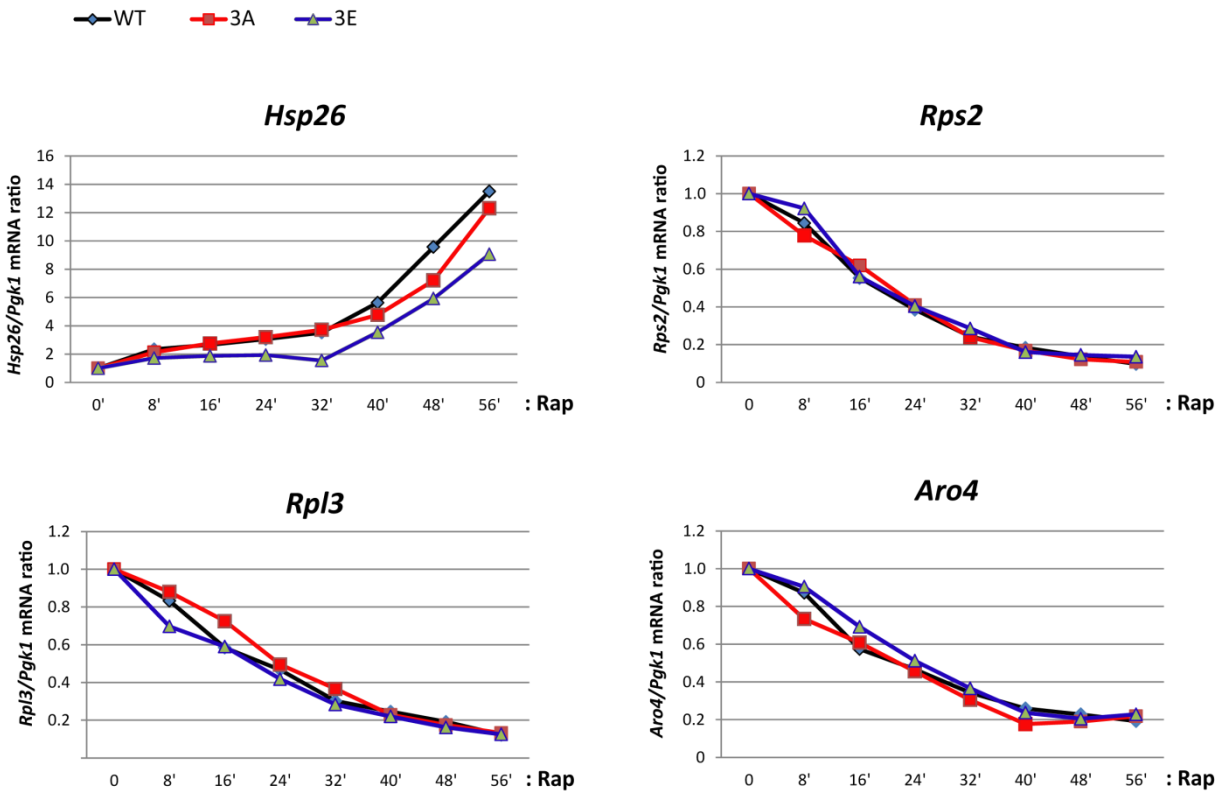

Figure 18. Rapamycin-dependent changes in *Hsp26*, *Rps2*, *Rpl3* and *Aro4* mRNA levels are not affected by Ccr4 phosphorylation.

Cells with plasmids expressing wild type or mutant alleles of *CCR4* were treated with rapamycin and the samples were collected at the indicated time-points. Following phenol-extraction of RNA and cDNA synthesis, mRNA levels of the indicated mRNAs were measured with qRT-PCR.

Ccr4 Phosphorylation and P-body Formation

Next, we investigated a potential role for Ccr4 phosphorylation in the formation of P-bodies. Edc3 is a non-essential protein involved in the decapping step of the mRNA decay pathway and is used as a marker of P-bodies (Balagopal & Parker, 2009). We induced P-body formation by starving the cells for glucose. Although we observed the localization of Edc3 into cytoplasmic foci, expression of different *CCR4* alleles had no clear effect on this process (Figure 19A). In our hands, we could not detect the

formation of the stress granules under these conditions even in wild type cells. Therefore, the question of whether Ccr4 phosphorylation affects stress granule formation remains to be further investigated. As shown before (Ramachandran et al, 2011), rapamycin did not induce P-body formation and different forms of Ccr4 had no effect on this observation (Figure 19B). We also localized Ccr4 in cells grown under glucose-rich and glucose-starved conditions by GFP tagging. Ccr4 seemed to disperse throughout the cytoplasm and the nucleus, and starvation for glucose did not significantly alter this localization neither in wild type nor in mutant cells (data not shown).

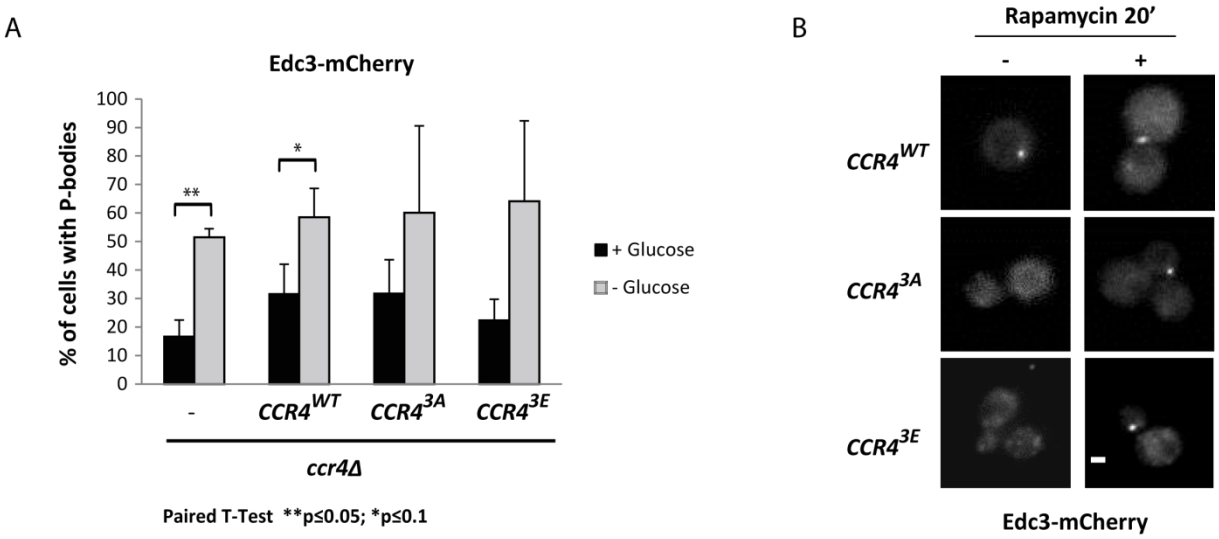

Figure 19. Phosphorylation status of Ccr4 does not affect the P-body formation.

(A) The indicated strains were grown to exponential growth phase in synthetic media with 2% glucose. Then, the cultures were split into two cultures containing or lacking glucose and incubated further for 20 minutes. Following formaldehyde fixation (4%, 20min), P-body formation was analyzed by using a Zeiss AXIOZ1 microscope. (-) 10µm

P-bodies are known to be important for cells survival at stationary phase (Shah et al, 2013). Hence, in parallel, we investigated whether Ccr4 phosphorylation influences the survival of long-term quiescent cells. We kept the cells in stationary phase for a number of days and finally, compared their abilities to resume growth upon glucose addition. The cells deleted for the *CCR4* gene seemed to have a diminished ability to regrow after staying in stationary phase for around 7 days (Figure 20). Cells expressing the phosphomutant allele of *CCR4* also exhibited altered survival after spending 12

days in stationary phase, thereby suggesting that Ccr4 phosphorylation may be playing a role in stationary phase cell survival. However, further confirmation and the repetition of this preliminary result will be required to confirm that Ccr4 phosphorylation is required to cope better with stationary–phase arrest and subsequent revival.

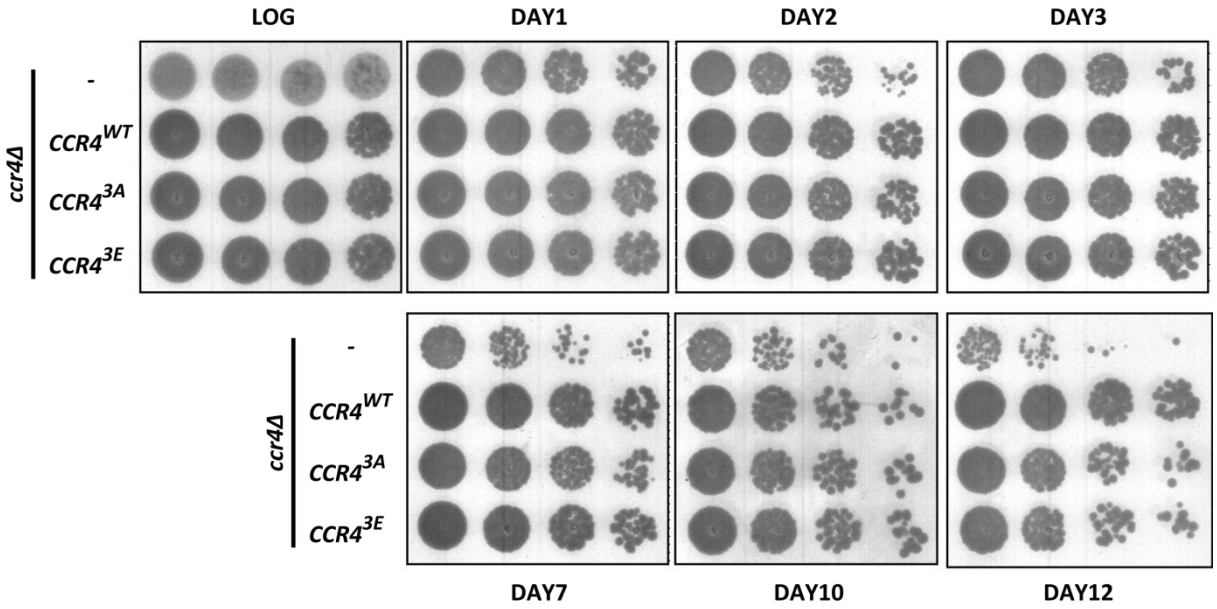

Figure 20. Phosphorylation of Ccr4 affects survival of cells following stationary-phase arrest.

The cells were grown in synthetic media for the indicated number of days. On the day of the assay, cells were diluted and grown in synthetic media for 2 hours. Cell numbers were normalized and serial dilutions were plated on synthetic media. The plates were kept at 30°C for 3 days before the pictures were taken.

Identification of Rapamycin-sensitive Interactome of Ccr4/Pop2

We hypothesized that TORC1 could be regulating the interaction between Ccr4/Pop2 and their partners. With the aim of identifying the rapamycin-sensitive interactome of Ccr4/Pop2, we did a mass spectrometry analysis of TAP-tagged Ccr4 or Pop2 immunoprecipitates before and after rapamycin treatment (Figure 21A). As expected, we identified all the known members of the Ccr4-Not complex as binding partners of both Ccr4 and Pop2 (Figure 21B). However, interactions between Ccr4/Pop2 and the rest of the complex did not seem to be affected by rapamycin treatment. This

analysis let us to identify novel interacting partners of Ccr4 and Pop2, which are involved in various cellular processes (Figure 21B). *CCR4* was previously shown to genetically interact with *NAM7* and *PAB1*, and *POP2* with *CDC14* and *PAB1* in large-scale studies (Mostafavi et al, 2008). All these candidate proteins appeared to interact with both Ccr4 and Pop2, whereas only the interaction with Pop2 was sensitive to TORC1-inhibition. Next, we attempted to confirm these interactions by means of co-immunoprecipitation and western blotting. Despite the fact that we managed to reproduce the interactions, none of the interactions was altered in response to rapamycin in these low-throughput assays (data not shown).

A

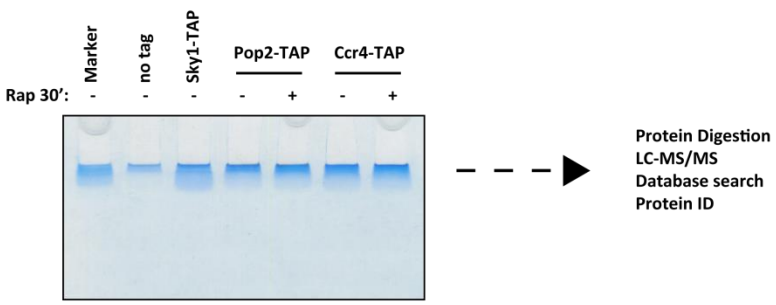

B

		Regulation of interaction with Ccr4 by rapamycin	Regulation of interaction with Pop2 by rapamycin
Ccr4	Ccr4-Not complex component		-
Pop2	Ccr4-Not complex component	-	
Not5	Ccr4-Not complex component	-	-
Cdc39	NOT1; Ccr4-Not complex component	-	-
Mot2	NOT4; Ccr4-Not complex component	-	-
Not3	Ccr4-Not complex component	-	-
Caf130	Ccr4-Not complex component	-	-
Caf40	Ccr4-Not complex component	-	-
Cdc36	NOT2; Ccr4-Not complex component	-	-
Net1	Core subunit of the RENT complex, which is a complex involved in nucleolar silencing and telophase exit	-	↗
Sup35	Translation termination factor eRF3	-	↗
Pma1	Plasma membrane H+-ATPase, pumps protons out of the cell	-	↗
Pab1	Poly(A) binding protein, part of the 3'-end RNA-processing complex	-	↗
Puf2	Member of the PUF protein family, which is defined by the presence of Pumilio homology domains that confer RNA binding activity	-	↗
Whi4	Putative RNA binding protein and partially redundant Whi3p homolog that regulates the cell size requirement for passage through Start and commitment to cell division	-	↗
Eap1	eIF4E-associated protein, competes with eIF4G for binding to eIF4E	-	↗
Upf1	ATP-dependent RNA helicase of the SFI superfamily involved in nonsense mediated mRNA decay	-	↗
Cdc14	Protein phosphatase required for mitotic exit	-	↗

Figure 21. Ccr4/Pop2 interactome

(A) Immunoprecipitation of Tap-tagged proteins from cells treated with vehicle or rapamycin were performed as mentioned before. The proteins were run into a 7.5% resolving gel until there was no samples left in the wells. The bands were cut out of the coomassie-stained gel and sent to Ammarer Laboratory in Vienna for the mass spectrometric analyses.
(B) List of the proteins found to interact with Ccr4 and Pop2. (↗) the interaction altered more than two fold upon rapamycin.

TORC1-dependent Regulation of Puf Proteins

Puf family proteins are well-characterized RNA-binding proteins. In yeast, there are six PUF proteins which recruit the Ccr4-Not complex to specific mRNAs and regulate their stability. Puf2 came out in our analysis of the rapamycin-dependent interactome of Pop2. Although we could not confirm the TORC1-dependency of this interaction, we found that Puf2, itself, is another rapamycin-responsive phosphoprotein (Figure 22A). Puf2 become hyper-phosphorylated upon rapamycin treatment just

like Ccr4 and Pop2. Similarly, another member of Puf family Puf4 appeared to display a slower migration pattern in response to rapamycin, suggesting that the phosphorylation status of Puf4 is altered in a TORC1-dependent manner (Figure 22B). Intriguingly, the absence of *PUF2* or *PUF4* genes rendered cells resistant to low concentrations of rapamycin (Figure 22C). *Rpl3* and *Rps4* mRNAs were suggested to bear putative Puf4-binding sites on their C-terminal ends (Foat et al, 2005). Thus, we decided to investigate a possible role for Puf4 in the regulation of poly(A) tail lengths of *Rpl3*, *Rpl21a* and *Rps4* mRNAs. However, we did not detect any significant, reproducible changes in poly(A) tail length before or after rapamycin treatment in *puf4* versus wild type cells (Figure 22D). One well-established mRNA target for Puf proteins in yeast is the *Cox17* mRNA which is regulated specifically by Puf3 (Olivas & Parker, 2000). Employing an RNA-immunoprecipitation assay, we explored whether the interaction of Puf3 with *Cox17* mRNA is affected by rapamycin – it is not (Figure 22E). In addition, no interaction between Puf3 and *Rpl3* or *Pgk1* mRNAs was observed. Altogether, the current data fail to illuminate the role of Puf family proteins in the TORC1-signaling pathway.

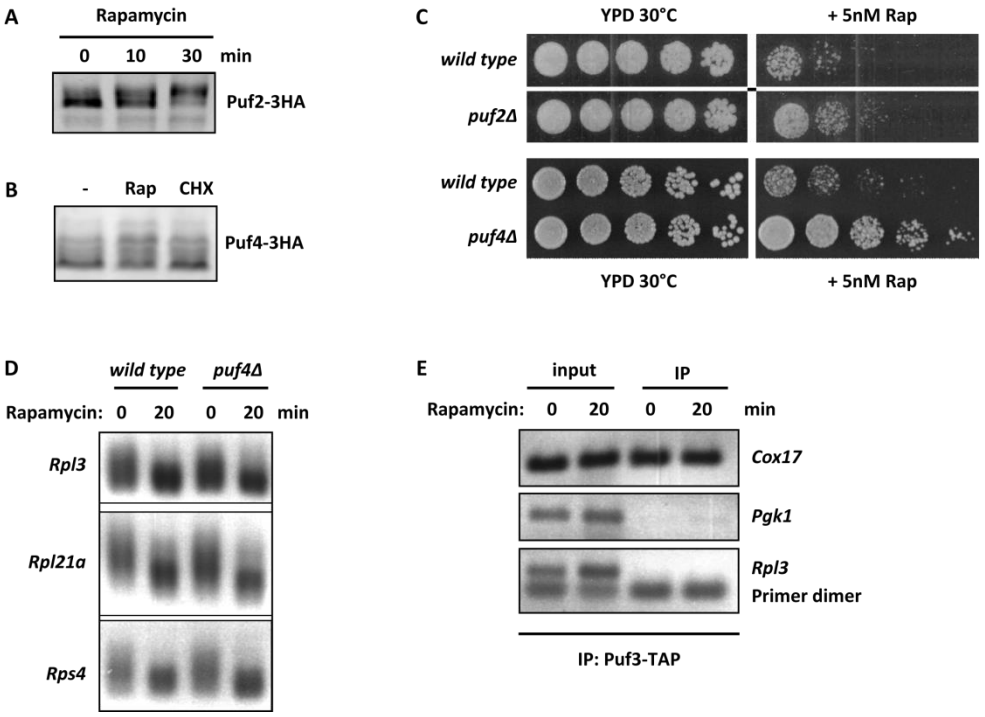

Figure 22. Puf2 and Puf4 are rapamycin-sensitive phosphoproteins.

(A-B) Exponentially growing cells expressing HA-tagged Puf2 or Puf4 were treated with 200nM rapamycin or 25µg/ml cycloheximide for 20 minutes. (C) Serial dilutions of the indicated strains were plated on YPD with rapamycin or vehicle. Pictures were taken following incubation at 30°C for 3 days. (D) mRNAs were extracted from the indicated strains following rapamycin treatment for 20 minutes. Poly(A) tail lengths were analyzed with LM-PAT. (E) Protein-RNA complexes were cross-linked with 1% formaldehyde (20min) prior to immunoprecipitation of TAP-tagged Puf3. The crosslink was reversed at 65°C for 1hour in the presence of 5M NaCl, and following RNA extraction and cDNA synthesis, mRNA levels were determined with PCR using specific primers.

Section III. Regulation and Function of Rps6 Phosphorylation in *Saccharomyces cerevisiae*

The Tools to Study Rps6 Phosphorylation

Rps6 is highly phosphorylated on its C-terminal end. In higher eukaryotes, there are five highly conserved phosphosites on this end, whereas in budding yeast only two of these sites are conserved. We started working on Rps6 by mutating these two phosphosites into alanine residues individually or in combination. With the aim of studying Rps6 phosphorylation intensively, we developed an antibody which binds total Rps6 protein. Taking advantage of the phosphomutant strains, we screened a number of commercially available antibodies which could recognize the phosphorylated form of Rps6 in different organisms. We found two antibodies which can bind differentially phosphorylated forms of Rps6 in *Saccharomyces cerevisiae*. The first phospho-antibody (we named as Rps6-PP) is able to recognize Rps6 only when both S232 and S233 residues are phosphorylated. The second antibody is an antibody against RXXS(T) motifs. Phosphorylation of S232 seemed to be sufficient for the recognition of Rps6 by the second phospho-antibody. However, as both serines are found in RXXS motifs, it is likely that this antibody binds either of the serines in a phosphorylated form. In relation to this, in our mutant strain in which only the first serine is mutated into alanine, we detected no signal with either of the phospho-antibodies suggesting that the phosphorylation of the first serine is a prerequisite for the phosphorylation of the second serine (Figure 23A).

In addition, we replaced these two serine residues with aspartic acid hoping to have a phosphomimetic copy of Rps6. However, we observed that insertion of aspartic acid residues into the protein was lethal. To address whether the lethality was due to the phosphomimetic nature of Rps6 or the instability of the protein, we created a repressible system. In this system, the promoter of the wild type *RPS6A* allele was replaced by the Galactose-inducible *GAL1* promoter, whereas the phosphomimetic version of *RPS6B* was under the control of its endogenous promoter (Figure 23B). On glucose, wild type *RPS6A* was not expressed as the Gal promoter was repressed leaving the phosphomimetic Rps6b as the only Rps6 copy in the cell. Under this condition, the cells did not grow, thereby confirming the lethal nature of the phosphomimetic allele of Rps6 (Figure 23C). To check if

the phosphomimetic Rps6 was stable, we switched the carbon source of the actively growing cells from galactose to glucose and followed the protein level of Rps6b in comparison to that of a reference protein, Hog1. We used the wild type and non-phosphorylatable alleles of *RPS6B* as controls. Accumulation of non-phosphorylatable Rps6b proved us that the system worked and the only copy of Rps6 at the time-points we chose was the Rps6b under the control of its endogenous promoter (Figure 23D). Under these conditions, we observed that the level of phosphomimetic Rps6b was much lower compared to the others, suggesting that the insertion of the aspartic acid residues rendered the Rps6 protein unstable.

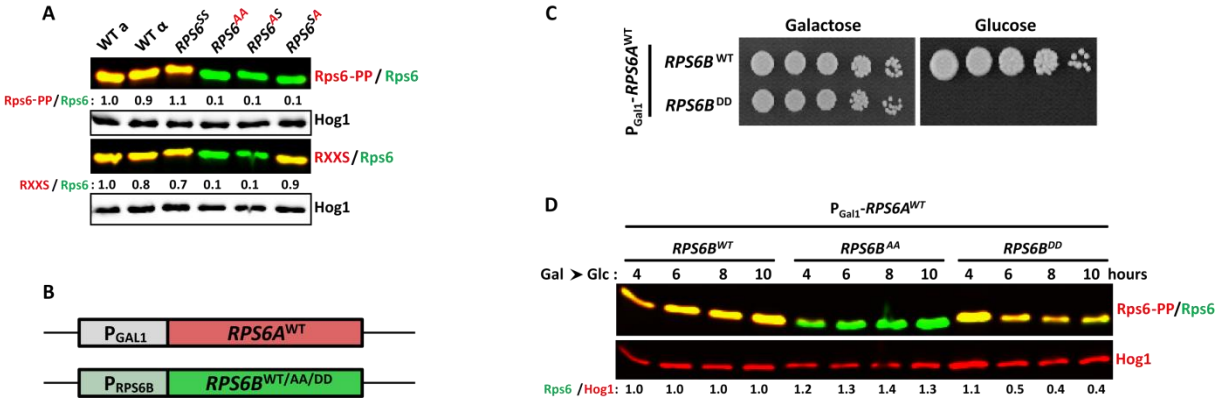

Figure 23. The phosphomimetic Rps6 is not stable.

(A) Total protein extracts were prepared from strains expressing the S6 mutants under denaturing conditions and resolved by 10% SDS-PAGE gels. Following transfer, membranes were probed with rabbit anti-phospho-S6 ribosomal protein (S235/S236) (Rps6-PP), rabbit anti-phospho-Akt substrate (RXXS*/T*), guinea pig anti-total Rps6 and rabbit anti-Hog1. Then, the signals were detected with IRDye®800CW anti-guinea pig IgG and IRDye®680CW anti-rabbit IgG. (B) Scheme illustrating the generation of the Rps6 repressible system. (C) Serial dilutions of the indicated strains were spotted on YP plates with 2% glucose or 2% galactose. (D) The indicated strains were grown in YPGal for two hours and transferred into YPD after wash. The samples were collected at the time-points indicated and processed for Western analyses.

Dynamics of Rps6 Dephosphorylation

Rps6 phosphorylation is sensitive to growth factors, mitogens and starvation for nutrients (Meyuhas, 2008). We employed the antibodies which recognized differentially phosphorylated forms of Rps6 to

investigate the dynamics of Rps6 dephosphorylation under a variety of conditions in budding yeast. Serine 233 residue of Rps6 was highly responsive to all the conditions we tested. Ser233 became dephosphorylated following rapamycin, caffeine, BHS treatments, and starvation for carbon and nitrogen sources (Figure 24A-C). On the other hand, Ser232 phosphorylation seemed to be resistant to rapamycin and caffeine treatments. Both BHS and nutrient starvation led to the dephosphorylation of both sites, however, with different kinetics. In all cases, dephosphorylation of the second site was followed by the dephosphorylation of the first site suggesting a hierarchy between these two sites (Figure 24B-C). Given that BHS and nutrient starvation result in the inhibition of both of the TOR complexes, the results suggested that the first site was a target of either TORC2 or both TORC1 and TORC2, whereas the second site was a TORC1 target only.

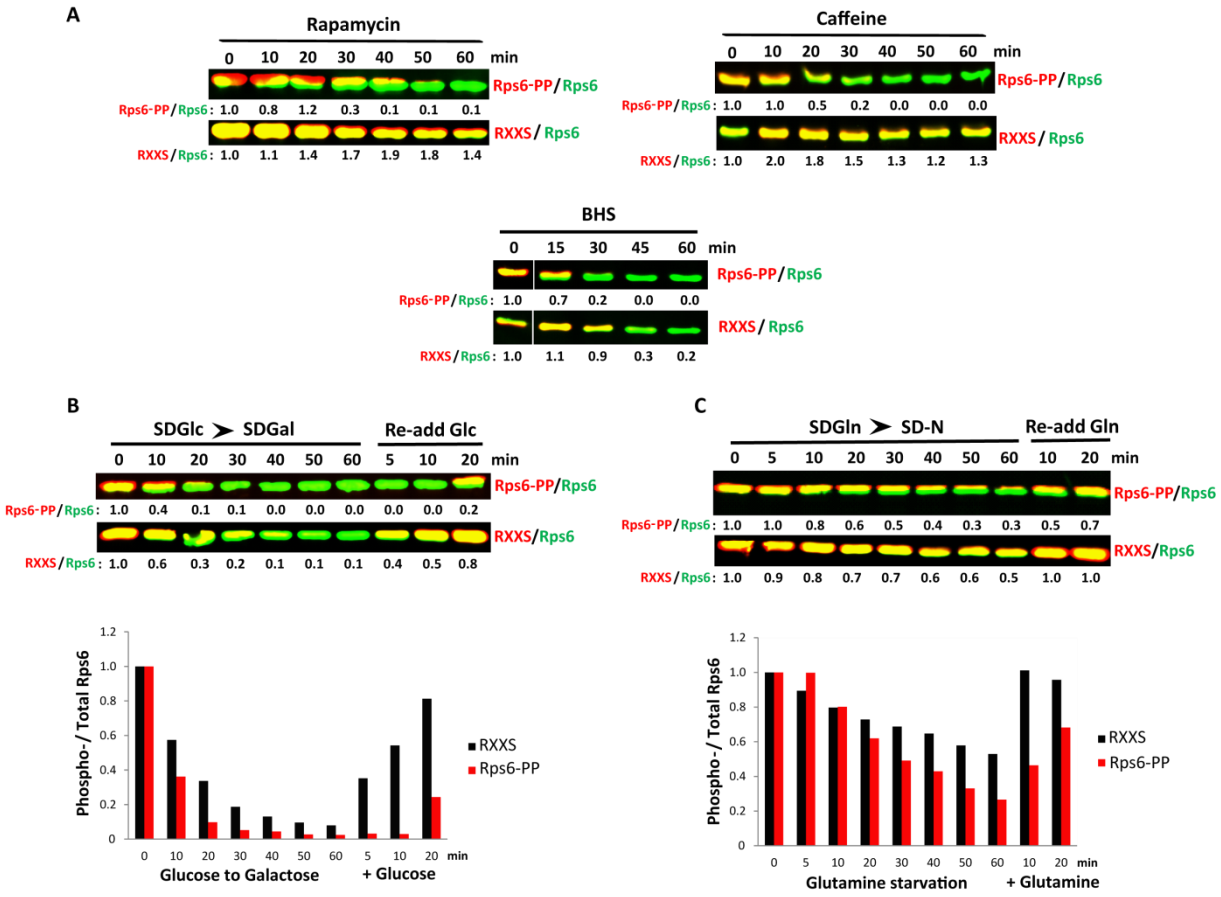

Figure 24. Rps6 phosphorylation is highly responsive to TORC1 and TORC2 inhibition.

(A) Exponentially growing wild type cells were treated with 200nM rapamycin, 10mM caffeine or 100µM BHS. Following treatment, the cells were collected at the indicated time-points and processed under denaturing conditions. (B) Prototroph wild type cells were grown in SD medium with 0.2% glutamine and 2% glucose until exponential growth phase, then filtered and transferred to medium with 2% galactose as the sole carbon source. Following 1 hour of carbon-source downshift, the cells were re-fed with 2% glucose and samples were taken at the indicated times. The graph represents the quantification of the western blot. (C) Prototroph wild type cells growing in SD media with 2% glucose and 0.2% glutamine were filtered and transferred into fresh medium without a nitrogen source. After 1 hour, 0.2% glutamine was added back onto the cells. The experiment was performed by Madeleine Meusburger.

The Role of Rps6 Phosphorylation in Cell Growth

We compared the growth rates of cells expressing either wild type Rps6 or the phosphomutant copy and found that the expression of the *RPS6*^{AA} allele resulted in an almost 30% decrease in the proliferation rate (Figure 25A-B). In accordance with the defect in cell proliferation, the *RPS6*^{AA} cells

also had lower protein content compared to the wild type cells as assessed by FITC staining and FACS analysis (Figure 25C-D).

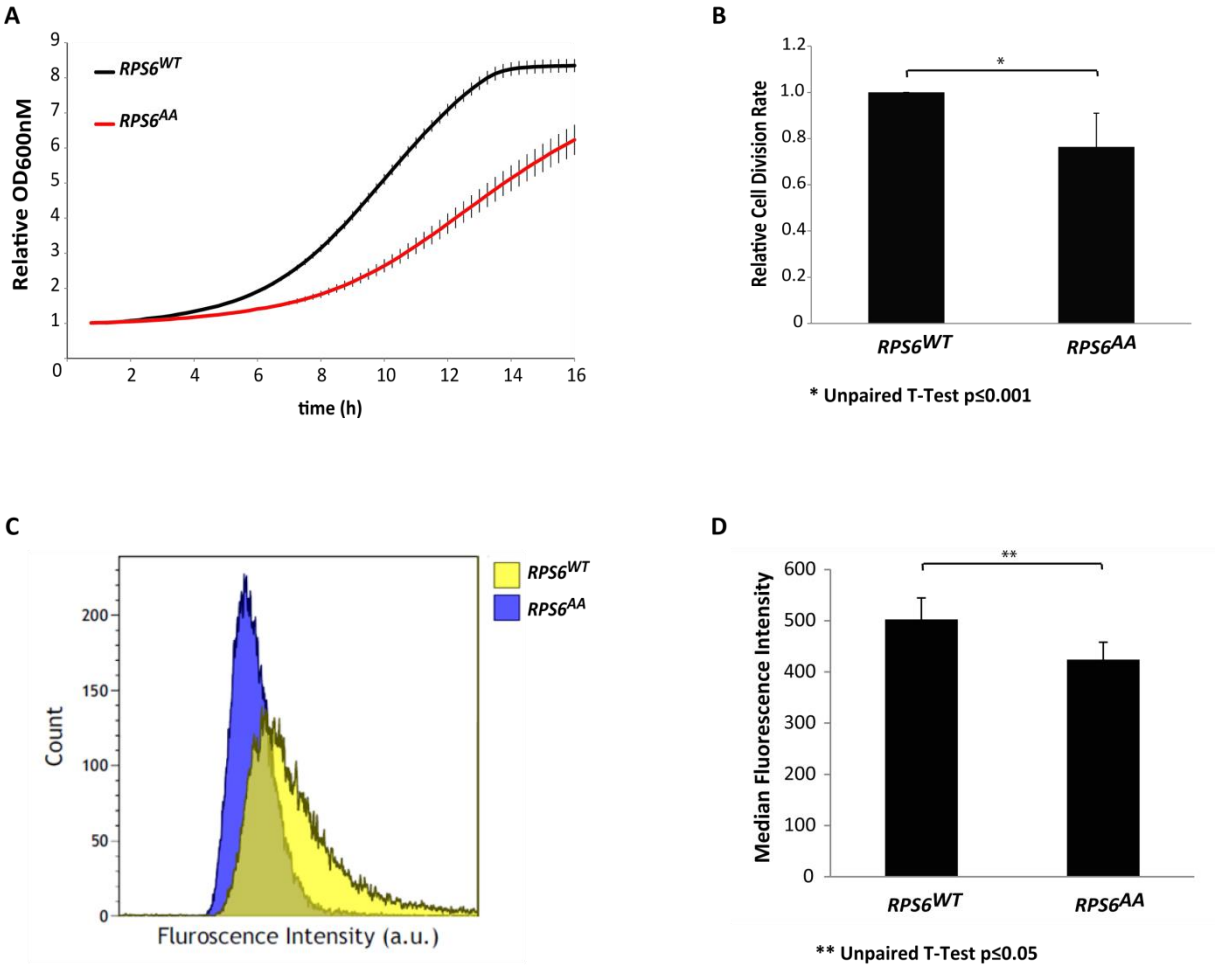

Figure 25. *RPS6*^{AA} cells are defective in cell growth.

(A) Indicated strains were grown in rich medium in 96-well plates at 30°C and the OD_{600nM} of the cells was recorded every 15min for 16 hours. (B) Quantification of the six-independent growth assays with wild type and *RPS6*^{AA} cells. (C) Protein content of exponentially growing cells was measured by FACS analysis. (D) Quantification of the FACS analysis results obtained in three independent experiments. One of the experiments was performed by Madeleine Meusburger.

The Role of Sch9 in Regulation of Rps6 Phosphorylation

When Sch9 was characterized as a direct effector of TORC1 (Urban et al, 2007), S6 kinase in mammalian cells was already known to be phosphorylated by mTORC1 (Burnett et al, 1998; Isotani et al, 1999). Considering that both Sch9 and mammalian S6 kinase belong to the AGC kinase family and

Sch9 phosphorylates Rps6 *in vitro,* Sch9 was proposed to be the yeast ortholog of S6 kinase (Urban et al, 2007). However, *in vivo* experiments were missing to support this notion. Curiously, we could not detect any change at the levels of Rps6 phosphorylation in the absence of Sch9 itself or its kinase activity (Figure 26A). Sch9 is required for proper cell growth and its absence results in a slow growth phenotype. However, cells missing Sch9 activity are able to adapt. For the controllable and acute inhibition of Sch9, we employed the analog-sensitive allele of *SCH9,* an allele which bears a point mutation in the ATP-binding pocket, thereby sensitizing the kinase to a specific inhibitor (Bishop et al, 2000). Rps6 phosphorylation, yet, remained constant even after the inhibition of Sch9 with the analog (Figure 26B). To ensure that the results were not due to the adaptation of the cells, we compared the growth abilities of the cells. As expected, the cells deleted for *SCH9* or expressing the kinase-dead allele of *SCH9* displayed a slow growth phenotype compared to the wild type cells (Figure 26C). Similarly, the growth of *sch9*^{as} allele-expressing cells was impaired upon addition of the analog. On the other hand, the expression of the *SCH9*^{DE} allele which uncouples Sch9 activity from TORC1 (Urban et al, 2007) intriguingly led to a delay in the Rps6 dephosphorylation upon rapamycin (Figure 26D).

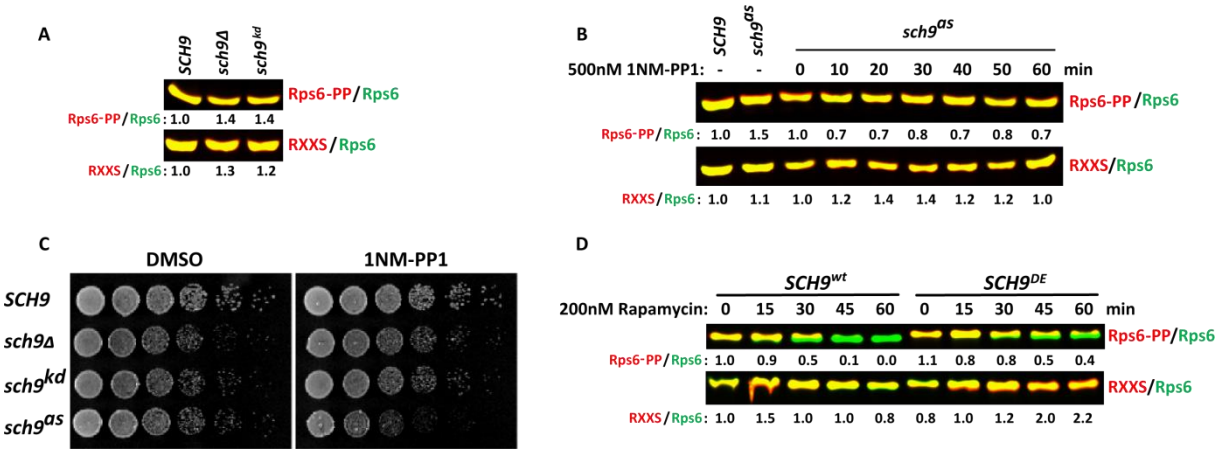

Figure 26. Sch9 is not the S6 kinase *in vivo*.

(A) Sch9 activity is dispensable for Rps6 phosphorylation. (B) Acute inhibition of Sch9 activity does not have a dramatic effect on Rps6 phosphorylation. (C) *sch9Δ* and *sch9*^{kd} cells display slow growth phenotypes. *sch9*^{as} cells are also defective in growth in the presence of the analog. (D) Expression of a rapamycin-insensitive allele of *SCH9* delays the rapamycin-induced dephosphorylation of Rps6.

Since lack of Sch9 activity had no effect on Rps6 phosphorylation, we hypothesized that Sch9 indirectly affects the kinetics of Rps6 dephosphorylation via its role in the regulation of translation initiation upstream of Gcn2. In accordance with the hypothesis, Rps6 dephosphorylation following rapamycin treatment was also delayed in the cells deleted for *GCN2* (Figure 27A). Furthermore, the hyperactive allele of *GCN2* was able to suppress the delay in the dephosphorylation of Rps6 due to the expression of *SCH9*^{DE} (Figure 27B). As expected, cells expressing the hyperactive allele of *GCN2* had higher levels of eIF2α phosphorylation compared to cells with the wild type *GCN2* allele. However, we could still detect an increase at the phosphorylation level upon rapamycin, which could be explained by the presence of the wild type *GCN2* copy in the cells. Based on these results, we hypothesized that Rps6 was not accessible to the phosphatase in the context of polysomes. In wild type cells, polysomes dissociate following rapamycin treatment as translation initiation is inhibited. However, in cells expressing *SCH9*^{DE}, translation continues even after rapamycin treatment and polysomes remain intact. In this context, Rps6 is not easily accessible for dephosphorylation. However, hyperactive Gcn2 triggers the translation inhibition, promoting the polysome dissociation

and thereby suppressing the delay due to *SCH9*^{DE}. Simultaneous treatment of cells with rapamycin and cycloheximide – a translation elongation inhibitor- resulted in a similar delay in Rps6 dephosphorylation strongly corroborating that Rps6 dephosphorylation required the dissociation of polysomes (Figure 27C).

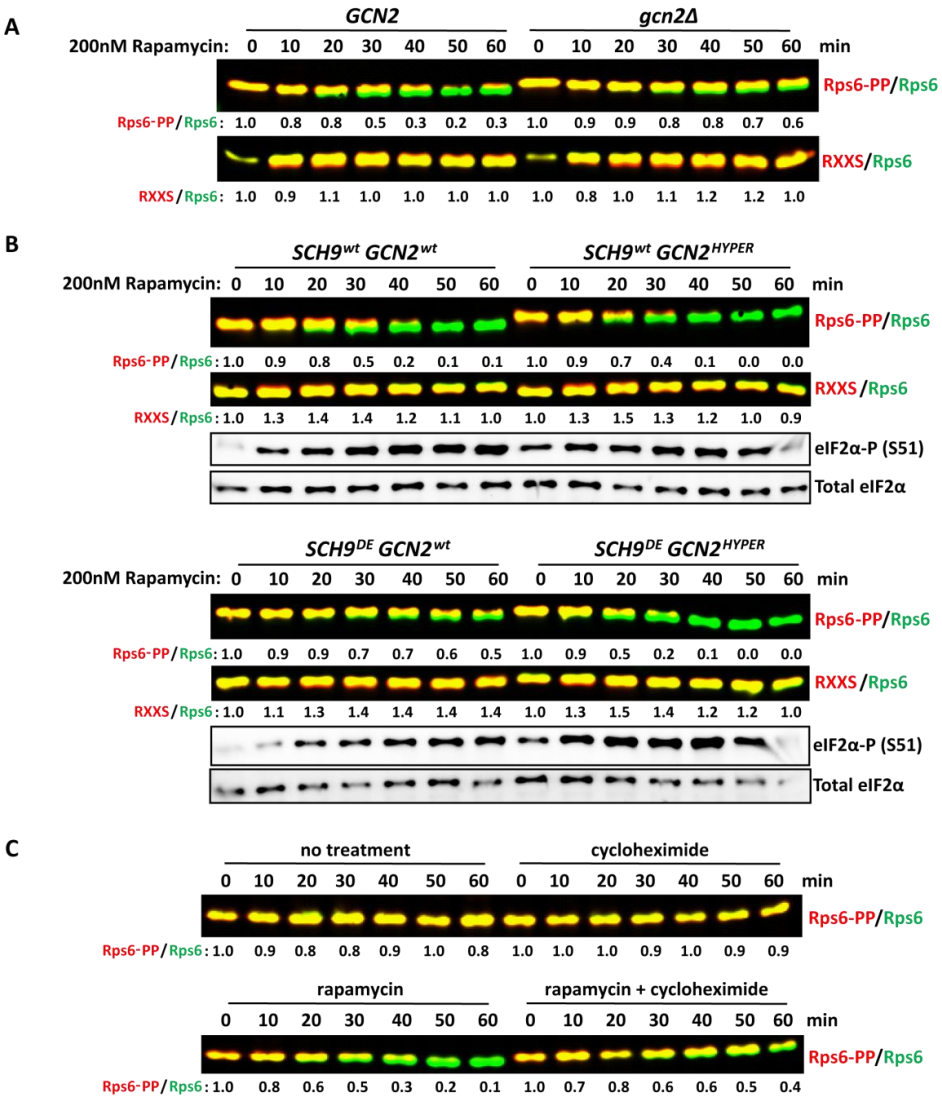

Figure 27. Ongoing translation delays the rapamycin-induced dephosphorylation of Rps6.

(A) Rps6 dephosphorylation upon rapamycin is delayed in cells deleted for *GCN2*. (B) Expression of the hyperactive allele of *GCN2* suppresses the *SCH9*^{DE}-dependent delay in Rps6 dephosphorylation. (C) While cycloheximide treatment alone has no effect on Rps6 phosphorylation, its presence delays rapamycin-induced dephosphorylation.

Characterization of Ypk3 as an S6 Kinase

Phylogenetic analysis of the Tor pathway indicated that Ypk3 is the yeast ortholog of S6K (van Dam et al). Based on this observation, we hypothesized that Ypk3 could be the S6K. Accordingly, we found that Ypk3 was essential for phosphorylation of Rps6 on Ser233 *in vivo* (Figure 28A). Deletion of the gene itself or the abolishment of its kinase activity impaired the phosphorylation of Rps6 on Ser233. We obtained the kinase-dead allele of *YPK3* by mutating the lysine 157 residue to alanine based on the conservation of the site in Ypk1 and Ypk2 proteins. Interestingly, the kinase-dead Ypk3 seemed to be less stable than the wild type protein. To further confirm the role of Ypk3 in S233 phosphorylation, we shifted cells to a poor carbon source so that we could trigger dephosphorylation of Rps6. Subsequently, we re-fed the cells with glucose. Under these conditions, we could detect the re-phosphorylation of Rps6. However, this re-phosphorylation event seemed to be dependent on Ypk3 activity as Rps6 stayed hypophosphorylated in *ypk3*^{as} cells treated with the ATP analog 1NM-PP1 (Figure 28B). Intriguingly, Ypk3, itself, seemed to go through phosphorylation in a carbon-source sensitive manner as reflected by the changes in SDS-PAGE migration of Flag-tagged Ypk3. Moreover, inhibition of Ypk3 activity with the analog treatment abolished its phosphorylation, implying that Ypk3 catalyzed autophosphorylation. In the absence of *YPK3*, we could still detect phosphorylation of Ser232. However, the lack of Ypk3 activity rendered Ser232 sensitive to rapamycin suggesting a role for Ypk3 in the phosphorylation of both sites (Figure 28C).

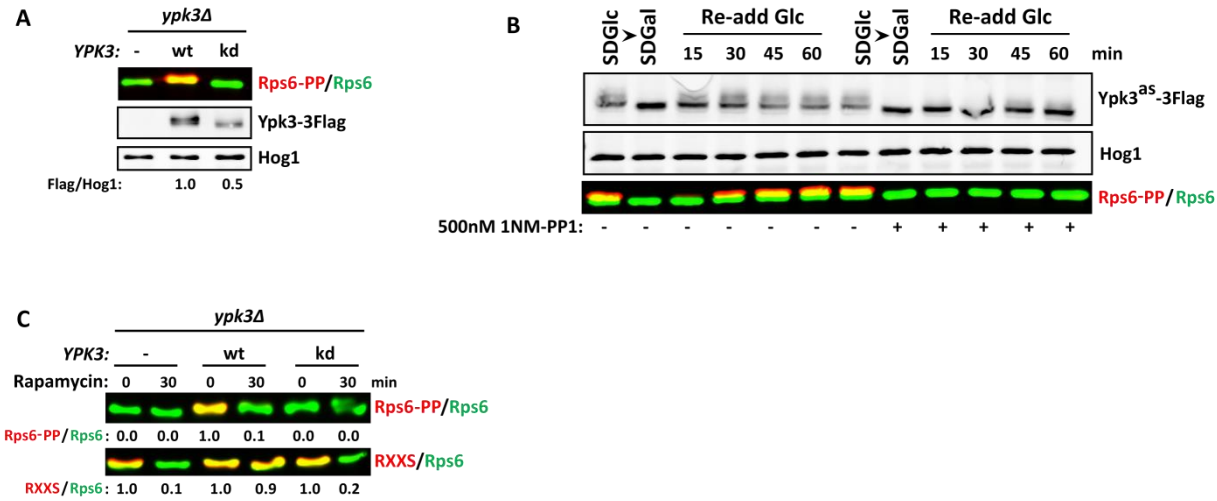

Figure 28. Ypk3 activity is indispensable for Rps6 phosphorylation on Ser233.

(A) Rps6 phosphorylation on Ser233 is impaired in cells lacking Ypk3 activity. (B) A *ypk3*^{as} strain was grown in SD medium with 2% glucose, filtered and resuspended in SD with 2% galactose. Following 1 hour of incubation at 30°C, the culture was split into two: one supplemented with 2% glucose and DMSO and the other with 2% glucose and 500nM 1NM-PP1. The experiment was performed by Madeleine Meusburger. (C) In the absence of Ypk3 activity, Ser232 phosphorylation is sensitive to rapamycin.

Like Sch9, Ypk1 and Ypk2, which are direct targets of TOR complexes, Ypk3 is a member of the AGC kinase family. Next, we wanted to address whether Ypk3 is likewise a target of TORCs. SDS-PAGE migration shift assay showed that Ypk3 was highly phosphorylated under normal conditions whereas it became hypophosphorylated under rapamycin-/BHS-treated and nutrient-limited conditions (Figure 29A-C) Rapamycin-dependent dephosphorylation of Ypk3 suggests that it is a TORC1 target. To see whether Ypk3 is a common target of TORC1 and TORC2, we employed an auxin-based degron system where TORC2 is specifically inhibited upon auxin treatment (Figure 29D). In this system, cells carry the E3 ubiquitin ligase SCF-TIR1 from plants and Avo1 tagged with auxin-interaction domain (AID). Treatment of these cells with auxin induces the interaction of the TIR complex with the AID tag, and eventually the degradation of the Avo1-AID fusion protein in the proteasome. We ensured that auxin treatment, itself, had no effect on either of the TOR complexes in wild type cells by showing that phosphorylation of the TOR-specific sites on Sch9 and Ypk1 were not influenced by the auxin treatment per se (Figure 29E). Auxin did not result in dephosphorylation of Ypk3 or Rps6 in the

Avo1-AID cells, although we could clearly see hypophosphorylation of Ypk1, the direct effector of TORC2, suggesting that inhibition of TORC2 is not sufficient to induce Ypk3 or Rps6 dephosphorylation (Figure 29F). We also excluded Snf1, Sch9, Mck1 and Kns1 from being mediators of TORC1 signaling to Ypk3 since inhibition or deletion of any of these kinases did not suppress hypophosphorylation of Ypk3 following rapamycin treatment (Figure 29G-I).

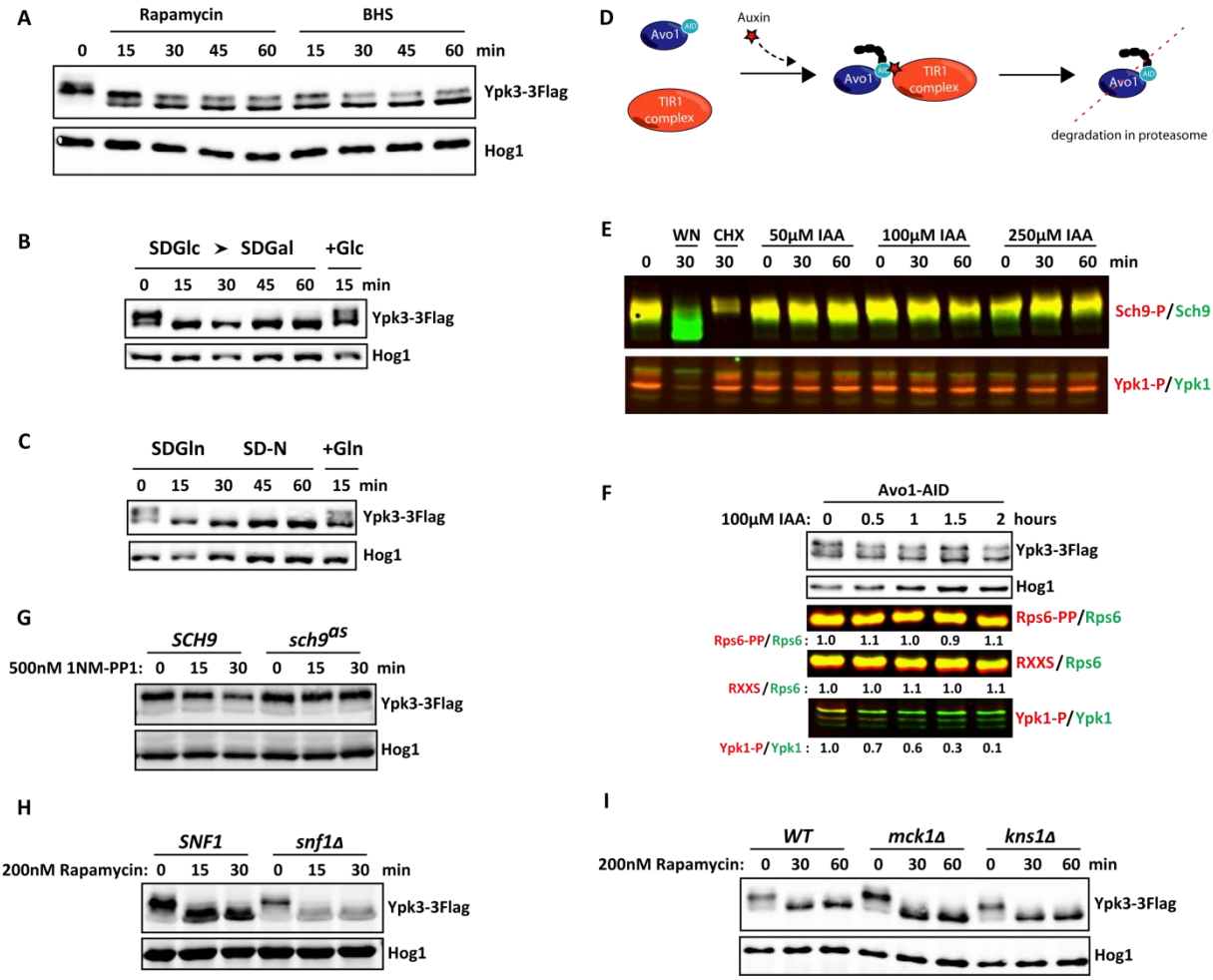

Figure 29. Ypk3 is a rapamycin- and nutrient-responsive phosphoprotein.

(A) The cells expressing Flag-tagged-Ypk3 were treated with 200nM rapamycin or 100μM BHS once they reached exponential growth phase. (B-C) Starvation experiments were performed as described previously with the cells carrying a plasmid which expresses Flag-tagged-Ypk3. (D) Scheme illustrating the Avo1-degron system. (E) Exponentially growing wild type cells with HA-tagged Sch9 were treated with wortmannin (WN), cycloheximide (CHX) or indole-3-acetic acid (IAA). Western analyses employed recognizing Sch9 phosphorylated on Ser737 or Ypk1 phosphorylated on Ser662 or total Ypk1. Total Sch9 levels were assessed with an antibody against the HA epitope. (F) Specific inhibition of TORC2 by the auxin system led to the dephosphorylation of Ypk1 on the TORC2-target site but not to that of Ypk3 or Rps6. (G-H-I) The indicated strains were transformed with a plasmid expressing Flag-tagged Ypk3 and treated with rapamycin when they reached exponential growth phase. The membranes were probed with anti-Flag and anti-Hog1 antibodies. Hog1 was used as a loading control.

PKA was proposed to be the kinase for Ypk3 mediating the signal from TORC1 (Soulard et al). We confirmed that inhibition of PKA led to the hypophosphorylation of Ypk3 (Figure 30A). However,

rapamycin-dependent dephosphorylation of Ypk3 was more drastic than PKA-dependent dephosphorylation suggesting that PKA could not be the only kinase for Ypk3 (Figure 30B). Moreover, we showed that Ypk3 interacted with TORC1 in a rapamycin-sensitive manner as well as with Rps6 (Figure 30C). Thus, these results together strongly suggest that Ypk3 is likely to be a direct effector of TORC1.

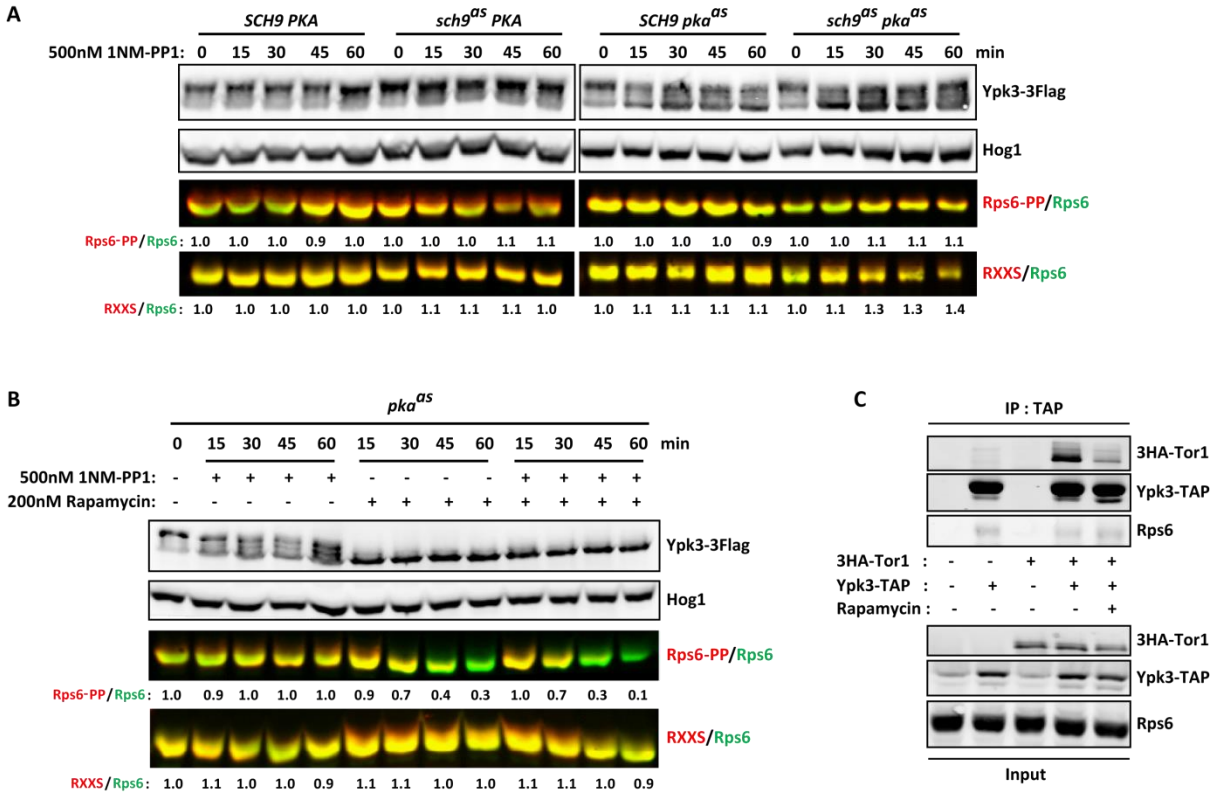

Figure 30. Ypk3 interacts with TORC1 and Rps6 *in vivo*.

(A) Strains carrying the analog-sensitive alleles of all three isoforms of PKA (*TPK1*, *TPK2* and *TPK3*) or that of *SCH9* individually or in combination were treated with the analog at the exponential growth phase. (B) Inhibition of PKA and TORC1 simultaneously revealed that TORC1 has a more profound effect on Ypk3 phosphorylation. (C) The strain bearing N-terminally tagged Tor1 and C-terminally tagged Ypk3 were grown in YPD. Total extracts were prepared under native conditions following 30 minutes of rapamycin treatment. Ypk3 was immunoprecipitated using IgG Dynabeads as described in the methods section.

TOR targets a highly conserved hydrophobic motif at the C-terminal end of AGC kinases. Based on the homology among Ypk1, Ypk2 and Ypk3, we predicted Ser513 to be the hydrophobic motif of Ypk3 and replaced this residue with alanine. Although the point mutation had little effect on the migration

of Ypk3, it did not affect the catalytic activity of the protein as reflected by Rps6 phosphorylation (Figure 31A). Substitution of the site with glutamic acid/aspartic acid to obtain a phosphomimetic Ypk3 did not suppress the rapamycin-induced hypophosphorylation of Rps6. To map other rapamycin-sensitive phosphorylation sites on Ypk3, we decided to do mass spectrometry analysis in collaboration with Gustav Ammarer's Laboratory in Vienna. We immunoprecipitated Flag-tagged Ypk3 from untreated- and rapamycin-treated cells and sent this material for mass spectrometric analysis. The analysis revealed three rapamycin-sensitive sites on the N-terminus (S86, S92, S94) and three other sites on the C-terminus of the protein (S505, S517, S519) (Figure 31B). Alanine substitution of the residues S505, S513, S86, S92 and S94 alone or in combination did not usably alter the activity of Ypk3, despite the fact that phosphorylation of Ypk3 decreased due to the mutations as observed by changes in migration in SDS-PAGE (Figure 31C). However, alanine substitution of S517 and S519 residues in combination with that of S505 and S513 greatly diminished the phosphorylation level of Rps6 to a comparable level to that observed in *ypk3* cells (Figure 31D). Next, we substituted these four sites with aspartic acid and glutamic acid and wanted to see whether the phosphomimetic Ypk3 suppressed Rps6 dephosphorylation induced by rapamycin. However, this was not the case leading us to think that Ypk3 is not the only player which mediates the rapamycin-dependent regulation of Rps6 phosphorylation (Figure 31D).

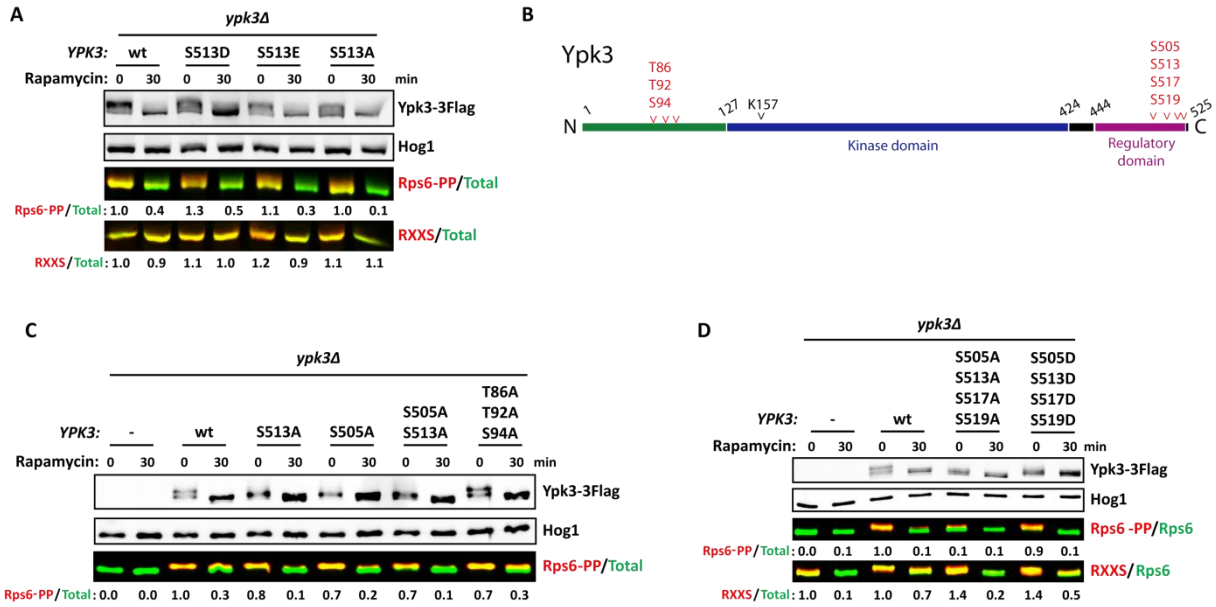

Figure 31. Ypk3 is phosphorylated on at least four residues on its C-terminal end.

(A) Substitution of only the hydrophobic motif with alanine, aspartic acid or glutamic acid affects neither phosphorylation of Ypk3 nor its function. (B) Schematic representation of the domains of Ypk3 and the mapped rapamycin-sensitive phosphorylation sites. (C) Alanine substitution of the turn motif and the hydrophobic motif individually or in combination does not impair Ypk3 activity. Similarly, mutation of the N-terminal phosphorylation sites does not abolish Ypk3 phosphorylation. (D) Substitution of the four phosphorylation sites on the C-terminal end of Ypk3 with alanine impairs its activity. However, their substitution with aspartic acid does not lead to the suppression of rapamycin-induced dephosphorylation of Rps6.

To gain insight into the role of Ypk3 and Rps6 phosphorylation in cells, we wanted to characterize the interactome of Ypk3. For this purpose, we again immunoprecipitated flag tagged-Ypk3 under rapamycin-treated and untreated conditions, cut out the bands detected with coomassie staining and sent them for identification by mass spectrometry. This analysis led us to the characterization of Rrp5, Rpg1 and Sup35 as Ypk3-interacting proteins (Figure 32A). More interestingly, Ypk3 interacted with ribosomal protein L3 in a TORC1 activity-dependent manner. Rrp5 is a component of the small subunit processosome (Dragon et al, 2002; Grandi et al, 2002) . Rpg1 is a component of the eIF3 complex involved in translation initiation, whereas Sup35 is a translation termination factor. Both factors are directly linked with translation, reinforcing the likelihood of a role for Ypk3 in the

ribosome system. Rpl3 was previously implicated in translation elongation (Meskauskas & Dinman, 2007). Accordingly, several mutations in Rpl3 affected the anisomycin-sensitivity of cells. Anisomycin is a translation inhibitor specific for the A-site and is also known to alter the efficiency of -1 ribosomal frameshifting in the cell (Dinman et al, 1997). Thus, we investigated the anisomycin-sensitivity of cells deleted for *YPK3* and found that loss of *YPK3* yielded hypersensitivity to anisomycin (Figure 32B-C). However, *RPS6*^{AA} mutants did not exhibit such strong growth phenotype in response to anisomycin (Figure 32D). The anisomycin phenotype of *ypk3* mutants could therefore be more related to its ability to regulate Rpl3. However, this hypothesis remains to be investigated in the future.

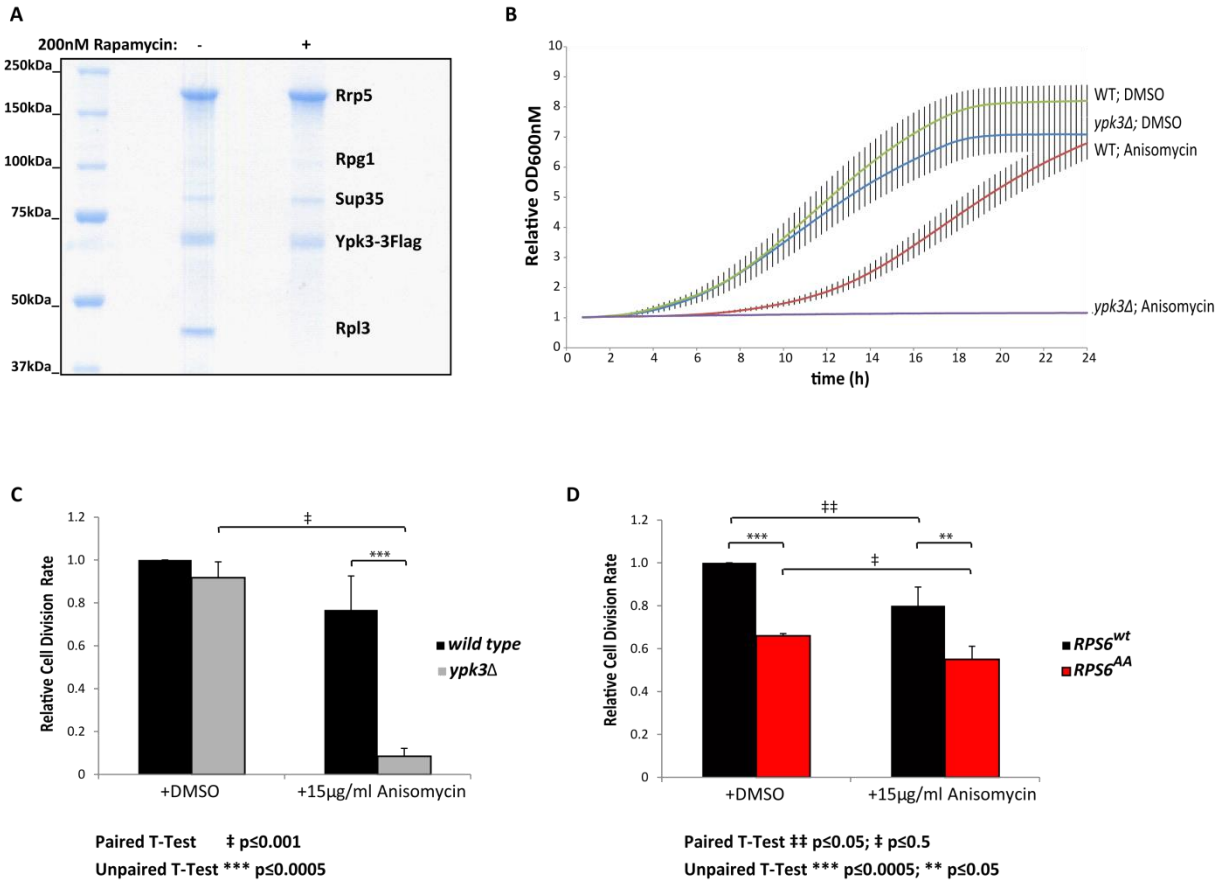

Figure 32. Cells deleted for *YPK3* are hypersensitive to anisomycin.

(A) Strains with Flag-tagged Ypk3 were treated with vehicle or 200nM rapamycin for 30min prior to the preparation of total extracts. Ypk3 was immunoprecipitated and co-precipitated proteins were identified by mass spectrometry as described previously. (B) Cells deleted for *YPK3* are not able to grow in the presence of anisomycin. (C-D) Quantification of the relative growth rates of the indicated strains under anisomycin-treated and untreated conditions obtained in three independent experiments.

Given a role for Rpl3 in ribosomal frameshifting (Peltz et al, 1999), we investigated whether Ypk3 or Rps6 phosphorylation had any effect on this process. We employed a dual-luciferase assay system previously established to study ribosomal frameshifting in yeast (Harger & Dinman, 2003). In these reporters, programmed -1 ribosomal frameshifting signals derived from HIV-1 and L-A viruses and programmed +1 ribosomal frameshifting signals derived from Ty-1 and Ty-3 viruses were replaced between the *Renilla* and firefly luciferase reporter genes. Thus, the ratio of firefly luciferase signal to the *Renilla* luciferase signal gives the efficiency of the translational decoding. Unfortunately,

preliminary experiments showed that neither the deletion of *YPK3* nor the expression of $RPS6^{AA}$ exhibited any effect on the ribosomal frameshifting compared to the wild type cells (Figure 33A-B). Thus, we concluded that neither Rps6 phosphorylation nor Ypk3 had an obvious role in ribosomal frameshifting.

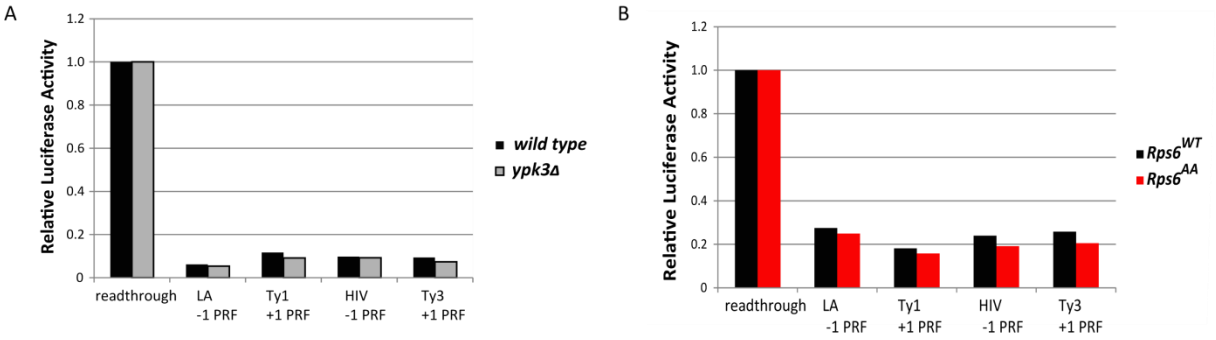

Figure 33. Rps6 phosphorylation has no effect on ribosomal frameshifting efficiency.

(A-B) Efficiency of frameshifting is represented as the ratio of firefly luciferase activity to *Renilla* luciferase activity.

Characterization of Ypk1 and Ypk2 as S6 Kinases

As mentioned earlier, BHS, an inhibitor of TORC1 and TORC2, triggers the dephosphorylation of both S232 and S233 on Rps6, whereas S232 phosphorylation is resistant to rapamycin treatment. As the inhibition of TORC2 by itself was not sufficient for the dephosphorylation of S232 (Figure 29F), we hypothesized that S232 could be a common target for TORC1 and TORC2. For further confirmation, we combined specific inhibition of TORC1 and TORC2 by employing rapamycin and the auxin-based degron system, respectively. We showed that simultaneous inhibition of both complexes led to the hypophosphorylation of Rps6 on S232 residue (Figure 34A). Ypk1 and Ypk2 are *bona fide* substrates of TORC2 and are also closely related to Ypk3 suggesting that all three kinases could redundantly be mediating Rps6 phosphorylation. Inhibition of Ypk1 and Ypk2 did not affect the phosphorylation levels of Rps6 (Figure 34B-C). However, inhibition of Ypk1 and Ypk2 in combination with rapamycin treatment induced hypophosphorylation of S232 (Figure 34D). Next, we combined the deletion of *YPK3* gene with the deletion of *YPK2* gene and analog-sensitive allele of *YPK1*. In the absence of the

activities of all three kinases, both S232 and S233 appeared to be dephosphorylated (Figure 34E). To see whether the activity of Ypk kinases was relevant for Rps6 phosphorylation under physiological conditions, we again starved the cells expressing the analog sensitive alleles of *YPK1* and *YPK3* in the absence of *YPK2* gene for glucose. Upon re-addition of glucose, Rps6 became re-phosphorylated. Re-phosphorylation of Rps6 under this condition was dependent on the activity of Ypk kinases as Rps6 re-phosphorylation was abolished when these cells were treated with the analog (Figure 34F).

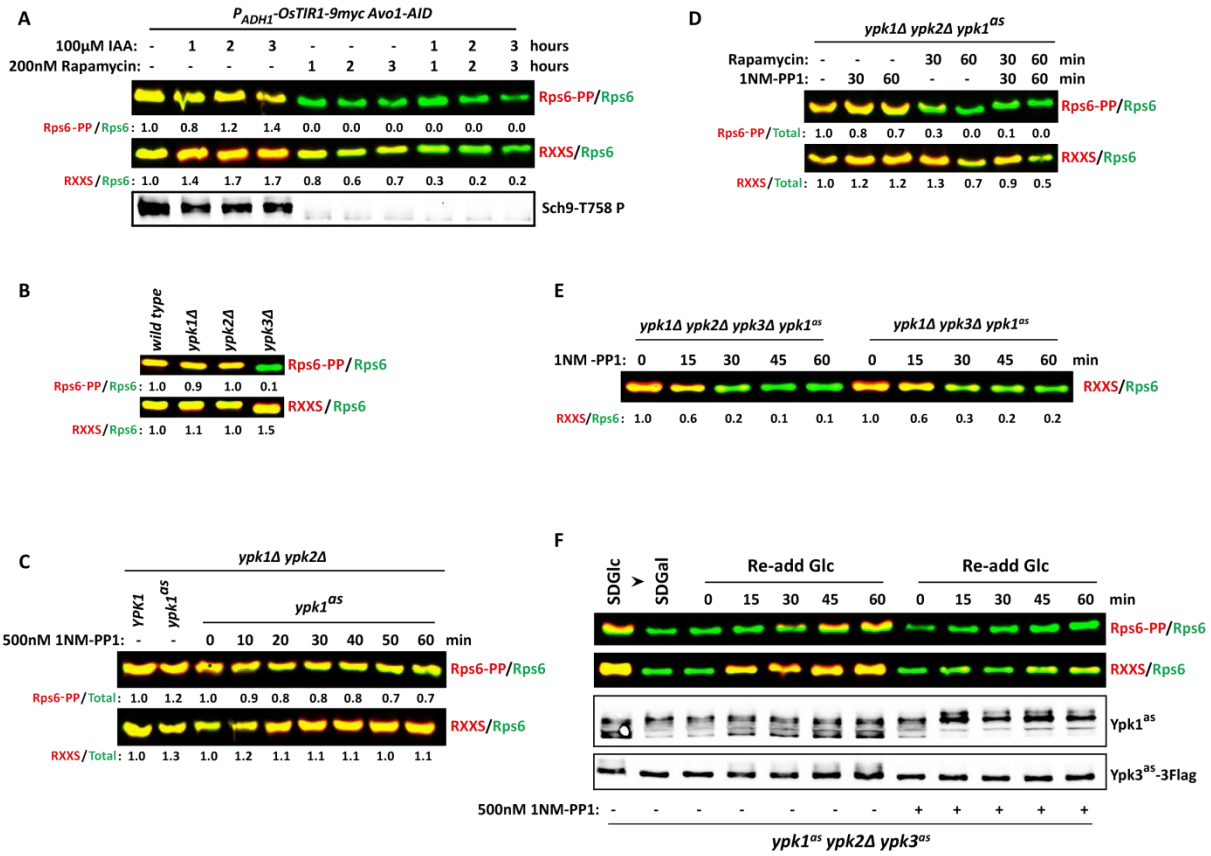

Figure 34. Both TORC1 and TORC2 contribute to the phosphorylation of Ser232.

(A) While inhibition of TORC1 and TORC2 individually has no strong effect on Ser232 phosphorylation, simultaneous inhibition of both complexes leads to the dephosphorylation of the site. (B) Individual deletion of *YPK1* and *YPK2* does not influence Rps6 phosphorylation. (C) Absence of both Ypk1 and Ypk2 activities does not trigger any change at the Rps6 phosphorylation levels. (D) Simultaneous treatment of ypk1-as ypk2 strains with rapamycin and the analog results in Rps6 dephosphorylation on both Ser232 and Ser233. (E) Ypk1 inhibition in *ypk2Δ* and *ypk3*Δ triggers loss of Ser232 phosphorylation. (F) Rps6 rephosphorylation upon glucose refeeding is dependent on the activity of the Ypk kinases.

Ypk1 and Ypk2 are redundant kinases as deletion of both genes is synthetically lethal (Casamayor et al, 1999). We observed that the deletion of *YPK1* and *YPK3* genes was also lethal suggesting that there is redundancy between these two Ypks (Figure 35). However, *YPK2* and *YPK3* were not synthetically lethal. Ypk1 is much more abundant than Ypk2 and Ypk3, so Ypk1 can be sufficient to compensate for the absence of both Ypk2 and Ypk3.

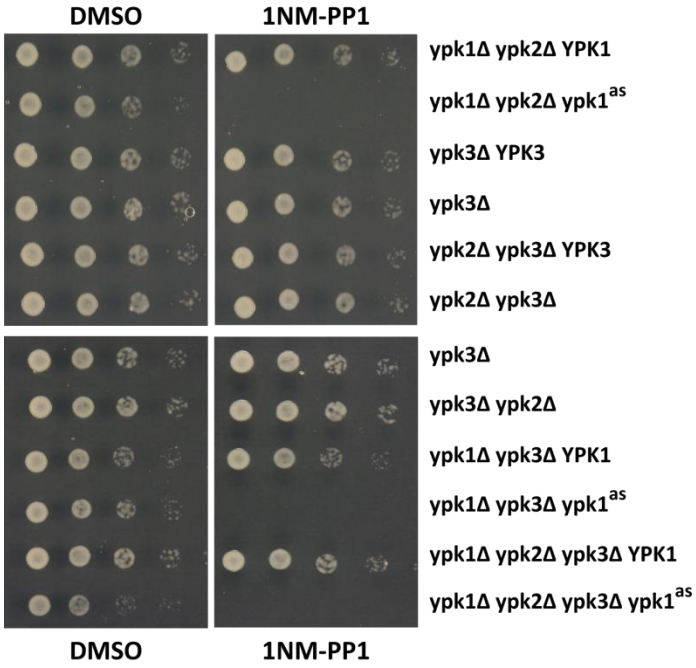

Figure 35. *YPK3* deletion is synthetic lethal with *ypk1*.

Indicated strains were spotted on synthetic media with DMSO/ 500nM 1NM-PP1 and incubated for 3 days at 30 °C.

As mentioned earlier, the deletion of *YPK3* renders phosphorylation of the S232 residue of Rps6 sensitive to rapamycin. Thus, we asked whether this hypophosphorylation event was due to the inhibition of Ypk1 and Ypk2 under these conditions. To answer this question, we tried to rescue the phenotype by expressing the hyperactive allele of *YPK2*, $YPK2^{D239A}$. However, hypophosphorylation of S232 was unaffected by the expression of $YPK2^{D239A}$ allele (Figure 36A). Next, we investigated whether the regulation went through Sch9 and Tap42/Tip41 downstream branches of TORC1. We hypothesized that as the regulation is dependent on rapamycin, bypass of TORC1 signaling can suppress the hypophosphorylation. Therefore, we combined the deletion of *YPK3* with the

expression of *SCH9*^{DE} allele and/or the temperature-sensitive allele of TAP42, *tap42-11*. Unexpectedly, we observed that expression of *SCH9*^{DE} led to lower levels of S232 phosphorylation and did not suppress the further hypophosphorylation upon rapamycin (Figure 36B). Similarly, expression of *tap42-11* resulted in a decrease in the levels of S232 phosphorylation, and in an even more drastic decrease in combination with *SCH9*^{DE}.

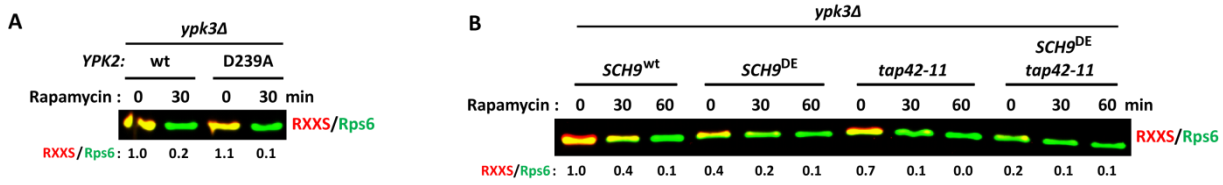

Figure 36. Sch9/Tap42 regulate the rapamycin-sensitivity of Ser232 in the absence of Ypk3 activity.

(A) Cells deleted for *YPK3* were transformed with plasmids carrying either the wild type or the hyperactive allele of *YPK2*. (B) Indicated strains were grown in YPD at 25°C, treated with 200nM rapamycin and processed as explained before.

Dephosphorylation of S233 upon rapamycin was not suppressed by the phosphomimetic allele of Ypk3 (Figure 31D). Similarly, dephosphorylation of S232 upon rapamycin in the *ypk3Δ* background was not suppressed by hyperactive Ypk2. Taken all the results together, we proposed that rapamycin-dependent regulation of Rps6 phosphorylation was not mediated solely by kinases, but also by phosphatases.

Characterization of PP1 as the S6 Phosphatase

Protein phosphatase 1 was recently proposed to mediate dephosphorylation of Ser-247 in Rps6 in mammalian cells (Hutchinson et al, 2011). Thus, we investigated the role of PP1 in Rps6 dephosphorylation in yeast employing numerous loss-of-function mutants of Glc7, the catalytic subunit of yeast PP1 (Baker et al, 1997). We observed that Rps6 phosphorylation levels were much higher in strains with lower Glc7 activity (Figure 37A). We continued our study using the *glc7-127* mutant as the effect on Rps6 phosphorylation of this mutant was more pronounced than that of the other mutants. The *glc7-127* allele contains two point mutations, K110A and K112A, and provokes phenotypes like defects in glycogen accumulation and elevated levels of phosphorylation of Histone

H3 (Baker et al, 1997). We showed that expression of the *glc7-127* allele blocked entirely the hypophosphorylation of Rps6 in response to rapamycin and BHS treatments, and even led to higher phosphorylation levels compared to the wild type cells under normal conditions (Figure 37B).

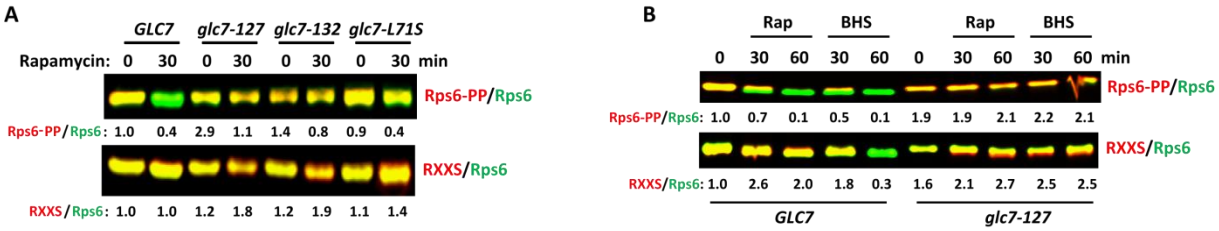

Figure 37. Rapamycin- and BHS-dependent dephosphorylation of Rps6 is mediated by Glc7.

(A) Expression of loss-of-function mutants of *GLC7* abolished the dephosphorylation of Rps6 upon rapamycin. (B) The indicated strains were treated with 200nM rapamycin or 100µM BHS when they reached exponential growth phase. The *glc7-127* allele suppressed both rapamycin- and BHS-induced dephosphorylation of Rps6.

Calyculin A is a known inhibitor of protein phosphatase 1 and protein phosphatase 2A. However, it was reported to be a more potent inhibitor of PP1 rather than PP2A in yeast (Hoon et al, 2008). Intriguingly, we found that strains expressing *RPS6*^{AA} exhibited resistance to calyculin A treatment compared to the wild type strains (Figure 38A). Calyculin A-sensitivity of the cells could be partially rescued by the overexpression of *GLC7* supporting the notion that Glc7 is the target of this drug (Figure 38B). This observation linked Glc7 activity and Rps6 phosphorylation physiologically. On the other hand, *ypk3* strains did not exhibit calyculin A resistance (Figure 38C). To ensure that the calyculin A-phenotype was due to non-phosphorylatable form of Rps6 rather than low levels of Rps6 due to the mutations, we tested whether the cells deleted for either of *RPS6A* or *RPS6B* genes exhibited the same phenotype. The deletion strains did not show any resistance to calyculin A treatment (Figure 38D), thereby supporting that it is the non-phosphorylatable form of Rps6 that renders cells resistant to calyculin A. To further confirm the synthetic interaction between Glc7 and Rps6 phosphorylation, we combined the *glc7-127* allele with *RPS6*^{AA}. The strains expressing either of the alleles have a growth defect with similar growth rates. We did not detect any additional growth defect in the cells in which these two alleles were combined, suggesting that Glc7 activity and Rps6

phosphorylation were functionally linked (Figure 38E). However, it is difficult to conclude which one is downstream and which one is upstream based on these results.

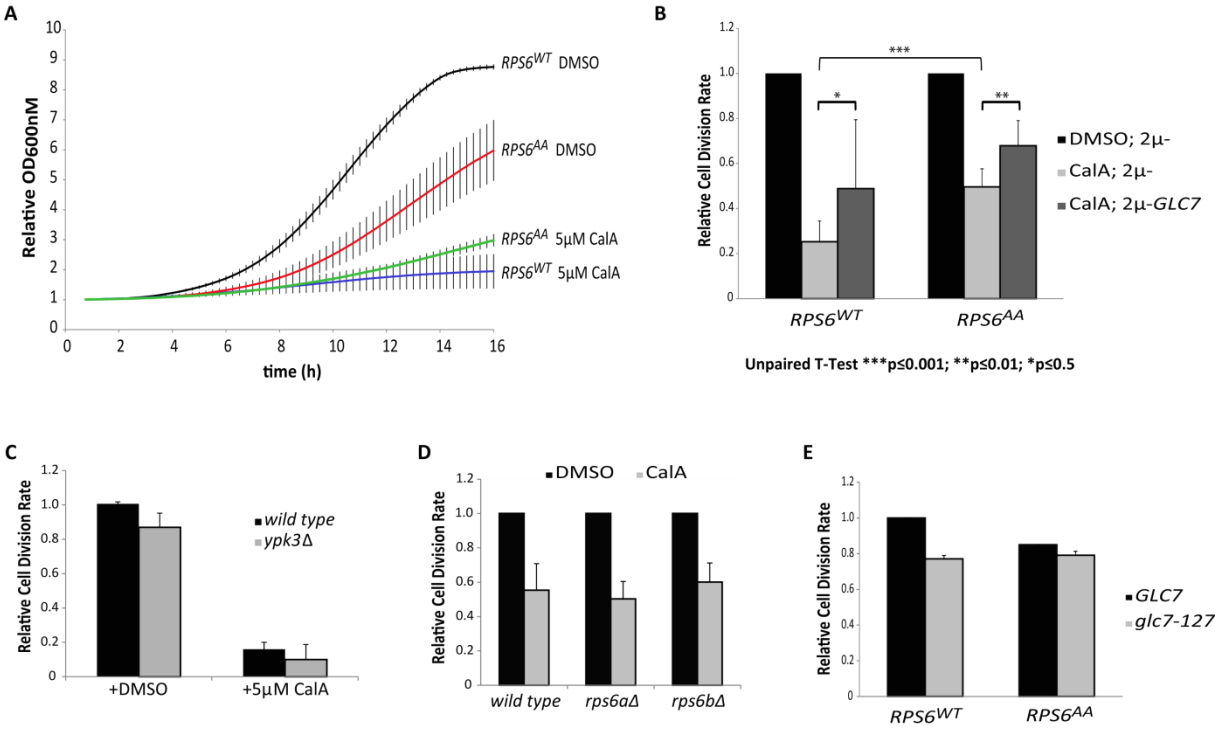

Figure 38. Cells expressing *RPS6*^{AA} exhibit slight resistance to calyculin A.

(A) Indicated strains were grown in the presence of the vehicle (DMSO) or 5µM calyculin A for 16 hours and their optical density was measured every 15min as explained in detail in the methods section. (B) Quantification of the relative cell division rates of *RPS6*^{AA} and wild type cells overexpressing, or not, *GLC7*. (C) Cells deleted for *YPK3* have similar growth rates to wild type cells and are not resistant to calyculin A. (D) Cells deleted for either copy of *RPS6* genes do not display a calyculin A-resistant phenotype. (E) *glc7-127* and *RPS6*^{AA} cells have similar proliferation rates.

Glc7 activity is regulated by numerous regulatory subunits. Next, we wanted to identify the regulatory subunit of Glc7 which played a role in Rps6 dephosphorylation. For this purpose, we screened all known non-essential proteins previously characterized as regulatory components of PP1 for any effect on Rps6 phosphorylation levels. We pinpointed Shp1 as a protein required for the dephosphorylation of Rps6 upon rapamycin (Figure 39A). Furthermore, deletion of *SHP1* suppressed the effect of rapamycin and BHS on Rps6 phosphorylation in a manner comparable to the expression of *glc7-127* allele (Figure 39B), pointing at a pronounced role for Shp1 in Rps6 dephosphorylation.

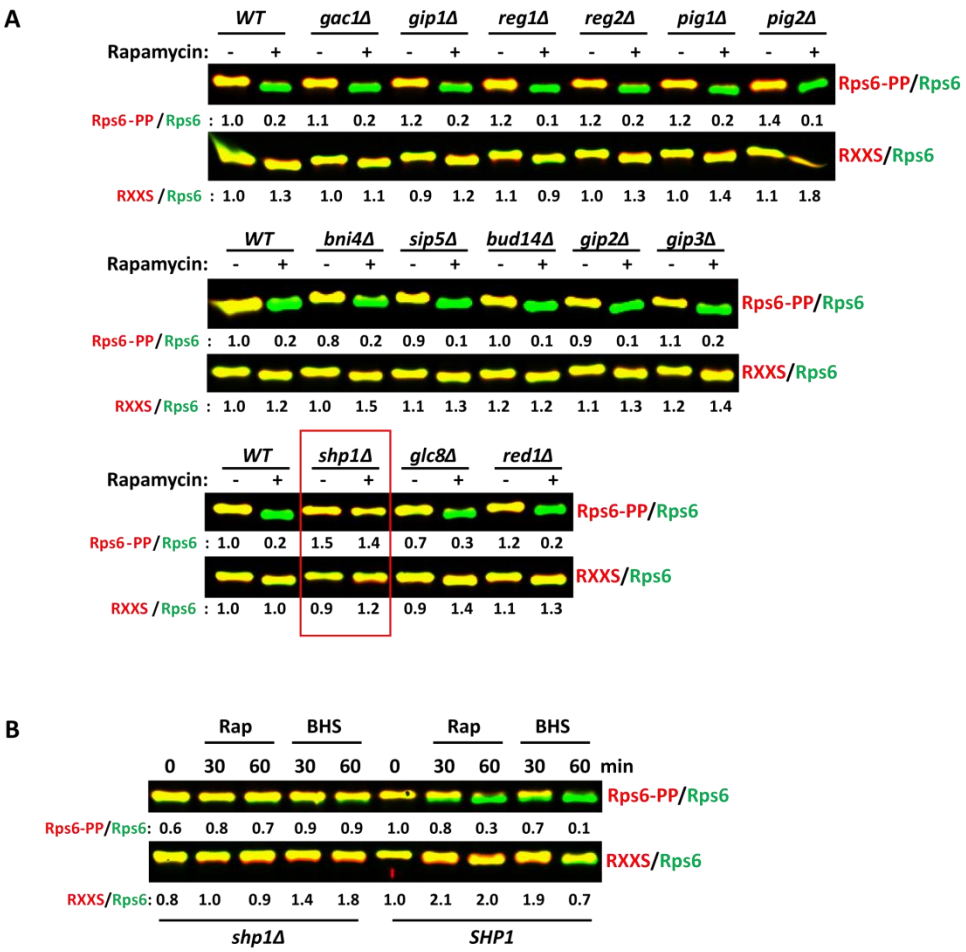

Figure 39. Shp1 activity is indispensable for dephosphorylation of Rps6 upon rapamycin and BHS.

(A) Cells deleted for genes which were previously implicated in the regulation of Glc7 activity were treated with 200nM rapamycin for 60min during exponential growth phase. Deletion of *SHP1* impaired the dephosphorylation of Rps6 upon rapamycin treatment. (B) Treatment of the cells deleted for SHP1 with 200nM rapamycin or 100µM BHS failed to induce dephosphorylation of Rps6.

To answer the question whether there is a synthetic genetic interaction between *SHP1* and *RPS6*^{AA}, we tested their growth abilities individually or in combination. However, we did not see any significant synthetic genetic interaction in contrast to what we observed between *GLC7* and *RPS6* (Figure 40A). However, because the cells deleted for *SHP1* were very sick, it was challenging to assess further effects on its growth abilities. Shp1 contains multiple functional domains: the UBA domain is required for its binding to ubiquitylated substrates, whereas the UBX and BS1 (binding site 1) domains function as Cdc48-binding sites (Figure 40B). In a recently published study, the effect of the

different domains of Shp1 on its activity was assessed (Bohm & Buchberger, 2013). Deletion of UBA domain did not have any impact on its ability to interact with Cdc48, whereas deletion of UBX domain completely abolished this interaction. Taking advantage of these mutants, we addressed the contribution of the different domains of Shp1 to the rapamycin sensitivity of Ser233. Interestingly, deletion of either of the UBA or UBX domains partially suppressed the rapamycin-induced dephosphorylation of Ser233 (Figure 40C). Furthermore, expression of these mutants partially suppressed the growth defect of *RPS6*^{AA} cells (Figure 40D). The mutations in the UBX and BS1 domains which completely blocked the interaction of Shp1 with Cdc48 completely abolished the rapamycin-sensitivity of the site. At this point, we wanted to investigate whether Cdc48 inhibition had any effect on Rps6 phosphorylation. Because Cdc48 is essential, we employed a temperature-sensitive allele of *CDC48*, *cdc48-3*. Inhibition of *CDC48* resulted in small suppression of Rps6 dephosphorylation in response to rapamycin treatment (Figure 40E).

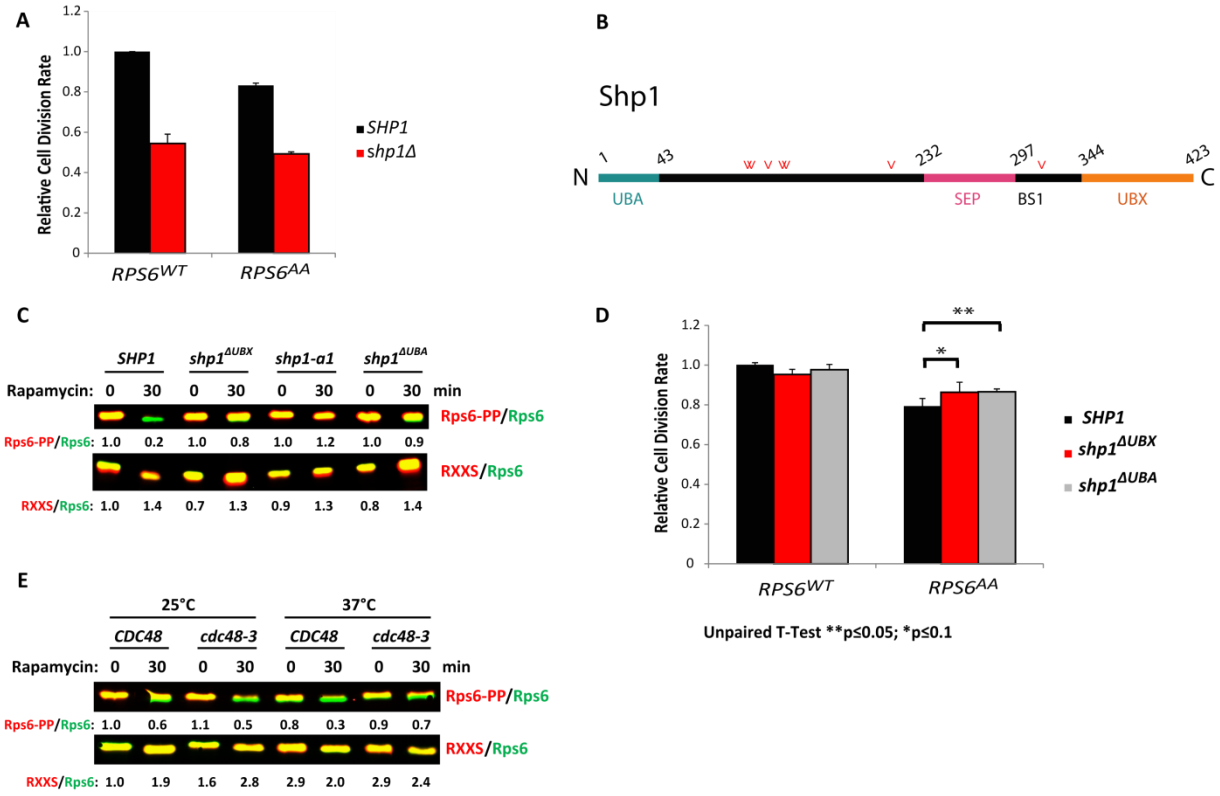

Figure 40. Full-length Shp1 is required for rapamycin-induced dephosphorylation of Rps6.

(A) Indicated strains were grown in YPD at 30°C and their growth rates were measured in a microplate reader as explained in in the methods section. (B) Schematic representation of the Shp1 domains. UBA: ubiquitin-associated domain, SEP: *shp1*, eyc and p47 domain, BS1: binding-site domain 1, UBX: a ubiquitin-like domain. (ˇ) putative phosphorylation sites found in RXXS motif. (C) Cells expressing the different mutants of *SHP1* were tested for their abilities to mediate Rps6 dephosphorylation upon 200nM rapamycin. (D) $shp1^{\Delta UBX}$ and $shp1^{\Delta UBA}$ mutants partially suppressed the proliferation defect of the $RPS6^{AA}$ cells. (E) Cells expressing wild type or a temperature-sensitive allele of *CDC48* were grown in YPD at 25°C. Once they reached exponential growth phase, cultures were split into two and one of the cultures was transferred to 37°C while the other was kept at 25°C. Following 1 hour of incubation, the cells treated with 200nM rapamycin.

As mentioned before, in the absence of Ypk3 activity, Ser232 is dephosphorylated upon rapamycin treatment. Based on the idea that the phosphatase branch mediates the regulation of Rps6 phosphorylation under various conditions, we assumed that Glc7/Shp1 could be responsible for the rapamycin sensitivity of Ser232 in the cells deleted for the *YPK3* gene. Accordingly, we found that expression of the *glc7-127* allele or that deletion of *SHP1* in combination with *ypk3* deletion was

sufficient to suppress the dephosphorylation of Ser232 following rapamycin treatment (Figure 41A-B).

Figure 41. Rapamycin-sensitivity of Ser232 in the absence of Ypk3 activity is dependent on Glc7/Shp1.

(A-B) Exponentially growing cells with the indicated genotypes were treated with 200nM rapamycin.

To better understand the regulation of Glc7/Shp1, we investigated whether Shp1 is a rapamycin-dependent phosphoprotein as suggested by a former phosphoproteomics study (Loewith Lab, unpublished data). The characterization of the rapamycin-sensitive phosphoproteome revealed two putative phosphorylation sites (Ser106 and Ser108) on Shp1 which could be targeted by TORC1 (Huber et al, 2009). These phosphorylation sites were found in RXXS motifs. Using the anti-RXXS antibody, we detected the phosphorylation of Shp1 on this motif (Figure 42A). More intriguingly, this phosphorylation of Shp1 seemed to be sensitive to rapamycin. We substituted the Ser106 and Ser108 residues with alanine to see whether these were the relevant phosphorylation sites. However, these alanine substitutions did not abolish the phosphorylation of Shp1 detected with anti-RXXS antibody (Figure 42A). We continued by mutating all putative phosphorylation sites found in RXXS motifs in Shp1 individually or in combination and thus, we mapped Ser210 as the target of this phosphorylation event (Figure 42B). None of these mutants appeared to be defective in cell division (Figure 42C). Next, we asked the question whether this phosphorylation event contributes to the regulation of Rps6 phosphorylation. None of the Shp1 mutants exhibited a defect in Rps6 dephosphorylation upon rapamycin except for the S315A mutant (Figure 42D). Interestingly, expression of the S315A mutant of *SHP1* accelerated the dephosphorylation of Rps6 in response to TORC1 activity. Currently, we are working on the role of the phosphomimetic mutants of Shp1 on

Rps6 phosphorylation to have a better insight into the function of Shp1 phosphorylation in the regulation of Rps6 phosphorylation. Moreover, we are investigating the roles of Ypk3 and Sch9 in the regulation of Shp1 phosphorylation and function.

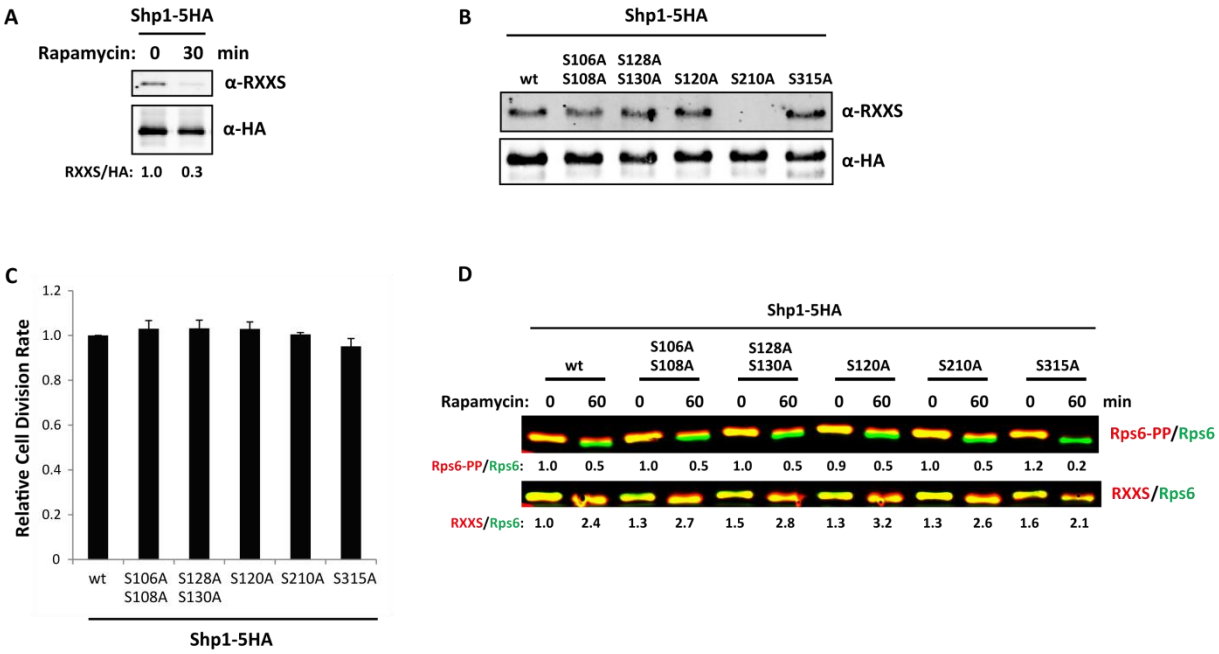

Figure 42. Shp1 is phosphorylated in a TORC1-dependent manner.

(A) Following the TCA treatment of the cells expressing HA-tagged Shp1, we immunoprecipitated Shp1, and probed the elute with anti-HA and anti-RXXS antibodies as described in the methods section. (B) We mutated all the serine codons found in RXXS motifs. *shp1Δ* cells were transformed with plasmids carrying the wild type or the mutated *SHP1* genes. (C) The steady state growth rates of the indicated strains were measured in a microplate reader for 16 hours at 30 °C. (D) Exponentially growing cells harboring the HA-tagged Shp1 plasmid with the indicated mutations were treated with 200nM rapamycin for 1 hour.

To address the role of Glc7 in translation, we compared the growth of wild type and *glc-127* cells in the presence of various translation elongation inhibitors. Expression of *glc7-127* rendered cells hypersensitive to hygromycin and paromomycin in a manner which could not be rescued by the expression of $RPS6^{AA}$ or the deletion of *YPK3* (Figure 43A-B). However, similar mutants of *GLC7* were previously shown to be sensitive to cationic drugs such as hygromycin and paromomycin due to the regulatory role of Glc7 in the electrochemical gradient of the plasma membrane (Williams-Hart et al,

2002). To see whether the drug sensitivity of the *glc7-127* strains we observed was also an indirect effect, we employed cycloheximide which is not a cationic drug. However, in this case, all the strains we tested reacted to the drug just like the wild type (Figure 43C-D). Thus, these results suggested that sensitivity of the *glc7-127* cells to translation inhibitors were most likely not due to translational defects.

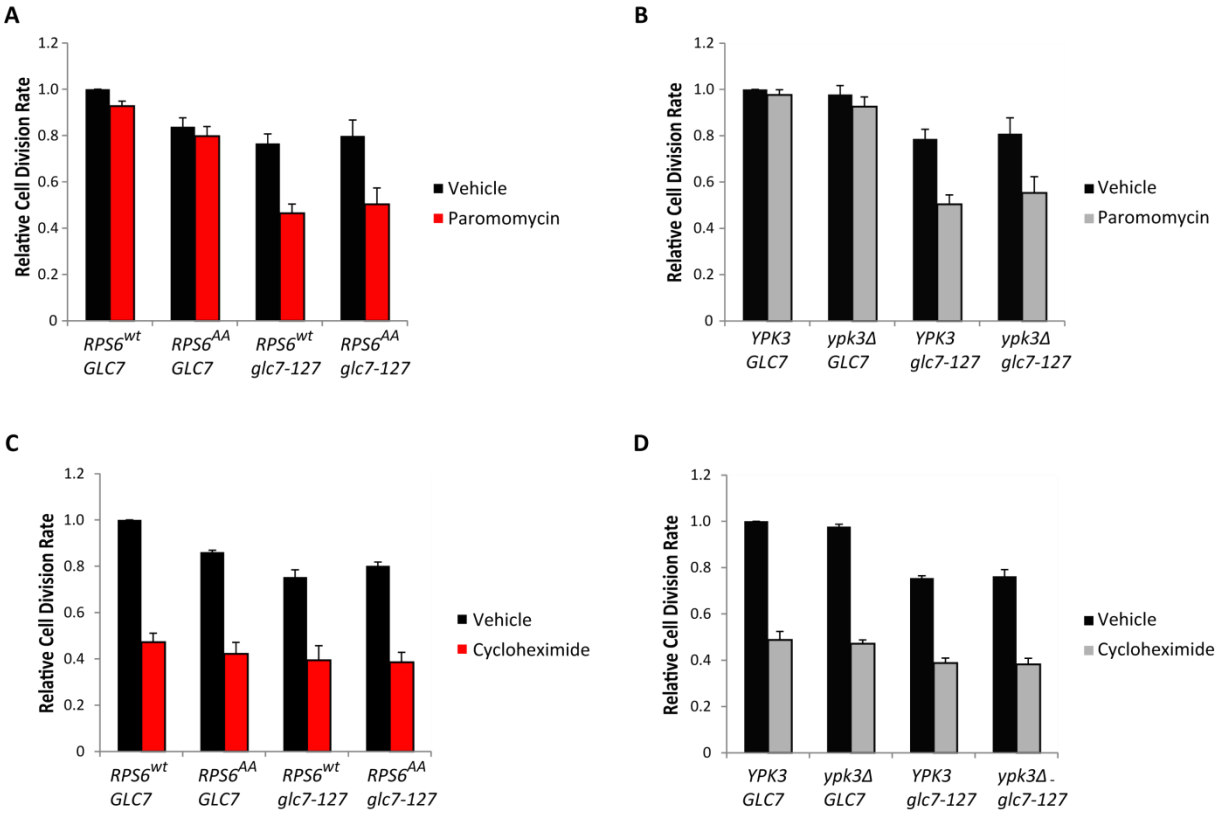

Figure 43. The *glc7-127* strains are hypersensitive to paromomycin, albeit in a Rps6-phosphorylation independent manner.

(A-D) Indicated strains were grown in YPD supplemented with 100µM paromomycin, 10ng/ml cycloheximide or the vehicle at 30°C for 16 hours.

The Role of Other Kinases/Phosphatases in Rps6 Phosphorylation

Phosphoproteomic analysis describing changes in phosphorylation events in cells deleted for various kinases/phosphatases revealed Rps6 as a target of numerous kinases and phosphatases including Ypk3 (Figure 44A) (Bodenmiller et al, 2010). We wanted to confirm the role of these proteins in Rps6 phosphorylation (Figure 44B). Cka1 and Cka2 are catalytic subunits of casein kinase 2, which is a

Ser/Thr kinase playing important roles in cell growth. We did not detect any significant change in the levels of Rps6 phosphorylation in the absence of Cka1, whereas deletion of *CKA2* seemed to delay rapamycin-dependent hypophosphorylation of S233 (Figure 44B). Pph21 and Pph22 are catalytic subunits of protein phosphatase 2A and are highly redundant. Deletion of *PPH21* led to a similar phenotype to the deletion of *YPK3* making S232 sensitive to rapamycin (Figure 44B). Despite the redundancy between Pph21 and Pph22, we found the opposite result with the deletion of *PPH22*. Psk1 and Psk2 are Ser/Thr kinases containing a PAS-domain, which regulate protein synthesis and carbohydrate metabolism. Deletion of *PSK1* or *PSK2* did not drastically change the levels of Rps6 phosphorylation. If and how these kinases and phosphatases contribute to the regulation of Rps6 phosphorylation remains to be further investigated.

Hrr25 is a Ser/Thr kinase which is known to regulate small ribosomal subunit biogenesis through the phosphorylation of Rps3 (Schafer et al, 2006). Thus, we investigated a possible role for Hrr25 in Rps6 phosphorylation. Hrr25 activity is essential for the survival of the cell. Therefore, we employed an analog-sensitive allele of *HRR25* to specifically inhibit the kinase. First, we determined the optimum concentration of analog necessary to inhibit Hrr25 using a cell division assay (Figure 44C). However, inhibition of Hrr25 alone or in combination with rapamycin did not induce any change at the Rps6 phosphorylation levels excluding Hrr25 in the regulation of Rps6 phosphorylation (Figure 44D).

A

Kinase/Phosphatase	Kinase Name	Rps6 Peptide
YOR061W	Cka2	R.RAS*S*LK
YML057W	Cmp2	R.RAS*S*LK
YKL190W	Cnb1	R.RAS*S*LK
YDL134C	Pph21	R.RAS*S*LK
YAL017W	Psk1	R.RAS*S*LK
YBR028C	Ypk3	R.RAS*S*LK

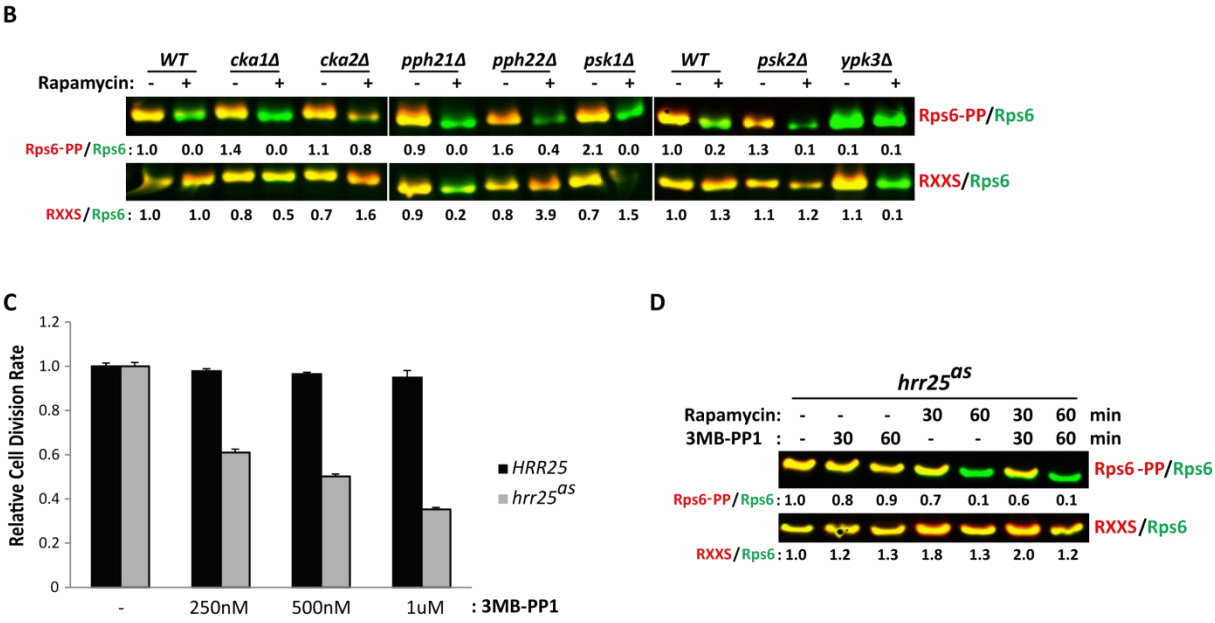

Figure 44. Multiple kinases/phosphatases have an impact on Rps6 phosphorylation.

(A) List of the kinases/phosphatases whose deletion leads to a change of more than two-fold in Rps6 phosphorylation (Bodenmiller et al, 2010). (B) Cells deleted for the indicated genes were treated with 200nM rapamycin for 60 min. (C) Cells deleted for *HRR25* gene and harboring a plasmid carrying wild type or an analog-sensitive allele of *HRR25* were grown in YPD supplemented with analog (3MB-PP1) or the vehicle (DMSO) at 30°C. (D) Cells expressing the analog-sensitive allele of *HRR25* were treated with rapamycin (200nM) and 3MB-PP1 (1µM) individually or in combination.

The Role of Rps6 Phosphorylation in Global Translation

To explore the impact of Rps6 phosphorylation on global translation, we monitored the abundance of free 40S, 60S and 80S subunits in addition to the actively translating ribosomes (polysomes) in wild type and $RPS6^{AA}$ cells using sucrose gradient centrifugation. The ratio of 80S to polysomes seemed to be the same in these two strains, suggesting that $RPS6^{AA}$ had no general effect on translation in accordance with the previous results (Ruvinsky et al, 2005) (Figure 45A). On the other hand, the

mutant strains exhibited an elevated 60S peak indicating an imbalance between the free subunits. This phenotype is similar to what is observed in the absence of one of the two copies of the *RPS6* genes (Pachler et al, 2004). Yet, we wanted to see whether there was a defect in ribosome biogenesis in the absence of phosphorylatable Rps6 in the cells. Preliminary experiments showed that the *RPS6*^{AA} cells were defective in pre-ribosomal rRNA processing (Figure 45B). However, the cells deleted for *YPK3* did not display the same phenotype, which could be explained by the fact that in the absence of the Ypk3 activity only the second serine (Ser233) is in a non-phosphorylated form. Nonetheless, the role of Rps6 phosphorylation in ribosome biogenesis and pre-rRNA processing will require further investigation.

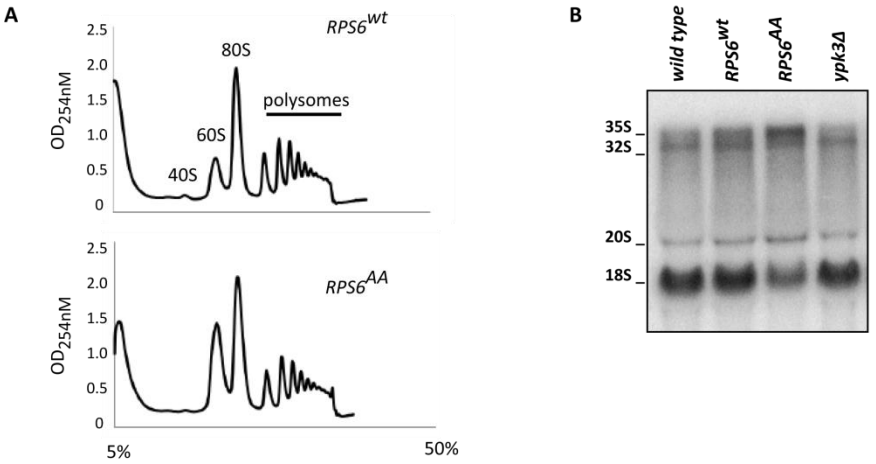

Figure 45. The cells expressing *RPS6*^{AA} display an elevated 60S peak.

Both of the experiments were performed by Madeleine Meusburger. (A) Exponentially growing cells with the indicated genotypes were treated with 20mg/ml cycloheximide prior to the ribosome extraction. Fractions corresponding to 10 OD_{260nM} of the extracts were loaded on top of sucrose gradients. (B) rRNA synthesis/processing was assessed by the northern blot.

To address whether the absence of the activity of the Rps6 kinases culminates in a similar polysome profile as the expression of the non-phosphorylatable Rps6, we starved cells deleted for all three YPKs, but expressing analog-sensitive alleles of *YPK1* and *YPK3* for glucose for 1 hour and refed them with glucose with or without the analog (1NM-PP1). Starvation for glucose led to the dephosphorylation of Rps6 and Ypk3, while refeeding triggered their rephosphorylation (Figure 46A).

However, treatment of cells with the analog and glucose in unison abrogated this rephosphorylation. Starvation for glucose induced a slower migration of Ypk1 in SDS-PAGE due to the inactivation of Ypk1 and consequent hyperactivation of Fpk1/2. Analysis of the abundance of the free subunits (40S and 60S), the monosomes (80S) and the polysomes collected after the refeeding with or without the analog revealed that inhibition of Ypks had no significant effect on the profiles under any of the conditions tested (Figure 46B). These results are in accordance with a recently published study which showed that the wild type and S6K1;S6K2^{-}/$^{-}$ liver polysome profiles did not exhibit any significant differences under starvation and refeeding conditions (Chauvin et al, 2013). Importantly, abolishment of the activities of the yeast Rps6 kinases did not induce a 60S peak as we observed with the Rps6 phosphomutant cells. Given that cells expressing only the *RPS6*^{AA} allele and that cells bearing only one copy of the two *RPS6* genes exhibit the same phenotype with regard to an increase in the 60S:40S ratio and that the inhibition of the S6 kinases do not result in the same profile, suggests that Rps6^{AA} may not be as stable as the wild type protein.

We repeated the starvation and refeeding experiment with the wild type and *RPS6*^{AA} cells and again analyzed the polysome profiles under these conditions. Although the *RPS6*^{AA} cells displayed an increase in the 60S peak in all the conditions we tested, we did not detect any other changes in the profiles compared to the wild type cells (data not shown).

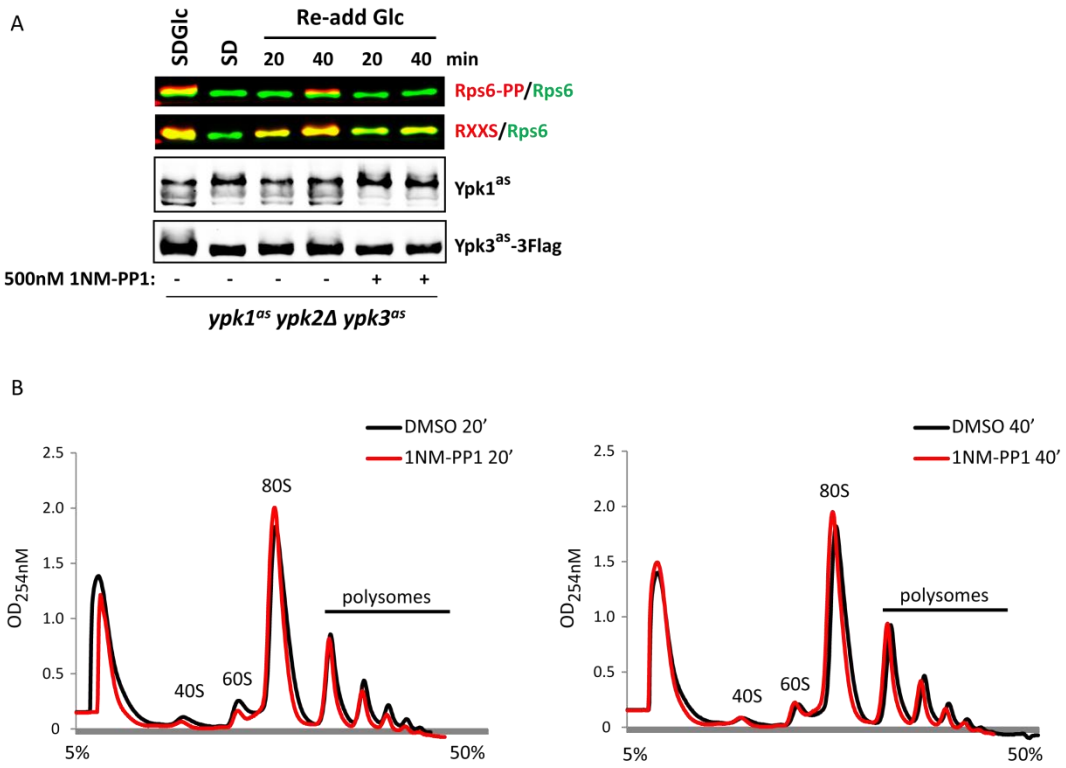

Figure 46. Global protein synthesis is not affected by the absence of the Ypk activity in the cell.

(A-B) *ypk1*^{as} *ypk2Δ ypk3*^{as} cells were grown to exponential growth phase in SD media with 2% glucose. Samples were collected for TCA protein extraction and the polysome profiling. Following filtering, the cells were resuspended in SD media without any carbon source and incubated at 30°C for 1 hour. After sample collection, remaining cells were split into two and treated with 2% glucose with or without the analog. At the indicated time-points, samples were collected. The samples were processed according to the protocols explained in the methods section.

The Role of Rps6 Phosphorylation in Reinitiation

Provided that Rps6 phosphorylation did not affect global translation, we hypothesized that it might rather alter the translation efficiency in specific cases. One such mechanism utilized for gene-specific translational control is reinitiation. To investigate if Rps6 phosphorylation affects the efficiency of reinitiation, we used a *GCN4-LacZ* reporter. We treated cells with 3-aminotriazole (3-AT) to induce *GCN4* expression. 3-AT is an inhibitor of *HIS3* gene production and thus causes histidine starvation. We did not detect any significant difference in the levels of *GCN4* expression between the Rps6-wild type and phosphomutant strains under 3-AT-treated or –untreated conditions (Figure 47A). We

argued that lack of a phenotype could be due to dephosphorylation of Rps6 upon 3-AT treatment. However, 3-AT treatment did not induce Rps6 dephosphorylation as shown by western blot (Figure 47B). Moreover, expression of *RPS6*^{AA} did not give any advantage/disadvantage in growth under conditions where cells were starved for amino acids (Figure 47C). Thus, we concluded that Rps6 phosphorylation has no significant effect on reinitiation efficiency, at least not in the case of *GCN4*.

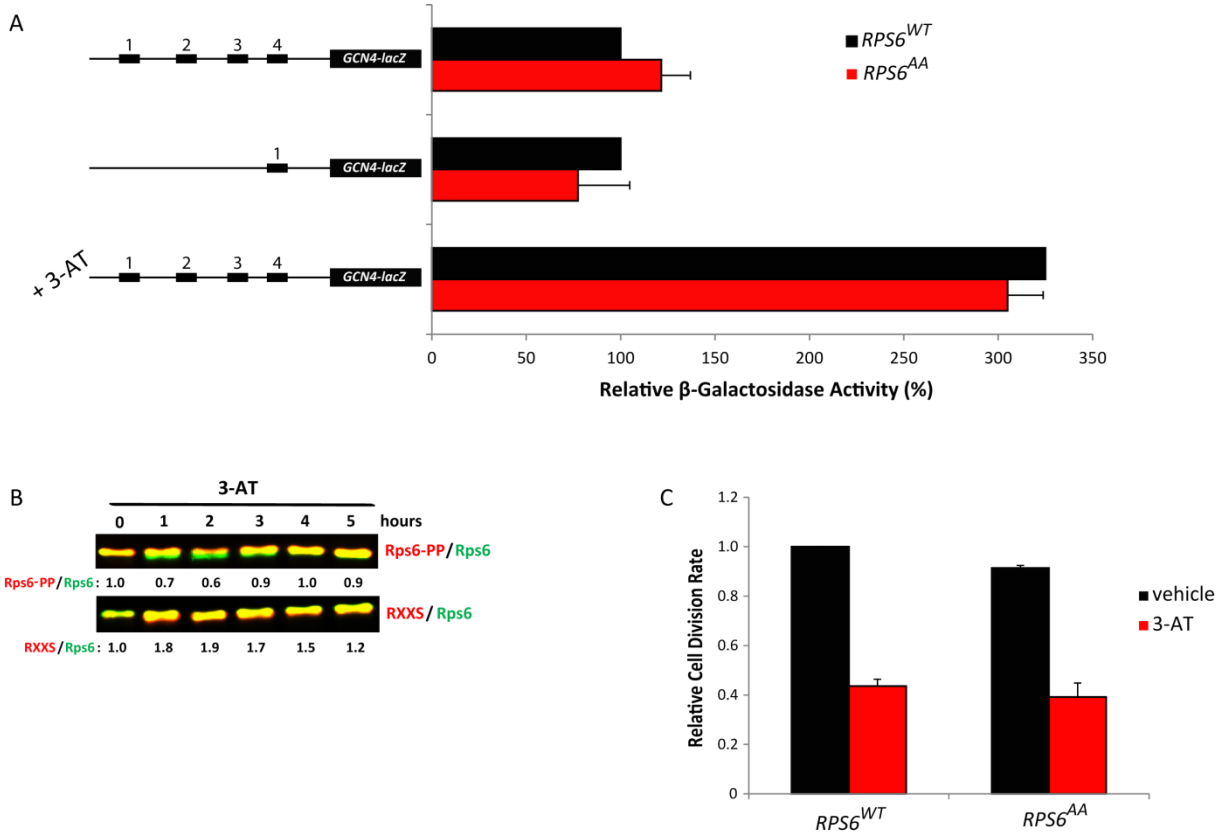

Figure 47. Rps6 phosphorylation does not play a role in the translational reiniation of the *Gcn4* mRNA.

(A) Prototrophic strains with the indicated genotypes were transformed with reporter plasmids carrying the four *Gcn4* upstream open reading frames (uORF), the first one or none. Relative β-galactosidase activities were assessed as the ratio of the reporter activity with the uORFs to the reporter activity in the absence of any uORFs. *GCN4-LacZ* expression was induced by treating cells with 30mM 3-aminotriazole for 5hours. (B) Exponentially growing wild type cells were treated with 30mM 3-AT up to 5hours to assess the effect of histidine starvation on Rps6 phosphorylation. (C) The indicated strains were grown in the presence of vehicle or 30mM 3-AT. The average and the standard deviation from three independent experiments are shown.

Synthetic Genetic Array to Identify the Function of Rps6 Phosphorylation

To identify mutants possessing synthetic genetic interactions with *RPS6*^{AA}, we performed a Synthetic Genetic Array (SGA) in collaboration with Charles Boone's Laboratory in Toronto. The SGA is a method based on "systematic construction of double mutants" by crossing the strain of interest with a collection of deletion mutants and subsequently an analysis of growth abilities of acquired mutants (Tong et al, 2001). We used wild type- and phosphomutant-Rps6 strains for the array and a number of genes associated with ribosome biogenesis, translation and mRNA decay scored suggesting that Rps6 phosphorylation might be implicated in these processes (Figure 48A). Next, we wanted to confirm some of these genetic interactions by remaking the triple mutants in our background. However, we could not detect any synthetic genetic interactions at 30°C (Figure 48B). Exceptionally, deletion of *HBS1* exhibited synthetic sickness with *RPS6*^{AA} at lower temperatures (Figure 48C). Hbs1 is a GTPase which is required for ribosomal subunit dissociation and release of the peptidyl-tRNA under conditions of ribosomal stalling, and is thus implicated in no-go decay (Carr-Schmid et al, 2002; Doma & Parker, 2006). No-go decay is a specialized mechanism which targets mRNAs harboring stalled ribosomes for degradation. Hbs1, in collaboration with Dom34, triggers release of the mRNA so that the fragments of the mRNA can be degraded by the exosome or Xrn1 following an endonucleolytic cleavage (Harigaya & Parker, 2010). Thus, with the purpose of investigating a possible role of Rps6 phosphorylation in no-go decay, we employed a previously established *PGK1-SL* reporter construct containing a stable stem loop which triggers elongation stalls (Doma & Parker, 2006). Unfortunately, wild type and *RPS6*^{AA} cells did not display any difference in no-go decay efficiency (data not shown).

A

deletion mutants which display 'synthetic' growth phenotypes with $RPS6^{AA}$		
YKR084C	Hbs1	facilitates ribosomal subunit dissociation and peptidyl-tRNA release when translation is stalled; genetically implicated in mRNA no-go decay
YOR141C	Arp8	Nuclear actin-related protein involved in chromatin remodeling
YBR131W	Ccz1	Protein involved in vacuolar assembly, essential for autophagy and the cytoplasm-to-vacuole pathway
YHR111W	Uba4	Protein that activates Urm1p before its conjugation to proteins (urmylation); also acts in thiolation of the wobble base of cytoplasmic tRNAs by adenylating and then thiolating Urm1p;
YDR159W	Sac3	Nuclear pore-associated protein; required for biogenesis of the small ribosomal subunit; component of TREX-2 complex (Sac3p-Thp1p-Sus1p-Cdc31p) involved in transcription elongation and mRNA export from the nucleus
YIL040W	Apq12	Protein required for nuclear envelope morphology, nuclear pore complex localization, mRNA export from the nucleus
YKR001C	Vps1	Dynamin-like GTPase required for vacuolar sorting; also involved in actin cytoskeleton organization, endocytosis, late Golgi-retention of some proteins, regulation of peroxisome biogenesis
YKL081W	Tef4	Gamma subunit of translational elongation factor eEF1B, stimulates the binding of aminoacyl-tRNA (AA-tRNA) to ribosomes by releasing eEF1A (Tef1p/Tef2p) from the ribosomal complex
YGL202W	Aro8	Aromatic aminotransferase I, expression is regulated by general control of amino acid biosynthesis
YCR016W		nuclear protein, involved in ribosome biogenesis

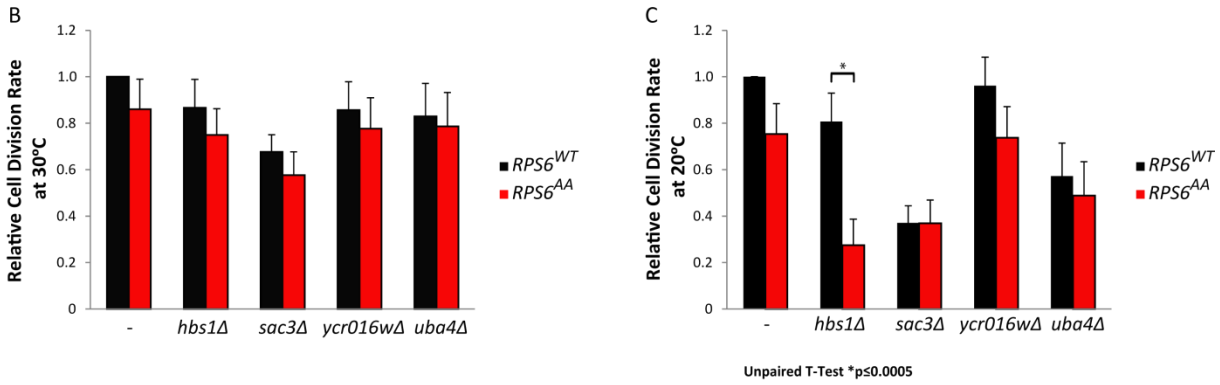

Figure 48. *RPS6*^{AA} and *HBS1* display a synthetic genetic interaction at 20°C.

(A) The list of hits which came out in the SGA analysis. (B-C) The growth rates of the indicated strains were measured over a 16 hour period at 30°C or 20°C. The growth rates of the mutant cells were normalized to that of the wild type. The assays performed at 20°C were done by Sedef Karayel.

Uba4 is implicated in the wobble base pairing through its ability to activate Urm1 which is required for thiolation of cytoplasmic tRNAs (Goehring et al, 2003; Leidel et al, 2009). Even though we did not manage to confirm the synthetic genetic interaction between the *RPS6*^{AA} and *UBA4* strains as suggested by the SGA, additional large-scale analyses suggested genetic interactions between *YPK3* and components of the Elongator complex. This prompted us to look into a possible role for Rps6 phosphorylation in wobble base pairing (Costanzo et al, 2010; Fiedler et al, 2009). To do so, we used a dual luciferase system in which arginine repeats were encoded with either AGA (translation permissive) or CGA (translation inhibitory) codons. The CGA codons require wobble decoding for

translation. The two sets of repeats were inserted between a *Renilla* and a firefly luciferase reporter (Figure 49A) (Letzring et al, 2010). Accordingly, the ratio between the *Renilla* and firefly luciferase signals gives the translation efficiency of the repeats. The strains bearing the non-phosphorylatable allele of *RPS6* displayed a slight defect in translation of the CGA repeats compared to the wild type cells (Figure 49B). However, the mechanism by which Rps6 contributes to the wobble base pairing remains to be elucidated.

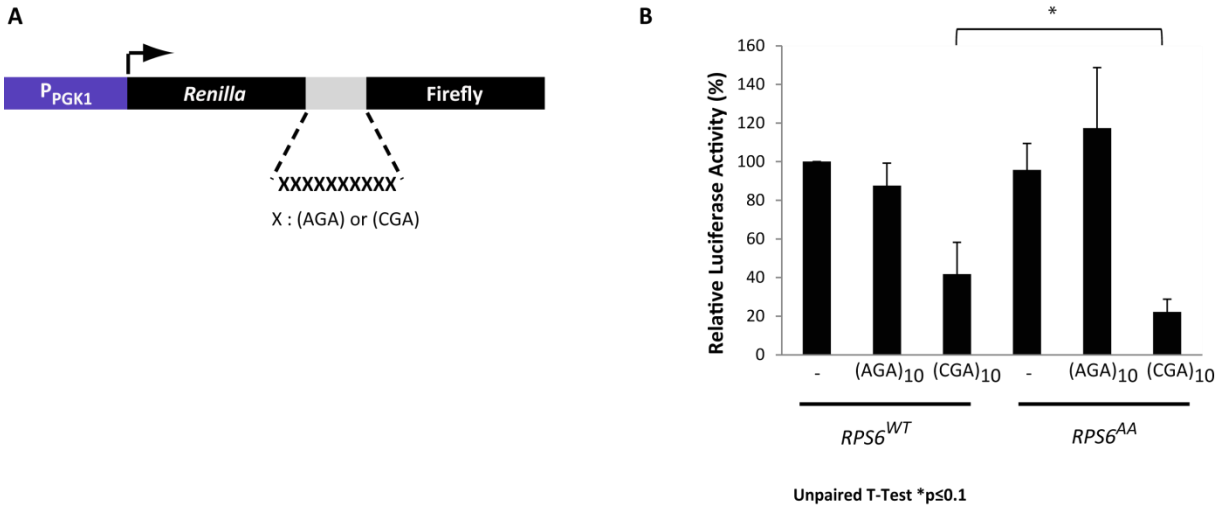

Figure 49. Efficiency of wobble base pairing is lower in cells expressing *RPS6*^{AA}.

(A) Scheme illustrating the dual luciferase system. Adapted from (Letzring et al, 2010) (B) The Dual-Luciferase Reporter Assay System from Promega was used to assess the luciferase expression of the exponentially growing cells in synthetic medium.

Localization of Rps6 Phosphorylation

One question which we wanted to address was whether Rps6 phosphorylation is an early event occurring during small subunit biogenesis or a late one which takes place in cytoplasm. To answer this question, we collaborated with the Vikram Panse Laboratory at the ETH, Zurich. Following the purification of the small subunit at different stages of biogenesis using Noc4-, Enp1-, Rio2- or Asc1-TAP tagged strains, we checked the phosphorylation level of Rps6 in these different contexts. Noc4 is a nucleolar protein which mediates the early steps of pre-40S maturation (Milkereit et al, 2003). Enp1 is another nucleolar protein, mostly interacting with the early 90S and intermediate pre-40S

particles (Chen et al, 2003). Rio2 and Asc1 are cytoplasmic proteins: Rio2 interacts with late cytoplasmic pre-40S particles, whereas Asc1 is a core component of the mature 40S and 80S (Gerbasi et al, 2004; Vanrobays et al, 2003). Rps6 seemed to be highly phosphorylated on Ser232 residue at every stage of the small subunit biogenesis we tested (Figure 50A). On the other hand, the phosphorylation of Ser233 appeared to be rather low in the context of immature 40S particles compared to the mature 40S. It is likely that the low levels of phosphorylation detected were due to contamination with abundant mature ribosomes. These results encouraged us to hypothesize that the phosphorylation of the two sites occurs in different compartments in the cell. Phosphorylation of Ser232 seemed to be a rather early event in 40S maturation, whereas Ser233 phosphorylation was likely to be a mature 40S-dependent event.

For further confirmation of the localization of Rps6 phosphorylation, we decided to do immune-cryo electron microscopy using the phospho-antibodies. This work was done in collaboration with the Olivier Gadal Laboratory in Toulouse, France. Unfortunately, we could not detect any signal with either of the antibodies we used (Figure 50B). As an alternative, we performed immunofluorescence with the phospho-antibodies. Immunofluorescence revealed that the signal detected with both Rps6-PP and RXXS antibodies concentrated in cytoplasm in wild type cells (Figure 50C). In *RPS6*^{AA} cells, no signal with either of the antibodies was detected suggesting that the signals in the wild type cells indeed reflected the phosphorylated form of Rps6. Surprisingly, we did not observe any signal with the strains in which only the second serine was substituted with alanine, either. This result could suggest that the RXXS signal we observed in wild type cells originated from the phosphorylated form of Ser233, rather than that of Ser232, thereby explaining why the signal was predominantly cytoplasmic in this case. However, there is also the possibility that absence of any clear phospho-signal in the nucleus was due to shielding of Rps6 by ribosome biogenesis factors in the nucleus. Further investigation is required to address these possibilities.

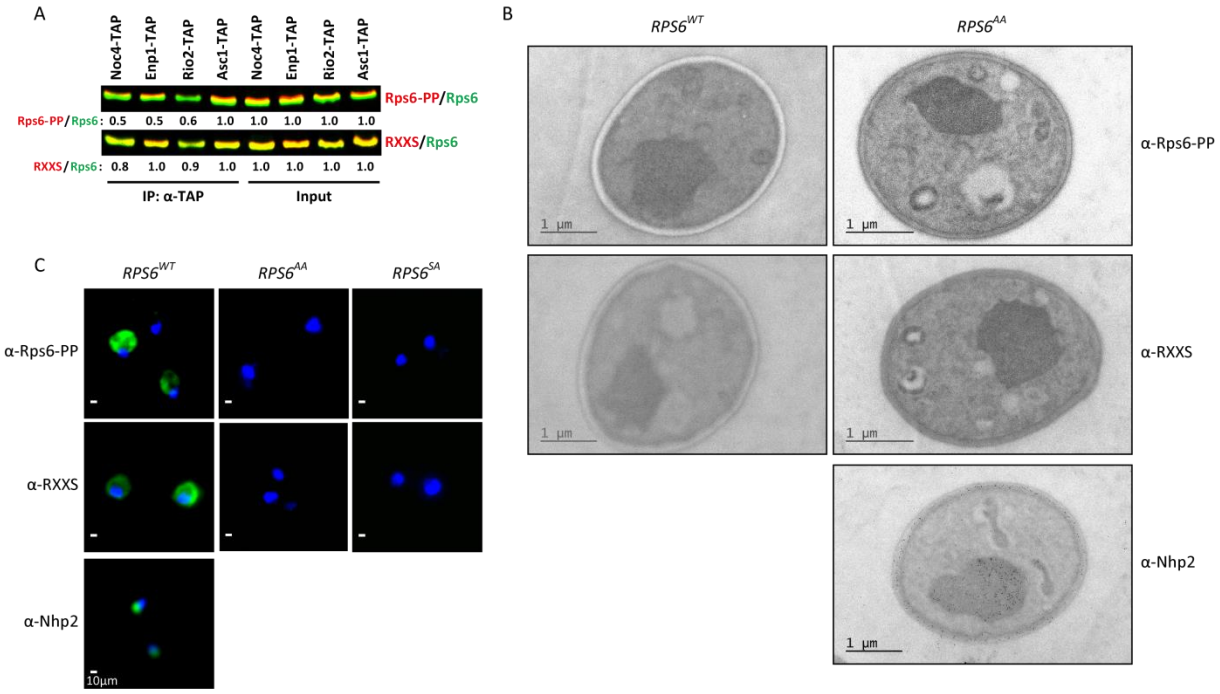

Figure 50. Differentially phosphorylated forms of Rps6 are found in different compartments of the cell.

(A) Rps6 phospho-signal from each TAP-purification was normalized to the signal from the corresponding input based on the observation that the phospho-signal weakens during the process of native protein extraction. (B) A range of concentrations from 1:50 to 1:5000 of the antibodies were tested for immune-cryo EM. However, no signal was detected under any conditions. Nhp2 is a nuclear protein and the antibody against Nhp2 protein was used as a positive control. (C) Spheroplasts prepared following paraformaldehyde fixation of the indicated strains were incubated with the indicated antibodies with a dilution of 1:50 from the original stocks. Nuclei were stained with DAPI (in blue). The images were analyzed by ImageJ.

Discussion

Characterization of Ccr4 as a Novel TORC1 Effector

In this study, we characterized Ccr4 as a downstream effector of TORC1. Current data show that Ccr4 is a phosphoprotein whose phosphorylation status is regulated according to nutrient availability and TORC1 activity. Moreover, we mapped the phosphorylation sites on Ccr4 by mass spectrometry and showed that the mutation of these sites into alanine abolished the rapamycin-dependent hyperphosphorylation of Ccr4 as well as its basal-level phosphorylation. However, we still cannot exclude the presence of additional sites which contribute to the phosphorylation-dependent regulation of Ccr4.

Although we so far failed to pinpoint the kinase which phosphorylates Ccr4, we managed to identify some players of the pathway signaling from TORC1 to Ccr4. Sch9 seemed to partially mediate this signaling event. However, the physiological condition which triggers the Sch9-dependent phosphorylation of Ccr4 remains yet to be elucidated. We excluded carbon source depletion and salt stress. Given that both Ccr4 phosphorylation and TORC1 are highly responsive to nitrogen source-depletion, it is feasible to test whether Sch9 participates in the regulation of Ccr4 in response to different nitrogen sources. On the other hand, hyperphosphorylation of Pop2 upon glucose starvation is dependent on Yak1 activity. However, its rapamycin-induced phosphorylation is mediated by the Sch9-Rim15 branch of TORC1 signaling. Again, the physiological conditions which activate this pathway require further investigation.

Intriguingly, we revealed that Yck1, Swe1 and Elm1 kinases were involved in the rapamycin-dependent hyperphosphorylation of Ccr4. Yck1 is a casein kinase I isoform. Despite the fact that Yck1 and Yck2 are redundant and Yck2 is more abundant than Yck1 in the cells, *YCK2* deletion did not result in any defect in the Ccr4 phosphorylation levels under untreated- and rapamycin-treated conditions, while *YCK1* deletion did. The cells deleted for *YCK1* were impaired in hyperphosphorylation of Ccr4 upon rapamycin treatment. Serine 281 which we mapped as one of

the rapamycin-responsive phosphorylation sites in Ccr4 is found in a casein kinase I recognition motif, thereby suggesting that Yck1 might be the kinase responsible for direct phosphorylation of Ccr4 upon inhibition of TORC1 activity. This hypothesis will require confirmation with an *in vitro* kinase assay. To date, no evidence for regulation of Yck1 by TORC1 has been reported, opening a new field of investigation for characterization of a novel effector of the TORC1 pathway.

One target of Yck1 is the RNA-binding protein Khd1 (also known as Hek2). Systematical analysis found that Khd1 binds to hundreds of mRNAs with a bias for ones which encode membrane-associated proteins (Hasegawa et al, 2008). One well-established target of Khd1 is the *Ash1* mRNA (Irie et al, 2002). Ash1 is a transcription factor which plays a role in filamentous growth, in response to nutrient limitation as well as in mating-type switch by repressing expression of the *HO* endonuclease expression in daughter cells in late anaphase (Chandarlapaty & Errede, 1998; Sil & Herskowitz, 1996). The roles of Ash1 in both processes necessitate the asymmetric localization of *Ash1* mRNA to daughter cells. Khd1 interacts with the *Ash1* mRNA in mother cells and represses its translation initiation (Paquin et al, 2007). On the other hand, phosphorylation of Khd1 by Yck1 hinders the interaction of Khd1 with the *Ash1* mRNA, thereby freeing its translational repression and promoting the production of Ash1 protein on the bud tip. Ccr4 was also implicated in the regulation of the *HO* mRNA levels in a Puf4/5-dependent manner (Goldstrohm et al, 2007; Hook et al, 2007). Moreover, Khd1 targets the *Flo11* mRNA and regulates its asymmetric localization during filamentous growth (Wolf et al, 2010). Another target of Khd1 is the *Rom2* mRNA. More interestingly, regulation of the *Rom2* mRNA by Khd1 is dependent on the presence of Ccr4 in the cell (Ito et al, 2011b). Rom2 is a GDP/GTP exchange factor which is involved in the cell wall integrity pathway. In addition, combinatorial deletion of the *CCR4*/*POP2* and *KHD1* genes results in a severe synthetic growth defect. On the other hand, TORC1 was recently shown to interact with multiple proteins related with filamentous growth under nitrogen-deprivation conditions (Laxman & Tu, 2011). Furthermore, TORC1 impinges on the regulation of the *Flo11* mRNA via the Gcn4 transcription factor upon amino acid starvation (Braus et al, 2003). Altogether, these data raise the possibility that Ccr4

phosphorylation might be involved in the regulation of mRNA repression/localization during filamentous growth or mating-type switching.

Elm1 is a serine-threonine kinase which modulates various cellular processes including cellular morphogenesis and septin organization. In addition, absence of Elm1 activity promotes filamentous growth (Koehler & Myers, 1997). Elm1 also contributes to the mitotic signaling pathway by phosphorylating a number of components of the pathway including the Swe1 kinase (Sreenivasan & Kellogg, 1999). Elm1, itself, is localized to the bud neck during the mitosis till the end of anaphase (Bouquin et al, 2000). Swe1, on the other hand, is another serine-threonine kinase which plays a major role in the regulation of G2/M transition (Booher et al, 1993). In a manner similar to Elm1, Swe1 assists in the promotion of filamentous growth under a variety of stress conditions (La Valle & Wittenberg, 2001). Considering the contribution of these two kinases to Ccr4 phosphorylation, the roles which the Elm1 and Swe1 kinases play in the filamentous growth further bolsters the idea that Ccr4 phosphorylation may be involved in the regulation of this process.

Septins are highly conserved proteins which form a structural scaffold during cytokinesis and bud formation. Swe1 and Elm1 kinases contribute to septin organization (Sreenivasan et al, 2003). Inhibition of Elm1 kinase activity at the G1 stage abolishes the proper polarization of septins. In parallel, Ccr4/Pop2 deadenylase activity contributes to the septin organization by regulating the stability of mRNAs encoding the proteins involved in the septin assembly including the *Elm1* mRNA (Traven et al, 2009). Moreover, *CCR4* and *POP2* genes exhibit synthetic genetic sickness with *ELM1*, thereby provoking the question of whether Ccr4 phosphorylation is critical for the regulation of septin organization.

Given that TORC1 regulates the transcription of ribosomal protein genes while Ccr4 modulates the degradation of ribosomal protein mRNAs, we hypothesized that TORC1 also contributes to the stability of *RP* mRNAs through the regulation of Ccr4. Our hypothesis-driven approach directed us to choose candidate *RP* mRNAs in addition to *Aro4* and *Hsp26* mRNAs to test. Unfortunately, we failed

to collect any evidence which would suggest such regulation. Yet, these results did not rule out the possibility for regulation of another specific subset of mRNAs by Ccr4 in a TORC1-dependent manner. The best approach to test this would be to measure changes at the levels of deadenylation in a transcriptome-wide manner in the presence of differentially phosphorylated forms of Ccr4. The technique is based on deep-sequencing (or microarray analysis) of mRNA populations classified based on the length of their poly(A) tails by "step-wise thermal elution" (Beilharz & Preiss, 2009).

One intriguing observation is the mitosis-dependent regulation of Ccr4 phosphorylation. Arrest of cells in interphase with α-factor treatment and their subsequent release revealed that Ccr4 is hyperphosphorylated at G1 and S phases, with phosphorylation levels returning to the basal levels by G2-M phase (Figure 14B). Given that Swe1 is a well-established regulator of mitosis, mitotic regulation of Ccr4 phosphorylation is likely to be functionally relevant. Moreover, another major player of the mRNA degradation pathway, Dcp1 was recently found to be differentially phosphorylated throughout the mitotic cycle in human cells and phosphorylation of Dcp1 was shown to affect its association with the P-bodies (Aizer et al, 2013). In addition, P-bodies are responsive to different stages of the mitotic cycle. P-bodies are smaller during the early stages of S phase, they become larger as the cells approach the end of S phase and the G2 phase and finally, they dissemble following the entry into mitosis (Aizer et al, 2013; Yang et al, 2004). Although the phosphorylation of Ccr4 had no clear effect on the formation of P-bodies under glucose-limited conditions, it would be feasible to investigate whether Ccr4 phosphorylation plays a role in the regulation of P-body formation during the mitotic cycle or in the recruitment of Ccr4 itself into the P-bodies during this process. Preliminary data suggested that Ccr4 phosphorylation influences the survival of cells in stationary phase. Taking the significance of the P-body formation in stationary phase survival into account, the question of whether Ccr4 phosphorylation is involved in the regulation of P-bodies and the stress granules deserves further investigation.

Finally, although Ccr4 was first identified as a transcription factor, its well-studied function as the major deadenylase in the cell has left its possible roles as a transcription factor in the shade. It might be still worthwhile to investigate whether Ccr4 phosphorylation has any role in the transcription of alcohol dehydrogenase II, its proposed target (Denis, 1984).

In this study, we mainly focused on the regulation and the function of phosphorylation of Ccr4, leaving unanswered the role of Pop2 phosphorylation in the cell. Considering that Pop2 is a highly conserved protein and has critical functions in glucose sensing in addition to its roles in Ccr4 recruitment, the investigation of the physiological role of Pop2 phosphorylation might provide further insight into its significance in the cell.

Regulation and Function of Rps6 Phosphorylation

The physiological role of Rps6 phosphorylation has remained mysterious for the last four decades. Similarly, the pathways signaling to Rps6 in budding yeast has also remained ambiguous, although it is fairly well characterized in higher eukaryotes. In this study, we showed that two phosphorylation sites on the C-terminus of Rps6 are differentially regulated in the cell. The dephosphorylation of the second site (Ser233) seemed to precede the dephosphorylation of the first site (Ser232) in response to nutrient limitations. In accordance, the phosphorylation of Ser232 recovered faster than that of Ser233 upon re-addition of nutrients. Moreover, mutation of Ser232 into alanine caused loss of phosphorylation on Ser233. Taken altogether, the data suggested that similar to the situation in mammalian cells, there is a hierarchy in the phosphorylation of these two sites.

Despite previous contention, here we show that Sch9 is not the S6 kinase *in vivo*, rather it contributes to the regulation of Rps6 phosphorylation only indirectly. The activity of Sch9 regulates translation initiation, and thereby the polysome abundance in the cell. We propose that Rps6 is not accessible to phosphatases in the context of polysomes. Hence, upon rapamycin treatment, Sch9 inhibits translation initiation leading to an increase in the 80S monosomes and free subunits and

assisting in the exposure of Rps6 to phosphatases. Additionally, we are currently trying to address the question of whether Sch9 contributes to the Glc7/Shp1 activity.

We characterized all three Ypks (Ypk1, Ypk2 and Ypk3) as S6 kinases in budding yeast. Despite the fact that we are still lacking the *in vitro* kinase assays, the dependency of Rps6 phosphorylation on the activity of these kinases, the interaction between Ypk3 and Rps6 and the strong homology between Ypks and S6K1/2 strongly suggest that Ypk kinases are the long missing S6 kinases of budding yeast.

In this study, we also characterize Ypk3 as a novel direct effector of TORC1. We showed that Ypk3 interacts with TORC1 *in vivo* in a TORC1 activity-dependent manner. We mapped four phosphorylation sites on the C-terminal end of the protein which are indispensable for its activity as an S6 kinase. *In vitro* kinase assays will be necessary to answer the question of which of these sites is directly phosphorylated by TORC1. AGC kinases are commonly phosphorylated by Pkh1/2/3 on their T-loop. Thus, it is plausible to suggest that the full activation of Ypk3 may also require the phosphorylation of its T-loop by the Pkh kinases. However, the regulation of Ypk3 by the Pkh kinases remains to be elucidated, as does its regulation by PKA.

Snf1 is a highly conserved AMP-activated serine-threonine kinase which is activated in response to glucose deprivation. Cells deficient in Snf1 activity exhibit a delay in dephosphorylation of Rps6 upon nutrient deprivation (data not shown). The mechanism by which Snf1 contributes to the regulation of Rps6 phosphorylation requires further investigation. One interesting observation we made was that Ypk3 was less stable in the absence of *SNF1* (Figure 29H). Moreover, Hinnebusch and his group had shown that Snf1 inhibits Glc7 activity in the absence of glucose (Cherkasova et al, 2010). Thus, we speculate that Snf1 signals to Rps6 via both the kinase and the phosphatase branches.

Immunofluorescence analyses revealed that phosphorylated Rps6 is predominantly cytoplasmic. However, affinity purification of pre-40S particles at different steps of maturation suggested that Rps6 phosphorylated on Ser232 is both cytoplasmic and nucleolar while Rps6 phosphorylated on

both Ser232 and Ser233 sites is prevailingly cytoplasmic. A previous study suggested that phosphorylated Rps6 was observed both in the cytoplasm and the nucleus (Pende et al, 2004). Glc7 was shown to be predominantly nucleolar and Shp1 contributes to the proper localization of Glc7 in the cell, even though these results were recently challenged (Bohm & Buchberger, 2013; Cheng & Chen, 2010; Hu et al, 2012). At this moment, it is particularly intriguing to investigate the cellular localization of Glc7 and Shp1 under different conditions which affect Rps6 phosphorylation. Our preliminary attempts to localize GFP-tagged Ypk3 suggested that Ypk3 is mainly cytoplasmic. However, we showed that Ypk3 interacts with a nucleolar protein Rrp5 suggesting that there might be a nucleolar pool of Ypk3.

The physiological role of Rps6 phosphorylation in cells has remained as an enigma for the last four decades. We attempted to take advantage of the novel players of the pathway which we characterized in this study to shed light on the function of Rps6 phosphorylation. So far, we showed that Rps6 phosphorylation and the yeast S6 kinases had no impact on global translation. Nonetheless, this result does not rule out that Rps6 phosphorylation may be involved in the translational regulation of specific subsets of mRNAs. To explore such possibility and single out the mRNAs regulated in an Rps6 phosphorylation-dependent manner, we would like to follow-up with a ribosome profiling strategy. Ribosome profiling is a method “based on deep sequencing of ribosome-protected mRNA fragments” which provides detailed information regarding which mRNAs are being actively transcribed (Ingolia et al, 2009). On the other hand, we excluded Rps6 phosphorylation from being an active player in translation reinitiation or ribosomal frameshifting. However, phosphorylatable Rps6 appeared to be required for efficient wobble decoding (Figure 49). Yet, the role of the Ypk kinases in this process and the mechanism by which Rps6 phosphorylation affects the wobble decoding remain to be elucidated.

Earlier attempts to address the impact of Rps6 phosphorylation on the life cycle of *Saccharomyces cerevisiae* led to the conclusion that Rps6 phosphorylation had no observable effect on growth under

a variety of stress conditions or on sporulation (Johnson & Warner, 1987; Kruse et al, 1985). However, we showed that the *RPS6*^{AA} cells had a lower proliferation rate and protein content compared to the wild type cells. In this study, we substituted both of the phosphorylatable serines of both *RPS6A* and *RPS6B* genes with alanine to obtain a phosphomutant Rps6 strain. Differently, in the previous study, one of the copies was deleted and the other copy was replaced with the phosphomutant allele (Kruse et al, 1985). Taking into consideration that deletion of one of the *RPS6* alleles already has phenotypic effects, it might not reflect the true nature of the cells defective in Rps6 phosphorylation. On the other hand, Meyuhas and his group created the first knock-in mice (rps6$^{P-/-}$) where all five Rps6 phosphorylation sites were substituted with alanine (Ruvinsky et al, 2005). The cells obtained from these mice displayed a decrease in cell size and defects in glucose homeostasis, albeit an increase in cell proliferation and amino acid incorporation into proteins. However, the question of which of these phenotypes are attributable to which specific sites still remains to be answered. Dissecting the specific roles of Ser240, Ser244 and Ser247 which are not conserved in yeast as well as those of Ser235 and Ser236 which are conserved in single-celled eukaryotes might help us to clarify the underlying reasons of the differences in the phenotypes which we observe.

Ribosomal proteins with extra-ribosomal functions are rather prevalent from prokaryotes to higher eukaryotes. For instance, there is substantial amount of evidence suggesting that ribosomal proteins are involved in the regulation of their own synthesis, splicing or degradation (Lindstrom, 2009; Warner & McIntosh, 2009). Moreover, some of the ribosomal proteins participate in apoptosis via direct association with Mdm2, an inhibitor of a pro-apoptotic protein p53 (Warner & McIntosh, 2009). More intriguingly, posttranslational modifications were shown to be a major regulator of the extra-ribosomal functions as in the example of Rpl13a in higher eukaryotes (Mazumder et al, 2003; Mukhopadhyay et al, 2008). Phosphorylation of Rpl13a triggers its dissociation from the ribosome and association with GAIT (interferon-*G*amma-*A*ctivated *I*nhibitor of *T*ranslation) complex, which is a negative translational regulator of specific mRNAs (Mukhopadhyay et al, 2008). In this context,

Rpl13a interacts with eIF4G and inhibits the recruitment of the preinitiation complex (PIC) to target mRNAs, thereby contributing to the inhibition of translation in collaboration with the GAIT complex (Kapasi et al, 2007). As another example, phosphorylation of Rps3 promotes its translocation from the cytoplasm to the nucleus in response to DNA damage, where it plays versatile roles in DNA repair (Warner & McIntosh, 2009; Yadavilli et al, 2007). On the other hand, Rps6 was previously shown to interact with heat-shock protein 90 (Hsp90) in an Hsp90 activity-dependent manner; thus, the free pool of Rps6 is supposedly protected from the proteasomal degradation (Kim et al, 2006). In addition, S6 heterozygous embryos seemed to prompt the p53-dependent checkpoint leading to the apoptosis (Panic et al, 2006). However, the question of whether the role of Rps6 in this process is linked with defects in ribosome biogenesis or if Rps6 directly participates in p53 regulation like other ribosomal proteins will require further investigation. The fact that Rps6 is highly phosphorylated in the context of ribosomes encourages us to speculate that Rps6 phosphorylation plays a role in the ribosomal system. However, we cannot rule out extra-ribosomal features of Rps6 in the cell and a conceivable role for its phosphorylation in such functions.

Materials and Methods

Yeast cultures and assays

Saccharomyces cerevisiae strains and plasmids used in the study are listed in Table 3 and 4. Standard protocols were followed to obtain the strains. Cells were grown in YPD (1% yeast extract, 2% peptone, 2% glucose) at 30°C if not indicated otherwise.

For the drug treatment assays, rapamycin was used at 200ng/ml, wortmannin at 10µg/ml, and cycloheximide at 25µg/ml concentrations.

Cells for carbon starvation experiments were grown in YPD, gently pelleted (2 min 1100 x g, 30 °C) and resuspended in YP medium. 20min after the medium change, either 2% glucose or equal amount of water was added into the cultures. After incubation for 20min, final aliquots of the cells were collected for protein extraction.

Cells for nitrogen starvation experiments were grown in YNB (-N) + 2 % Glc, 0.2 % Gln, gently pelleted (2 min 1100 x g, 30 °C) and resuspended in YNB (-N) + 2 % Glc. 20min later, either 0.2% glutamine or equal amount of water was added to the cell cultures.

Table 3. List of yeast strains used in this study

Name	Genotype	Source	Figure
TB50a	MATa*; trp1 leu2 ura3 his3 rme1*	wt	Figure 7A-B; 17A; 23A; 24A-C; 29E; 32B-C; 33A; 45B
TB50α	MATa; *trp1 leu2 ura3 his3 rme1*	wt	Figure 23A
BY4741	MATa; *his3 leu2 met15 ura3*	wt	Figure 14A; 29H
SY33	MATa; *ccr4Δ::KanMX6 [TB50]*	This study	Figure 7A; 12B; 13; 15; 17A; 18; 19A-B; 20
SY34	MATa; *pop2Δ::KanMX6 [TB50]*	This study	Figure 7A; 15
SY47-a	MATa; *dhh1Δ::TRP1 [TB50]*	This study	Figure 7A
SY48-a	MATa; *pat1Δ::TRP1 [TB50]*	This study	Figure 7A
SY39-a	*MATa; CCR4-3HA[KanMX6] [TB50]*	This study	Figure 8A-B; 9A-B; 10,; 11A-E; 14B
SY40-a	MATa; *POP2-3HA[KanMX6] [TB50]*	This study	Figure 8A; 9A-B; 10; 11A-D
SY41	MATa; *NOT2-3HA[KanMX6] [TB50]*	This study	Figure 10
SY42	MATa; *NOT3-3HA[KanMX6] [TB50]*	This study	Figure 10
SY43	MATa; *NOT4-3HA[KanMX6] [TB50]*	This study	Figure 10
SY44	MATa; *NOT5-3HA[KanMX6] [TB50]*	This study	Figure 10
SY65	MATa; *CAF40-3HA[KanMX6] [TB50]*	This study	Figure 10
SY66	MATa; *CAF130-3HA[KanMX6] [TB50]*	This study	Figure 10

SY140	MATa; *yck1Δ::KanMX6 CCR4-3HA [NatMX4] [BY4741]*	This study	Figure 14A
SY143	MATa; *swe1Δ::KanMX6 CCR4-3HA [NatMX4] [BY4741]*	This study	Figure 14A
SY144	MATa; *elm1Δ::KanMX6 CCR4-3HA [NatMX4] [BY4741]*	This study	Figure 14A
DM45-2C	MATa; *crfΔ::KanMX6 [TB50]*	Martin et al., 2004.	Figure 16A
AH248	MATα; *rpd3Δ::HphMX4 [TB50]*	Huber et al., 2011.	Figure 16B-C
AH251	MATα; *sds3Δ::HphMX4 [TB50]*	Huber et al., 2011.	Figure 16B-C
SY73	MATa; *TetR'-Ssn6 tTA [URA3] TetO7-3HA-ARO4[HIS3MX6] [TB50]*	This study	Figure 17C
SY74	MATa; *ccr4Δ::KanMX6 pAH346(Ura3) TetO7-3HA-ARO4[HIS3MX6] [TB50]*	This study	Figure 17C
SY57-a	MATa; *CCR4-TAP[HIS3MX6] [TB50]*	This study	Figure 21
SY58	MATa; *POP2-TAP[HIS3MX6] [TB50]*	This study	Figure 21
MS073	MATa; *SKY1-TAP[HIS3MX6] [TB50]*	Michael Stahl, Loewith Lab	Figure 21
SY5	MATa; *PUF2-3HA[KanMX6] [TB50]*	This study	Figure 22A
SY45-a	MATa; *PUF4-3HA[KanMX6] [TB50]*	This study	Figure 22B
SY13	MATa; *puf2Δ::KanMX6 [TB50]*	This study	Figure 22C
SY46-a	MATa; *puf4Δ::HIS3MX6 [TB50]*	This study	Figure 22C-D
SY20	MATa; *PUF3-TAP[HIS3MX6] [TB50]*	This study	Figure 22E
AH111	MATa; *RPS6A^{WT}::HphMX4 RPS6B^{WT}::NatMX4 [TB50]*	Alexandre Huber, Loewith Lab	Figure 23A; 25A-D; 32D; 33B; 38A-B; 45A-B; 47A-C; 48B-C; 49A; 50B-C
AH114	MATa; *rps6a^{AA}::HphMX4 rps6b^{AA}::NatMX4 [TB50]*	Alexandre Huber, Loewith Lab	Figure 23A; 25A-D; 32D; 33B; 38A-B; 45A-B; 47A-C; 48B-C; 49A; 50B-C
MM121	MATa; *rps6a^{AS}::HphMX4 rps6b^{AS}::NatMX4 [TB50]*	Madeleine Meusburger, Loewith Lab	Figure 23A
MM122	MATα; *rps6a^{SA}::HphMX4 rps6b^{SA}::NatMX4 [TB50]*	Madeleine Meusburger, Loewith Lab	Figure 23A; 50B-C
SY121	MATa; *pGal1-RPS6A[KanMX6] RPS6B[NatMX4] [TB50]*	This study	Figure 23C-D
SY123	MATa; *pGal1-RPS6A[KanMX6] rps6b^{AA}[NatMX4] [TB50]*	This study	Figure 23D
SY125	MATa; *pGal1-RPS6A[KanMX6] rps6b^{DD}[NatMX4] [TB50]*	This study	Figure 23C-D
AH308	MATa; *SCH9::TRP1 [TB50]*	Huber et al., 2009.	Figure 26A-D; 27B-C; 29G
SY155	MATa; *sch9as::TRP1 [TB50]*	This study	Figure 26B-C; 29G
SY158	MATa; *sch9kd::TRP1 [TB50]*	This study	Figure 26A-C
SY161	MATa; *sch9Δ::TRP1 [TB50]*	This study	Figure 26A-C
AH333	MATa; *sch9DE::TRP1 [TB50]*	Huber et al., 2009.	Figure 26D; 27B
RL276-2B	MATa; *HIS3 [TB50]*	Robbie Loewith, Loewith Lab	Figure 27A
AH215	MATa; *gcn2Δ::HIS3MX6 [TB50]*	Alexandre Huber, Loewith Lab	Figure 27A
SY106	MATa; *ypk3Δ::HIS3MX6 [TB50]*	This study	Figure 28A-C; 31A-D; 32B-C; 33A; 45B

MM138	MATa; *YPK3-3Flag::HIS3MX6 [TB50]*	Madeleine Meusburger, Loewith Lab	Figure 29A-C
	MATa; *snf1Δ::KanMX6 [BY4741]*	Claudio De Virgilio Lab	Figure 29H
	MATa; *mck1Δ::KanMX6 [BY4741]*	Yeast deletion collection	Figure 29I
	MATa; *kns1Δ::KanMX6 [BY4741]*	Yeast deletion collection	Figure 29I
MS150	MATa; *pADH1-OsTIR1-9Myc::URA3 AVO1-AID::KanMX6[TB50]*	Michael Stahl, Loewith Lab	Figure 29F; 34A
AH477	MATa; *RPC82-TAP::HIS3MX6 [TB50]*	Alexandre Huber, Loewith Lab	Figure 30A
AH478	MATa; *sch9-as RPC82-TAP::HIS3MX6 [TB50]*	Alexandre Huber, Loewith Lab	Figure 30A
AH479	MATa; *tpk1-as tpk2-as tpk3-as RPC82-TAP::HIS3MX6 [TB50]*	Alexandre Huber, Loewith Lab	Figure 30A-B
AH480	MATa; *sch9-as tpk1-as tpk2-as tpk3-as RPC82-TAP::HIS3MX6 [TB50]*	Alexandre Huber, Loewith Lab	Figure 30A
MM153	MATa; *YPK3-TAP::HIS3MX6 3HA-TOR1 [TB50]*	Madeleine Meusburger, Loewith Lab	Figure 30C
MM125	MATa; *YPK3-TAP::HIS3MX6 [TB50]*	Madeleine Meusburger, Loewith Lab	Figure 32A
RL276-5B	MATa; *TRP1 [TB50]*	Robbie Loewith, Loewith Lab	Figure 34B; 38C; 39B
SY132	MATa; *a ypk3Δ::TRP1 [TB50]*	This study	Figure 34B; 36A; 38C; 41B
MP14	MATa; *a ypk1Δ::KanMX6 TRP1 [TB50]*	Manuele Piccolis, Loewith Lab	Figure 34B
MP15	MATa; *a ypk2Δ::HIS3MX6 [TB50]*	Manuele Piccolis, Loewith Lab	Figure 34B
MP57	MATa; *a ypk1Δ::KanMX6 ypk2Δ::HIS3MX6 YPK1::URA3 [TB50]*	Manuele Piccolis, Loewith Lab	Figure 35
MP58	MATa; *a ypk1Δ::KanMX6 ypk2Δ::HIS3MX6 ypk1as::URA3 [TB50]*	Manuele Piccolis, Loewith Lab	Figure 34C-D; 35
SY210	MATa; *ypk1Δ:: KanMX6 ypk2Δ:: HIS3MX6 ypk3Δ::TRP1 YPK1::URA3 [TB50]*	This study	Figure 35
SY212	MATa; *ypk1Δ:: KanMX6 ypk2Δ:: HIS3MX6 ypk3Δ::TRP1 ypk1as::URA3 [TB50]*	This study	Figure 34E-F; 35; 46A-B
SY214	MATa; *ypk2Δ:: HIS3MX6 ypk3Δ::TRP1 [TB50]*	This study	Figure 35
SY216	MATa; *ypk1Δ:: KanMX6 ypk3Δ::TRP1 YPK1::URA3 [TB50]*	This study	Figure 35
SY226	MATa; *ypk1Δ:: KanMX6 ypk3Δ::TRP1 ypk1as::URA3 [TB50]*	This study	Figure 34E; 35
SY239	MATa; *ypk3Δ::HIS3MX6 SCH9::TRP1 tap42Δ::HphMX4 pRS415::TAP42 [TB50]*	This study	Figure 36B
SY240-a	MATa; *ypk3Δ::HIS3MX6 sch9DE::TRP1 tap42Δ::HphMX4 pRS415::TAP42 [TB50]*	This study	Figure 36B
SY241	MATα; *ypk3Δ::HIS3MX6 SCH9::TRP1 tap42Δ::HphMX4 pRS415::tap42-11 [TB50]*	This study	Figure 36B
SY242-a	MATa; *ypk3Δ::HIS3MX6 sch9DE::TRP1 tap42Δ::HphMX4 pRS415::tap42-11 [TB50]*	This study	Figure 36B
JC482	MATα; *leu2 ura3-52 his3*	Baker et al., 1997.	Figure 37A
KT1623	MATα; *glc7-127 [JC482]*	Baker et al., 1997.	Figure 37A
KT1639	MATα; *glc7-132 [JC482]*	Baker et al., 1997.	Figure 37A
KT2968	MATα; *glc7-L71S [JC482]*	Baker et al., 1997.	Figure 37A
SY251	MATa; *HIS3 GLC7::LEU2 [TB50]*	This study	Figure 37B

SY259	MATa; *HIS3 glc7-127::LEU2 [TB50]*	This study	Figure 37B
MM48	MATa; *rps6aΔ::KanMX6 [TB50]*	Madeleine Meusburger, Loewith Lab	Figure 37D
MM49	MATa; *rps6bΔ::KanMX6 [TB50]*	Madeleine Meusburger, Loewith Lab	Figure 37D
SY255	MATa; *GLC7::LEU2 RPS6A::HphMX4 RPS6B::NatMX4 [TB50]*	This study	Figure 37E; 42A; 42C
SY257	MATa; *GLC7::LEU2 rps6a^{AA}::HphMX4 rps6b^{AA}::NatMX4 [TB50]*	This study	Figure 37E; 42A; 42C
SY263	MATa; *glc7-127::LEU2 RPS6A::HphMX4 RPS6B::NatMX4 [TB50]*	This study	Figure 37E; 42A; 42C
SY265	MATa; *glc7-127::LEU2 rps6a^{AA}::HphMX4 rps6b^{AA}::NatMX4 [TB50]*	This study	Figure 37E; 42A; 42C
SY116	MATa; *shp1Δ::TRP1 [TB50]*	This study	Figure 39B; 40C; 42A-D
SY228	MATa; *TRP1 RPS6A::HphMX4 RPS6B::NatMX4 [TB50]*	This study	Figure 40A
SY230	MATa; *TRP1 rps6a^{AA}::HphMX4 rps6b^{AA}::NatMX4 [TB50]*	This study	Figure 40A
SY247	MATa; *shp1Δ::TRP1 RPS6A::HphMX4 RPS6B::NatMX4 [TB50]*	This study	Figure 40A
SY249	MATa; *shp1Δ::TRP1 rps6a^{AA}::HphMX4 rps6b^{AA}::NatMX4 [TB50]*	This study	Figure 40A
RJD360	MATa; *can1-100, leu2-3,-112, his3-11,-15, trp1-1, ura3-1, ade2-1*	Bohm et al., 2013.	Figure 40D
RJD3411	MATa; *cdc48-3, leu2-3, his3-11,-15, trp1-1, ura3-1, ade2-1*	Bohm et al., 2013.	Figure 40D
SY251	MATa; *HIS3 GLC7::LEU2 [TB50]*	This study	Figure 41A; 42B; 42D
SY253	MATa; *ypk3Δ::HIS3MX6 GLC7::LEU2 [TB50]*	This study	Figure 41A; 42B; 42D
SY259	MATa; *HIS3 glc7-127::LEU2 [TB50]*	This study	Figure 41A; 42B; 42D
SY261	MATa; *ypk3Δ::HIS3MX6 glc7-127::LEU2 [TB50]*	This study	Figure 41A; 42B; 42D
SY243	MATa; *HIS3 shp1Δ::TRP1 [TB50]*	This study	Figure 41B
SY245	MATa; *ypk3Δ::HIS3 shp1Δ::TRP1 [TB50]*	This study	Figure 41B
RL343-F0	MATa; *a hrr25Δ::KanMX6 HRR25::URA3 [BY4741]*	Joerg Urban, Loewith Lab	Figure 44C-D
RL343-F1	MATa; *a hrr25Δ::KanMX6 hrr25^{I82G}::URA3 [BY4741]*	Joerg Urban, Loewith Lab	Figure 44C-D
MM46	MATa; *hbs1Δ::HIS3MX6 RPS6A::HphMX4 RPS6B::NatMX4 [TB50]*	Madeleine Meusburger, Loewith Lab	Figure 48B-C
MM47	MATa; *hbs1Δ::HIS3MX6 rps6a^{AA}::HphMX4 rps6b^{AA}::NatMX4 [TB50]*	Madeleine Meusburger, Loewith Lab	Figure 48B-C
MM128	MATa; *sac3Δ::HIS3MX6 RPS6A::HphMX4 RPS6B::NatMX4 [TB50]*	Madeleine Meusburger, Loewith Lab	Figure 48B-C
MM129	MATa; *sac3Δ::HIS3MX6 rps6a^{AA}::HphMX4 rps6b^{AA}::NatMX4 [TB50]*	Madeleine Meusburger, Loewith Lab	Figure 48B-C
MM132	MATa; *ycr016wΔ::HIS3MX6 RPS6A::HphMX4 RPS6B::NatMX4 [TB50]*	Madeleine Meusburger, Loewith Lab	Figure 48B-C
MM133	MATa; *ycr016wΔ::HIS3MX6 rps6a^{AA}::HphMX4 rps6b^{AA}::NatMX4 [TB50]*	Madeleine Meusburger, Loewith Lab	Figure 48B-C

MM135	MATa; *uba4Δ::HIS3MX6 RPS6A::HphMX4 RPS6B::NatMX4 [TB50]*	Madeleine Meusburger, Loewith Lab	Figure 48B-C
MM142	MATα; *uba4Δ::HIS3MX6 rps6a^{AA}::HphMX4 rps6b^{AA}::NatMX4 [TB50]*	Madeleine Meusburger, Loewith Lab	Figure 48B-C

Table 4. List of plasmids used in this study

Name	Vector::Insert	Source	Figure
pRS416			Figure 13; 19A; 20; 24; 31C-D; 35;
pRS426			Figure 38B
pJU450	pRS415::TRP1 HIS3	Joerg Urban, Loewith Lab	Figure 24
pSY22	pRS416::CCR4-6HA	This study	Figure 12B
pSY23	pRS416::CCR4^{3A}-6HA	This study	Figure 12B
pSY30	pRS416::CCR4	This study	Figure 13;18; 19A-B; 20
pSY31	pRS416::CCR4^{3A}	This study	Figure 13;18; 19A-B; 20
pSY32	pRS416::CCR4^{3E}	This study	Figure 13;18; 19A-B; 20
pRP1574	EDC3-mCherry	Buchan et al., 2008.	Figure 19A
pAH138	pRS416::GCN2	Alexandre Huber, Loewith Lab	Figure 27B
pHQ1253	pRS316::GCN2$^{T882A\ T887A}$	Qui et al., 2002.	Figure 27B
pSY56	pRS416::YPK3-3Flag	This study	Figure 28A-C; 29A-I; 30A-B; 31A; 31C-D; 35
pMM105	pRS416::YPK3^{L231G}-3Flag	Madeleine Mesuburger, Loewith Lab	Figure 28B
pSY63	pRS416::YPK3^{K157A}-3Flag	This study	Figure 28C
pSY57	pRS416::YPK3^{S513D}-3Flag	This study	Figure 31A
pSY58	pRS416::YPK3^{S513E}-3Flag	This study	Figure 31A
pSY59	pRS416::YPK3^{S513A}-3Flag	This study	Figure 31A; 31C;
pSY71	pRS416::YPK3^{1A}-3Flag	This study	Figure 31C
pSY72	pRS416::YPK3^{2A}-3Flag	This study	Figure 31C
pSY73	pRS416::YPK3^{3A}-3Flag	This study	Figure 31C
pSY78	pRS416::YPK3^{4A}-3Flag	This study	Figure 31D
pSY90	pRS415::YPK3^{4D}-3Flag	This study	Figure 31D
pSD375	pYDL	Harger and Dinman, 2003.	Figure 33
pSD376	pYDL-LA	Harger and Dinman, 2003.	Figure 33
pSD377	pYDL-Ty1	Harger and Dinman, 2003.	Figure 33
pSD378	pYDL-HIV1	Harger and Dinman, 2003.	Figure 33
pSD379	pYDL-Ty3	Harger and Dinman, 2003.	Figure 33
	YEp352::YPK2	Loewith Lab	Figure 36A
	YEp352::YPK2^{D239A}	Loewith Lab	Figure 36A
pSY75	pRS426::GLC7	This study	Figure 38B
pAB855	YCplac111::SHP1	Böhm et al., 2013.	Figure 40C
pAB1845	YCplac111::shp1-a1	Böhm et al., 2013.	Figure 40C
pAB856	YCplac111::shp1^{UBAΔ}	Böhm et al., 2013.	Figure 40C
pAB857	YCplac111::shp1^{UBXΔ}	Böhm et al., 2013.	Figure 40C
pMS93	pRS415::SHP1-5HA	Michael Stahl, Loewith Lab	Figure 42A
pSY79	pRS415::SHP1^{S106AS108A}-5HA	This study	Figure 42B-D

pSY102	pRS415::SHP1^{S128130A}-5HA	This study	Figure 42B-D
pSY103	pRS415::Shp1^{S120A}-5HA	This study	Figure 42B-D
pSY104	pRS415::Shp1^{S210A}-5HA	This study	Figure 42B-D
pSY105	pRS415::Shp1^{S315A}-5HA	This study	Figure 42B-D
B180	YCp50::GCN4-lacZ	Grant et al., 1994.	Figure 47A
B4163	YCp50::GCN4^{ORF1}-lacZ	Grant et al., 1994.	Figure 47A
pDL202	*pRS425::p_{PGK1}-Fluc-Rluc* (RF)	Letzring et al., 2010.	Figure 49B
pDL221	pRS425::RF-ArgAGA10	Letzring et al., 2010.	Figure 49B
pDL230	pRS425::RF-ArgCGA10	Letzring et al., 2010.	Figure 49B

Denaturing Protein extraction

PPi: 10 mM NaF, 10 mM p-nitrophenylphosphate, 10 mM $Na_2P_2O_4$, and 10 mM β-glycerophosphate; PI: 1× Roche protease inhibitor cocktail and 1 mM PMSF.

Protein extraction was performed based on TCA-Urea extraction method as previously described (Urban et al, 2007).

Immunoprecipitation and lambda phosphatase treatment

Ccr4 tagged with HA-epitope was precipitated and treated with lambda phosphatase based on the procedure as described in a previous study (Berset et al, 1998).

Tandem affinity purification for mass spectrometry analysis

3L cultures of the strains with TAP-tagged proteins were grown to OD_{600} 0.8 and treated with either rapamycin or the vehicle for 20min. Native protein extracts were prepared as previously described (Berset et al, 1998). Protein concentrations were normalized. 10^7 magnetic beads (Epoxy M270 Dynabeads, Invitrogen) covalently coated with purified rabbit IgG were added to the samples and bound for 2h at 4°C. Beads were washed four times with lysis buffer without Tween-20 and suspended in SDS-PAGE sample buffer. Samples were run in 7.5% SDS-PAGE gel. The gel was washed in distilled water for 30min, incubated in Coomassie stain (Bio-RAD) for 1h. Following the wash in distilled water for another 30min, the bands corresponding to the proteins of interest were cut out with a clean razor. The bands were sent for mass spectrometry analysis.

RNA Extraction and Reverse Transcription

For total RNA extraction, a previously published method was followed (Urban et al, 2007). cDNA was synthesized using BioRad's iScript system.

Quantitative PCR

The Roche LightCycler 480 system was used for qPCR. 10µl reaction per well was prepared in 384-well plates according to the manufacturer's instructions.

Ligation-mediated Poly(A) Test

LM-PAT assay was performed as described previously (Beilharz & Preiss, 2009). The gene –specific forward primers are: 5'-CGATCACCACTGCTTCCACAC-3' for *Mfa2*, 5'-GGAATTATTGGAAGGTAAGG-3' for *Pgk1*, 5'-GAGATTCTAAGCTTGTTGTC-3' for *Rps4*, 5'-CATGGGTACTTTGAAGAAGG-3' for *Rpl3* and 5'-TCATCTAATTTACCCGATGC-3' for *Rpl21a*. Finally, the PCR product was run on 2.5% agarose gel with ethidium bromide for visualization.

Spot Assay

Cells grown overnight were diluted to an OD_{600nM} of 0.1 and grown to exponential phase. 1:10 serial dilutions were spotted following the normalization of the cell numbers. The plates were incubated for 2-3days at 30°C if not indicated otherwise.

Microscopy

Saturated cells were diluted to an OD_{600nM} of 0.1 and grown to exponential phase in synthetic media. Following the indicated treatments, the cells were fixed with formaldehyde with a final concentration of 3.7% for 20min at room temperature and then, washed twice with water. The cells were observed under Zeiss AXIOZ1. P-body formation was induced and analyzed with ImageJ according to the protocol by Parker Lab (Nissan & Parker, 2008).

RNA Immunoprecipitation

RNA immunoprecipitation was performed according to a previously described protocol (Gilbert & Svejstrup, 2006).

Growth Assay

Exponentially growing cells were diluted to an OD_{600nM} of 0.005 in the indicated media. 200µl cells with 2% treatment per well were dispensed in 96-well plates and the OD_{600nM} of the cells was recorded every 15min for 16 to 24 hours at 30°C if not indicated otherwise. The average and standard deviation values were obtained from at least three independent experiments if not indicated otherwise.

B-Galactosidase Assay

β-galactosidase activity in the indicated cells was assayed using the Beta-Glo System (E4720) from Promega. According to the manufacturer's instructions, Beta-Glo reagent was mixed with exponentially growing cell with ratio of 1:1 in 96-well plates. Following 30min of incubation, luminescence was measured in Relative Luminescence Units (RLU) using a luminometer with a 10-sec shake, 2-sec delay and a 5-sec measurement.

Dual-Luciferase Reporter Assay

Luciferase assays were conducted as described previously using the Dual-Luciferase Reporter Assay System (E1910) from Promega (Letzring et al, 2010). The average values shown are from at least three independent experiments.

Sucrose Density Gradient Centrifugation

Exponentially growing cells were treated with 20mg/ml cycloheximide. After 10min of incubation, cells were harvested, washed and lysed with lysis buffer (10mM Tris-HCl pH 7.4, 100mM NaCl, 30mM $MgCl_2$, 100ug/ml CHX, 200ug/ml Heparin). The extract was centrifuged for 10min at 13000rpm at 4°C. OD_{260} of 1:100 dilutions of the supernatant were measured. Following the addition of glycerol with the final concentration of 10%, the samples were stored at -70°C. 10 OD_{260} of the supernatant was loaded on top of a 7-50% sucrose gradient prepared in Gradient Buffer (50mM Tris-AcO pH 7.0, 50mM NH_4Cl, 12mM $MgCl_2$, 1mM DTT). Gradients were ultracentrifuged for 3.5 hours at 35000 rpm and the UV profile was recorded using an IG gradient fractionator.

Immunofluorescence

Following the fixation of cells with paraformaldehyde, cell wall was digested with Zymolase to prepare spheroplasts. The samples were incubated with primary antibodies, rabbit anti-phospho-S6 ribosomal protein (S235/S236) 4858S from Cell Signaling, and rabbit anti-phospho-Akt substrate (RXXS*/T*) 9614S from Cell Signaling for 2 hours at room temperature. Following washing step, the samples were further incubated with a second antibody conjugated to a green fluorochrome Alexa 488 (Alexa Fluor 488 Goat anti-Rabbit IgG) for 1 hour at room temperature. Then, the samples were mounted between glassslide and coverslip. The pictures taken were analyzed with ImageJ.

Abbreviations

mRNA	messenger RNA
rRNA	ribosomal RNA
tRNA	transfer RNA
TOR	Target Of Rapamycin
TORC	TOR Complex
FAT	FRAP-ATM-TRRAP
PRD	PIKK regulatory domain
PIKK	Phosphatidyl Inositol Kinase-like Kinase
FATC	FAT C-terminus
HEAT	Huntingtin, Elongation factor 3, PR65/A, TOR
FRB	FKBP12-binding
FKBP12	FK506-Binding Protein 12 kDa
mTOR	mammalian Target Of Rapamycin
HM	Hydrophobic motif
TM	Turn motif
PP1	Type-1 protein phosphatase
PP2A	Type-2A protein phosphatase
UBA	Ubiquitin-associated domain
SEP	Shp1, Eyc, p47
UBX	Ubiquitin-like domain
BS1	Binding-site 1
AAA	ATPases associated with diverse cellular activities
ER	Endoplasmic reticulum
RPS	Ribosomal Protein of the Small Subunit
RPL	Ribosomal Protein of the Large Subunit
CHX	Cycloheximide
DNA	Deoxyribonucleic Acid
RNA	Ribonucleic acid
eIF	eukaryotic Initiation Factor
ORF	Open Reading Frame
PCR	Polymerase Chain Reaction
qPCR	quantitative PCR
rDNA	ribosomal DNA
Ribi	Ribosome biogenesis
RP	Ribosomal Protein

References

Aizer A, Kafri P, Kalo A, Shav-Tal Y (2013) The P body protein Dcp1a is hyper-phosphorylated during mitosis. *PloS one* **8:** e49783

Alba MM, Guigo R (2004) Comparative analysis of amino acid repeats in rodents and humans. *Genome research* **14:** 549-554

Albert TK, Hanzawa H, Legtenberg YI, de Ruwe MJ, van den Heuvel FA, Collart MA, Boelens R, Timmers HT (2002) Identification of a ubiquitin-protein ligase subunit within the CCR4-NOT transcription repressor complex. *The EMBO journal* **21:** 355-364

Albig AR, Decker CJ (2001) The target of rapamycin signaling pathway regulates mRNA turnover in the yeast Saccharomyces cerevisiae. *Mol Biol Cell* **12:** 3428-3438

Anderson P, Kedersha N (2008) Stress granules: the Tao of RNA triage. *Trends in biochemical sciences* **33:** 141-150

Aronova S, Wedaman K, Aronov PA, Fontes K, Ramos K, Hammock BD, Powers T (2008) Regulation of ceramide biosynthesis by TOR complex 2. *Cell metabolism* **7:** 148-158

Audhya A, Loewith R, Parsons AB, Gao L, Tabuchi M, Zhou H, Boone C, Hall MN, Emr SD (2004) Genome-wide lethality screen identifies new PI4,5P2 effectors that regulate the actin cytoskeleton. *The EMBO journal* **23:** 3747-3757

Baker SH, Frederick DL, Bloecher A, Tatchell K (1997) Alanine-scanning mutagenesis of protein phosphatase type 1 in the yeast Saccharomyces cerevisiae. *Genetics* **145:** 615-626

Balagopal V, Parker R (2009) Polysomes, P bodies and stress granules: states and fates of eukaryotic mRNAs. *Current opinion in cell biology* **21:** 403-408

Beilharz TH, Preiss T (2009) Transcriptome-wide measurement of mRNA polyadenylation state. *Methods* **48:** 294-300

Belandia B, Brautigan D, Martin-Perez J (1994) Attenuation of ribosomal protein S6 phosphatase activity in chicken embryo fibroblasts transformed by Rous sarcoma virus. *Molecular and cellular biology* **14:** 200-206

Belew AT, Advani VM, Dinman JD (2011) Endogenous ribosomal frameshift signals operate as mRNA destabilizing elements through at least two molecular pathways in yeast. *Nucleic acids research* **39:** 2799-2808

Belli G, Gari E, Piedrafita L, Aldea M, Herrero E (1998) An activator/repressor dual system allows tight tetracycline-regulated gene expression in budding yeast. *Nucleic acids research* **26:** 942-947

Ben-Shem A, Garreau de Loubresse N, Melnikov S, Jenner L, Yusupova G, Yusupov M (2011) The structure of the eukaryotic ribosome at 3.0 A resolution. *Science* **334:** 1524-1529

Berchtold D, Piccolis M, Chiaruttini N, Riezman I, Riezman H, Roux A, Walther TC, Loewith R (2012) Plasma membrane stress induces relocalization of Slm proteins and activation of TORC2 to promote sphingolipid synthesis. *Nature cell biology* **14:** 542-547

Berchtold D, Walther TC (2009) TORC2 plasma membrane localization is essential for cell viability and restricted to a distinct domain. *Molecular biology of the cell* **20:** 1565-1575

Berset C, Trachsel H, Altmann M (1998) The TOR (target of rapamycin) signal transduction pathway regulates the stability of translation initiation factor eIF4G in the yeast Saccharomyces cerevisiae. *Proceedings of the National Academy of Sciences of the United States of America* **95:** 4264-4269

Beugnet A, Tee AR, Taylor PM, Proud CG (2003) Regulation of targets of mTOR (mammalian target of rapamycin) signalling by intracellular amino acid availability. *The Biochemical journal* **372:** 555-566

Bharucha JP, Larson JR, Konopka JB, Tatchell K (2008) Saccharomyces cerevisiae Afr1 protein is a protein phosphatase 1/Glc7-targeting subunit that regulates the septin cytoskeleton during mating. *Eukaryotic cell* **7:** 1246-1255

Bianchin C, Mauxion F, Sentis S, Seraphin B, Corbo L (2005) Conservation of the deadenylase activity of proteins of the Caf1 family in human. *RNA* **11:** 487-494

Bishop AC, Ubersax JA, Petsch DT, Matheos DP, Gray NS, Blethrow J, Shimizu E, Tsien JZ, Schultz PG, Rose MD, Wood JL, Morgan DO, Shokat KM (2000) A chemical switch for inhibitor-sensitive alleles of any protein kinase. *Nature* **407:** 395-401

Bodenmiller B, Wanka S, Kraft C, Urban J, Campbell D, Pedrioli PG, Gerrits B, Picotti P, Lam H, Vitek O, Brusniak MY, Roschitzki B, Zhang C, Shokat KM, Schlapbach R, Colman-Lerner A, Nolan GP, Nesvizhskii AI, Peter M, Loewith R, von Mering C, Aebersold R (2010) Phosphoproteomic analysis reveals interconnected system-wide responses to perturbations of kinases and phosphatases in yeast. *Sci Signal* **3:** rs4

Bohm S, Buchberger A (2013) The budding yeast Cdc48(Shp1) complex promotes cell cycle progression by positive regulation of protein phosphatase 1 (Glc7). *PloS one* **8:** e56486

Booher RN, Deshaies RJ, Kirschner MW (1993) Properties of Saccharomyces cerevisiae wee1 and its differential regulation of p34CDC28 in response to G1 and G2 cyclins. *The EMBO journal* **12:** 3417-3426

Bouquin N, Barral Y, Courbeyrette R, Blondel M, Snyder M, Mann C (2000) Regulation of cytokinesis by the Elm1 protein kinase in Saccharomyces cerevisiae. *Journal of cell science* **113 (Pt 8):** 1435-1445

Braus GH, Grundmann O, Bruckner S, Mosch HU (2003) Amino acid starvation and Gcn4p regulate adhesive growth and FLO11 gene expression in Saccharomyces cerevisiae. *Molecular biology of the cell* **14:** 4272-4284

Brown CE, Sachs AB (1998) Poly(A) tail length control in Saccharomyces cerevisiae occurs by message-specific deadenylation. *Molecular and cellular biology* **18:** 6548-6559

Brown JA, Roberts TL, Richards R, Woods R, Birrell G, Lim YC, Ohno S, Yamashita A, Abraham RT, Gueven N, Lavin MF (2011) A novel role for hSMG-1 in stress granule formation. *Molecular and cellular biology* **31:** 4417-4429

Brunn GJ, Fadden P, Haystead TA, Lawrence JC, Jr. (1997) The mammalian target of rapamycin phosphorylates sites having a (Ser/Thr)-Pro motif and is activated by antibodies to a region near its COOH terminus. *The Journal of biological chemistry* **272:** 32547-32550

Budovskaya YV, Stephan JS, Deminoff SJ, Herman PK (2005) An evolutionary proteomics approach identifies substrates of the cAMP-dependent protein kinase. *Proceedings of the National Academy of Sciences of the United States of America* **102:** 13933-13938

Burnett PE, Barrow RK, Cohen NA, Snyder SH, Sabatini DM (1998) RAFT1 phosphorylation of the translational regulators p70 S6 kinase and 4E-BP1. *Proceedings of the National Academy of Sciences of the United States of America* **95:** 1432-1437

Carr-Schmid A, Pfund C, Craig EA, Kinzy TG (2002) Novel G-protein complex whose requirement is linked to the translational status of the cell. *Molecular and cellular biology* **22:** 2564-2574

Carrozza MJ, Florens L, Swanson SK, Shia WJ, Anderson S, Yates J, Washburn MP, Workman JL (2005) Stable incorporation of sequence specific repressors Ash1 and Ume6 into the Rpd3L complex. *Biochimica et biophysica acta* **1731:** 77-87; discussion 75-76

Casamayor A, Torrance PD, Kobayashi T, Thorner J, Alessi DR (1999) Functional counterparts of mammalian protein kinases PDK1 and SGK in budding yeast. *Current biology : CB* **9:** 186-197

Castermans D, Somers I, Kriel J, Louwet W, Wera S, Versele M, Janssens V, Thevelein JM (2012) Glucose-induced posttranslational activation of protein phosphatases PP2A and PP1 in yeast. *Cell research* **22:** 1058-1077

Chandarlapaty S, Errede B (1998) Ash1, a daughter cell-specific protein, is required for pseudohyphal growth of Saccharomyces cerevisiae. *Molecular and cellular biology* **18:** 2884-2891

Charneski CA, Hurst LD (2013) Positively charged residues are the major determinants of ribosomal velocity. *PLoS biology* **11:** e1001508

Chauvin C, Koka V, Nouschi A, Mieulet V, Hoareau-Aveilla C, Dreazen A, Cagnard N, Carpentier W, Kiss T, Meyuhas O, Pende M (2013) Ribosomal protein S6 kinase activity controls the ribosome biogenesis transcriptional program. *Oncogene*

Chen J, Chiang YC, Denis CL (2002) CCR4, a 3'-5' poly(A) RNA and ssDNA exonuclease, is the catalytic component of the cytoplasmic deadenylase. *EMBO J* **21:** 1414-1426

Chen J, Rappsilber J, Chiang YC, Russell P, Mann M, Denis CL (2001) Purification and characterization of the 1.0 MDa CCR4-NOT complex identifies two novel components of the complex. *Journal of molecular biology* **314:** 683-694

Chen J, Young SM, Allen C, Seeber A, Peli-Gulli MP, Panchaud N, Waller A, Ursu O, Yao T, Golden JE, Strouse JJ, Carter MB, Kang H, Bologa CG, Foutz TD, Edwards BS, Peterson BR, Aube J, Werner-Washburne M, Loewith RJ, De Virgilio C, Sklar LA (2012) Identification of a small molecule yeast TORC1 inhibitor with a multiplex screen based on flow cytometry. *ACS chemical biology* **7:** 715-722

Chen RH, Sarnecki C, Blenis J (1992) Nuclear localization and regulation of erk- and rsk-encoded protein kinases. *Molecular and cellular biology* **12:** 915-927

Chen W, Bucaria J, Band DA, Sutton A, Sternglanz R (2003) Enp1, a yeast protein associated with U3 and U14 snoRNAs, is required for pre-rRNA processing and 40S subunit synthesis. *Nucleic acids research* **31:** 690-699

Cheng YL, Chen RH The AAA-ATPase Cdc48 and cofactor Shp1 promote chromosome bi-orientation by balancing Aurora B activity. *J Cell Sci* **123:** 2025-2034

Cheng YL, Chen RH (2010) The AAA-ATPase Cdc48 and cofactor Shp1 promote chromosome bi-orientation by balancing Aurora B activity. *J Cell Sci* **123:** 2025-2034

Cherkasova V, Qiu H, Hinnebusch AG (2010) Snf1 promotes phosphorylation of the alpha subunit of eukaryotic translation initiation factor 2 by activating Gcn2 and inhibiting phosphatases Glc7 and Sit4. *Molecular and cellular biology* **30:** 2862-2873

Cherkasova VA, Hinnebusch AG (2003) Translational control by TOR and TAP42 through dephosphorylation of eIF2alpha kinase GCN2. *Genes & development* **17:** 859-872

Collart MA, Panasenko OO (2012) The Ccr4--not complex. *Gene* **492:** 42-53

Collart MA, Struhl K (1994) NOT1(CDC39), NOT2(CDC36), NOT3, and NOT4 encode a global-negative regulator of transcription that differentially affects TATA-element utilization. *Genes & development* **8:** 525-537

Coller JM, Tucker M, Sheth U, Valencia-Sanchez MA, Parker R (2001) The DEAD box helicase, Dhh1p, functions in mRNA decapping and interacts with both the decapping and deadenylase complexes. *RNA* **7:** 1717-1727

Costanzo M, Baryshnikova A, Bellay J, Kim Y, Spear ED, Sevier CS, Ding H, Koh JL, Toufighi K, Mostafavi S, Prinz J, St Onge RP, VanderSluis B, Makhnevych T, Vizeacoumar FJ, Alizadeh S, Bahr S, Brost RL, Chen Y, Cokol M, Deshpande R, Li Z, Lin ZY, Liang W, Marback M, Paw J, San Luis BJ, Shuteriqi E, Tong AH, van Dyk N, Wallace IM, Whitney JA, Weirauch MT, Zhong G, Zhu H, Houry WA, Brudno M, Ragibizadeh S, Papp B, Pal C, Roth FP, Giaever G, Nislow C, Troyanskaya OG, Bussey H, Bader GD, Gingras AC, Morris QD, Kim PM, Kaiser CA, Myers CL, Andrews BJ, Boone C (2010) The genetic landscape of a cell. *Science* **327:** 425-431

Crick FH (1958) On protein synthesis. *Symposia of the Society for Experimental Biology* **12:** 138-163

Crick FH (1966) Codon--anticodon pairing: the wobble hypothesis. *Journal of molecular biology* **19:** 548-555

Cui DY, Brown CR, Chiang HL (2004) The type 1 phosphatase Reg1p-Glc7p is required for the glucose-induced degradation of fructose-1,6-bisphosphatase in the vacuole. *The Journal of biological chemistry* **279:** 9713-9724

Cui Y, Ramnarain DB, Chiang YC, Ding LH, McMahon JS, Denis CL (2008) Genome wide expression analysis of the CCR4-NOT complex indicates that it consists of three modules with the NOT module controlling SAGA-responsive genes. *Molecular genetics and genomics : MGG* **279:** 323-337

Dai N, Christiansen J, Nielsen FC, Avruch J (2013) mTOR complex 2 phosphorylates IMP1 cotranslationally to promote IGF2 production and the proliferation of mouse embryonic fibroblasts. *Genes & development* **27:** 301-312

Daugeron MC, Mauxion F, Seraphin B (2001) The yeast POP2 gene encodes a nuclease involved in mRNA deadenylation. *Nucleic acids research* **29:** 2448-2455

De Virgilio C, Loewith R (2006) Cell growth control: little eukaryotes make big contributions. *Oncogene* **25:** 6392-6415

Decker CJ, Teixeira D, Parker R (2007) Edc3p and a glutamine/asparagine-rich domain of Lsm4p function in processing body assembly in Saccharomyces cerevisiae. *The Journal of cell biology* **179:** 437-449

Denis CL (1984) Identification of new genes involved in the regulation of yeast alcohol dehydrogenase II. *Genetics* **108:** 833-844

Di Como CJ, Arndt KT (1996) Nutrients, via the Tor proteins, stimulate the association of Tap42 with type 2A phosphatases. *Genes & development* **10:** 1904-1916

Dinman JD (2012) Mechanisms and implications of programmed translational frameshifting. *Wiley interdisciplinary reviews RNA* **3:** 661-673

Dinman JD, Ruiz-Echevarria MJ, Czaplinski K, Peltz SW (1997) Peptidyl-transferase inhibitors have antiviral properties by altering programmed -1 ribosomal frameshifting efficiencies: development of model systems. *Proceedings of the National Academy of Sciences of the United States of America* **94:** 6606-6611

Dlakic M (2000) Functionally unrelated signalling proteins contain a fold similar to Mg2+-dependent endonucleases. *Trends in biochemical sciences* **25:** 272-273

Doerfel LK, Wohlgemuth I, Kothe C, Peske F, Urlaub H, Rodnina MV (2013) EF-P is essential for rapid synthesis of proteins containing consecutive proline residues. *Science* **339:** 85-88

Doma MK, Parker R (2006) Endonucleolytic cleavage of eukaryotic mRNAs with stalls in translation elongation. *Nature* **440:** 561-564

Dorrello NV, Peschiaroli A, Guardavaccaro D, Colburn NH, Sherman NE, Pagano M (2006) S6K1- and betaTRCP-mediated degradation of PDCD4 promotes protein translation and cell growth. *Science* **314:** 467-471

Dragon F, Gallagher JE, Compagnone-Post PA, Mitchell BM, Porwancher KA, Wehner KA, Wormsley S, Settlage RE, Shabanowitz J, Osheim Y, Beyer AL, Hunt DF, Baserga SJ (2002) A large nucleolar U3 ribonucleoprotein required for 18S ribosomal RNA biogenesis. *Nature* **417:** 967-970

Draper MP, Salvadore C, Denis CL (1995) Identification of a mouse protein whose homolog in Saccharomyces cerevisiae is a component of the CCR4 transcriptional regulatory complex. *Mol Cell Biol* **15:** 3487-3495

Du W, Halova L, Kirkham S, Atkin J, Petersen J (2012) TORC2 and the AGC kinase Gad8 regulate phosphorylation of the ribosomal protein S6 in fission yeast. *Biology open* **1:** 884-888

Dudley AM, Janse DM, Tanay A, Shamir R, Church GM (2005) A global view of pleiotropy and phenotypically derived gene function in yeast. *Mol Syst Biol* **1:** 2005 0001

Dummler BA, Hauge C, Silber J, Yntema HG, Kruse LS, Kofoed B, Hemmings BA, Alessi DR, Frodin M (2005) Functional characterization of human RSK4, a new 90-kDa ribosomal S6 kinase, reveals constitutive activation in most cell types. *The Journal of biological chemistry* **280:** 13304-13314

Erikson E, Maller JL (1985) A protein kinase from Xenopus eggs specific for ribosomal protein S6. *Proceedings of the National Academy of Sciences of the United States of America* **82:** 742-746

Feldman ME, Apsel B, Uotila A, Loewith R, Knight ZA, Ruggero D, Shokat KM (2009) Active-site inhibitors of mTOR target rapamycin-resistant outputs of mTORC1 and mTORC2. *PLoS biology* **7:** e38

Feng Y, Zhang F, Lokey LK, Chastain JL, Lakkis L, Eberhart D, Warren ST (1995) Translational suppression by trinucleotide repeat expansion at FMR1. *Science* **268:** 731-734

Fernandez-Vazquez J, Vargas-Perez I, Sanso M, Buhne K, Carmona M, Paulo E, Hermand D, Rodriguez-Gabriel M, Ayte J, Leidel S, Hidalgo E (2013) Modification of tRNA(Lys) UUU by Elongator Is Essential for Efficient Translation of Stress mRNAs. *PLoS genetics* **9:** e1003647

Ferrari S, Pearson RB, Siegmann M, Kozma SC, Thomas G (1993) The immunosuppressant rapamycin induces inactivation of p70s6k through dephosphorylation of a novel set of sites. *The Journal of biological chemistry* **268:** 16091-16094

Fiedler D, Braberg H, Mehta M, Chechik G, Cagney G, Mukherjee P, Silva AC, Shales M, Collins SR, van Wageningen S, Kemmeren P, Holstege FC, Weissman JS, Keogh MC, Koller D, Shokat KM, Krogan NJ (2009) Functional organization of the S. cerevisiae phosphorylation network. *Cell* **136:** 952-963

Flotow H, Thomas G (1992) Substrate recognition determinants of the mitogen-activated 70K S6 kinase from rat liver. *The Journal of biological chemistry* **267:** 3074-3078

Foat BC, Houshmandi SS, Olivas WM, Bussemaker HJ (2005) Profiling condition-specific, genome-wide regulation of mRNA stability in yeast. *Proceedings of the National Academy of Sciences of the United States of America* **102:** 17675-17680

Fournier MJ, Coudert L, Mellaoui S, Adjibade P, Gareau C, Cote MF, Sonenberg N, Gaudreault RC, Mazroui R (2013) Inactivation of the mTORC1-eukaryotic translation initiation factor 4E pathway alters stress granule formation. *Molecular and cellular biology* **33:** 2285-2301

Francisco L, Wang W, Chan CS (1994) Type 1 protein phosphatase acts in opposition to IpL1 protein kinase in regulating yeast chromosome segregation. *Molecular and cellular biology* **14:** 4731-4740

Fumagalli SaTG (2000) *S6 phosphorylation and signal transduction in translational control of gene expression*, Cold Spring Harbor, NY: Cold Spring Harbor Laboratory Press.

Gelperin D, Horton L, DeChant A, Hensold J, Lemmon SK (2002) Loss of ypk1 function causes rapamycin sensitivity, inhibition of translation initiation and synthetic lethality in 14-3-3-deficient yeast. *Genetics* **161:** 1453-1464

Gerbasi VR, Weaver CM, Hill S, Friedman DB, Link AJ (2004) Yeast Asc1p and mammalian RACK1 are functionally orthologous core 40S ribosomal proteins that repress gene expression. *Molecular and cellular biology* **24:** 8276-8287

Gilbert C, Svejstrup JQ (2006) RNA immunoprecipitation for determining RNA-protein associations in vivo. *Current protocols in molecular biology / edited by Frederick M Ausubel [et al]* **Chapter 27:** Unit 27 24

Goehring AS, Rivers DM, Sprague GF, Jr. (2003) Attachment of the ubiquitin-related protein Urm1p to the antioxidant protein Ahp1p. *Eukaryotic cell* **2:** 930-936

Goldstrohm AC, Hook BA, Seay DJ, Wickens M (2006) PUF proteins bind Pop2p to regulate messenger RNAs. *Nature structural & molecular biology* **13:** 533-539

Goldstrohm AC, Seay DJ, Hook BA, Wickens M (2007) PUF protein-mediated deadenylation is catalyzed by Ccr4p. *The Journal of biological chemistry* **282:** 109-114

Gowrishankar G, Winzen R, Dittrich-Breiholz O, Redich N, Kracht M, Holtmann H (2006) Inhibition of mRNA deadenylation and degradation by different types of cell stress. *Biol Chem* **387:** 323-327

Grandi P, Rybin V, Bassler J, Petfalski E, Strauss D, Marzioch M, Schafer T, Kuster B, Tschochner H, Tollervey D, Gavin AC, Hurt E (2002) 90S pre-ribosomes include the 35S pre-rRNA, the U3 snoRNP, and 40S subunit processing factors but predominantly lack 60S synthesis factors. *Molecular cell* **10:** 105-115

Green H, Wang N (1994) Codon reiteration and the evolution of proteins. *Proceedings of the National Academy of Sciences of the United States of America* **91:** 4298-4302

Gressner AM, Wool IG (1974) The phosphorylation of liver ribosomal proteins in vivo. Evidence that only a single small subunit protein (S6) is phosphorylated. *The Journal of biological chemistry* **249:** 6917-6925

Grigull J, Mnaimneh S, Pootoolal J, Robinson MD, Hughes TR (2004) Genome-wide analysis of mRNA stability using transcription inhibitors and microarrays reveals posttranscriptional control of ribosome biogenesis factors. *Molecular and cellular biology* **24:** 5534-5547

Gutierrez E, Shin BS, Woolstenhulme CJ, Kim JR, Saini P, Buskirk AR, Dever TE (2013) eIF5A Promotes Translation of Polyproline Motifs. *Molecular cell* **51:** 35-45

Hannan KM, Brandenburger Y, Jenkins A, Sharkey K, Cavanaugh A, Rothblum L, Moss T, Poortinga G, McArthur GA, Pearson RB, Hannan RD (2003) mTOR-dependent regulation of ribosomal gene transcription requires S6K1 and is mediated by phosphorylation of the carboxy-terminal activation domain of the nucleolar transcription factor UBF. *Molecular and cellular biology* **23:** 8862-8877

Harada H, Andersen JS, Mann M, Terada N, Korsmeyer SJ (2001) p70S6 kinase signals cell survival as well as growth, inactivating the pro-apoptotic molecule BAD. *Proceedings of the National Academy of Sciences of the United States of America* **98:** 9666-9670

Harger JW, Dinman JD (2003) An in vivo dual-luciferase assay system for studying translational recoding in the yeast Saccharomyces cerevisiae. *RNA* **9:** 1019-1024

Harigaya Y, Parker R (2010) No-go decay: a quality control mechanism for RNA in translation. *Wiley interdisciplinary reviews RNA* **1:** 132-141

Hasegawa Y, Irie K, Gerber AP (2008) Distinct roles for Khd1p in the localization and expression of bud-localized mRNAs in yeast. *RNA* **14:** 2333-2347

He W, Parker R (1999) Analysis of mRNA decay pathways in Saccharomyces cerevisiae. *Methods* **17:** 3-10

Heitman J, Movva NR, Hall MN (1991) Targets for cell cycle arrest by the immunosuppressant rapamycin in yeast. *Science* **253:** 905-909

Herruer MH, Mager WH, Raue HA, Vreken P, Wilms E, Planta RJ (1988) Mild temperature shock affects transcription of yeast ribosomal protein genes as well as the stability of their mRNAs. *Nucleic Acids Res* **16:** 7917-7929

Hook BA, Goldstrohm AC, Seay DJ, Wickens M (2007) Two yeast PUF proteins negatively regulate a single mRNA. *The Journal of biological chemistry* **282:** 15430-15438

Hoon S, Smith AM, Wallace IM, Suresh S, Miranda M, Fung E, Proctor M, Shokat KM, Zhang C, Davis RW, Giaever G, St Onge RP, Nislow C (2008) An integrated platform of genomic assays reveals small-molecule bioactivities. *Nature chemical biology* **4:** 498-506

Hsieh AC, Liu Y, Edlind MP, Ingolia NT, Janes MR, Sher A, Shi EY, Stumpf CR, Christensen C, Bonham MJ, Wang S, Ren P, Martin M, Jessen K, Feldman ME, Weissman JS, Shokat KM, Rommel C, Ruggero D (2012) The translational landscape of mTOR signalling steers cancer initiation and metastasis. *Nature* **485:** 55-61

Hu K, Li W, Wang H, Chen K, Wang Y, Sang J (2012) Shp1, a regulator of protein phosphatase 1 Glc7, has important roles in cell morphogenesis, cell cycle progression and DNA damage response in Candida albicans. *Fungal genetics and biology : FG & B* **49:** 433-442

Huber A, Bodenmiller B, Uotila A, Stahl M, Wanka S, Gerrits B, Aebersold R, Loewith R (2009) Characterization of the rapamycin-sensitive phosphoproteome reveals that Sch9 is a central coordinator of protein synthesis. *Genes Dev* **23:** 1929-1943

Huber A, French SL, Tekotte H, Yerlikaya S, Stahl M, Perepelkina MP, Tyers M, Rougemont J, Beyer AL, Loewith R (2011) Sch9 regulates ribosome biogenesis via Stb3, Dot6 and Tod6 and the histone deacetylase complex RPD3L. *The EMBO journal* **30:** 3052-3064

Humphrey EL, Shamji AF, Bernstein BE, Schreiber SL (2004) Rpd3p relocation mediates a transcriptional response to rapamycin in yeast. *Chemistry & biology* **11:** 295-299

Hutchinson JA, Shanware NP, Chang H, Tibbetts RS (2011) Regulation of ribosomal protein S6 phosphorylation by casein kinase 1 and protein phosphatase 1. *The Journal of biological chemistry* **286:** 8688-8696

Iadevaia V, Caldarola S, Tino E, Amaldi F, Loreni F (2008) All translation elongation factors and the e, f, and h subunits of translation initiation factor 3 are encoded by 5'-terminal oligopyrimidine (TOP) mRNAs. *RNA* **14:** 1730-1736

Ingolia NT, Ghaemmaghami S, Newman JR, Weissman JS (2009) Genome-wide analysis in vivo of translation with nucleotide resolution using ribosome profiling. *Science* **324:** 218-223

Irie K, Tadauchi T, Takizawa PA, Vale RD, Matsumoto K, Herskowitz I (2002) The Khd1 protein, which has three KH RNA-binding motifs, is required for proper localization of ASH1 mRNA in yeast. *The EMBO journal* **21:** 1158-1167

Isotani S, Hara K, Tokunaga C, Inoue H, Avruch J, Yonezawa K (1999) Immunopurified mammalian target of rapamycin phosphorylates and activates p70 S6 kinase alpha in vitro. *The Journal of biological chemistry* **274:** 34493-34498

Ito K, Inoue T, Yokoyama K, Morita M, Suzuki T, Yamamoto T (2011a) CNOT2 depletion disrupts and inhibits the CCR4-NOT deadenylase complex and induces apoptotic cell death. *Genes to cells : devoted to molecular & cellular mechanisms* **16:** 368-379

Ito W, Li X, Irie K, Mizuno T (2011b) RNA-binding protein Khd1 and Ccr4 deadenylase play overlapping roles in the cell wall integrity pathway in Saccharomyces cerevisiae. *Eukaryotic cell* **10:** 1340-1347

Jacinto E, Guo B, Arndt KT, Schmelzle T, Hall MN (2001) TIP41 interacts with TAP42 and negatively regulates the TOR signaling pathway. *Molecular cell* **8:** 1017-1026

Jacinto E, Lorberg A (2008) TOR regulation of AGC kinases in yeast and mammals. *The Biochemical journal* **410:** 19-37

Jackson RJ, Hellen CU, Pestova TV (2010) The mechanism of eukaryotic translation initiation and principles of its regulation. *Nature reviews Molecular cell biology* **11:** 113-127

Jacobs JL, Belew AT, Rakauskaite R, Dinman JD (2007) Identification of functional, endogenous programmed -1 ribosomal frameshift signals in the genome of Saccharomyces cerevisiae. *Nucleic acids research* **35:** 165-174

Jiang Y, Broach JR (1999) Tor proteins and protein phosphatase 2A reciprocally regulate Tap42 in controlling cell growth in yeast. *The EMBO journal* **18:** 2782-2792

Johnson SP, Warner JR (1987) Phosphorylation of the Saccharomyces cerevisiae equivalent of ribosomal protein S6 has no detectable effect on growth. *Molecular and cellular biology* **7:** 1338-1345

Jona G, Choder M, Gileadi O (2000) Glucose starvation induces a drastic reduction in the rates of both transcription and degradation of mRNA in yeast. *Biochim Biophys Acta* **1491:** 37-48

Kabat D (1970) Phosphorylation of ribosomal proteins in rabbit reticulocytes. Characterization and regulatory aspects. *Biochemistry* **9:** 4160-4175

Kamada Y, Fujioka Y, Suzuki NN, Inagaki F, Wullschleger S, Loewith R, Hall MN, Ohsumi Y (2005) Tor2 directly phosphorylates the AGC kinase Ypk2 to regulate actin polarization. *Molecular and cellular biology* **25:** 7239-7248

Kamada Y, Yoshino K, Kondo C, Kawamata T, Oshiro N, Yonezawa K, Ohsumi Y (2010) Tor directly controls the Atg1 kinase complex to regulate autophagy. *Molecular and cellular biology* **30:** 1049-1058

Kapasi P, Chaudhuri S, Vyas K, Baus D, Komar AA, Fox PL, Merrick WC, Mazumder B (2007) L13a blocks 48S assembly: role of a general initiation factor in mRNA-specific translational control. *Molecular cell* **25:** 113-126

Kennelly PJ, Krebs EG (1991) Consensus sequences as substrate specificity determinants for protein kinases and protein phosphatases. *The Journal of biological chemistry* **266:** 15555-15558

Kim TS, Jang CY, Kim HD, Lee JY, Ahn BY, Kim J (2006) Interaction of Hsp90 with ribosomal proteins protects from ubiquitination and proteasome-dependent degradation. *Molecular biology of the cell* **17:** 824-833

Koehler CM, Myers AM (1997) Serine-threonine protein kinase activity of Elm1p, a regulator of morphologic differentiation in Saccharomyces cerevisiae. *FEBS letters* **408:** 109-114

Koltin Y, Faucette L, Bergsma DJ, Levy MA, Cafferkey R, Koser PL, Johnson RK, Livi GP (1991) Rapamycin sensitivity in Saccharomyces cerevisiae is mediated by a peptidyl-prolyl cis-trans isomerase related to human FK506-binding protein. *Molecular and cellular biology* **11:** 1718-1723

Kondo H, Rabouille C, Newman R, Levine TP, Pappin D, Freemont P, Warren G (1997) p47 is a cofactor for p97-mediated membrane fusion. *Nature* **388:** 75-78

Krick R, Bremer S, Welter E, Schlotterhose P, Muehe Y, Eskelinen EL, Thumm M Cdc48/p97 and Shp1/p47 regulate autophagosome biogenesis in concert with ubiquitin-like Atg8. *J Cell Biol* **190:** 965-973

Kruk JA, Dutta A, Fu J, Gilmour DS, Reese JC (2011) The multifunctional Ccr4-Not complex directly promotes transcription elongation. *Genes & development* **25:** 581-593

Kruse C, Johnson SP, Warner JR (1985) Phosphorylation of the yeast equivalent of ribosomal protein S6 is not essential for growth. *Proceedings of the National Academy of Sciences of the United States of America* **82:** 7515-7519

La Valle R, Wittenberg C (2001) A role for the Swe1 checkpoint kinase during filamentous growth of Saccharomyces cerevisiae. *Genetics* **158:** 549-562

LaGrandeur TE, Parker R (1998) Isolation and characterization of Dcp1p, the yeast mRNA decapping enzyme. *EMBO J* **17:** 1487-1496

Lai KP, Leong WF, Chau JF, Jia D, Zeng L, Liu H, He L, Hao A, Zhang H, Meek D, Velagapudi C, Habib SL, Li B (2010) S6K1 is a multifaceted regulator of Mdm2 that connects nutrient status and DNA damage response. *The EMBO journal* **29:** 2994-3006

Latterich M, Frohlich KU, Schekman R (1995) Membrane fusion and the cell cycle: Cdc48p participates in the fusion of ER membranes. *Cell* **82:** 885-893

Lau NC, Mulder KW, Brenkman AB, Mohammed S, van den Broek NJ, Heck AJ, Timmers HT (2010) Phosphorylation of Not4p functions parallel to BUR2 to regulate resistance to cellular stresses in Saccharomyces cerevisiae. *PloS one* **5:** e9864

Laxman S, Tu BP (2011) Multiple TORC1-associated proteins regulate nitrogen starvation-dependent cellular differentiation in Saccharomyces cerevisiae. *PloS one* **6:** e26081

Lee J, Moir RD, McIntosh KB, Willis IM (2012) TOR signaling regulates ribosome and tRNA synthesis via LAMMER/Clk and GSK-3 family kinases. *Molecular cell* **45:** 836-843

Leidel S, Pedrioli PG, Bucher T, Brost R, Costanzo M, Schmidt A, Aebersold R, Boone C, Hofmann K, Peter M (2009) Ubiquitin-related modifier Urm1 acts as a sulphur carrier in thiolation of eukaryotic transfer RNA. *Nature* **458:** 228-232

Lempiainen H, Uotila A, Urban J, Dohnal I, Ammerer G, Loewith R, Shore D (2009) Sfp1 interaction with TORC1 and Mrs6 reveals feedback regulation on TOR signaling. *Molecular cell* **33:** 704-716

Lenssen E, James N, Pedruzzi I, Dubouloz F, Cameroni E, Bisig R, Maillet L, Werner M, Roosen J, Petrovic K, Winderickx J, Collart MA, De Virgilio C (2005) The Ccr4-Not complex independently controls both Msn2-dependent transcriptional activation--via a newly identified Glc7/Bud14 type I protein phosphatase module--and TFIID promoter distribution. *Molecular and cellular biology* **25:** 488-498

Letzring DP, Dean KM, Grayhack EJ (2010) Control of translation efficiency in yeast by codon-anticodon interactions. *RNA* **16:** 2516-2528

Levy S, Avni D, Hariharan N, Perry RP, Meyuhas O (1991) Oligopyrimidine tract at the 5' end of mammalian ribosomal protein mRNAs is required for their translational control. *Proceedings of the National Academy of Sciences of the United States of America* **88:** 3319-3323

Liko D, Slattery MG, Heideman W (2007) Stb3 binds to ribosomal RNA processing element motifs that control transcriptional responses to growth in Saccharomyces cerevisiae. *The Journal of biological chemistry* **282:** 26623-26628

Lindstrom MS (2009) Emerging functions of ribosomal proteins in gene-specific transcription and translation. *Biochemical and biophysical research communications* **379:** 167-170

Lippman SI, Broach JR (2009) Protein kinase A and TORC1 activate genes for ribosomal biogenesis by inactivating repressors encoded by Dot6 and its homolog Tod6. *Proceedings of the National Academy of Sciences of the United States of America* **106:** 19928-19933

Liu HY, Badarinarayana V, Audino DC, Rappsilber J, Mann M, Denis CL (1998) The NOT proteins are part of the CCR4 transcriptional complex and affect gene expression both positively and negatively. *The EMBO journal* **17:** 1096-1106

Liu HY, Chiang YC, Pan J, Chen J, Salvadore C, Audino DC, Badarinarayana V, Palaniswamy V, Anderson B, Denis CL (2001) Characterization of CAF4 and CAF16 reveals a functional connection between the CCR4-NOT complex and a subset of SRB proteins of the RNA polymerase II holoenzyme. *J Biol Chem* **276:** 7541-7548

Liu HY, Toyn JH, Chiang YC, Draper MP, Johnston LH, Denis CL (1997) DBF2, a cell cycle-regulated protein kinase, is physically and functionally associated with the CCR4 transcriptional regulatory complex. *The EMBO journal* **16:** 5289-5298

Liu Q, Ren T, Fresques T, Oppliger W, Niles BJ, Hur W, Sabatini DM, Hall MN, Powers T, Gray NS (2012) Selective ATP-competitive inhibitors of TOR suppress rapamycin-insensitive function of TORC2 in Saccharomyces cerevisiae. *ACS chemical biology* **7:** 982-987

Loewith R. (2010) TORC1 Signaling in Budding Yeast. In Hall MT, F. (ed.), *The Enzymes*. Academic Press, USA, Vol. 27.

Lupas AN, Martin J (2002) AAA proteins. *Current opinion in structural biology* **12:** 746-753

Ma XJ, Lu Q, Grunstein M (1996) A search for proteins that interact genetically with histone H3 and H4 amino termini uncovers novel regulators of the Swe1 kinase in Saccharomyces cerevisiae. *Genes & development* **10:** 1327-1340

Ma XM, Blenis J (2009) Molecular mechanisms of mTOR-mediated translational control. *Nature reviews Molecular cell biology* **10:** 307-318

Magnuson B, Ekim B, Fingar DC (2012) Regulation and function of ribosomal protein S6 kinase (S6K) within mTOR signalling networks. *The Biochemical journal* **441:** 1-21

Maillet L, Tu C, Hong YK, Shuster EO, Collart MA (2000) The essential function of Not1 lies within the Ccr4-Not complex. *Journal of molecular biology* **303:** 131-143

Malvar T, Biron RW, Kaback DB, Denis CL (1992) The CCR4 protein from Saccharomyces cerevisiae contains a leucine-rich repeat region which is required for its control of ADH2 gene expression. *Genetics* **132:** 951-962

Manukyan A, Zhang J, Thippeswamy U, Yang J, Zavala N, Mudannayake MP, Asmussen M, Schneider C, Schneider BL (2008) Ccr4 alters cell size in yeast by modulating the timing of CLN1 and CLN2 expression. *Genetics* **179:** 345-357

Mar Alba M, Santibanez-Koref MF, Hancock JM (1999) Amino acid reiterations in yeast are overrepresented in particular classes of proteins and show evidence of a slippage-like mutational process. *Journal of molecular evolution* **49:** 789-797

Marion RM, Regev A, Segal E, Barash Y, Koller D, Friedman N, O'Shea EK (2004) Sfp1 is a stress- and nutrient-sensitive regulator of ribosomal protein gene expression. *Proceedings of the National Academy of Sciences of the United States of America* **101:** 14315-14322

Martin-Perez J, Thomas G (1983) Ordered phosphorylation of 40S ribosomal protein S6 after serum stimulation of quiescent 3T3 cells. *Proceedings of the National Academy of Sciences of the United States of America* **80:** 926-930

Martin DE, Soulard A, Hall MN (2004) TOR regulates ribosomal protein gene expression via PKA and the Forkhead transcription factor FHL1. *Cell* **119:** 969-979

Mayer C, Zhao J, Yuan X, Grummt I (2004) mTOR-dependent activation of the transcription factor TIF-IA links rRNA synthesis to nutrient availability. *Genes & development* **18:** 423-434

Mazumder B, Sampath P, Seshadri V, Maitra RK, DiCorleto PE, Fox PL (2003) Regulated release of L13a from the 60S ribosomal subunit as a mechanism of transcript-specific translational control. *Cell* **115:** 187-198

Meier KD, Deloche O, Kajiwara K, Funato K, Riezman H (2006) Sphingoid base is required for translation initiation during heat stress in Saccharomyces cerevisiae. *Molecular biology of the cell* **17:** 1164-1175

Meskauskas A, Dinman JD (2007) Ribosomal protein L3: gatekeeper to the A site. *Molecular cell* **25:** 877-888

Metspalu A, Saarma M, Villems R, Ustav M, Lind A (1978) Interaction of 5-S RNA, 5.8-S RNA and tRNA with rat-liver ribosomal proteins. *European journal of biochemistry / FEBS* **91:** 73-81

Meyer HH, Kondo H, Warren G (1998) The p47 co-factor regulates the ATPase activity of the membrane fusion protein, p97. *FEBS letters* **437:** 255-257

Meyuhas O (2008) Physiological roles of ribosomal protein S6: one of its kind. *International review of cell and molecular biology* **268:** 1-37

Milkereit P, Strauss D, Bassler J, Gadal O, Kuhn H, Schutz S, Gas N, Lechner J, Hurt E, Tschochner H (2003) A Noc complex specifically involved in the formation and nuclear export of ribosomal 40 S subunits. *The Journal of biological chemistry* **278:** 4072-4081

Morel AP, Sentis S, Bianchin C, Le Romancer M, Jonard L, Rostan MC, Rimokh R, Corbo L (2003) BTG2 antiproliferative protein interacts with the human CCR4 complex existing in vivo in three cell-cycle-regulated forms. *Journal of cell science* **116:** 2929-2936

Moriya H, Shimizu-Yoshida Y, Omori A, Iwashita S, Katoh M, Sakai A (2001) Yak1p, a DYRK family kinase, translocates to the nucleus and phosphorylates yeast Pop2p in response to a glucose signal. *Genes & development* **15:** 1217-1228

Mostafavi S, Ray D, Warde-Farley D, Grouios C, Morris Q (2008) GeneMANIA: a real-time multiple association network integration algorithm for predicting gene function. *Genome biology* **9 Suppl 1:** S4

Muhlrad D, Parker R (2005) The yeast EDC1 mRNA undergoes deadenylation-independent decapping stimulated by Not2p, Not4p, and Not5p. *The EMBO journal* **24:** 1033-1045

Mukhopadhyay R, Ray PS, Arif A, Brady AK, Kinter M, Fox PL (2008) DAPK-ZIPK-L13a axis constitutes a negative-feedback module regulating inflammatory gene expression. *Molecular cell* **32:** 371-382

Mulder KW, Brenkman AB, Inagaki A, van den Broek NJ, Timmers HT (2007a) Regulation of histone H3K4 tri-methylation and PAF complex recruitment by the Ccr4-Not complex. *Nucleic acids research* **35:** 2428-2439

Mulder KW, Inagaki A, Cameroni E, Mousson F, Winkler GS, De Virgilio C, Collart MA, Timmers HT (2007b) Modulation of Ubc4p/Ubc5p-mediated stress responses by the RING-finger-dependent ubiquitin-protein ligase Not4p in Saccharomyces cerevisiae. *Genetics* **176:** 181-192

Nakano K, Yamamoto T, Kishimoto T, Noji T, Tanaka K (2008) Protein kinases Fpk1p and Fpk2p are novel regulators of phospholipid asymmetry. *Molecular biology of the cell* **19:** 1783-1797

Nakashima A, Otsubo Y, Yamashita A, Sato T, Yamamoto M, Tamanoi F (2012) Psk1, an AGC kinase family member in fission yeast, is directly phosphorylated and controlled by TORC1 and functions as S6 kinase. *Journal of cell science* **125:** 5840-5849

Nakashima A, Tanimura-Ito K, Oshiro N, Eguchi S, Miyamoto T, Momonami A, Kamada S, Yonezawa K, Kikkawa U (2013) A positive role of mammalian Tip41-like protein, TIPRL, in the amino-acid dependent mTORC1-signaling pathway through interaction with PP2A. *FEBS letters*

Niles BJ, Mogri H, Hill A, Vlahakis A, Powers T (2012) Plasma membrane recruitment and activation of the AGC kinase Ypk1 is mediated by target of rapamycin complex 2 (TORC2) and its effector proteins Slm1 and Slm2. *Proceedings of the National Academy of Sciences of the United States of America* **109:** 1536-1541

Nissan T, Parker R (2008) Analyzing P-bodies in Saccharomyces cerevisiae. *Methods in enzymology* **448:** 507-520

Nygard O, Nika H (1982) Identification by RNA-protein cross-linking of ribosomal proteins located at the interface between the small and the large subunits of mammalian ribosomes. *The EMBO journal* **1:** 357-362

Oberholzer U, Collart MA (1998) Characterization of NOT5 that encodes a new component of the Not protein complex. *Gene* **207:** 61-69

Oh WJ, Wu CC, Kim SJ, Facchinetti V, Julien LA, Finlan M, Roux PP, Su B, Jacinto E (2010) mTORC2 can associate with ribosomes to promote cotranslational phosphorylation and stability of nascent Akt polypeptide. *The EMBO journal* **29:** 3939-3951

Ohanna M, Sobering AK, Lapointe T, Lorenzo L, Praud C, Petroulakis E, Sonenberg N, Kelly PA, Sotiropoulos A, Pende M (2005) Atrophy of S6K1(-/-) skeletal muscle cells reveals distinct mTOR effectors for cell cycle and size control. *Nature cell biology* **7:** 286-294

Olivas W, Parker R (2000) The Puf3 protein is a transcript-specific regulator of mRNA degradation in yeast. *The EMBO journal* **19:** 6602-6611

Pachler K, Karl T, Kolmann K, Mehlmer N, Eder M, Loeffler M, Oender K, Hochleitner EO, Lottspeich F, Bresgen N, Richter K, Breitenbach M, Koller L (2004) Functional interaction in establishment of ribosomal integrity between small subunit protein rpS6 and translational regulator rpL10/Grc5p. *FEMS yeast research* **5:** 271-280

Panasenko O, Landrieux E, Feuermann M, Finka A, Paquet N, Collart MA (2006) The yeast Ccr4-Not complex controls ubiquitination of the nascent-associated polypeptide (NAC-EGD) complex. *The Journal of biological chemistry* **281:** 31389-31398

Panic L, Tamarut S, Sticker-Jantscheff M, Barkic M, Solter D, Uzelac M, Grabusic K, Volarevic S (2006) Ribosomal protein S6 gene haploinsufficiency is associated with activation of a p53-dependent checkpoint during gastrulation. *Molecular and cellular biology* **26:** 8880-8891

Paquin N, Menade M, Poirier G, Donato D, Drouet E, Chartrand P (2007) Local activation of yeast ASH1 mRNA translation through phosphorylation of Khd1p by the casein kinase Yck1p. *Molecular cell* **26:** 795-809

Parker R (2012) RNA degradation in Saccharomyces cerevisae. *Genetics* **191:** 671-702

Parker R, Song H (2004) The enzymes and control of eukaryotic mRNA turnover. *Nat Struct Mol Biol* **11:** 121-127

Pearce LR, Komander D, Alessi DR (2010) The nuts and bolts of AGC protein kinases. *Nature reviews Molecular cell biology* **11:** 9-22

Pedruzzi I, Dubouloz F, Cameroni E, Wanke V, Roosen J, Winderickx J, De Virgilio C (2003) TOR and PKA signaling pathways converge on the protein kinase Rim15 to control entry into G0. *Molecular cell* **12:** 1607-1613

Peltz SW, Hammell AB, Cui Y, Yasenchak J, Puljanowski L, Dinman JD (1999) Ribosomal protein L3 mutants alter translational fidelity and promote rapid loss of the yeast killer virus. *Molecular and cellular biology* **19:** 384-391

Pende M, Um SH, Mieulet V, Sticker M, Goss VL, Mestan J, Mueller M, Fumagalli S, Kozma SC, Thomas G (2004) S6K1(-/-)/S6K2(-/-) mice exhibit perinatal lethality and rapamycin-sensitive 5'-terminal oligopyrimidine mRNA translation and reveal a mitogen-activated protein kinase-dependent S6 kinase pathway. *Molecular and cellular biology* **24:** 3112-3124

Poyry TA, Kaminski A, Jackson RJ (2004) What determines whether mammalian ribosomes resume scanning after translation of a short upstream open reading frame? *Genes & development* **18:** 62-75

Ptacek J, Devgan G, Michaud G, Zhu H, Zhu X, Fasolo J, Guo H, Jona G, Breitkreutz A, Sopko R, McCartney RR, Schmidt MC, Rachidi N, Lee SJ, Mah AS, Meng L, Stark MJ, Stern DF, De Virgilio C, Tyers M, Andrews B, Gerstein M, Schweitzer B, Predki PF, Snyder M (2005) Global analysis of protein phosphorylation in yeast. *Nature* **438:** 679-684

Rabouille C, Levine TP, Peters JM, Warren G (1995) An NSF-like ATPase, p97, and NSF mediate cisternal regrowth from mitotic Golgi fragments. *Cell* **82:** 905-914

Radimerski T, Mini T, Schneider U, Wettenhall RE, Thomas G, Jeno P (2000) Identification of insulin-induced sites of ribosomal protein S6 phosphorylation in Drosophila melanogaster. *Biochemistry* **39:** 5766-5774

Ramachandran V, Shah KH, Herman PK (2011) The cAMP-dependent protein kinase signaling pathway is a key regulator of P body foci formation. *Molecular cell* **43:** 973-981

Raught B, Peiretti F, Gingras AC, Livingstone M, Shahbazian D, Mayeur GL, Polakiewicz RD, Sonenberg N, Hershey JW (2004) Phosphorylation of eucaryotic translation initiation factor 4B Ser422 is modulated by S6 kinases. *The EMBO journal* **23:** 1761-1769

Reinke A, Chen JC, Aronova S, Powers T (2006) Caffeine targets TOR complex I and provides evidence for a regulatory link between the FRB and kinase domains of Tor1p. *The Journal of biological chemistry* **281:** 31616-31626

Robinson LC, Bradley C, Bryan JD, Jerome A, Kweon Y, Panek HR (1999) The Yck2 yeast casein kinase 1 isoform shows cell cycle-specific localization to sites of polarized growth and is required for proper septin organization. *Molecular biology of the cell* **10:** 1077-1092

Robinson LC, Phillips J, Brou L, Boswell EP, Tatchell K (2012) Suppressors of ipl1-2 in components of a Glc7 phosphatase complex, Cdc48 AAA ATPase, TORC1, and the kinetochore. *G3 (Bethesda)* **2:** 1687-1701

Roelants FM, Baltz AG, Trott AE, Fereres S, Thorner J (2010) A protein kinase network regulates the function of aminophospholipid flippases. *Proceedings of the National Academy of Sciences of the United States of America* **107:** 34-39

Roelants FM, Torrance PD, Thorner J (2004) Differential roles of PDK1- and PDK2-phosphorylation sites in the yeast AGC kinases Ypk1, Pkc1 and Sch9. *Microbiology* **150:** 3289-3304

Romeo Y, Zhang X, Roux PP (2012) Regulation and function of the RSK family of protein kinases. *The Biochemical journal* **441:** 553-569

Rosner M, Hengstschlager M (2011) Nucleocytoplasmic localization of p70 S6K1, but not of its isoforms p85 and p31, is regulated by TSC2/mTOR. *Oncogene* **30:** 4509-4522

Rosner M, Schipany K, Hengstschlager M (2012) p70 S6K1 nuclear localization depends on its mTOR-mediated phosphorylation at T389, but not on its kinase activity towards S6. *Amino acids* **42:** 2251-2256

Roux PP, Shahbazian D, Vu H, Holz MK, Cohen MS, Taunton J, Sonenberg N, Blenis J (2007) RAS/ERK signaling promotes site-specific ribosomal protein S6 phosphorylation via RSK and stimulates cap-dependent translation. *The Journal of biological chemistry* **282:** 14056-14064

Rubenstein EM, Schmidt MC (2007) Mechanisms regulating the protein kinases of Saccharomyces cerevisiae. *Eukaryotic cell* **6:** 571-583

Russell P, Benson JD, Denis CL (2002) Characterization of mutations in NOT2 indicates that it plays an important role in maintaining the integrity of the CCR4-NOT complex. *Journal of molecular biology* **322:** 27-39

Ruvinsky I, Sharon N, Lerer T, Cohen H, Stolovich-Rain M, Nir T, Dor Y, Zisman P, Meyuhas O (2005) Ribosomal protein S6 phosphorylation is a determinant of cell size and glucose homeostasis. *Genes & development* **19:** 2199-2211

Saitoh M, Pullen N, Brennan P, Cantrell D, Dennis PB, Thomas G (2002) Regulation of an activated S6 kinase 1 variant reveals a novel mammalian target of rapamycin phosphorylation site. *The Journal of biological chemistry* **277:** 20104-20112

Salles FJ, Strickland S (1995) Rapid and sensitive analysis of mRNA polyadenylation states by PCR. *PCR Methods Appl* **4:** 317-321

Sarkaria JN, Busby EC, Tibbetts RS, Roos P, Taya Y, Karnitz LM, Abraham RT (1999) Inhibition of ATM and ATR kinase activities by the radiosensitizing agent, caffeine. *Cancer research* **59:** 4375-4382

Schafer T, Maco B, Petfalski E, Tollervey D, Bottcher B, Aebi U, Hurt E (2006) Hrr25-dependent phosphorylation state regulates organization of the pre-40S subunit. *Nature* **441:** 651-655

Schalm SS, Blenis J (2002) Identification of a conserved motif required for mTOR signaling. *Current biology : CB* **12:** 632-639

Schuberth C, Buchberger A (2008) UBX domain proteins: major regulators of the AAA ATPase Cdc48/p97. *Cellular and molecular life sciences : CMLS* **65:** 2360-2371

Schuberth C, Richly H, Rumpf S, Buchberger A (2004) Shp1 and Ubx2 are adaptors of Cdc48 involved in ubiquitin-dependent protein degradation. *EMBO Rep* **5:** 818-824

Shah KH, Zhang B, Ramachandran V, Herman PK (2013) Processing body and stress granule assembly occur by independent and differentially regulated pathways in Saccharomyces cerevisiae. *Genetics* **193:** 109-123

Sheth U, Parker R (2003) Decapping and decay of messenger RNA occur in cytoplasmic processing bodies. *Science* **300:** 805-808

Shibata Y, Oyama M, Kozuka-Hata H, Han X, Tanaka Y, Gohda J, Inoue J (2012) p47 negatively regulates IKK activation by inducing the lysosomal degradation of polyubiquitinated NEMO. *Nature communications* **3:** 1061

Shimada K, Filipuzzi I, Stahl M, Helliwell SB, Studer C, Hoepfner D, Seeber A, Loewith R, Movva NR, Gasser SM (2013) TORC2 Signaling Pathway Guarantees Genome Stability in the Face of DNA Strand Breaks. *Molecular cell*

Shin CS, Kim SY, Huh WK (2009) TORC1 controls degradation of the transcription factor Stp1, a key effector of the SPS amino-acid-sensing pathway in Saccharomyces cerevisiae. *Journal of cell science* **122:** 2089-2099

Sil A, Herskowitz I (1996) Identification of asymmetrically localized determinant, Ash1p, required for lineage-specific transcription of the yeast HO gene. *Cell* **84:** 711-722

Soulard A, Cremonesi A, Moes S, Schutz F, Jeno P, Hall MN The rapamycin-sensitive phosphoproteome reveals that TOR controls protein kinase A toward some but not all substrates. *Mol Biol Cell* **21:** 3475-3486

Sreenivasan A, Bishop AC, Shokat KM, Kellogg DR (2003) Specific inhibition of Elm1 kinase activity reveals functions required for early G1 events. *Molecular and cellular biology* **23:** 6327-6337

Sreenivasan A, Kellogg D (1999) The elm1 kinase functions in a mitotic signaling network in budding yeast. *Molecular and cellular biology* **19:** 7983-7994

Stark C, Su TC, Breitkreutz A, Lourenco P, Dahabieh M, Breitkreutz BJ, Tyers M, Sadowski I (2010) PhosphoGRID: a database of experimentally verified in vivo protein phosphorylation sites from the budding yeast Saccharomyces cerevisiae. *Database : the journal of biological databases and curation* **2010:** bap026

Szamecz B, Rutkai E, Cuchalova L, Munzarova V, Herrmannova A, Nielsen KH, Burela L, Hinnebusch AG, Valasek L (2008) eIF3a cooperates with sequences 5' of uORF1 to promote resumption of scanning by post-termination ribosomes for reinitiation on GCN4 mRNA. *Genes & development* **22:** 2414-2425

Takahara T, Maeda T (2012) Transient sequestration of TORC1 into stress granules during heat stress. *Molecular cell* **47:** 242-252

Takahashi Y, Ogata K (1981) Ribosomal proteins cross-linked to natural mRNA by UV irradiation of rat liver polysomes. *Journal of biochemistry* **90:** 1549-1552

Tan YS, Morcos PA, Cannon JF (2003) Pho85 phosphorylates the Glc7 protein phosphatase regulator Glc8 in vivo. *The Journal of biological chemistry* **278:** 147-153

Tang H, Hornstein E, Stolovich M, Levy G, Livingstone M, Templeton D, Avruch J, Meyuhas O (2001) Amino acid-induced translation of TOP mRNAs is fully dependent on phosphatidylinositol 3-kinase-mediated signaling, is partially inhibited by rapamycin, and is independent of S6K1 and rpS6 phosphorylation. *Molecular and cellular biology* **21:** 8671-8683

Thedieck K, Holzwarth B, Prentzell MT, Boehlke C, Klasener K, Ruf S, Sonntag AG, Maerz L, Grellscheid SN, Kremmer E, Nitschke R, Kuehn EW, Jonker JW, Groen AK, Reth M, Hall MN, Baumeister R (2013) Inhibition of mTORC1 by Astrin and Stress Granules Prevents Apoptosis in Cancer Cells. *Cell* **154:** 859-874

Thoreen CC, Chantranupong L, Keys HR, Wang T, Gray NS, Sabatini DM (2012) A unifying model for mTORC1-mediated regulation of mRNA translation. *Nature* **485:** 109-113

Thoreen CC, Kang SA, Chang JW, Liu Q, Zhang J, Gao Y, Reichling LJ, Sim T, Sabatini DM, Gray NS (2009) An ATP-competitive mammalian target of rapamycin inhibitor reveals rapamycin-resistant functions of mTORC1. *The Journal of biological chemistry* **284:** 8023-8032

Tong AH, Evangelista M, Parsons AB, Xu H, Bader GD, Page N, Robinson M, Raghibizadeh S, Hogue CW, Bussey H, Andrews B, Tyers M, Boone C (2001) Systematic genetic analysis with ordered arrays of yeast deletion mutants. *Science* **294:** 2364-2368

Tourriere H, Chebli K, Tazi J (2002) mRNA degradation machines in eukaryotic cells. *Biochimie* **84:** 821-837

Traven A, Beilharz TH, Lo TL, Lueder F, Preiss T, Heierhorst J (2009) The Ccr4-Pop2-NOT mRNA deadenylase contributes to septin organization in Saccharomyces cerevisiae. *Genetics* **182:** 955-966

Tucker M, Staples RR, Valencia-Sanchez MA, Muhlrad D, Parker R (2002) Ccr4p is the catalytic subunit of a Ccr4p/Pop2p/Notp mRNA deadenylase complex in Saccharomyces cerevisiae. *The EMBO journal* **21:** 1427-1436

Tucker M, Valencia-Sanchez MA, Staples RR, Chen J, Denis CL, Parker R (2001) The transcription factor associated Ccr4 and Caf1 proteins are components of the major cytoplasmic mRNA deadenylase in Saccharomyces cerevisiae. *Cell* **104:** 377-386

Uchiyama K, Jokitalo E, Kano F, Murata M, Zhang X, Canas B, Newman R, Rabouille C, Pappin D, Freemont P, Kondo H (2002) VCIP135, a novel essential factor for p97/p47-mediated membrane fusion, is required for Golgi and ER assembly in vivo. *The Journal of cell biology* **159:** 855-866

Uchiyama K, Jokitalo E, Lindman M, Jackman M, Kano F, Murata M, Zhang X, Kondo H (2003) The localization and phosphorylation of p47 are important for Golgi disassembly-assembly during the cell cycle. *The Journal of cell biology* **161:** 1067-1079

Ude S, Lassak J, Starosta AL, Kraxenberger T, Wilson DN, Jung K (2013) Translation elongation factor EF-P alleviates ribosome stalling at polyproline stretches. *Science* **339:** 82-85

Urban J, Soulard A, Huber A, Lippman S, Mukhopadhyay D, Deloche O, Wanke V, Anrather D, Ammerer G, Riezman H, Broach JR, De Virgilio C, Hall MN, Loewith R (2007) Sch9 is a major target of TORC1 in Saccharomyces cerevisiae. *Molecular cell* **26:** 663-674

Usdin K (2008) The biological effects of simple tandem repeats: lessons from the repeat expansion diseases. *Genome research* **18:** 1011-1019

van Dam TJ, Zwartkruis FJ, Bos JL, Snel B Evolution of the TOR pathway. *J Mol Evol* **73:** 209-220

Vanrobays E, Gelugne JP, Gleizes PE, Caizergues-Ferrer M (2003) Late cytoplasmic maturation of the small ribosomal subunit requires RIO proteins in Saccharomyces cerevisiae. *Molecular and cellular biology* **23:** 2083-2095

Versees W, De Groeve S, Van Lijsebettens M (2010) Elongator, a conserved multitasking complex? *Molecular microbiology* **76:** 1065-1069

Wade CH, Umbarger MA, McAlear MA (2006) The budding yeast rRNA and ribosome biosynthesis (RRB) regulon contains over 200 genes. *Yeast* **23:** 293-306

Wang PC, Vancura A, Mitcheson TG, Kuret J (1992) Two genes in Saccharomyces cerevisiae encode a membrane-bound form of casein kinase-1. *Molecular biology of the cell* **3:** 275-286

Wang X, Li W, Williams M, Terada N, Alessi DR, Proud CG (2001) Regulation of elongation factor 2 kinase by p90(RSK1) and p70 S6 kinase. *The EMBO journal* **20:** 4370-4379

Wanke V, Cameroni E, Uotila A, Piccolis M, Urban J, Loewith R, De Virgilio C (2008) Caffeine extends yeast lifespan by targeting TORC1. *Molecular microbiology* **69:** 277-285

Warner JR, McIntosh KB (2009) How common are extraribosomal functions of ribosomal proteins? *Molecular cell* **34:** 3-11

Wei M, Fabrizio P, Hu J, Ge H, Cheng C, Li L, Longo VD (2008) Life span extension by calorie restriction depends on Rim15 and transcription factors downstream of Ras/PKA, Tor, and Sch9. *PLoS Genet* **4:** e13

Wettenhall RE, Erikson E, Maller JL (1992) Ordered multisite phosphorylation of Xenopus ribosomal protein S6 by S6 kinase II. *The Journal of biological chemistry* **267:** 9021-9027

Wickens M, Bernstein DS, Kimble J, Parker R (2002) A PUF family portrait: 3'UTR regulation as a way of life. *Trends in genetics : TIG* **18:** 150-157

Williams-Hart T, Wu X, Tatchell K (2002) Protein phosphatase type 1 regulates ion homeostasis in Saccharomyces cerevisiae. *Genetics* **160:** 1423-1437

Wippich F, Bodenmiller B, Trajkovska MG, Wanka S, Aebersold R, Pelkmans L (2013) Dual specificity kinase DYRK3 couples stress granule condensation/dissolution to mTORC1 signaling. *Cell* **152:** 791-805

Wolf JJ, Dowell RD, Mahony S, Rabani M, Gifford DK, Fink GR (2010) Feed-forward regulation of a cell fate determinant by an RNA-binding protein generates asymmetry in yeast. *Genetics* **185:** 513-522

Xie MW, Jin F, Hwang H, Hwang S, Anand V, Duncan MC, Huang J (2005) Insights into TOR function and rapamycin response: chemical genomic profiling by using a high-density cell array method. *Proc Natl Acad Sci U S A* **102:** 7215-7220

Yadavilli S, Hegde V, Deutsch WA (2007) Translocation of human ribosomal protein S3 to sites of DNA damage is dependant on ERK-mediated phosphorylation following genotoxic stress. *DNA repair* **6:** 1453-1462

Yamasaki S, Anderson P (2008) Reprogramming mRNA translation during stress. *Current opinion in cell biology* **20:** 222-226

Yamashita A, Chang TC, Yamashita Y, Zhu W, Zhong Z, Chen CY, Shyu AB (2005) Concerted action of poly(A) nucleases and decapping enzyme in mammalian mRNA turnover. *Nature structural & molecular biology* **12:** 1054-1063

Yang Z, Jakymiw A, Wood MR, Eystathioy T, Rubin RL, Fritzler MJ, Chan EK (2004) GW182 is critical for the stability of GW bodies expressed during the cell cycle and cell proliferation. *Journal of cell science* **117:** 5567-5578

Yin Z, Wilson S, Hauser NC, Tournu H, Hoheisel JD, Brown AJ (2003) Glucose triggers different global responses in yeast, depending on the strength of the signal, and transiently stabilizes ribosomal protein mRNAs. *Mol Microbiol* **48:** 713-724

Yoon JH, Choi EJ, Parker R (2010) Dcp2 phosphorylation by Ste20 modulates stress granule assembly and mRNA decay in Saccharomyces cerevisiae. *The Journal of cell biology* **189:** 813-827

Zhang S, Guha S, Volkert FC (1995) The Saccharomyces SHP1 gene, which encodes a regulator of phosphoprotein phosphatase 1 with differential effects on glycogen metabolism, meiotic differentiation, and mitotic cell cycle progression. *Mol Cell Biol* **15:** 2037-2050

Zhao Y, Bjorbaek C, Weremowicz S, Morton CC, Moller DE (1995) RSK3 encodes a novel pp90rsk isoform with a unique N-terminal sequence: growth factor-stimulated kinase function and nuclear translocation. *Molecular and cellular biology* **15:** 4353-4363

Zhou F, Roy B, von Arnim AG (2010) Translation reinitiation and development are compromised in similar ways by mutations in translation initiation factor eIF3h and the ribosomal protein RPL24. *BMC plant biology* **10:** 193

Zhu C, Byers KJ, McCord RP, Shi Z, Berger MF, Newburger DE, Saulrieta K, Smith Z, Shah MV, Radhakrishnan M, Philippakis AA, Hu Y, De Masi F, Pacek M, Rolfs A, Murthy T, Labaer J, Bulyk ML (2009) High-resolution DNA-binding specificity analysis of yeast transcription factors. *Genome research* **19:** 556-566

Zinzalla V, Stracka D, Oppliger W, Hall MN (2011) Activation of mTORC2 by association with the ribosome. *Cell* **144:** 757-768